Distribution Agreement

In presenting this thesis or dissertation as a partial fulfillment of the requirements for an advanced degree from Emory University, I hereby grant to Emory University and its agents the non-exclusive license to archive, make accessible, and display my thesis or dissertation in whole or in part in all forms of media, now or hereafter known, including display on the world wide web. I understand that I may select some access restrictions as part of the online submission of this thesis or dissertation. I retain all ownership rights to the copyright of the thesis or dissertation. I also retain the right to use in future works (such as articles or books) all or part of this thesis or dissertation.

Signature:

_____ _____

Luke S. Uebelhoer Date

Binding, entry, and immune escape mechanisms of hepatitis C virus

By

Luke S. Uebelhoer
Doctor of Philosophy

Graduate Division of Biological and Biomedical Sciences
Immunology and Molecular Pathogenesis

_____
Arash Grakoui, Ph.D.
Advisor

_____
Brian D. Evavold, Ph.D.
Committee Member

_____
Joshy Jacob, Ph.D.
Committee Member

_____
Robert S. Mittler, Ph.D.
Committee Member

_____
Samuel H. Speck, Ph.D.
Committee Member

Accepted:

_____
Lisa A. Tedesco, Ph.D.
Dean of the James T. Laney School of Graduate Studies

_____
Date

Binding, entry, and immune escape mechanisms of hepatitis C virus

By

Luke S. Uebelhoer
B.S., Cornell University, 2004

Advisor: Arash Grakoui, Ph.D.

An Abstract of
A dissertation submitted to the Faculty of the James T. Laney School of Graduate Studies of Emory University in partial fulfillment of the requirements for the degree of Doctor of Philosophy

Graduate Division of Biological and Biomedical Sciences
Immunology and Molecular Pathogenesis

2011

ABSTRACT

Binding, entry, and immune escape mechanisms of hepatitis C virus

By

Luke S. Uebelhoer

Hepatitis C virus (HCV) infection is a global health problem, affecting more than 170 million people worldwide. Currently, no vaccine exists and treatment options are limited, highlighting the importance of elucidating factors that lead to viral persistence. One of the most important mechanisms of HCV pathogenesis is the high variability of its genome. Like most small RNA viruses, HCV has an extremely high replication rate, and the highly error prone NS5B polymerase allows for robust production of minor viral variants that may subvert host immune responses to establish persistent infection. The work presented here focuses on two highly variable HCV proteins, the NS3 helicase/protease and the E2 envelope glycoprotein. First, we examine the evolution of a dominant NS3 major histocompatibility complex (MHC) class I epitope during the acute and chronic phases of infection in a chimpanzee through seven years of follow-up. *In vitro* assessment of the fitness of viral variants that arose *in vivo*, as well as the host immune response directed against these variants, indicate that genomes encoding cytotoxic T lymphocyte (CTL) escape mutations that emerge early in infection are not necessarily optimized for replication and are eventually replaced by variants that successfully balance escape from cellular immune pressure and replicative fitness in the chronic phase of infection. Second, we analyze the conserved disulfide bonding patterns in the highly variable HCV E2 protein to determine potential impact on viral life cycle. A mutagenesis approach identified phenotypically relevant cysteine residues of E2, and we report that the majority of these residues are essential at early steps in viral assembly, while two allow for low levels of egress, and one allows for high levels of viral particle formation and secretion but ablates CD81 coreceptor binding. In parallel to these experiments, a system using high-resolution deconvolution microscopy was developed to aid in future binding and entry studies of relevant HCV mutants. We additionally report a recombinant chimeric antibody technique for the delivery of epitopes to antigen-specific T cells. This work highlights the competing forces of viral infection and the immune system, and presents a novel attenuated HCV vaccine candidate.

Binding, entry, and immune escape mechanisms of hepatitis C virus

By

Luke S. Uebelhoer
B.S., Cornell University, 2004

Advisor: Arash Grakoui, Ph.D.

A dissertation submitted to the Faculty of the James T. Laney School of Graduate Studies of Emory University in partial fulfillment of the requirements for the degree of Doctor of Philosophy

Graduate Division of Biological and Biomedical Sciences
Immunology and Molecular Pathogenesis

2011

ACKNOWLEDGMENTS

I am extremely thankful for all the people who have helped and supported me over the past seven years of my graduate studies. First and foremost, I would like to thank my mentor, Arash Grakoui, for his guidance, patience, and scientific training. He gave me the freedom to pursue areas of research which I found interesting, at considerable expense to his funding and mental well-being. His office door was always open to me, and our daily discussions have shaped how I think about experiments and who I am as a scientist. He taught me the importance of proper controls, the importance of hard work, and the importance of personal reputation, and for these things I am grateful. Cheers, my friend.

A special thanks to the members of my thesis committee, Drs. Brian Evavold, Joshy Jacob, Bob Mittler, and Sam Speck. Their experimental input has been invaluable in guiding my research to its full potential. I would like to thank Bob in particular for allowing me full access to his lab without question to purify numerous antibodies.

The members of my lab, both past and present, have been unwavering in their optimism and friendship over the years. Hiro “Tomes” Nakahara, you taught me how to eat like a champion, and introduced me to Rodenbach, the nectar of the gods. Hank “The Tank” Radziewicz, I will always be in awe of your ability to incorporate every experiment you do into a figure, and your choice of titles for manuscripts. Holly, thank you for reading every sentence I have ever written, and for the numerous free samples without which I would be unable to keep my clothes clean and hypoallergenic. Ragi, thank you for the tea and for keeping me sane when we were the only ones in lab at midnight on Fridays.

Victoria, Hannah, Aryn, Bethy, and Sooki, your excellent discussions and ability to carve a liver like a pumpkin make you my honorary Grakoui lab surgeons (and makes this only child feel like he has many sisters). Last but not least, I would like to acknowledge Guaniri “Kelly” Mateu, for without her help I would still be adrift in a sea of useless HCV clones. Thanks for being there for me through the good, the bad, and the ugly.

Throughout my tenure at Emory, I have made more friends than I ever dreamed possible. Pablo Romagnoli, David Loria, Kristen Rosenthal, and Lisa Gargano all deserve special recognition as my greatest supporters. Craig Chappell and Tim Denning proved to me that mentors can be found anywhere, whether it be on a century bike race or on a lazy boat drifting through the waters of South Carolina. I owe a special debt of gratitude to Brian Norris, who was the driving force behind many immunological experiments and a close friend to boot. There is no one I would rather work with in BSL-3 than him.

I am grateful for my loving family, including my mother Gail and my father Bernie who have given me every opportunity to succeed in this world no matter what the cost. I cannot express in words the thanks they deserve. I hope to make them proud.

Finally, I would like to acknowledge my best friend, scientific confidant, partner-in-crime, and Pnut, Ruth Napier. She has been with me through thick and thin, without question or hesitation, and I strive to be her strength as she is mine. Ruth, you are my inspiration. I love you.

TABLE OF CONTENTS

LIST OF FIGURES AND TABLES

Chapter 5

Chapter 6

LIST OF ABBREVIATIONS

APC:	antigen presenting cell
ARFP:	alternate reading-frame protein
BCR:	B cell receptor
CLDN1:	claudin-1
DC:	dendritic cell
DC-SIGN:	dendritic cell-specific intercellular adhesion molecule 3-grabbing nonintegrin
eE2:	ectodomain E2
ELISA:	enzyme-linked immunosorbent assay
GAG:	glycosaminoglycan
HBV:	hepatitis B virus
HCV:	hepatitis C virus
HCVcc:	hepatitis C virus cell culture
HCVpp:	hepatitis C virus pseudoparticle
HDL:	high density lipoprotein
HIV:	human immunodeficiency virus
HLA:	human leukocyte antigen
HVR:	hypervariable region
IFN:	interferon
IRES:	internal ribosomal entry site
ISG:	interferon-stimulated gene
JAK/STAT:	Janus kinase/signal transducer and activator of transcription

JFH-1: Japanese fulminant hepatitis clone 1

L-SIGN: liver-specific intercellular adhesion molecule 3-grabbing nonintegrin

LCMV: lymphocytic choriomeningitis virus

LDL: low density lipoprotein

LDLr: low density lipoprotein receptor

LEL: large extracellular loop

mDC: myeloid dendritic cell

MHC: major histocompatibility complex

NCR: non-coding region

NK: natural killer

OCLN: occluding

ORF: open reading frame

PAMP: pathogen-associated molecular pattern

PD: programmed death

pDC: plasmacytoid dendritic cell

PRR: pattern recognition receptor

rAb: recombinant antibody

RdRp: RNA-dependent RNA polymerase

rE2: recombinant E2

RIG-I: retinoic acid-inducible gene I

RNAi: RNA interference

sE2: soluble E2

SEL: small extracellular loop

siRNA:	small interfering RNA, short interfering RNA, silencing RNA
SR-BI:	scavenger receptor class B type 1
STAT-C:	specifically targeted antiviral therapy for HCV
TCR:	t cell receptor
TLR:	Toll-like receptor
TNF:	tumor necrosis factor
Treg:	regulatory T cell
VLDL:	very low density lipoprotein
VSV:	vesicular stomatitis virus

CHAPTER 1

INTRODUCTION

Hepatitis C virus: a deadly human pathogen

Epidemiology, impact, significance

It is estimated that over 170 million people worldwide are infected with hepatitis C virus (HCV), and although the rate of new infections is rapidly declining, the prevalence of HCV infection is not predicted to decrease in the near future [1]. The global scale of HCV is not well known, owing to the asymptomatic nature of the acute phase of infection. However, it is accepted that approximately 2-4 million individuals are chronically infected in the United States, 5-10 million in Europe, and upwards of 12 million in India. Especially alarming are numerous Middle Eastern and African countries such as Egypt, with HCV prevalence ranging anywhere from 1-12% of the entire population [2]. In fact, HCV has been found in every part of the world where it has been sought, highlighting the virus' successful transmission and persistence in the human population. HCV causes persistent infection in approximately 70% of all documented cases, and can lead to liver failure, portal hypertension, and hepatocellular carcinoma [3,4]. Indeed, infection with HCV has become the leading cause of orthotopic liver transplant in the United States, and a serious burden on our public health. Infection accounts for 40-50% of individuals receiving or waiting for liver transplant, and the rate of viral recurrence is high, often leading to graft loss and retransplantation [5,6,7]. Taking into account that fewer than 5,000 liver transplants are performed every year, HCV confounds our transplantation network by adding a pool of individuals with a low probability of success post-operation. With over 17,000 patients currently awaiting this

operation, the demand for organs vastly outstrips the supply, and this imbalance continues to increase mortality rates across the United States [5]. Virus is transmitted percutaneously or permucosally, and before diagnostic tests had been established, blood products, haemodialysis, and solid organ transplantation were the main routes of transmission [8,9,10,11]. In the current era of screened blood products, intravenous drug users and their sexual partners represent the largest fraction of infected individuals [12]. HCV is becoming uncontrollable in United States correctional facilities, where the rate of infection is more than ten times that of the general population (20-40% versus ~2-3%) [13]. Even more concerning is the fact that approximately 25% of human immunodeficiency virus (HIV) -infected individuals are also infected with HCV, a number that increases dramatically (50-90%) among injecting drug users. These co-infected individuals can have higher HCV titers, and experience a more rapid progression to cirrhosis [14]. Clearly, HCV has taken and will continue to extract a toll on the human species until successful treatment and eradication protocols can be established.

The viral life cycle

HCV is an enveloped single-stranded RNA (ssRNA) virus that is both hepatotrophic and non-cytopathic, belonging to the genus *Hepacivirus* and the family *Flaviviridae* [6]. Virions typically have a short half-life of 3 hours, and viral loads between 10^3-10^7 genomes per ml of serum are common in most patients [15]. These factors combined with a highly error-prone RNA-dependent RNA replication mechanism have generated a remarkably diverse virus, with HCV being grouped into at least six major genotypes comprised of numerous subtypes that exist as a quasispecies swarm inside infected

individuals [16]. HCV particles are thought to be approximately 50 nm in diameter, based on limited imaging data and predictions using analogous flaviviruses [17,18]. The HCV nucleocapsid is composed of copies of the core protein studded with heterodimer pairs of the E1 and E2 glycoproteins, all of which encapsidate the RNA genome [19]. Interestingly, plasma-derived HCV has been shown to associate with both low-density lipoproteins (LDL) and very low-density lipoproteins (VLDL), and infectivity of particles may be enhanced as a result ([20], reviewed in [21]). In general, the infectious life cycle of an HCV virion can be broken down into the following stages. First, binding and entry of the virus occurs in a permissive cell, typically a hepatocyte. This process is mediated by specific molecules on both the cell and virion, and most likely occurs in a stepwise manner. We will devote a comprehensive review to the description of this process, as it pertains directly to work contained herein. Second, the lipid bilayer of the virion fuses with the host endosomal membrane, releasing the positive-sense ssRNA genome into the cytoplasm of the cell. Although this process is not well understood, it is known that a low pH-triggering event is necessary for this step to occur, and a recent publication has postulated that motifs in viral surface molecules may adopt specific conformations to aid in fusion [22]. Third, the newly released genome undergoes direct translation at the endoplasmic reticulum and potentially other membranes, as well as replication through a negative-strand intermediate, followed by packaging into a finished virion assembled from the processed viral proteins. Finally, mature virions bud from the endoplasmic reticulum or associated membranes, and are released from the host cell through traditional secretory pathways to begin the process anew.

Binding and entry

Upon encounter of a permissive cell, the HCV virion undergoes a highly coordinated set of binding interactions with several cellular (co-) receptors that lead to its eventual internalization. It is currently accepted that HCV particles are associated with LDL in infected plasma, and many studies have demonstrated that the LDL receptor (LDLr) is involved in initial HCV binding [20,23,24,25,26]. However, this interaction may be confined to the LDL molecule alone, and the association of HCV with LDL particles is not well correlated with subsequent infectivity [27]. Additional data exists correlating inhibition of HCV pseudoparticle (HCVpp) entry with antibodies to apolipoprotein E (a component of VLDL, [28]), as well as LDL and VLDL [29], but the latter study has yet to be confirmed by others [28,30,31]. During or immediately after lipoprotein-receptor interactions, HCV undergoes a low-affinity interaction with glycosaminoglycans (GAGs) that serves to retain the viral particle at the cell surface and facilitate subsequent high-affinity binding. The highly sulfated forms of these linear polysaccharides permiscuously bind several viruses, and in HCV this process is thought to be mediated by E2, a finding that has been confirmed in our lab using both HCV cell culture (HCVcc) virus and a purified form of recombinant ectodomain E2 (eE2) protein ([23,32,33], see *Chapter 5* for data). Other promiscuous initial HCV binding partners include dendritic cell-specific intercellular adhesion molecule 3-grabbing nonintegrin (DC-SIGN) and liver-specific intercellular adhesion molecule 3-grabbing nonintegrin (L-SIGN), both of which bind soluble E2 (sE2) and plasma-derived HCV [34,35,36]. These receptors are not found on hepatocytes, and most likely mediate *in vivo* trans-infection of HCV. In addition to DC-SIGN and L-SIGN, the asialoglycoprotein receptor has been implicated in early HCV binding, due to its interaction with HCV structural proteins expressed in a surrogate

baculovirus expression system [37]. However, the functional interaction of asialoglycoprotein receptor and HCV has yet to be demonstrated.

Although many receptors have been implicated in HCV binding, the minimal set of factors necessary for infection currently include CD81, scavenger receptor class B type 1 (SR-B1, SR-BI), claudin-1 (CLDN1), and occludin (OCLN). The best studied of these factors is CD81, a 236-amino acid protein containing four membrane-spanning segments, intracellular N- and C- termini, and two extracellular loops (large, CD81LEL; small, CD81SEL) [38]. CD81 was initially implicated as a potential receptor using sE2, and antibodies against both CD81 and the CD81LEL were able to greatly reduce infectivity in HCVpp [28,39,40,41,42], HCVcc [17,43,44], plasma-derived HCV [45], and plasma-derived HCVcc systems [46]. These data were supported by the fact that decreased expression of this molecule by RNA interference (RNAi) results in low permissivity of infection [42,47,48]. In essence, a "threshold" level of this cell surface molecule needed to be present to pass a critical checkpoint in infectivity. The necessity of CD81 in HCV infection was further confirmed using HepG2 cells, an immortalized liver carcinoma line that lacks this molecule and is refractory to HCV infection [49]. When engineered to express CD81, these cells become fully susceptible to both HCVpp and HCVcc infection as determined by luciferase expression and infectious titer assays [42,43,49]. Indeed, complementing this molecule in HepG2 cells results in comparable HCV permissivity to what is seen using Huh-7.5 cells, a derivative of the human hepatoma liver cancer line Huh-7 that has been cleared of self-replicating subgenomic RNA by prolonged interferon (IFN) -α treatment (see *Chapter 1, Model systems to study hepatitis C virus*) [50]. While

antibodies to this molecule inhibit infection, they are unable to inhibit HCVpp and plasma-derived HCV attachment to cells, suggesting that the HCV E2-CD81 interaction occurs after initial virion binding [47,51,52]. CD81 has been implicated in sperm-egg fusion, arguing for a role in fusion of the viral envelope and cell membrane [53]. Despite exhaustive studies, the exact role of CD81 in HCV infection remains a mystery. Even the physiological role of CD81 has yet to be determined. This molecule is part of the B cell receptor (BCR) complex, but does not seem to be essential for the humoral immune response [54]. Additionally, the closest relative to CD81, the CD9 tetraspanin, is unable to mediate HCV uptake. However, chimeric CD9 expressing the CD81LEL can mediate HCV uptake as efficiently as wild type CD81, highlighting the point that motifs in the extracellular loops of this molecule are critical for HCV infectivity, and may represent an attractive candidate for targeted therapies [42]. Because HCV can attach to cells in the presence of anti-CD81 antibodies, it is accepted that this molecule is one of (potentially) many needed for initial infectivity of HCV particles. It is clear that further study of this molecule is needed in both HCV and cellular immunology systems to solidify its role in HCV uptake and infectivity.

A second molecule deemed necessary for initial HCV binding and entry is SR-BI, a 509-amino acid protein that was also identified by sE2 binding screens in hepatoma cell lines [55]. This protein contains two transmembrane domains and intracellular N- and C-termini, and alternative splicing of the SR-BI mRNA can yield a protein in which 42 C-terminal amino acid residues have been replaced by 40 residues encoded by a downstream exon (termed SR-BII, [56]). SR-BI's role in basic physiology makes it a

likely candidate for assistance in initial HCV binding, as it functions in selective lipid uptake, acting as a bridge for cholesterol esters to flow from liver high density lipoproteins (HDL) into receptor-HDL-bound cell membranes [56]. Like LDL and VLDL, HDL enhances both HCVpp and HCVcc entry during infection [30,31,57]. These studies suggest that SR-BI may facilitate HCV entry by enriching the cell membrane in cholesterol, a hypothesis supported by another study demonstrating that cholesterol depletion mildly inhibits HCVpp and HCVcc entry [58]. Like CD81, antibodies to SR-BI and small interfering RNA (siRNA) -mediated downregulation of SR-BI expression results in both HCVpp and HCVcc inhibition, although these results are often variable when using different genotypic clones [41,46,49,58]. Interestingly, plasma-derived HCVcc is equally as susceptible to anti-SR-BI antibodies [46,59]. Unlike CD81 and HepG2 cells, a non-permissive cell line lacking SR-BI has yet to be engineered to express SR-BI and allow for HCV infectivity. However, a very convincing study demonstrated that HCVcc could be bound by SR-BI but not CD81 or CLDN1 when these molecules were overexpressed in Chinese hampster ovary cells [47]. This observation, along with the observation that sE2 directly interacts with SR-BI, has led many to believe that SR-BI may be the primary receptor to which the virus initially binds.

Over the last decade, it has been known that expression of the two previously mentioned candidate receptors is not enough to render cells permissive for HCV infection, and it was hypothesized that other factor(s) may be required [39,49](reviewed in [18]). Recently, two key factors supporting HCV entry have been identified. The first, CLDN1, is a tight-junction protein highly expressed in the liver that was found using an expression

cloning approach [47]. Claudin family members are critical to forming the epithelial barrier at the apical and basolateral membrane compartments, interacting with one another on adjacent cells like zippers to eliminate the intercellular space [60]. CLDN1 is similar to CD81 in both structure (four transmembrane domains, intracellular N- and C-termini) and size (211 amino acids), but shares no sequence homology with the tetraspanin receptor. Indeed, the first large extracellular loop of CLDN1 is similar to the CD81LEL in the sense that both are critical for HCV entry [47]. However, the first extracellular loop of CLDN1 does not bind sE2, HCVcc, or any other viral component yet probed, arguing against a direct interaction between the virus and this molecule. After its identification, overexpression of CLDN1 in the SR-BI- and CD81-expressing 293T (human embryonic kidney) and SW13 (human adrenocortex carcinoma) cell lines rendered these previously refractory cells susceptible to HCV infection [47]. Subsequent silencing of CLDN1 transcripts using siRNA targeting approaches blocked HCV entry in the normally permissive Hep3B and Huh-7.5 cell lines. Despite this molecule's lack of direct HCV interaction (or interaction with an unidentified intermediate factor), it seems that CLDN1 acts as a late-stage entry co-factor, downstream of CD81 and SR-BI. This hypothesis has been supported by a recent study demonstrating that adjacent cell spread of HCV is dependent on CLDN1 but not CD81 [61]. Interestingly, additional claudin molecules (CLDN6, CLDN9) have been implicated in HCV infection, strengthening the idea that a late stage HCV-claudin interaction may lead to internalization near or at liver epithelial tight junctions [62]. The second key factor in HCV entry was recently identified by two groups as another tight junction protein, OCLN. One group used an siRNA approach to target specific molecules implicated in polarized cell infection by

group B coxsackievirus [63], while the other group used an elegant cyclic retrovirus-based repackaging screen combined with a reductionist approach employing several permissive and non-permissive cell lines [64]. Both studies demonstrate that downregulation of OCLN results in ablation of HCVpp and HCVcc infectivity. Interestingly, Liu *et al*. show that infection of Huh-7 cells with HCVcc downregulates OCLN, preventing superinfection and possibly contributing to morphological changes seen in HCV-infected hepatocytes. Ploss *et al*. additionally demonstrate that overexpression of the human forms of CD81 and OCLN along with murine or human forms of SR-BI and CLDN1 break a species barrier, rendering several types of non-human cells permissive for HCVpp entry. Furthermore, these experiments solidify the idea that four factors, human CD81, SR-BI, CLDN1, and human OCLN, are absolutely required for HCV infectivity. Because of their association with tight junctions, we can extrapolate that a spatial and temporal relationship exists between CLDN1 and OCLN. These two recently identified cell-specific factors are likely the last to interact with an HCV particle before its ensuing endocytosis.

Fusion and uncoating

Currently, very little is known about how HCV undergoes membrane fusion and releases its genome contents once endocytosis has occurred. Through the use of siRNA targeting and the drug chlorpromazine, both HCVpp and HCVcc have been shown to be internalized via clathrin-coated vesicles in hepatoma cells [65,66,67]. Proteinase-K protection experiments further demonstrated that HCV endocytosis is relatively slow, with half of HCVpp reaching protected compartments by 53 min. By comparison, membrane fusion usually occurs in this same system by 73 min, indicating a significant

delay between initial internalization and end-stage fusion [66]. Furthermore, treating cells with drugs known to inhibit endosomal acidification ablated HCVpp and HCVcc entry, suggesting that HCV most likely utilizes an endosomal pathway, and that fusion is an acid-triggered event [28,39,65,66,68]. This hypothesis was confirmed using acidic environments of pH 5-5.5 to trigger membrane fusion events [69]. Additional experiments utilizing Rab5 or Rab7 dominant-negative cell lines further narrowed the HCV entry pathway to early, but not late, endosomes [66]. Because of the protected nature of the endosomal compartment, it remains unknown whether any HCV co-receptors accompany the incoming virion in the endosome. Perhaps the most interesting observation is that HCVcc infectivity prior to internalization is pH-insensitive, indicating that a post-binding "priming" event may prepare the virion for membrane fusion [51,66,68]. Our lab and others have hypothesized that this event may depend on a restructuring of the E2 glycoprotein at the surface of the virion (potentially in concert with a bound co-receptor), allowing for direct insertion of the genome into the host cell cytoplasm [22] (see *Chapter 3, Discussion*).

RNA replication, genome translation, processing

Once released into the host cell cytoplasm, the incoming 9.6 kilobase positive-sense ssRNA undergoes cap-independent translation from a single open reading frame (ORF) to yield a polyprotein precursor of approximately 3,000 amino acids. Translation is initiated from an internal ribosomal entry site (IRES) found in the 5'-noncoding region (NCR) of the genome, which is highly conserved among HCV genotypes and organized into four separate domains based on unique RNA secondary structures (domains I-IV, [70]). Although domain I is not essential for IRES activity (domains II-IV and the first

24-40 nucleotides are essential), domains I and II are critical for RNA replication [71]. The HCV IRES is bound by the 40S ribosomal subunit with such high avidity that initiation factors are not needed, and the subunit adopts an mRNA-bound conformation [72]. After initial subunit binding, eukaryotic initiation factor 3 is recruited along with the Met-tRNA-eIF2-GTP complex to form a 48S intermediate, followed by a kinetically slow transition to the 80S active complex [73,74]. The amino-terminal one-third of the polyprotein encodes the HCV structural proteins, which include the core (C) protein that assembles the viral nucelocapsid and the E1 and E2 glycoproteins that decorate the mature viral particle. A putative ion channel protein, p7, follows the structural proteins, while the remainder of the genome encodes the nonstructural proteins NS2, NS3, NS4A, NS4B, NS5A, and NS5B which orchestrate the intracellular life processes of HCV. The RNA genome terminates with a 3' -NCR consisting of (in 5'-3' direction) i) a short variable sequence, ii) a poly(U/UC) tract of approximately 80 nucleotides, and iii) a highly-conserved 98 base pair HCV-specific sequence (referred to as the "X-tail") [75,76]. While deletion of the variable sequence impairs replication, only 26-50 nucleotides of the poly(U/UC) tract are needed for efficient cell culture replication, suggesting that this region may act as a spacer to facilitate interactions of the 3' -NCR with the replicase machinery [77,78]. In support of this hypothesis, a cis-acting replication element was discovered in the C-terminal region of NS5B (specifically a stem-loop, termed 5B-SL3.2) that assembles a pseudoknot with a stem-loop in the X-tail region and is essential for RNA replication [79]. The X-tail consists of three stem-loop structures, one of which is highly stable (3' SL1) and two of which are metastable (3' SL2, SL3), and this entire region is required for *in vitro* replication and *in vivo* infectivity

[77,78,80,81]. Although the role of the 3' -NCR in translation remains controversial, it is likely that this region has essential function in direct de novo initiation of minus-strand RNA synthesis. During and after cap-independent 5'-IRES-mediated translation, the structural and p7 proteins are processed by the endoplasmic reticulum signal peptidase and signal peptide peptidase, while the nonstructural proteins are processed by the NS2-3 protease (traditionally referred to as the "autoprotease") and the NS3-4A serine protease (see [70] and [82] for excellent diagrams and reviews).

The core protein of HCV is an alpha-helical protein that forms the viral nucelocapsid and has been found in numerous locations throughout infected cells, including the endoplasmic reticulum, the membranous web (active HCV replication sites, discussed below), and in association with lipid droplets [83]. An internal signal sequence between core and E1 targets the nascent proteins to the endoplasmic reticulum, ensures their proper orientation on the cytoplasmic (core) or lumenal (ectodomain E1) surfaces, and is cleaved by host signal peptidase to release E1 and yield an immature form of core. Core undergoes further C-terminal processing by host signal peptide peptidases, resulting in the mature 21-kDa protein of 173-179 amino acids [84]. Aside from being critical for mature particle formation, the core protein has three peculiar features. First, a concentration of basic amino acid residues is found in the amino-terminal hydrophilic region of core, and has been implicated in both RNA binding and homo-oligomerization [70]. Second, the association of the central hydrophobic region of this protein with lipid droplets may impact virion morphogenesis, and emerging data suggests that this association may account for HCV-related steatosis that is common in genotype 3-infected

patients [85]. Third, initiation of translation is often imprecise in genotype 1a viruses, leading to altered versions of the core protein. A -2+1 ribosomal frameshift has been documented, resulting in a ~160 amino acid protein termed alternative reading frame protein (ARFP) or F (frameshift) protein [86]. Although the ARFP/F version of core is dispensable for HCV RNA replication *in vitro* and *in vivo*, T cells and antibodies to this protein have been detected in HCV patients suggesting that it is expressed during infection [87].

The HCV envelope glycoproteins E1 and E2 are the building blocks of the viral envelope, and play an important role in early binding and entry events. As they are exposed to the host environment, these proteins are also critical determinants of the host immune response. Like most viral envelope glycoproteins, E1 and E2 are thought of as dynamic proteins both in sequence and in function: they contain regions with high mutation rates, and may undergo dramatic conformation changes at precise times in the viral life cycle to aid in attachment, membrane fusion, and genome release. Studying these proteins has traditionally been difficult, due to a lack of an efficient HCVcc system. Instead, transient cell culture expression and surrogate model systems were used to initially characterize E1 and E2 [88]. It was not until the development of pseudotyping systems combining retroviral particles and native HCV glycoproteins that the full biogenesis of these proteins could be appreciated (see *Chapter 1, Model systems to study hepatitis C virus*). Cleavage at the core/E1 junction was previously discussed, and complete cleavage of the E1/E2 junction also occurs by host signal peptidases. Partial cleavages occur at E2/p7 and p7/NS2 sites (discussed below), and while NS2 is quickly

liberated from the E2p7NS2 intermediate, E2p7 separation is often incomplete, resulting in finished products that include E2, E2p7, p7, and NS2 [89]. When fused to reporter proteins, the signal peptides located immediately to the N-terminal side of the E2/p7 and p7/NS2 cleavage sites are efficiently cut, indicating that the partial cleavage seen during HCV polyprotein processing is not due to suboptimal signaling [90]. Instead, this delayed processing may serve to sequester E2, p7, or NS2 proteins until they are needed. Deleting the C-terminal hydrophobic regions of both E1 and E2 results in their secretion, confirming signal sequence-mediated endoplasmic reticulum retention data and the role of these regions in membrane anchoring [91,92,93]. The topology of these C-terminal transmembrane domains was unknown for a long time, with both single- and double-spanning models proposed [94,95,96]. Elegant experiments tagging both E1 and E2 with epitopes and tracking their accessibility before and after signal sequence cleavage in selectively permeabilized cells revealed that the transmembrane domains undergo a dramatic conformational change during processing [97]. Before cleavage, these domains adopt a hairpin structure, bending away from the cytosolic side of the endoplasmic reticulum to face the lumen. After cleavage, the hairpin snaps away from the lumenal face, forming a single membrane pass oriented towards the cytosol (see Figure 1 in [89]).

The amino-terminal ectodomains of E1 and E2 reside in the lumenal space of the endoplasmic reticulum, and are heavily modified post-translationally by N- and O-linked glycans that aid in protein folding, transport, function [98]. Additionally, these glycans may modulate the immune response by shielding exposed functional domains from neutralizing antibodies, a phenomenon that has been well documented in HIV-1 infection

[99]. E1 possesses up to 6 potential N-linked glycosylation sites, 5 of which are highly conserved across all HCV genotypes, and 4 of these 5 have been shown to be occupied [100,101,102]. 9 of 11 potential N-linked sites in E2 are similarly conserved, with the remaining 2 showing some degree of conservation (75% for N5 and 89% for N7) [101,102]. All 11 sites in E2 have repeatedly been shown to be occupied [98,103,104]. Both HCV glycoproteins are inextricably linked, forming noncovalent heterodimers at the surface of the virion [105]. Amazingly, the proper folding of E1 is dependent on E2 coexpression and vice-versa, although a small degree of E2 folding can be achieved without E1 [106,107,108,109]. Proper folding occurs slowly, dependent on an interaction with calnexin and most likely other endoplasmic reticulum chaperones [110]. Data on whether E1 alone or the E1E2 complex interacts with calnexin is conflicting, but this chaperone's affinity for monoglucosylated N-linked oligosaccharides suggests that glycosylation patterns in HCV glycoproteins are critical for proper folding [111]. This has been confirmed using a HepG2 E1 mutant expression system [100], pseudotyped retroviral particle infectivity [104], and cell-binding assays with purified recombinant eE2 protein (*Chapter 4, Supplementary Figure 4*).

The presence of the E1E2 complex at the surface of the viral particle makes it the most likely candidate ligand for host cell receptors. The HCV E2 glycoprotein itself has received much attention, owing to its initial discovery as a direct binding partner of both CD81 and SR-BI. The CD81 binding residues of E2 have been deduced through reverse epitope discovery using antibodies that block the CD81-E2 interaction, and map to discrete segments localized to a single domain [39,112,113,114,115]. Another interesting

feature of the E2 protein is a 27 amino acid stretch of mostly basic residues located at the N-terminus, called the hypervariable region 1 (HVR1) [116]. As its name implies, HVR1 evolves rapidly in HCV-infected patients, presumably because it is a primary target of the host immune system [117,118]. However, despite this pressure, HVR1 manages to retain its conformation and chemicophysical properties. Studies have shown HVR1 to be linked to HCVpp and *in vivo* infectivity, and it is hypothesized that an indirect association may exist between this region and a host molecule involved in HCV entry [31,49,119]. Additional E2 conformation-dependent and -independent targets exist outside of HVR1, including three immunogenic domains that have been elucidated through characterization of HCVpp with monoclonal antibodies [120,121]. Tremendous effort has gone into determining the crystal structure of HCV E2, and all attempts thus far have been unsuccessful, presumably due to its intimate association with both E1 and the endoplasmic reticulum. The ectodomain of E2, which has been mapped to the first 334 amino acids, contains 18 cysteines that (potentially) contribute to 9 intramolecular disulfide bonds [106]. It has been proposed that these cysteines may also pair with the 8 absolutely conserved cysteines in the ectodomain of E1, forming complexes via intermolecular bonds that appear as high molecular weight aggregates on SDS-PAGE gels [122] (G. Mateu, L. Uebelhoer, et al., unpublished results). Indeed, aggregation is so common in E2 expression systems that a non-productive folding pathway is now accepted as a physiologically relevant part of the HCV life cycle [123]. Recently, an excellent system for the production of significant quanitites of non-aggregated eE2 using human cells was developed [122]. Subsequent experiments determined the oligomerization state, glycosylation pattern, and secondary structure of this molecule. In

this system, eE2 to exists mostly in dimeric (60-70%) and monomeric form, with a very small population of trimers. Circular dichroism spectroscopy revealed a secondary structure of mostly beta sheets and random coil, and this study also convincingly demonstrated evidence of disulfide bonding between the 17th and 18th cysteine of eE2. Following this work, a group has recently proposed the tertiary organization of the HCV E2 using an expression system in *Drosophila melanogaster* cells [22]. Using a structural template from related flavi- and alphaviruses, researchers were able to incorporate data from circular dichroism, infrared spectroscopy, and previously known CD81 binding regions along with reported E2 deletion mutants to fashion a model of E2 as a class II fusion protein [22]. This remains controversial, as others have suggested that HCV E1 may contain a fusion peptide in its ectodomain [124,125]. Currently, only two classes of viral fusion proteins are known. Class I fusion proteins are synthesized as a precursor before being cleaved by host cell proteases into a metastable state, forming trimeric spikes that transiently extend upon a triggering event to insert an alpha-helical fusion subunit into the target membrane, inducing hemifusion between host and viral membranes (*e.g.* influenza HA, HIV Env) [126,127]. Class II fusion proteins are quite different, containing mostly beta-sheet secondary structure making up three separate domains with an internal fusion peptide in a loop conformation [126]. These proteins are normally synthesized in complex with another glycoprotein (prM for flavirivurses; pE2 for alphaviruses), and fusogenic potential is activated by cellular endoproteases as the mature virion exits the cell through the secretory pathway. By these standards, it is difficult to label one or both of the HCV glycoproteins as the viral fusion candidate, as neither are matured by cellular endoproteases during their export from the cell [128].

Additionally, both HCV glycoproteins contain many glycans, whereas other described class II fusion proteins do not. Krey *et al*. have proposed that the fusion peptide loop resides in domain II of E2, but further functional studies are needed to support this model. Regardless, it is clear from decades of research on binding, entry, and fusion that both E1 and E2 glycoproteins play a critical role in the HCV life cycle.

The p7 protein of HCV represents perhaps the greatest enigma of the viral genome. Nestled between the structural and nonstructural proteins, p7 has yet to be classified in either group because little is known about this small (63 amino acid) polytopic protein. Often incompletely cleaved from E2, p7 is restricted to the endoplasmic reticulum via two transmembrane domains and intraluminal N- and C-termini with genotype-specific functions [129,130]. The greater function of p7 remains a mystery, although studies have reported it as an oligomeric cation channel [131,132]. Interestingly, this protein is not required for *in vitro* RNA replication, but is indispensable for productive infection in chimpanzees [130]. Further studies are needed to elucidate the contribution of p7 to the overall viral life cycle, but if it is indeed a member of the viroporin family, it may represent an attractive target for future antiviral drugs.

The NS2 and NS4A proteins both share function with the interceding NS3 protein. Operating in concert, the C-terminus of NS2 and the N-terminus of NS3 form an autoprotease that serves to liberate these proteins at their juncture. Proteolytic activity is further dependent on amino acids His143, Glu163, and Cys184, as determined by site-directed mutagenesis studies [133,134]. The NS2 protein is peculiar in the sense that two

monomers of NS2 make up the active site, with one monomer supplying residues His143 and Glu163 and the other supplying Cys184 [135]. Because dimerization is necessary for NS2-3 autocleavage, one can hypothesize that NS2 concentration represents a rate-limiting step in formation of an active HCV replication complex. Like all HCV proteins, NS2 is associated with intracellular membranes. However, the number and nature of its N-terminal transmembrane segments remain unknown, although deletion studies have shown them to be dispensable for enzymatic activity [136,137]. The protein is necessary for the complete HCV replication cycle, and it was recently discovered that chimeric genotype swapping in this region yields high titers of HCVcc virus [138,139]. These results are intriguing, because similar intra- and intergenotypic chimeras have been identified in HCV patients [140,141]. These observations, combined with its role in polyprotein cleavage and replication complex formation, suggest that NS2 is critical both during early establishment of infection and at later steps in the viral life cycle.

Unlike NS2, NS4A is more dependent on NS3, functioning as a dedicated cofactor for serine protease activity. The N-terminal portion of NS4A serves to tether the NS3-4A complex to intracellular (presumably endoplasmic reticulum) membranes and increase the mean protein half-life, while the central portion of NS4A functions in the enzymatic core [142]. In collaboration with NS4A, the amino-terminal one third of NS3 makes up the rest of the serine protease. This HCV-specific enzymatic complex has been the target of small molecule and substrate-based inhibitors, with the assumption that ablation of proteolytic function would halt further genomic processing [143,144]. Many determinants of substrate specificity exist, with the catalytic triad of His57, Asp81, and

Ser139 recognizing both cis- and trans-cleavage sites (see [70] for review). Recent data has also ascribed anti-host-immune function to this protease complex, which has changed the way the field thinks about the host-pathogen interface during HCV infection (described in detail in *Chapter 1, Hepatitis C virus and the host immune response, Innate immune response and viral evasion*). Although it serves as a functional partner for both NS2 and NS4A, NS3 also has a critical independent function as a superfamily 2 DExH/D-box RNA helicase/NTPase. The C-terminal two thirds of NS3 functions to unwind dsRNA or ssRNA forming secondary structures, and couples this process to ATP hydrolysis. The unwinding process is analogous to cytoskeletal motor proteins, proceeding along the duplex substrate by quickly unzipping and then pausing at regular intervals of approximately 11 base pairs (known as "fast ripping" and "local pausing", [145,146,147]). It remains unknown why the HCV NS3 proteolytic and helicase domains are physically linked, but emerging data suggests that these two enzymatic activities are inextricably linked in function during the viral life cycle [148]. The necessity of the NS3 helicase and its association with foreign RNA species may make this protein an attractive target for host immune responses, a hypothesis supported by numerous studies documenting extensive cytotoxic T lymphocyte (CTL) epitope escape mutations in this region (see *Chapter 2* for review).

Currently, little is known about the HCV protein NS4B, other than its predicted topology and potential involvement in the viral replication complex. This protein is thought to contain four transmembrane regions, is palmitoylated at two C-terminal cysteine residues, and may form oligomers [149]. Using tetracycline-regulated cell lines expressing

different combinations of HCV proteins, one group has shown that expression of NS4B alone is sufficient to induce a compact intracellular vesicular structure, termed "membranous web" [150]. In this expression system, all HCV proteins tested localized to this area, suggesting that this web may actually be the HCV replication complex. Further studies into the nature of NS4B oligomerization and its role in HCV replication may yield interesting clues as to how the virus assembles and buds at intracellular surfaces.

NS5A is a monotopic phosphoprotein with an N-terminal amphipathic alpha-helix buried in-plane at the cytosolic leaflet of the host membrane bilayer, serving to anchor three distinct domains that face outwards into the cytosol [151]. This anchoring is possible due to alternating hydrophobic charges (mainly tryptophan residues) facing into the bilayer and polar charges facing outwards toward the cytosol [152]. The crystal structure of domain I has been solved, and forms a claw-like dimer with a groove that has been hypothesized to accommodate RNA, cellular proteins, and membranes [153]. Indeed, biochemical analyses have shown NS5A to have RNA-binding properties, allowing researchers to hypothesize that multiple NS5A proteins may form a two-dimensional lattice that serves to shuttle RNA through a highly basic cleft while acidic residues higher towards the tip of the dimers prevent bound molecules from exiting the groove [154]. This is an attractive hypothesis for many reasons. First, by creating a tunnel through which genomic material can be shuttled, the protein may protect nascent HCV RNA from cellular RNAse degradation or pathogen-associated molecular pattern (PAMP) -based immune attack. Second, because budding of newly formed virions is dependent on an excess of core to form nucleocapsids, this shuttling system may hold the newly created

genome at membrane surfaces for immediate packaging and delivery to secretory routes. Finally, it has been demonstrated using HCV replicon systems that only a small proportion of nonstructural proteins are actively involved in RNA replication [155,156]. This accumulation of proteins, especially ones such as NS5A that form recognizable repeating structures, may serve as PAMP-like decoys to draw the host innate antiviral response away from actively replicating RNA complexes.

HCV is a positive-strand RNA virus, and genome replication proceeds via a negative-strand intermediate that serves as a template for positive-strand amplification. The NS5B protein is the replication workhorse of the virus, functioning solely as an RNA-dependent RNA polymerase (RdRp) to create both positive- and negative-strand transcripts. Post-translational mechanisms target 21 amino acids in the C-terminus of this protein to membranes, and oligomerization is necessary for cooperative RNA synthesis activity [157]. The crystal structure of NS5B has been characterized as a classic right-handed RdRp, with palm, fingers, and thumb subdomains that close to form the active site of RNA replication [158,159,160]. Like most RdRps, extensive interactions of the thumb and fingers subdomains create a highly structured enclosed enzymatic site [161]. NS5B contains the classical GDD sequence within motif C, which is absolutely conserved across HCV genotypes and additionally across select nonstructural proteins of all known positive-strand RNA viruses. We and others have shown that alteration of this sequence leads to severe replication defects in numerous HCV model systems, and mutation of the GDD motif serves as a negative control in most of the replication-sensitive assays described in this thesis.

Although translation of the HCV genome occurs rather simply from a single ORF and produces a single polyprotein, the actual assembly of the viral replication complex is a complicated, multistep process. HCV, and indeed all positive-strand RNA viruses, form replication complexes involving a coordination of post-translational processing events and associations of viral proteins, altered membrane compartments, and replicating RNA. The nature and function of membranes and the membranous web in HCV replication complexes remains poorly understood, but several ideas have been proposed. These include, but are not limited to, i) shepherding viral products into discreetly organized environments for ease of complex formation [162], ii) providing a supporting framework for complexes [163], iii) shielding nascent viral RNA from host factors or immune responses, and iv) donation of necessary lipid constituents to the complex. Current studies are targeted at determining host factors that may be involved in replication complex development, and several novel interactions have already been found, including a cyclophilin B-induced stimulation of NS5B RNA-binding and an FKBP8/Hsp90 association with NS5A that may alter HCV RNA replication [164,165]. The HCV viral proteins and the host involvement in HCV replication will likely remain intense areas of research, as both offer many unique targets for pharmacological manipulation and therapeutic intervention.

Virion maturation and egress

Along with fusion and uncoating, the latter stages of HCV assembly and exit are poorly understood. Thanks to recent developments in HCVcc systems, the complete life cycle of the virus is able to be studied, and many new observations have been made regarding host

or viral determinants for virion production, as well as the biophysical properties of secreted virions. The host cell environment is known to be critical for virion release, with clonal derivatives of Huh-7 cells producing higher titers of HCVcc JFH-1 than the parental Huh-7 line [43,44]. Conversely, the virus itself can affect production, with different chimeric genotype 2a-matched clones producing higher titers than the parental JFH-1 virus [43,139,166]. Merely culturing the JFH-1 virus for prolonged periods of time in permissive cells results in an increase in infectious particle titers, which may reflect either an adaptation to the culture environment, or a correction of a previous unidentified replication defect inherent to this viral clone [44,167]. Additionally, assembly and egress of infectious particles may be intimately linked to the NS2 protein, a feature reminiscent of classic flaviviruses and pestiviruses. Extensive full-length HCV chimeric genotype construction has hinted that forced interactions (due to an optimized polyprotein breakpoint) between the N-terminus of NS2 and structural proteins, as well as the C-terminus of NS2 and the replicase region may influence virion assembly [139]. Currently, an intense area of research in HCV egress revolves around the association of secreted particles with VLDLs. Inhibition of pathways necessary for apolipoprotein B and microsomal triglyceride transfer protein production results in a decrease of infectious HCV particles [168]. Simple buoyant density analysis of intracellular versus extracellular virions yields differing results, with intracellular HCV sedimenting at 1.15-1.20 g/ml and extracellular at 1.03-1.16 g/ml [169]. Additionally, our lab and others have utilized sucrose density gradients to demonstrate that lower density fractions remain highly infectious, despite apparently low levels of HCV RNA (see *Chapter 3, Figure 3*) [43]. A recent publication has also shown that HCV core protein associates with both early and

late endosomes during egress-specific timeframes, but not mitochondria or peroxisomes [170]. Although research on late-stage HCV assembly and egress is still in its infancy, it is clear from recent data that the virion undergoes a density shift and matures as it is transported out of the cell, presumably via classical secretory pathways.

Current and future therapies

Worldwide, hundreds of millions of individuals are infected with HCV, and at present a cure is not available. Current therapies are not optimal, and the development of new therapies has traditionally been hampered by the lack of a high quality testable *in vitro* model as well as the very nature of the virus, which has proven an excellent survivor under even the most strict drug regimens. Although outside of the scope of work presented in the following chapters, the development of novel antivirals is an area of intense research with high potential future impact, and as such warrants a short review.

Well before identification of the virus, IFN-α therapy was known to have beneficial effects in chronic HCV patients [171]. After diagnostic tests had been established, IFN-α therapy was shown to cause a rapid decline in serum HCV RNA levels, and more surprisingly sustained this decline over time in both serum and liver of patients who resolved chronic infection [172]. This potent antiviral activity is not due to direct virus or replication complex interaction, but rather to the induction of IFN-stimulated genes (ISGs) involved in multiple cellular processes including lipid metabolism, apoptosis, protein degradation, and inflammation [173]. This induction leads to the establishment of an antiviral state in the cell that is not specific for HCV [174,175]. However, treatment

with IFN-α alone only elicited a 6-12% or 16-20% response rate dependent on 6-month or 12-month administration, respectively [176]. IFN-α monotherapy has since undergone two significant advances. First, the addition of ribavirn, a broad-spectrum guanosine analogue antiviral agent, has more than doubled the sustained antiviral response rate to 35-40% [177]. Although the mechanism(s) by which ribavirin augments the response rate to IFN is unknown, several ideas have been proposed with experimental support, including misincorporation of a phosphorylated form of ribavirin into nascent viral RNA, inhibition of inosine monophosphate dehydrogenase leading to depletion of GTP, increasing HCV genomic mutation frequency, alteration of the Th1/Th2 CD4+ T cell response, and stabilization of intracellular mediators of IFN activity (reviewed in [178]) [179,180,181,182,183,184]. Second, the covalent attachment of polyethylene glycol to recombinant IFN-α has improved the pharmacokinetic profile of the drug and further increased its half-life [185,186,187,188]. Combined, the current regimen of 24 or 48 weeks pegylated-IFN-α with ribavirin yields sustained response rates of 54-56% [189,190,191]. Although this is encouraging, this statistic does not include those with co-morbidities that often accompany HCV infection [192]. Approximately 50% of those treated still remain unresponsive to therapy, most likely due to numerous competing host and viral factors (see [178] for an overview). Perhaps most significantly, combination therapy is very expensive and associated with severe side effects due to the induction of a systemic antiviral state. Clearly, modulation of existing HCV therapies as well as novel approaches to combat infection are needed.

There are currently hundreds of compounds and therapies for HCV in various stages of clinical trials. The most promising new class of drugs for therapeutic intervention is "specifically targeted antiviral therapy for HCV" (STAT-C), which is made up of numerous compounds that target viral proteins or functional epitopes. The NS3-4A protease and the NS5B RdRp have emerged as the most popular targets of STAT-C. The protease inhibitors have been developed to be preferentially targeted to the active site of the viral enzyme by inclusion of specific moieties. The first of these inhibitors, BILN2061 (Ciluprevir; Boehringer Ingelheim), showed impressive dose-dependent effects, exceeding a 2-$\log_{10}$ reduction in viral load at higher administrated concentrations [144,193]. Unfortunately, this compound was abandoned after apparent cardiac toxicity in laboratory animals [194]. Another promising protease inhibitor is VX-950 (Vertex/Mitsubishi), which is targeted to the HCV NS3-4A active site through inclusion of an α-ketoamide and is well-tolerated with outstanding antiviral activity (reviewed in [1]). However, both BILN2061 and VX-950 have been shown to develop cross-resistance through single amino acid mutation in HCV, suggesting that such compounds may have limited clinical efficacy [195]. Drugs targeting the NS5B RdRp include both nucleoside analogues (NM283/Valopicitabine, others) and non-nucleoside inhibitors (JTK-103, Japan Tobacco; HCV-796, ViroPharma/Wyeth; others). Nucleoside analogues act as "chain terminators", stopping synthesis of viral RNA by misincorporation into the nascent RNA molecule by the polymerase, whereas non-nucleoside inhibitors are thought to block a conformational change in the RdRp needed for initiation of RNA synthesis [196]. In addition to STAT-C candidates, several other approaches are in the developmental pipeline for HCV therapy. Synthetic nucleic acids, such as ribozymes,

antisense oligonucleotides, and siRNAs, may represent an effective alternative to the previously mentioned inhibitors by directly targeting the viral genome [197,198,199,200,201,202]. The success of these agents will depend heavily on their *in vivo* delivery method(s), the specific genomic target, and the ability of HCV to engender mutational resistance to such compounds (which has been shown for an siRNA approach, [203]). In recent years, the most interesting new approaches to anti-HCV drug development have focused on the host rather than the virus. Building on decades of IFN-based antiviral research, novel immunomodulatory agents and host-targeting compounds have entered clinical trials with the hope of aiding the native immune response while avoiding resistance that all too commonly arises during traditional HCV therapy. Synthetic agonists of Toll-like receptors (TLRs) 7 and 9 (ANA245/Isatoribine, Anadys Pharmaceuticals; Actilon/CpG-10101, Coley Pharmaceutical Group) have already shown much promise by stimulating an antiviral response directly, through type 1 (α and β) IFN-producers such as plasmacytoid dendritic cells (pDCs), and indirectly, through secondary effects on adaptive immunity, such as antigen-presenting cell (APC) and natural killer (NK) cell maturation [1,204]. These and other immunomodulatory approaches operate on the assumption that restoration of aberrant innate and adaptive immune responses in HCV-infected individuals will have a significant impact on control of viremia, and may complement therapies that seek to directly target the virus [205]. With the recent development of a novel HCVcc system (see *Chapter 1, Model systems to study hepatitis C virus*), new antiviral candidates against all viral proteins and many human molecules can be further screened before entering chimpanzee or human clinical trials, increasing confidence of safety and *in vivo* efficacy. For excellent reviews on

current and upcoming HCV drugs/therapies, please refer to [1,206,207] and the website http://clinicaltrials.gov.

Model systems to study hepatitis C virus

Initial approaches: biochemistry and chimpanzees

Since the breakthrough cDNA cloning of the agent responsible for non-A non-B hepatitis in 1989, researchers have fought an uphill battle in the study of HCV, owing in large part to the inability of the virus to grow in primary or immortalized cell lines. Additionally, HCV exhibits an extremely narrow host range, with chimpanzees and humans representing the only well-studied *in vivo* animal models. There are clear ethical and cost considerations associated with both of these hosts, and as such the history of HCV model systems is a winding road involving many imperfect methods, each designed to build upon previous knowledge to garner as much information on the viral life cycle as possible. The first experiments performed simply tried to demonstrate replication of the newly found agent in cell culture, to no avail [19]. Almost a decade passed until a highly conserved 3' RNA sequence element was shown to be an integral part of the viral genome, and the first full-length functional cDNA clones could be constructed containing what is now known as the 3'-NCR [75,208]. In lieu of a suitable cell culture system to monitor viral RNA replication, chimpanzees were intrahepatically inoculated with these clones to demonstrate that HCV RNA transcripts alone were adequate to cause disease in animals [208]. Indeed, most of what was known about HCV genome structure, proteolytic processing, protein topology, and protein function at the time was deduced through a tour-de-force effort employing surrogate biochemical methods.

Subgenomic and full-length replicons

The first major breakthrough in studying the replication of HCV came in 1999, with the advent of a subgenomic genotype 1b replicon system that allowed for metabolic radiolabeling of viral RNA and proteins [209]. This replicon was a bicistronic RNA under the translational control of two separate IRES elements. The first cistron consisted of a neomycin phosphotransferase gene under the control of the 5' HCV IRES, while the second cistron consisted of the minimal necessary HCV replicase proteins NS3-5B under the control of a heterologous IRES from encephylomyocarditis virus. Following electroporation of subgenomic RNA into human hepatoma cell lines, replication produces the selectable gene product, allowing transduction of G418 drug-resistance as an indirect readout of replication efficiency. This replication was, on the whole, inefficient, but it paved the way for further advances that immediately followed. Replicon-transfected Huh cells cured by IFN-α treatment were subcloned to establish lines highly permissive for HCV RNA replication [50]. One particularly useful clone isolated in this screen, termed Huh-7.5, harbors a defect in the retinoic-acid inducible gene I (RIG-I), known to be involved in several antiviral pathways [210]. This clone has been invaluable in the development of model systems, as well as studies of the immune response to HCV (discussed in *Chapter 1, Hepatitis C virus and the host immune response*). By parsing out different replicon-transfected cell clones, researchers were able to identify a number of adaptive mutations in nonstructural genes that greatly enhanced replication of viral RNA [211,212]. Soon after this, adaptive mutations were found that rendered genotypes 1a and 2a replication-competent, and greater knowledge of the replicon life cycle allowed for

expansion of this system into other hepatic and non-hepatic cell lines [70,213]. Indeed, the replicon system has become so well established that numerous reporter genes can be employed across the genome, including an insertion of green fluorescent protein in HCV NS5A that allows for tracking of functional HCV replication complexes in living cells [214]. However, no matter how malleable, full-length HCV replicons were unable to yield infectious virus despite robust RNA replication [213,215,216].

Glycoprotein expression systems, vesicular stomatitis virus-pseudotyping, virus-like particles

The failure of virion production using full-length adaptive mutation-containing replicons was perplexing, and it was postulated that either i) necessary host factors were lacking, or ii) the adaptive mutations required for efficient replication were interfering with some phase of the viral life cycle, most likely genome packaging, particle assembly, or egress. In the meantime, parallel surrogate systems were being developed, each with their own pros and cons. Soluble forms of the HCV E2 glycoprotein were produced using C-terminal truncations previously shown to be critical in membrane tethering [38,55,106,112]. These sE2 molecules proved invaluable in probing the virus-cell interactions, and led to the discovery of two previously unknown putative receptors, CD81 and SR-BI [38,55]. Unfortunately, the expression of sE2 in complex with truncated sE1 led to misfolding issues, production of properly folded sE2 was inefficient, and concentrations of secreted protein used in assays did not necessarily reflect an *in vivo* viral infection [106]. A lingering concern throughout these experiments was that sE2 was produced in non-human cell lines, which may have affected glycosylation or

oligomerization patterns of these sE2 molecules. It would take another decade of research before sE2 could be produced in sufficient quantity using human cells, but the codependency of the HCV glycoproteins and the reluctance of sE1 to follow suit remains a current issue even today [122]. Other attempts at studying the envelope glycoproteins included cell surface expression of chimeric E2 fused to the cytoplasmic and transmembrane domains of influenza HA and E1-E2 liposomes [97,124]. The first successful attempts towards construction of complete viral particles involved vesicular stomatitis virus (VSV) pseudotyping schemes where the ectodomains of HCV E1 and E2 were fused to the VSV G glycoprotein, producing VSV particles with functional surface E1-E2 complexes [217,218,219]. The E1 and E2 glycoproteins were also expressed on virus-like particles produced in insect cell lines, although the functional nature of these complexes is questionable, as they bound cells independently of CD81 and failed to associate with lipoproteins [220,221].

Hepatitis C virus pseudoparticles

Building upon the previous pseudotyped viral particle systems, a major advance in HCV model systems was the generation of retroviral particles with unmodified HCV glycoprotein surface expression [28,39]. In this system, 293T cells are transfected with three separate plasmids and function as particle production factories. The first plasmid encodes the HCV E1E2, the second encodes the Gag-pol proteins of HIV or murine leukemia virus, and the third encodes a retroviral genome with a reporter to moniter subsequent entry in permissive cell lines. Because HCVpp contain unmodified E1 and E2, it is thought that infection of naïve Huh-7.5 cells closely resembles the cell entry

properties of complete HCV virions. However, the assembly of the nucleocapsid is retroviral-specific, and the stoichiometry of E1-E2 complexes on the surface of these particles may differ greatly from HCV. Perhaps the greatest limitation of this system is the inability of infection to spread to neighboring cells, allowing for only a partial dissection of the infectious life cycle. A retroanalysis of the subgenomic and full-length replicon systems containing adaptive mutations shed some light on the inability of this system (and all tested up to this point) to produce infectious viral particles. Most adaptive mutations analyzed affected the degree of NS5A phosphorylation, with hypophosphorylated forms yielding better replication results than hyperphosphorylated forms [212,222,223]. These results were confirmed through chemical inhibition of cellular kinases responsible for NS5A hyperphosphorylation, as well as mutation of critical hyperphosphorylation sites [222]. Although the mechanism behind this phenomenon remains unknown, it is hypothesized that adaptive mutations ablating hyperphosphorylation may facilitate replicase construction and stability, but hinder downstream processes of packaging and assembly (see [224] for a review of NS5A phosphorylation). The fact that most genomes with adaptive mutations replicate but do not produce infectious virus and are attenuated or non-infectious in chimpanzees supports this hypothesis, and gave hope that discovery of a replicating genome without adaptive mutations might yield infectious virus [213,215,216,225].

Hepatitis C virus full-length infectious cell culture systems

In 2003, a peculiar HCV isolate was cloned from a Japanese patient suffering from an acute case of fulminant hepatitis. Termed JFH-1, the consensus sequence of this genotype

2a virus was cloned into replicons and shown to efficiently replicate in both hepatic and non-hepatic cell lines without acquiring adaptive mutations [226,227,228]. Amazingly, when JFH-1 full-length RNA was transfected into Huh-7 cells, viral particles were produced that were filterable and capable of infecting naïve cells [17]. Efficiency of particle production was low, but similar experiments performed in the subclone Huh-7.5 and a derivative yielded higher infectious titers [43,44]. Importantly, HCVcc JFH-1 is infectious in both chimpanzees and uPA-SCID mice transplanted with human hepatocytes (discussed below), and virus recovered from these animals remains infectious in cell culture, fulfilling Koch's postulates [17,229]. In these studies, autologous genome swapping using the HCV genotype 2a J6 sequence in the C-NS2 regions of JFH-1 was found to increase virion production [43]. Since the development of HCVcc systems, much work has gone into the optimization and characterization of cell culture-grown particles. By further altering the fusion junction of NS2/3 to a breakpoint just after the first predicted transmembrane segment of NS2, a chimera producing approximately 10^5 TCID50/ml was generated (Jc1), along with heterologous genotype (1a, 1b, 3a) chimeras [139]. Our lab has shown that this Jc1 chimera (termed "Cp7" in our studies) causes greater cell death than the parent JFH-1 virus, can be highly concentrated using sucrose gradient ultracentrifugation, and may be used to track early infection events using monoclonal antibodies raised against the previously described eE2 protein (see *Chapters 3, 4*) [122,166].

The future of hepatitis C virus model systems

With the advent of these new systems to study the complete life cycle of HCV, we are entering an exciting era where technology is no longer a limiting factor. Different genotypic clones such as H77S (1a) are being moved into the HCVcc system, and analysis of subsequent infectivity and adaptive mutation generation will shed light on critical factors for particle assembly and release [230,231]. In addition, novel systems for infectious particle release from integrated cDNA (genotype 2a) and cDNA flanked by two self-cleaving ribozymes (genotypes 1a, 1b, 2a) have increased the repertoire of tools used to stabilize cell culture virion production for long-term HCVcc analysis [232,233]. Arguably the most critical avenue of HCV research in upcoming years will be the development of a small animal model. Such a model would be instrumental in drug/vaccine development, and would greatly contribute to our understanding of *in vivo* HCV pathogenesis and liver disease progression. This could be envisioned either through adaptation of HCV to infect non-human cells, or humanization of rodent (or other small animal) tissues. The initial block in adapting HCV to non-human cells is most likely entry, as critical coreceptors CD81 and OCLN must be of human origin for infection to proceed [64]. Interestingly, the virus can be adapted to interact with murine CD81 through *in vitro* serial passage, highlighting the plasticity of HCV glycoproteins [234]. However, this process may be more difficult with OCLN or other unidentified coreceptors similar to OCLN, as physical association with E2 has not been proven. The second block in murine cell infection occurs post-translation. Hydrodynamic transfection of RNA into mouse hepatocytes failed to initiate replication, suggesting that the viral replicase machinery may be incompatible with murine counterparts [235]. Lastly, it is unknown whether HCV virions can be packaged and assembled in mouse cells, although

initial experiments with mouse hepatoma cells harboring full-length genomes suggested this is not possible [236]. In addition, altering the species tropism of HCV may affect the pathogenesis or resultant immune response, making this model unfaithful to that which is seen in human infection. For these reasons, humanization of current mouse strains may represent a preferable alternative. These models are already in development, and fall into two categories: xenotransplantation and genetic manipulation. The first category has been explored using urokinase-type plasminogen activator transgenic mice with transgene overexpression in the liver driven by the albumin promoter (Alb-uPA) [237]. These mice are severely immunocompromised, with rapidly progressing hepatotoxicity that can be rescued through human hepatocytic transplantation [237,238]. When inoculated with HCV-infected patient sera or HCVcc, these mice become viremic for several weeks [229,239,240]. Unfortunately, Alb-uPA transgenic mice are time-consuming and expensive to create, and individual animal grafting often results in substantial variability. Their immunocompromised status (to avoid xenograft rejection) also hinders analysis of the immune response during HCV infection. To combat this, several groups are using human haematopoetic progenitor stem cell engraftment in immunocompromised animals to create chimeric mice with humanized livers and human haematolymphoid systems, and virus-specific immune responses have already been demonstrated [241,242]. As opposed to xenotransplantation, genetic manipulation of animals for HCV permissiveness is not well studied. After the discovery of CD81, transgenic mice expressing the human version of this molecule in many tissues were shown to bind rE2 but remained resistant to infection [243]. Although the minimal human factors for HCV uptake are now known, a

more complete knowledge of host factors involved in replication, assembly, and egress will be required before further genetic manipulation is feasible.

Hepatitis C virus and the host immune response

Onset of disease, potential outcomes, severity of infection

Upon infection with HCV, the virus and the host immune system do not wage war on one another, but rather begin a delicate relationship in which slight perturbations in either participant can mean the difference between resolution and chronicity. Early onset of disease is usually mild, meaning that most patients are chronically infected at the time of clinical presentation. It is known that the first six months of infection are critical in determining outcome, and the asymptomatic nature of HCV in the early incubation phase confounds treatment approaches, skewing towards therapeutic rather than prophylactic regimens. Up to 70% of those infected will become chronically infected carriers for life, and 20% of these individuals will go on to develop liver cirrhosis, greatly increasing their chances for hepatocellular carcinoma [244]. Initial diagnosis usually coincides with a rise in alanine aminotransferase levels, which occurs in the first 8-12 weeks and coincides with a late (detectable) onset of both HCV-specific antibodies and T cells [245]. Because of delayed detection, study of innate immune responses is difficult, and adaptive immune studies have traditionally been relegated to the chronic phase. Indeed, prospective studies of chimpanzees and individuals at a high risk for exposure have only recently begun to shed light on the virus-host interaction during the acute phase. This section is divided into the three known phases of HCV infection: incubation, acute, and chronic. In each, we

describe the immune response to the virus, the key players in this response, and the mechanisms by which HCV undermines virus-specific immunity.

Incubation phase of infection

Innate immune response and viral evasion

Within days of infection, HCV RNA can be found in hepatocytes, and mathematical modeling predicts that HCV titers rise rapidly, doubling every 12 hours, until an induction of intrahepatic type I IFN responses that slow this rate to 7.5 days [246,247,248]. Although the proportion of infected hepatocytes remains uncertain, sensitive *in situ* hybridziation methods indicate that up to 50% may contain viral RNA [249]. In this very early phase of the infection, it is thought that IFN-β is primarily generated by these infected hepatocytes. DNA microarrays confirmed these predictions, implicating several factors involved in PAMP recognition of HCV [250,251]. These factors include the pattern recognition receptors (PRRs) TLR3 and RIG-I, which sense dsRNA in endosomes and recognize the poly(U/UC) tract in the HCV 3' -NCR, respectively [252]. Following PAMP-sensing, TLR3 recruits the adapter molecule Toll-IL-1 receptor domain-containing adaptor inducing IFN-β (TRIF or TICAM-1) while RIG-I recruits IFN-β promoter stimulator protein 1 (IPS-1 or MAVS or VISA or CARDIF), all of which function to induce a downstream signaling cascade resulting in increased IFN production (see [253] for a review of TLR and RIG-I signaling). Increased IFN-β leads to induction of an antiviral state through autocrine/paracrine activation of Janus Kinase/Signal Transducer and Activator of Transcription (JAK/STAT) and induction of ISGs, as well as production of antiviral mediators like P56, protein kinase R,

2'-5' oligoadenylate synthetase, and IRF7 [254,255,256]. HCV proteins are the main antagonists of this innate immune response, and evasion usually involves disruption of the IFN pathway at multiple different steps. HCV core protein has been shown to directly inhibit STAT1 phosphorylation, as well as induce SOCS3 and protein phosphatase 2A, inhibiting the JAK/STAT pathway and decreasing the transcriptional activity of ISG factor 3 [257,258,259]. NS5A has also been shown to be an IFN antagonist, inhibiting 2'-5' oligoadenylate synthetase activity and contributing to a global suppression of ISGs through production of the inflammatory cytokine IL-8 [260]. In addition to the IFN pathway, protein kinase R has been shown to be a direct target for HCV proteins. NS5A heterodimerizes with this kinase, while E2 acts as a decoy target, inhibiting or reducing its antiviral effectiveness [261,262]. Perhaps the most elegant innate immune evasion mechanism HCV employs is a dual function of the NS3-4A serine protease. This protease was found to cleave IPS-I and TRIF, releasing these molecules from their mitochondrial- and endosomal-associations and preventing downstream IRF3 and nuclear factor-kappa B signaling, critical steps of an effective innate response [263,264,265]. It should be noted that these observations enjoy substantial biochemical support, but still need to be demonstrated in an HCV-infected liver.

Dendritic cells (DC) have also been proposed as master regulators of the anti-HCV innate immune response, based on their ability to both produce type 1 IFNs and transport antigen to draining lymph nodes for presentation to circulating T cells. Two lineage-specific subsets of DCs have been implicated thus far: plasmacytoid and myeloid. pDCs isolated from the blood of treatment-naïve HCV patients are functional, but their

frequency and ability to produce IFN-α upon *in vitro* TLR9-stimulation is greatly diminished compared to uninfected patients [266,267]. pDCs express CD81 but not CLDN1, and as such cannot be infected with HCVcc [268]. This indicates that, unlike primary hepatocytes, HCV or HCV proteins may have an indirect role in inhibiting the pDC type 1 IFN response. Indeed, both core and NS3 decrease IFN-α production and increase apoptosis in pDCs via TLR2-dependent stimulation of monocytes [267,269]. Additionally, some evidence exists that infectious or heat-killed HCV can inhibit IFN-α production by pDCs *in vitro*, but this needs to be confirmed (reviewed in [245]). Because HCV cannot infect these cells, it is possible that HCV or a component of HCV directly interacts with pDCs, but does not result in productive infection. Unlike pDCs, mDCs may bridge the gap between innate and adaptive immune responses to HCV, as they are the likely APCs during infection and can influence how responding T cells are activated. *In vitro* cultured mDCs from chronic patients show a decrease in IL-12 and an increase in IL-10 production, suggesting an immature phenotype [270,271]. This defect can be induced upon core or NS3 stimulation and rescued by lipopolysaccharide-induced maturation, but this same maturation does not rescue similarly stimulated mDCs from chronic HCV patients, indicating *in vivo* defects apart from HCV protein antagonism [271]. Decreased IL-12 production may be due in part to core binding with gC1qR, the globular domain of complement receptor, and suppression of activator protein 1, which supports a suppressive mechanism rather than an induction of IL-10 [272]. Reports surrounding the allostimulatory capacities of *ex vivo*-derived mDCs remain controversial, but the absence of global immunosuppression in HCV patients argues for functionality in this subset.

NK cells represent another innate immune cell subset, and their rapid cytokine production and cytotoxicity make them an attractive candidate for control of HCV or HCV-infected hepatocytes. A meta-analysis demonstrated a link between clearance of viremia and specific killer cell Ig-like receptor/human leukocyte antigen pairs in patients, suggesting that genetic determinants may predispose certain people for rapid degranulation, IFNγ release, and effective HCV clearance [273,274]. NK cells from HCV patients secrete IL-10 and TGF-β, display high surface levels of inhibitory receptor complex CD94/NKG2A, and fail to fully mature DCs *in vitro* [275]. How HCV influences NK function is not known, but it has been proposed that CD81-crosslinking by E2 may be involved [276,277]. However, these observations were made using purified E2 protein preparations. E2 from HCVcc failed to crosslink the tetraspanin on NK cells, and their function remained intact even after exposure to high levels of virus or HCV-antibody complexes [269]. As described in this section, it is clear that *in vitro* stimulation experiments using whole viral proteins may not accurately reflect the *in vivo* situation of HCV-infected individuals. So far, we have a snapshot of the innate immune response during infection. Development of new *in vivo* models will aid in the study of these very early events, and may allow for the creation of novel diagnostics or reliable predictive methods that influence acute-phase treatment options.

Acute phase of infection

Drastic increases in serum transaminase levels demark the movement of infection from the incubation phase into the acute phase, approximately 8-12 weeks after primary viral

inoculation. HCV-specific T cells become detectable along with HCV-specific antibodies, and the strength of the overall immune response in this phase likely dictates outcome of infection. Regardless of outcome, HCV RNA genomes in plasma peak between 6-10 weeks, and three patterns of infection emerge that correlate with the strength and breadth of the adaptive immune response [278]. First, poorly controlled viremia coincides with a weak (or absent) CD4+ T cell response which is rapidly lost and a weak CD8+ T cell response that wanes over time but may be detectable for several years. Second, viremia is initially controlled by a robust CD4+/CD8+ T cell response, but contraction of the HCV-specific CD4+ T cell subset results in viral recrudescence despite an endurance of the CD8+ T cell subset. Third, viremia becomes undetectable in plasma following the delayed onset of a robust CD4+/CD8+ T cell response, which endures for the life of the host [279,280,281,282,283]. The neutralizing capacity of the humoral immune response in the acute phase and the chronic phase is less well known, and as such we will only devote a small section to its review. Adaptive cellular immunity is currently the only reliable determinant of HCV infection outcome, and as such HCV adopts multiple viral evasion strategies to persist into the chronic phase.

Humoral immune response

Seroconversion after exposure to HCV has been shown to occur around 10-12 weeks in hemodialysis, transfusion, and accidental needle-stick transmission events [284,285,286,287,288,289]. However, the *in vivo* neutralization capacity of anti-HCV antibodies remains questionable; acute resolving patients have been shown to develop neutralizing antibody responses, but hypogammaglobulinemic patients are equally able to clear infection [29,290,291,292]. Several chimpanzee studies have supported antibody-

mediated neutralization. In these experiments, virus was cultured with antibodies against the E2 HVR-1, immunoglobulins pooled from infected individuals, or serum from a chronically infected patient before inoculation into seronegative animals, and in each case HCV replication was prevented [117,293,294]. Conversely, anti-HCV antibodies do not protect against rechallenge in both chimpanzees and humans, and, similar to humans, resolution has occurred in chimpanzees without the development of anti-HCV antibodies [279,295,296,297]. HCVpp studies have also been confounding, as neutralizing antibodies to these particles found at time of seroconversion in humans are weak or strain-specific but then broaden to become cross-protective [29,41,291,292,298]. Our lab has also shown that serum from mice immunized with a recombinant form of E2 is able to efficiently block HCVcc infectivity, but the long-term consequences of this glycoprotein-specific antibody generation are not known. In an *in vivo* situation, an expansion of HCV-specific antibodies may actually contribute to persistence as these immunoglobulins exert selective pressure on highly immunogenic regions of the virus (HVR-1, glycoproteins, etc.) [299,300].

T cell-mediated immune response

Much work has been done to determine how a successful T cell response is mounted against HCV. T cell-mediated immunity may be the sole determining factor of infection outcome, and the nature of CD4+ and CD8+ T cell responses in the acute phase controls progression to the chronic phase. These responses are more complicated than (and may depend on) the previously mentioned hard-wired innate responses, and as such most HCV-related T cell studies have been comparisons of resolved versus chronically infected chimpanzee and human cohorts. Both the kinetics and scope of CD4+ and CD8+

T cell responses differ in controlled versus uncontrolled infection. T cells are slow to expand in all individuals who contract HCV, appearing in the blood 5-10 weeks after infection, and data from chimpanzees have suggested a similar delay exists at the site of initial viral replication in the liver [279,289,301,302,303]. However, expansion of T cells after this initial lag phase is fundamentally different in controlled infections. A robust CD4+ T cell population capable of proliferating in response to HCV proteins must persist throughout the acute phase and after viremia is undetectable to prevent persistence [280,282,289,301,304]. High resolution mapping has shown that these CD4+ T cells target multiple different epitopes (average=10, range 3-28) presented by multiple major histocompatibility (MHC) class II molecules, and that these epitopes are mainly located in the HCV core and nonstructural proteins [305]. The evolution of this response is complex, and responses in a chimpanzee demonstrate that a complex hierarchy exists with certain dominant epitopes targeted by CD4+ T cells during clearance of viremia, followed by subdominant populations that only become detectable once viremia is controlled [306]. In addition to this multi-faceted, mutli-epitope response, evidence exists that certain MHC class II genes may correlate with viral control [307]. In particular, human leukocyte antigen (HLA) DQB1*0301 and DRB1*1101 alleles present many HCV epitopes, and DRB1*1101 has been linked to a sustained helper T cell response [308]. CD8+ T cells also increase in frequency during the acute phase, although acquisition of effector functions such as IFNγ secretion or cytotoxicity lag behind their initial expansion [283,301,302,309,310,311,312,313]. These effector functions arise 8-12 weeks after initial infection (~3 weeks or so after detection of cells using MHC class I tetramers) as assessed by intrahepatic mRNA levels of IFNγ, CD3ε, tumor necrosis factor

(TNF) alpha, and monocyte-induced protein 1 alpha [289,314]. The hepatic localization of these mRNAs suggests that the liver is not only the primary site of infection, but also a key microenvironment in determining resolution. The breadth of the CD8+ T cell response differs from the CD4+ T cell response in several ways. First, there is no preferential localization of epitopes in the HCV polyprotein; epitopes have been found in all regions [315]. Second, there is currently no genetic association of MHC class I haplotype with viral clearance, although some epitopes are cross-reactive with other human pathogens (i.e. Influenza, see $NS3_{1073\text{-}1081}$ below) [303,316]. Instead, the most common acute phase features of resolved infections are an overall increase in CD8+ T cell frequency and a vigorous, mutli-epitope response spanning the entire polyprotein. Like most viral infections, CD4+ and CD8+ T cells go through a contraction phase after spontaneous resolution, but this contraction remains poorly defined. Circulating virus-specific CD8+ T cells can be found intermittently in the weeks following termination of viremia, and may represent specific populations tasked with eliminating cellular reservoirs containing low levels of replicating genomes [301,317,318].

The story of acute phase T cells in uncontrolled HCV infections is markedly different. CD4+ T cells fail to significantly expand, or expand but are quickly lost before viremia can be controlled [281,282,319]. These cells also experience defects in IL-2 production, which is an early indicator of proliferative dysfunction and known to predict persistence [320]. Unlike the mutli-epitope-specific response discussed above, the average number of targeted MHC class II epitopes is very low (average=1, range 0-8) [305]. It is thought that the disappearance of CD4+ T cells during the acute phase may contribute to

inappropriate CD8+ T cell responses during the chronic phase, a hypothesis that is supported by *in vivo* CD4+ T cell depletion in chimpanzees followed by rechallenge [321]. Similarly, CD8+ T cells in uncontrolled infections do not undergo a large expansion in the acute phase, although one study has observed a large CD8+ clonal T cell outgrowth directed towards a single HLA-A2-restricted epitope in the NS3 protein, termed $NS3_{1073-1081}$ [303,312,317,322]. Whether particular viral quasispecies retain such immunogenic epitopes to purposefully serve as decoys for the immune response is not currently known. These data indicate that CD8+ T cells in the acute phase of uncontrollable infections are by some measure multispecific, but virus is able to persist nonetheless.

Functional circulating and intrahepatic CD4+ and CD8+ T cells represent a predictive signature of viral control. Protective immunity is a common feature in those who spontaneously resolve their infections, and is durable for years and potentially decades [302,323,324]. Indeed, T cell immunity is often the only indicator of a prior infection in seronegative individuals [325,326,327,328]. An epidemiological study of intravenous drug users has shown that persistence of viremia is less frequent in individuals who have had at least one previously confirmed spontaneously resolving infection [329]. The mechanisms behind this protection are unknown, but likely revolve around long-lived cellular rather than humoral immunity, as previously resolving chimpanzees rechallenged with the identical HCV strain showed a decrease in viremia that correlates with an increase in intrahepatic IFNγ and TNFα mRNA expression [302,323,324]. In these studies, incoming virus was not eliminated, arguing against a sterilizing antibody

response. Control of secondary challenge in animals is also associated with transient and lower peak levels of viremia, as well as increased kinetics and breadth of HCV-specific effector cells (2-3 week onset compared to 10-12 week, 10-fold higher frequency of cells targeting dominant class I epitopes), all features of a classical memory response [302,306]. These studies also demonstrated that CD4+ and CD8+ T cell subsets contribute differently to the HCV memory response. Antibody-mediated depletion of memory CD8+ T cells between a second and third round of infection resulted in prolonged viremia despite endurance of memory CD4+ T cells, and viral elimination did not occur until recovery of the intrahepatic HCV-specific CD8+ subset [302]. Similar depletion of CD4+ T cells resulted in a more drastic phenotype, with memory CD8+ T cells unable to control infection and a permanent loss of memory CD4+ T cell activity leading to chronic infection [321]. Interestingly, absence of CD4+ protection in this study allowed for emergence of viral escape variants in MHC class I epitopes, meaning that critical cross-talk events between T cell subsets are necessary for an effective memory response [321]. Taken together, these results indicate that for small RNA viruses such as HCV that establish chronic infection and have a high propensity to mutate, CD8+ T cells are likely the final effector cells for elimination of infection, but these cells must be primed and maintained by antigen-specific CD4+ T cells.

Chronic phase of infection

Inadequate or poorly functioning T cell responses during the acute phase of infection are a major factor in progression to chronic disease. Individuals who maintain these infections for life greatly increase their chance of hepatic cirrhosis and end-stage liver

disease. The chronic phase of infection is marked by several interesting features. First, levels of HCV RNA drop 2-3 $\log_{10}$ below what is seen in the acute phase, and are highly stable, varying less than 1 $\log_{10}$ for the remainder of infection [248]. This baseline level may vary greatly between individuals, and it is currently unknown whether intrahepatic CD8+ T cells contribute to this wide inter-variation, or instead are responsible for the tightly-controlled RNA maintenance [330,331,332,333]. Second, the levels of HCV-specific antibodies increase. This increase includes neutralizing antibodies against multiple HCV strains, which lends strength to the hypothesis that humoral immunity has little influence over viral control [248]. Third, HCV-specific T cell reactivity decreases over time, as assessed by *in vitro* recall responses to HCV antigens. This last feature seems to be limited to functionality, as large numbers of HCV-specific CD8+ T cells can be found in the liver during the chronic phase [248,334,335,336,337]. Longitudinal studies of T cell receptor rearrangement have even shown that some of these CD8+ populations can be stable for years [338]. These CD8+ T cells are stunted early in development as defined by high expression of CCR7, CD27 and/or CD28, combined with functionality defects that include low IFNγ production, low intracellular stores of perforin, poor *ex vivo* proliferation, and an inability to degranulate for target cell lysis [311,339,340,341]. This global dysfunction of adaptive immunity does not, however, arise without direct and indirect subversion by HCV. These mechanisms are just now starting to be fully defined, and as they represent a critical determinant in progression and maintenance of chronicity, necessitate a comprehensive review.

Persistent antigen stimulation, anergy, deletion of T cells

The persistence of low levels of HCV for the life of the host provides a nearly limitless source of antigen to which T cells eventually become desensitized. Similar to what is seen in other chronic infections such as lymphocytic choriomeningitis virus (LCMV) and HIV, CD4+ and CD8+ T cells in HCV become gradually more impaired in effector function as time progresses, with weak IFNγ levels remaining as the only indicator of responsiveness [283,301,341,342]. In this anergic state, reduced IL-2 production by CD4+ T cells has important consequences for CD8+ T cell function, with a recent report showing that loss of IL-2-mediated killing preceeds chronic hepatitis [310,343]. Exhaustion of HCV-specific T cells has been demonstrated during chronic infection, with high levels of the inhibitory receptor programmed death-1 (PD-1) expressed on both circulating and intrahepatic CD8+ subsets [344,345]. In chronic HCV infection, the ligand for PD-1, PD-L1, is highly expressed on many cells of the liver parenchyma (stellate cells, liver sinusoidal endothelial cells, Kupffer cells), and the PD-1/PD-L1 interaction both inhibits effector functions and increases T cell apoptosis [346]. Building on data generated in the LCMV model system, *in vitro* antibody blockade of this interaction reestablishes proliferative capacity in these exhausted cells, indicating that chronic antigen stimulation is an indirect HCV-specific subversion of the immune response [345,347,348,349]. Differences in levels of exhaustion between circulating and intrahepatic T cells have also been demonstrated, with liver-resident effectors expressing very high levels of PD-1 as well as low levels of the IL-7 receptor alpha chain (CD127) and requiring a more complex costimulatory molecule blockade to restore function [345,350].

IL-10-mediated suppression of T cell responses, induction of regulatory T cells

The cytokine IL-10 is a global attenuator of inflammatory responses, able to inhibit the production of pro-inflammatory cytokines such as IFNγ, IL-2, and TNFα (for review, see [351]). Produced mainly by monocytes, this cytokine has been known to have a profound effect during the HCV incubation phase, with innate immune responses suffering as a consequence of increased DC and NK cell IL-10 production. The first indication that this cytokine also played a role in adaptive immunity came in a study where IL-10-producing HCV-specific CD8+ T cell lines were derived from the liver of a chronically infected patient and shown to suppress antiviral T cells [352]. Since then, CD8+ T cells capable of producing IL-10 have been isolated from multiple human liver biopsies [353]. These cells were capable of suppressing function and proliferation of virus-specific T cells, and were shown to be localized to areas of low hepatocellular apoptosis and low laminin expression [353,354]. From these very limited studies, it appears that a chronically infected liver can be further divided into microenvironments of varying inflammation. Regions of low inflammation tend to be enriched for CD8+ T cells secreting IL-10, which suppresses inflammatory cytokine secretion and encourages HCV replication, while regions of high inflammation are distinguished by active protein rearrangement and a high concentration of functional, IFNγ-secreting T cell infiltrates. However, the CD8+ T cell subset is not the only suppressive population found in HCV infection. Regulatory T cells (Treg), a subset of naturally occurring CD4+ cells expressing the transcription factor forkhead box P3 (FoxP3) and the IL-2 receptor alpha chain (IL-2Rα, CD25), are known to be enriched in the peripheral circulation of chronically infected individuals [355,356,357]. *Ex vivo* depletion of these cells has been shown to increase the frequency of functional HCV-specific CD8+ T cells in both humans and chimpanzees, suggesting

that Tregs suppress an otherwise competent viral-specific response through a cell contact-dependent mechanism [355,356,357,358,359]. Despite this convincing evidence, several observations have hinted that this association is not so straightforward. First, this suppression was not HCV-specific, as cytomegalovirus, Epstein-Barr virus, and influenza virus-specific CD8+ T cells were also shown to rebound after Treg depletion [357,358]. Second, there is no difference in FoxP3 levels and Treg suppression in the acute phase between individuals who clear their infection and those who remain chronic [360]. Finally, *in vivo* Tregs have not been found in secondary lymphoid organs, the liver, or other sites of antigen-specific interaction, casting doubt on their *in vitro* cell contact-dependent nature. These data suggest that Treg generation and suppression in HCV infection may be a result of acute inflammation rather than an HCV-specific response.

Mutational escape of CD4+ and CD8+ T cell epitopes

For chronically infected individuals with detectable HCV-specific T cells, mutational escape represents a likely mechanism of adaptive immune evasion. Like other small RNA viruses, HCV contains a highly error-prone RdRp (NS5B) that introduces random mutations into replicating HCV genomes and allows for subsequent escape of developing humoral and cellular immunity. Mutations that allow for escape of CD4+ T cell pressure have been difficult to document, as this subset is usually lost early in the acute phase of infection, confounding the identification of dominant epitopes. Exceptions to this rule do exist, and amino acid changes in several well-studied MHC class II epitopes have been documented [361,362,363]. Some of these mutations ablated cytokine production and proliferation of CD4+ T cells, while others skewed cytokine production from a Th1 to a Th2 response [362,364]. A more recent longitudinal study in chimpanzees demonstrated

that CD4+ T cell epitopes undergo far fewer amino acid changes than CD8+ T cell epitopes [365]. In addition, changes in restricted CD4+ epitopes occur no more frequently than non-restricted epitopes or regions flanking epitopes, suggesting that CD4+ T cell pressure is not significant enough to engender mutational escape for persistence in the chronic phase [365].

Unlike CD4+ epitope evolution, mutational escape in MHC class I-restricted T cell epitopes is frequently observed and is likely a mechanism by which HCV subverts the adaptive immune response. Depending on where in the epitope these mutations arise, variation can i) alter peptide-MHC binding, ii) ablate T cell contact residues, or iii) affect the pattern of proteasomal cleavage, ruining the epitope during processing (reviewed in [366]). These variations can be highly advantageous to the virus, rendering T cell responses to the wild type sequence useless, and interfering with priming of naïve T cell subsets [367,368]. The rate of nonsynonymous (coding) to synonymous (non-coding) mutation in CD8+ T cell epitopes has been found to be statistically significant in chronically infected chimpanzees when compared to non-restricted epitopes or flanking regions, strongly indicating that a link between CD8+ T cell pressure and mutational escape exists [369]. Longitudinal studies in humans at high risk of infection have confirmed this link, proving that amino acid substitutions in MHC class I epitopes can impair *ex vivo* immune recognition, as assessed by tetramer staining and IFNγ ELISA [370,371,372]. As one might expect, MHC donor and recipient haplotypes play a large role in the evolution of CD8+ T cell epitopes. When virus is transmitted into an individual that does not share the donor haplotype, HCV is able to spontaneously revert

to its original sequence [372,373]. This is also seen in both HIV and simian immunodeficiency virus, and is the direct result of a "fitness cost" to replication that coincides with escape from immune pressure [374,375]. The most successful T cell responses target regions or epitopes that are critical to the propagation of HCV, so it is reasonable to hypothesize that similar fitness costs constrain the evolution of HCV quasispecies. With the advent of the HCVcc system, it is now possible to test the fitness of HCV mutant quasispecies that arise during *in vivo* infection through a reverse genetics approach. Using this approach, we have shown that mutations in HCV CD8+ T cell epitopes that arise early in the acute phase of infection are not necessarily fixed, but may further mutate away from or revert back to the parental sequence [376]. HCV seeks a balance between immune evasion and fitness: regions critical for viral replication will tolerate mutation to escape T cell pressure, but only to a degree that the viral life cycle is not severely impaired. This is the first published report demonstrating that single amino acid substitutions in known HCV CD8+ T cell epitopes impair *in vitro* viral fitness, and has important implications for the evolution of *in vivo* viral quasispecies. Whether the fixed chronic phase variant seen in this study would undergo further mutation in an HLA-mismatched chimpanzee is unknown, but such a study would help to further demonstrate the criticality of single amino acid mutations in the establishment of persistence, as well as provide a correlation between *in vitro* and *in vivo* observations. Another study has confirmed this fitness constraint utilizing an HLA-B27-restricted HCV epitope, but showed instead that a clustering of mutations was required to escape T cell recognition [377]. It is unknown whether single or multiple substitution in a single epitope is the prevailing mechanism for T cell escape in HCV, but it is likely that this pattern may vary

depending on the genomic locale and the strength of the T cell response to that particular epitope.

It should be noted that although epitope escape in HCV infection is a well-studied phenomenon, it is not the only mechanism for evading antigen-specific T cells, as many epitopes remain intact during chronic infection despite highly focused CD8+ T cell responses [303]. Aside from affecting viral quasispecies inside a single host, CTL escape mutations may also select for dominant quasispecies at the human population level. It is currently unknown as to whether HCV imparts "footprints" of associated polymorphisms when transmitted from individual to individual, as is common in HIV infection [378]. However, the high mutation rate of HCV combined with the plasticity of sequence variation upon transmission to HLA-mismatched individuals suggest that immunodominant epitopes restricted by particular alleles may be lost over time, creating a new hierarchy of circulating virus in the general population [372,373]. As in HIV, additional compensating mutations with negligible fitness costs would most likely accompany these new quasispecies, further serving to outpace or confound de novo immune responses [379]. More metanalyses of large HCV cohorts will be needed to confirm these hypotheses, but taken together it is clear that this small, hepatotropic RNA virus has efficiently evolved to outpace immune defense while retaining the capability to propagate its genome in naïve human hosts.

Lymphocytic choriomeningitis virus: a surrogate model of chronic viral infections

Pathogenesis in humans and rodents

LCMV is a prototypical model of chronic viral infections, often used to deduce how the human immune system reacts to persistent antigenic exposure [380]. LCMV has proven indispensable as a model for chronic infection and as a tool for studying immune function, but the virus also poses very serious real world clinical health risks. Since its first isolation in 1933 by Armstrong and Lillie, the virus has confounded clinicians with a variety of nonspecific symptoms in adults and a host of life-threatening conditions in neonates [381]. Although human-to-human transmission of LCMV has not been documented, a recent case report citing transmission via organ transplantation has underscored the need for diagnostic testing in both immunocompromised patients and in pregnant women throughout each trimester [382].

The natural reservoir of LCMV infection is restricted mainly to rodents, which can either remain asymptomatic in the case of vertical transmission in wild mice (*Mus musculus*) or develop variable maladies in the case of common Syrian hamsters (*Mesocricetus auratus*) [383]. Virus is shed in rodent saliva, urine, feces, nasal secretions, milk, and semen, and the two routes of rodent-to-human transmission are inhalation of aerosolized viral particles or contact with infected fomites [384]. Infected adults usually present with biphasic disease symptoms of headache, fever, nausea, vomiting, myalgia, or adenopathy, and can progress to more severe central nervous system disease such as meningitis and meningoencephalitis. The symptoms in liveborn infants are more severe and include (but are not limited to) nonobstructive hydrocephalus with periventricular calcifications, sensorineural deafness, and psychomotor retardation (reviewed in [385]). Furthermore,

the disease can mimic congenital toxoplasmosis or cytomegalovirus infection, and is often misdiagnosed due to clinical similarities [386]. Congenital infection was first recognized in Great Britain, followed by cases of spontaneous fetal abortion, chorioretinitis, and hydrocephalus in Germany, France, and Lithuania [387,388,389].

While viral isolation is possible, serological testing remains the standard for LCMV diagnosis, and is becoming the standard in cases of unexplained infant/child hydrocephalus, micro- or macrocephaly, chorioretinitis, and various intracranial abnormalities. Detection of IgM and IgG with an immunofluorescent antibody test has been shown to be extremely sensitive and widely available, while standard ELISA has been shown to be ideal for prolonged tracking of LCMV-specific immunoglobulin [390,391]. More recently, several groups have shown that reverse transcriptase PCR can provide rapid and accurate antenatal and postnatal diagnosis, opening the door for standardized testing in pregnant women [392]. However, despite the many advances made in serological testing over the past two decades, education on the dangers that rodents pose to both the general public and to pregnant women remains the key factor in preventing LCMV infection.

Genome organization

LCMV is a prototypic member of the family *Arenaviridae*, and has long been studied as an ideal model of both acute and chronic infection, proving invaluable as a proxy model for studying the human immune system. The natural host of LCMV is the mouse, which has greatly facilitated both *in vitro* and *in vivo* studies of this non-cytopathic virus.

Vertical transmission is almost exclusive within the natural host, causing an induction of immune tolerance and persistent infection for the life of the animal [393]. The viral genome is made up of two negative-sense RNA strands, both having an ambisense protein coding strategy [394,395]. The large (L) strand codes for the viral RdRp, while the short (S) strand codes for the nucleoprotein NP and GP-C, a polypeptide that is processed into both the peripheral glycoprotein GP-1 and the transmembrane glycoprotein GP-2 [396,397,398]. More recent studies have proven the genome to be relatively dispensable, with the NP and L proteins representing the minimal viral elements sufficient for RNA transcription and replication of RNA analogs [399].

Acute versus chronic variants

Throughout the development of LCMV as a model infectious system, much work has focused on the cellular tropism of the virus and the viral variants that have been seen throughout its manipulation *in vivo*. Central nervous system isolates from mice infected at birth caused distinctively different infection courses than those found in lymphoid tissues. Further investigation led to the discovery, isolation, and cloning of two separate viral variants. The first, termed Armstrong 53b (Armstrong, ARM), caused robust IFNγ CTL responses in mice when injected intravenously, and was eventually cleared 7-10 days post infection. The second, termed Clone13 (Cl13), suppressed this response and led to persistent infection when administered via the same route [400,401,402]. Genome sequencing and comparison studies went on to show that despite their markedly different patterns of infection, the two isolates differed in only five nucleotides throughout their entire genome, two of which caused amino acid substitutions [403,404,405]. These mutations were mapped to the L protein and the GP-1 protein, with the latter correlating

(in Cl13) to a higher binding affinity for α-dystroglycan, the main cellular receptor for the virus [406,407,408]. Since these seminal discoveries, both variants have been used extensively to model both acute and chronic viral infection in mice, and continue to provide invaluable correlations in chronic human diseases such as tuberculosis, leprosy, HBV, HCV, and HIV [409].

Host immune response

Humoral and cellular immune response

The immune response to LCMV has been extensively characterized thanks to the use of transgenic mouse models, and the interplay of both cellular and humoral components has proven crucial in tissue damage and the outcome of infection. Indeed, the immune system is responsible for death in infected mice, as LCMV is a non-cytopathic agent [410] (L. Uebelhoer, unpublished data). Cellular protection is not limited to the naïve or memory subsets; rather, priming and recall responses must be equally represented for effective control. Loss of both types of CD8+ T cells has been demonstrated, and exhaustion as well as peripheral deletion pave the way for persistent infection [347,411,412]. Additionally, perforin-deficient transgenic mice have almost no ability to control acute infection, due to poorly cytotoxic CD8+ T and natural killer cells [413]. The generation of a CD4+ transgenic "SMARTA" mouse with an I-A^b restricted TCR specific for the GP61-80 epitope of LCMV (formerly termed P13) helped to exclude the possibility of inefficient CD4+ T cell induction upon infection, and lent even more support to the importance of the CD8+ T cell response [414]. This mouse model has also opened the

door for new studies that closely examine CD4+ T cell help in both acute and persistent infections.

While CD8+ CTL responses have proven essential for short-term viral control, they are not the only determining factor in long-term protective immunity. CD4+ T cell-deficient mice are able to clear LCMV, but it was determined that they establish a carrier status with much higher frequency than wild type mice [415]. It was also found that beta-2 microglobulin knockout mice still succumb to immunopathology despite their lack of functional CD8+ T cells [416]. These mice mounted a rare LCMV class II-restricted response, suggesting that CD4+ T cells are able to compensate for CD8+ T cells in this system [417]. One of these "lytic CD4+ T cells" was also shown to be cross-protective during lethal LCMV challenge, arguing strongly for the importance of this cell subset [418]. Even more interesting is the finding that long-term responsiveness of CD8+ CTLs is dependent on early CD4+ T cell priming, the absence of which results in viral recrudescence and death [419]. This crosstalk between cell subsets extends into the realm of humoral immunity, and establishes a niche for both CD4+ T cells and B cells in prolonged viral control. Knocking out either B cells or CD4+ T cells in mice resulted in persistent LCMV infection after apparent control, with CTL exhaustion the culprit of susceptibility [420,421].

It has been known for many years that LCMV-specific humoral responses are CD4+ T cell-dependent, and the specific aspects of this humoral response have been well characterized [422,423,424,425]. High titers of both NP- and GP-specific isotype-

switched antibodies are present as early as eight days post infection (as detected by ELISA), but effective neutralizing Abs do not arise until months later [426]. In contrast, elimination of the CTL response led to a surprising acceleration of neutralizing antibody kinetics, with greater and more specific titers detected 25-30 days post infection [427].

Decades of experimentation have proven three fundamental principles in LCMV infection. First, robust CD8+ T cell expansion early in acute infection is a dual-edged sword; while being necessary for viral control, this subset also contributes to the severe immunopathology that is seen in this non-cytopathic virus. Second, as the acute infection shifts to long-term persistence, the role of both CD4+ T cells and B cells becomes more pronounced. Third, the immune response to LCMV can no longer be compartmentalized. Each component of the adaptive immune response occupies a specific niche in battling the infection, but crosstalk is a necessary step for effective clearance. Initial priming of future CD8+ memory responses by CD4+ T cells is critical, and CD4+ T cell-B cell interactions help to isotype switch neutralizing Abs that are necessary for targeting viral surface molecules and intermittent suppression of disease. If anything, extensive experimentation has proven CD4+ T cells to be the master regulator in the immune response to LCMV. These cells are the choreographers of an intricate dance, a middleman that is essential for effective viral control.

Memory T cell response

The characteristics of a robust memory T cell response have traditionally eluded researchers, due to experimental limitations and an unknown marker profile that was only discovered within the last decade. Prior to these advancements, it was known that

secondary immune responses tended to be more efficient, stronger, and faster than primary responses. Studies employing LCMV and the use of new models such as the P14 CD8+ T cell transgenic mouse greatly advanced the current base of knowledge in the field of T cell memory [428]. In the context of LCMV infection, there are similarities and differences in the naïve, effector, and memory T cell pools, and also critical differences at the single cell level [429]. By transferring naïve P14 cells into recipient mice and infecting with LCMV, a stable memory pool of T cells was created that expressed a defined TCR, and could be efficiently tracked upon secondary transfer for memory studies [411,430]. Upon establishment of this system, comparisons could be made between naïve and memory populations. It was found that although the threshold for activation was relatively similar on a single cell basis, the kinetics of the memory response was indeed greatly enhanced. Cytokines such as IFNγ and IL-2 were secreted much more rapidly (1-2 h) than by naïve cells (24 h) [431]. Interestingly, these memory cells also became committed to proliferation 2 h after restimulation with antigen, and remained so even after antigen was withdrawn [432]. Subsequent experiments went on to show that the efficient recall response was due largely to a reorganization of the TCR signaling machinery, in particular the association of the kinase Lck with the CD8 coreceptor [433].

The CD4+ memory T cell response in LCMV has been less extensively studied, mainly because of the dominating interest in CD8+ T cell exhaustion during non-cytopathic viral infections such as LCMV, HBV, and HCV. Indeed, early studies failed to demonstrate a role for these cells in LCMV resolution, because the chronic phase of infection had not

been examined [434,435]. Groups began to explore the idea that functional CD4+ T cells were critical during the establishment of persistent infection, and to the survival of the host, through cytokine and migratory studies both in LCMV and VSV systems [436,437]. Subsequently, studies focused on the role of CD4+ T cells in priming the memory CD8+ T cell (or B cell) response during chronic infection, and it has become apparent that this help is necessary for effective viral control [438]. CD4+ T cells were proven dispensable in the primary immune response, since CD8+ T cells were able to proliferate, secrete IFNγ, and efficiently perform cytolytic duties upon stimulation with antigen in a surrogate system [439,440]. Numerous groups then went on to define a role for CD4+ T cells in the maintenance of long-term functional memory, and the necessary imprinting steps involved during the priming phase in LCMV infection [441,442,443,444].

B cells as antigen-presenting cells

Antigen-presenting cell transfer as therapy

Antigen-specific T cell transfer in allogeneic recipients has long been recognized experimentally and clinically as a promising therapy for the treatment of viral infection, tumors, and relapsed hematological malignancies [445]. However, low precursor frequencies and the difficulty of preparing these T cells directly *ex vivo* necessitated new therapies. The use of adoptive transfer of autologous APC populations to stimulate T cells specific for foreign or tumor antigens has been a very popular area of research in the last 15 years, and initial studies using DCs loaded with single tumor antigens or even single epitopes showed much promise in small animal models. Since the first report on DC vaccination in 1996, clinical response rates in over 100 trials have failed to faithfully

reproduce pre-clinical results, with most of these vaccination trials and adoptive transfer therapies being DC-focused [446,447]. Investigators initially operated on the assumption that DCs are superior to B cells and macrophages in their ability to stimulate CD4+ T cells with the proper costimulation needed to generate an effective immune response [448]. This view has been revised, however, upon findings that other APCs such as CD40-stimulated B cells and artificially engineered APCs are equivalent to DCs in their ability to prime T cells [445,449,450,451,452]. Additionally, DC therapies pose numerous challenges such as low (0.1-0.5%) frequencies in peripheral blood, a decrease in long-term proliferation/presentation, and the necessity for multiple high-count cellular doses, all of which highlight the need for additional APC vaccination approaches [453,454,455].

CD40-activation in B cell priming of T cells

In contrast to DCs, B cells represent a population of APCs that has been less well studied in adoptive transfer experiments using both tumor and virus challenge models. As with DCs, there are both pros and cons in harnessing the antigen processing and presentation abilities of B cells. Naïve B cells are present at a much higher frequency than DCs, both in the peripheral blood and in the spleen (10-15% and 40-45%, respectively) (reviewed in [456]). They can be expanded to large numbers *ex vivo*, and are able to capture, process, and present rare foreign antigens in as little as 20 minutes upon specific B cell receptor interaction [457]. Perhaps most importantly, initial studies have shown that CD40-activated B cells can expand rare naïve and memory CD8+ T cell populations in peripheral blood mononuclear cells (PBMCs) directly *ex vivo* up to 10^6-fold

[445,458,459,460,461,462]. Priming of CD4+ T cells has also been achieved in the context of protein antigens both *in vitro* and *in vivo* [463,464]. Unfortunately, CD40 manipulation on freshly isolated B cells adds a layer of complexity to the therapeutic process, as was evident with the extensive testing needed to meet Good Manufacturing Practices of trimeric soluble CD40L. Another limitation is that CD40-stimulated B cells have only been modified with exogenous peptide or RNA/retroviral vector transfection, without specifically targeting the BCR [459,461,464]. Whether such an approach would further enhance B cell presentation or increase the risk of lymphoblastic malignancies is currently not known.

Naïve B cell-T cell interactions

Interestingly, the role of resting, or naïve, B cells in the activation of both naïve and memory T cells is still unclear, as they seemingly induce tolerance or block anti-tumor activity *in vivo* [465,466]. It has been known for quite some time that B cells express high levels of MHC class I, and can thereby act as APCs to CD8+ T cells [467]. Several *in vitro* studies have also showed the ability of B cells to induce CTL activity or stimulate IL-2 production in CD8+ T cell clones or hybridoma lines [468,469,470]. Paradoxically, B cells were also shown to directly induce tolerance in naïve CD8+ T cells, and it was later found that this phenomenon occurred via CD95-mediated activation-induced deletion [467,471]. Even less is known about the role that B cells (naïve or otherwise) may play in the activation and differentiation of CD4+ T cells into memory cells.

Recombinant chimeric antibodies: a novel system to probe APC-T cell interactions

Studies have suggested that targeting specific cell surface molecules on naïve B cells (and on all professional APCs) with protein-associated peptide complexes may provide an alternative route of CD4+ T cell priming, and in doing so eliminate the need for adoptive transfers or deliberate B cell activation in therapy [472,473,474]. Immunoglobulin molecules in particular have provided an attractive choice for recombinant protein-peptide technology, due to their long half-life and ability to be internalized via Fc (or other) receptors on APCs [475,476]. The complementarity determining regions of Igs are loops that connect the various beta strands of these molecules, and are surprisingly plastic in their ability to accommodate foreign sequences without altering native antibody structure [477]. Several groups have shown that insertion of foreign peptides into these heavy chain regions resulted in efficient processing and presentation by APCs, and in some cases a 100-1000 fold increase in T cell activation both *in vitro* and *in vivo* over free synthetic peptide [478,479,480,481,482,483]. Additionally, sequences for these recombinant antibodies (rAbs, "troybodies") can be cloned into expression cassettes, allowing for rapid epitope insertion mutations of the heavy chain and simultaneous expression of both light and heavy chains in permissive cells [484]. With this in mind, it is feasible that rAb molecules could be constructed using variable regions that target surface molecules on B cells, thereby eliminating the need for passive uptake and processing of the complex. For example, targeting of IgD on the surface of naïve B cells would be expected to cluster BCRs, and could potentially induce costimulation molecules needed for efficient T cell priming as seen in CD40-stimulated B cells. Deliberate targeting to this APC subset, coupled with the precursor frequencies of B cells mentioned above, eliminates the need to adoptively transfer cells. This system

could also allow for multiple epitope insertions into the numerous CDRs of these rAbs, creating a molecule bearing several foreign peptide sequences that would target naïve B cells and enhance the priming of T cell populations. The potential for CD4+ T cell response improvement in the context of chronic infection has remained relatively unexplored, but one could hypothesize that augmenting the function of this subset would in turn augment a network of complex cellular responses, providing a novel approach that may help in the elimination of many types of persistent human pathogens. rAbs specific for naïve B cells and bearing integrated CD4+ T cell epitopes would give further insight into the interaction of these two cell subsets, and could be modified to develop a potentially multivalent, efficacious class II-restricted vaccine strategy.

References

1. De Francesco R, Migliaccio G (2005) Challenges and successes in developing new therapies for hepatitis C. Nature 436: 953-960.

2. Organization WH (2000) Hepatitis C--global prevalence (update). Wkly Epidemiol Rec 75: 18-19.

3. Hoofnagle JH (2002) Course and outcome of hepatitis C. Hepatology 36: S21-29.

4. Hoofnagle JH (1997) Hepatitis C: the clinical spectrum of disease. Hepatology 26: 15S-20S.

5. Brown RS (2005) Hepatitis C and liver transplantation. Nature 436: 973-978.

6. Chisari FV (2005) Unscrambling hepatitis C virus-host interactions. Nature 436: 930-932.

7. Chen SL, Morgan TR (2006) The natural history of hepatitis C virus (HCV) infection. Int J Med Sci 3: 47-52.

8. Alter HJ, Seeff LB (2000) Recovery, persistence, and sequelae in hepatitis C virus infection: a perspective on long-term outcome. Semin Liver Dis 20: 17-35.

9. Alter MJ (1996) Epidemiology of hepatitis C. Eur J Gastroenterol Hepatol 8: 319-323.

10. Alter HJ, Conry-Cantilena C, Melpolder J, Tan D, Van Raden M, et al. (1997) Hepatitis C in asymptomatic blood donors. Hepatology 26: 29S-33S.

11. Alter MJ (1999) Hepatitis C virus infection in the United States. J Hepatol 31 Suppl 1: 88-91.

12. Alter MJ (2002) Prevention of spread of hepatitis C. Hepatology 36: S93-98.

13. Spaulding A, Greene C, Davidson K, Schneidermann M, Rich J (1999) Hepatitis C in state correctional facilities. Prev Med 28: 92-100.

14. Sulkowski MS, Mast EE, Seeff LB, Thomas DL (2000) Hepatitis C virus infection as an opportunistic disease in persons infected with human immunodeficiency virus. Clin Infect Dis 30 Suppl 1: S77-84.

15. Neumann AU, Lam NP, Dahari H, Gretch DR, Wiley TE, et al. (1998) Hepatitis C viral dynamics *in vivo* and the antiviral efficacy of interferon-alpha therapy. Science 282: 103-107.

16. Simmonds P (2004) Genetic diversity and evolution of hepatitis C virus--15 years on. J Gen Virol 85: 3173-3188.

17. Wakita T, Pietschmann T, Kato T, Date T, Miyamoto M, et al. (2005) Production of infectious hepatitis C virus in tissue culture from a cloned viral genome. Nat Med 11: 791-796.

18. von Hahn T, Rice CM (2008) Hepatitis C virus entry. J Biol Chem 283: 3689-3693.

19. Lindenbach BD, Thiel, H.-J., and Rice, C.M. (2007) Flaviviridae: the viruses and their replication. Fields Virology 5th Ed.: 1101-1152.

20. Molina S, Castet V, Fournier-Wirth C, Pichard-Garcia L, Avner R, et al. (2007) The low-density lipoprotein receptor plays a role in the infection of primary human hepatocytes by hepatitis C virus. J Hepatol 46: 411-419.

21. von Hahn T, McKeating JA (2007) *In vitro* veritas? The challenges of studying hepatitis C virus infectivity in a test tube. J Hepatol 46: 355-358.

22. Krey T, d'Alayer J, Kikuti CM, Saulnier A, Damier-Piolle L, et al. (2010) The disulfide bonds in glycoprotein E2 of hepatitis C virus reveal the tertiary organization of the molecule. PLoS Pathog 6: e1000762.

23. Germi R, Crance JM, Garin D, Guimet J, Lortat-Jacob H, et al. (2002) Cellular glycosaminoglycans and low density lipoprotein receptor are involved in hepatitis C virus adsorption. J Med Virol 68: 206-215.

24. Agnello V, Abel G (1997) Localization of hepatitis C virus in cutaneous vasculitic lesions in patients with type II cryoglobulinemia. Arthritis Rheum 40: 2007-2015.

25. Monazahian M, Bohme I, Bonk S, Koch A, Scholz C, et al. (1999) Low density lipoprotein receptor as a candidate receptor for hepatitis C virus. J Med Virol 57: 223-229.

26. Agnello V, Abel G, Elfahal M, Knight GB, Zhang QX (1999) Hepatitis C virus and other flaviviridae viruses enter cells via low density lipoprotein receptor. Proc Natl Acad Sci U S A 96: 12766-12771.

27. Wunschmann S, Medh JD, Klinzmann D, Schmidt WN, Stapleton JT (2000) Characterization of hepatitis C virus (HCV) and HCV E2 interactions with CD81 and the low-density lipoprotein receptor. J Virol 74: 10055-10062.

28. Bartosch B, Dubuisson J, Cosset FL (2003) Infectious hepatitis C virus pseudo-particles containing functional E1-E2 envelope protein complexes. J Exp Med 197: 633-642.

29. Meunier JC, Engle RE, Faulk K, Zhao M, Bartosch B, et al. (2005) Evidence for cross-genotype neutralization of hepatitis C virus pseudo-particles and enhancement of infectivity by apolipoprotein C1. Proc Natl Acad Sci U S A 102: 4560-4565.

30. Bartosch B, Verney G, Dreux M, Donot P, Morice Y, et al. (2005) An interplay between hypervariable region 1 of the hepatitis C virus E2 glycoprotein, the

scavenger receptor BI, and high-density lipoprotein promotes both enhancement of infection and protection against neutralizing antibodies. J Virol 79: 8217-8229.

31. Voisset C, Callens N, Blanchard E, Op De Beeck A, Dubuisson J, et al. (2005) High density lipoproteins facilitate hepatitis C virus entry through the scavenger receptor class B type I. J Biol Chem 280: 7793-7799.

32. Barth H, Schafer C, Adah MI, Zhang F, Linhardt RJ, et al. (2003) Cellular binding of hepatitis C virus envelope glycoprotein E2 requires cell surface heparan sulfate. J Biol Chem 278: 41003-41012.

33. Barth H, Schnober EK, Zhang F, Linhardt RJ, Depla E, et al. (2006) Viral and cellular determinants of the hepatitis C virus envelope-heparan sulfate interaction. J Virol 80: 10579-10590.

34. Lozach PY, Lortat-Jacob H, de Lacroix de Lavalette A, Staropoli I, Foung S, et al. (2003) DC-SIGN and L-SIGN are high affinity binding receptors for hepatitis C virus glycoprotein E2. J Biol Chem 278: 20358-20366.

35. Gardner JP, Durso RJ, Arrigale RR, Donovan GP, Maddon PJ, et al. (2003) L-SIGN (CD 209L) is a liver-specific capture receptor for hepatitis C virus. Proc Natl Acad Sci U S A 100: 4498-4503.

36. Pohlmann S, Zhang J, Baribaud F, Chen Z, Leslie GJ, et al. (2003) Hepatitis C virus glycoproteins interact with DC-SIGN and DC-SIGNR. J Virol 77: 4070-4080.

37. Saunier B, Triyatni M, Ulianich L, Maruvada P, Yen P, et al. (2003) Role of the asialoglycoprotein receptor in binding and entry of hepatitis C virus structural proteins in cultured human hepatocytes. J Virol 77: 546-559.

38. Pileri P, Uematsu Y, Campagnoli S, Galli G, Falugi F, et al. (1998) Binding of hepatitis C virus to CD81. Science 282: 938-941.

39. Hsu M, Zhang J, Flint M, Logvinoff C, Cheng-Mayer C, et al. (2003) Hepatitis C virus glycoproteins mediate pH-dependent cell entry of pseudotyped retroviral particles. Proc Natl Acad Sci U S A 100: 7271-7276.

40. McKeating JA, Zhang LQ, Logvinoff C, Flint M, Zhang J, et al. (2004) Diverse hepatitis C virus glycoproteins mediate viral infection in a CD81-dependent manner. J Virol 78: 8496-8505.

41. Lavillette D, Tarr AW, Voisset C, Donot P, Bartosch B, et al. (2005) Characterization of host-range and cell entry properties of the major genotypes and subtypes of hepatitis C virus. Hepatology 41: 265-274.

42. Zhang J, Randall G, Higginbottom A, Monk P, Rice CM, et al. (2004) CD81 is required for hepatitis C virus glycoprotein-mediated viral infection. J Virol 78: 1448-1455.

43. Lindenbach BD, Evans MJ, Syder AJ, Wolk B, Tellinghuisen TL, et al. (2005) Complete replication of hepatitis C virus in cell culture. Science 309: 623-626.

44. Zhong J, Gastaminza P, Cheng G, Kapadia S, Kato T, et al. (2005) Robust hepatitis C virus infection *in vitro*. Proc Natl Acad Sci U S A 102: 9294-9299.

45. Aly HH, Watashi K, Hijikata M, Kaneko H, Takada Y, et al. (2007) Serum-derived hepatitis C virus infectivity in interferon regulatory factor-7-suppressed human primary hepatocytes. J Hepatol 46: 26-36.

46. Grove J, Huby T, Stamataki Z, Vanwolleghem T, Meuleman P, et al. (2007) Scavenger receptor BI and BII expression levels modulate hepatitis C virus infectivity. J Virol 81: 3162-3169.

47. Evans MJ, von Hahn T, Tscherne DM, Syder AJ, Panis M, et al. (2007) Claudin-1 is a hepatitis C virus co-receptor required for a late step in entry. Nature 446: 801-805.

48. Koutsoudakis G, Herrmann E, Kallis S, Bartenschlager R, Pietschmann T (2007) The level of CD81 cell surface expression is a key determinant for productive entry of hepatitis C virus into host cells. J Virol 81: 588-598.

49. Bartosch B, Vitelli A, Granier C, Goujon C, Dubuisson J, et al. (2003) Cell entry of hepatitis C virus requires a set of co-receptors that include the CD81 tetraspanin and the SR-B1 scavenger receptor. J Biol Chem 278: 41624-41630.

50. Blight KJ, McKeating JA, Rice CM (2002) Highly permissive cell lines for subgenomic and genomic hepatitis C virus RNA replication. J Virol 76: 13001-13014.

51. Koutsoudakis G, Kaul A, Steinmann E, Kallis S, Lohmann V, et al. (2006) Characterization of the early steps of hepatitis C virus infection by using luciferase reporter viruses. J Virol 80: 5308-5320.

52. Cormier EG, Tsamis F, Kajumo F, Durso RJ, Gardner JP, et al. (2004) CD81 is an entry coreceptor for hepatitis C virus. Proc Natl Acad Sci U S A 101: 7270-7274.

53. Rubinstein E, Ziyyat A, Wolf JP, Le Naour F, Boucheix C (2006) The molecular players of sperm-egg fusion in mammals. Semin Cell Dev Biol 17: 254-263.

54. Levy S, Shoham T (2005) The tetraspanin web modulates immune-signalling complexes. Nat Rev Immunol 5: 136-148.

55. Scarselli E, Ansuini H, Cerino R, Roccasecca RM, Acali S, et al. (2002) The human scavenger receptor class B type I is a novel candidate receptor for the hepatitis C virus. EMBO J 21: 5017-5025.

56. Rigotti A, Miettinen HE, Krieger M (2003) The role of the high-density lipoprotein receptor SR-BI in the lipid metabolism of endocrine and other tissues. Endocr Rev 24: 357-387.

57. Voisset C, Op de Beeck A, Horellou P, Dreux M, Gustot T, et al. (2006) High-density lipoproteins reduce the neutralizing effect of hepatitis C virus (HCV)-infected patient antibodies by promoting HCV entry. J Gen Virol 87: 2577-2581.

58. Kapadia SB, Barth H, Baumert T, McKeating JA, Chisari FV (2007) Initiation of hepatitis C virus infection is dependent on cholesterol and cooperativity between CD81 and scavenger receptor B type I. J Virol 81: 374-383.

59. Catanese MT, Graziani R, von Hahn T, Moreau M, Huby T, et al. (2007) High-avidity monoclonal antibodies against the human scavenger class B type I receptor efficiently block hepatitis C virus infection in the presence of high-density lipoprotein. J Virol 81: 8063-8071.

60. Furuse M, Tsukita S (2006) Claudins in occluding junctions of humans and flies. Trends Cell Biol 16: 181-188.

61. Timpe JM, Stamataki Z, Jennings A, Hu K, Farquhar MJ, et al. (2008) Hepatitis C virus cell-cell transmission in hepatoma cells in the presence of neutralizing antibodies. Hepatology 47: 17-24.

62. Zheng A, Yuan F, Li Y, Zhu F, Hou P, et al. (2007) Claudin-6 and claudin-9 function as additional coreceptors for hepatitis C virus. J Virol 81: 12465-12471.

63. Liu S, Yang W, Shen L, Turner JR, Coyne CB, et al. (2009) Tight junction proteins claudin-1 and occludin control hepatitis C virus entry and are downregulated during infection to prevent superinfection. J Virol 83: 2011-2014.

64. Ploss A, Evans MJ, Gaysinskaya VA, Panis M, You H, et al. (2009) Human occludin is a hepatitis C virus entry factor required for infection of mouse cells. Nature 457: 882-886.

65. Blanchard E, Belouzard S, Goueslain L, Wakita T, Dubuisson J, et al. (2006) Hepatitis C virus entry depends on clathrin-mediated endocytosis. J Virol 80: 6964-6972.

66. Meertens L, Bertaux C, Dragic T (2006) Hepatitis C virus entry requires a critical postinternalization step and delivery to early endosomes via clathrin-coated vesicles. J Virol 80: 11571-11578.

67. Codran A, Royer C, Jaeck D, Bastien-Valle M, Baumert TF, et al. (2006) Entry of hepatitis C virus pseudotypes into primary human hepatocytes by clathrin-dependent endocytosis. J Gen Virol 87: 2583-2593.

68. Tscherne DM, Jones CT, Evans MJ, Lindenbach BD, McKeating JA, et al. (2006) Time- and temperature-dependent activation of hepatitis C virus for low-pH-triggered entry. J Virol 80: 1734-1741.

69. Kobayashi M, Bennett MC, Bercot T, Singh IR (2006) Functional analysis of hepatitis C virus envelope proteins, using a cell-cell fusion assay. J Virol 80: 1817-1825.

70. Moradpour D, Penin F, Rice CM (2007) Replication of hepatitis C virus. Nat Rev Microbiol 5: 453-463.

71. Friebe P, Lohmann V, Krieger N, Bartenschlager R (2001) Sequences in the 5' nontranslated region of hepatitis C virus required for RNA replication. J Virol 75: 12047-12057.

72. Spahn CM, Kieft JS, Grassucci RA, Penczek PA, Zhou K, et al. (2001) Hepatitis C virus IRES RNA-induced changes in the conformation of the 40s ribosomal subunit. Science 291: 1959-1962.

73. Ji H, Fraser CS, Yu Y, Leary J, Doudna JA (2004) Coordinated assembly of human translation initiation complexes by the hepatitis C virus internal ribosome entry site RNA. Proc Natl Acad Sci U S A 101: 16990-16995.

74. Otto GA, Puglisi JD (2004) The pathway of HCV IRES-mediated translation initiation. Cell 119: 369-380.

75. Kolykhalov AA, Feinstone SM, Rice CM (1996) Identification of a highly conserved sequence element at the 3' terminus of hepatitis C virus genome RNA. J Virol 70: 3363-3371.

76. Tanaka T, Kato N, Cho MJ, Sugiyama K, Shimotohno K (1996) Structure of the 3' terminus of the hepatitis C virus genome. J Virol 70: 3307-3312.

77. Friebe P, Bartenschlager R (2002) Genetic analysis of sequences in the 3' nontranslated region of hepatitis C virus that are important for RNA replication. J Virol 76: 5326-5338.

78. Yi M, Lemon SM (2003) 3' nontranslated RNA signals required for replication of hepatitis C virus RNA. J Virol 77: 3557-3568.

79. Friebe P, Boudet J, Simorre JP, Bartenschlager R (2005) Kissing-loop interaction in the 3' end of the hepatitis C virus genome essential for RNA replication. J Virol 79: 380-392.

80. Yi M, Lemon SM (2003) Structure-function analysis of the 3' stem-loop of hepatitis C virus genomic RNA and its role in viral RNA replication. RNA 9: 331-345.

81. Yanagi M, St Claire M, Emerson SU, Purcell RH, Bukh J (1999) *In vivo* analysis of the 3' untranslated region of the hepatitis C virus after *in vitro* mutagenesis of an infectious cDNA clone. Proc Natl Acad Sci U S A 96: 2291-2295.

82. Tellinghuisen TL, Evans MJ, von Hahn T, You S, Rice CM (2007) Studying hepatitis C virus: making the best of a bad virus. J Virol 81: 8853-8867.

83. Boulant S, Montserret R, Hope RG, Ratinier M, Targett-Adams P, et al. (2006) Structural determinants that target the hepatitis C virus core protein to lipid droplets. J Biol Chem 281: 22236-22247.

84. McLauchlan J, Lemberg MK, Hope G, Martoglio B (2002) Intramembrane proteolysis promotes trafficking of hepatitis C virus core protein to lipid droplets. EMBO J 21: 3980-3988.

85. Asselah T, Rubbia-Brandt L, Marcellin P, Negro F (2006) Steatosis in chronic hepatitis C: why does it really matter? Gut 55: 123-130.

86. Branch AD, Stump DD, Gutierrez JA, Eng F, Walewski JL (2005) The hepatitis C virus alternate reading frame (ARF) and its family of novel products: the alternate reading frame protein/F-protein, the double-frameshift protein, and others. Semin Liver Dis 25: 105-117.

87. McMullan LK, Grakoui A, Evans MJ, Mihalik K, Puig M, et al. (2007) Evidence for a functional RNA element in the hepatitis C virus core gene. Proc Natl Acad Sci U S A 104: 2879-2884.

88. Op De Beeck A, Cocquerel L, Dubuisson J (2001) Biogenesis of hepatitis C virus envelope glycoproteins. J Gen Virol 82: 2589-2595.

89. Lavie M, Goffard A, Dubuisson J (2006) HCV Glycoproteins: Assembly of a Functional E1-E2 Heterodimer.

90. Carrere-Kremer S, Montpellier C, Lorenzo L, Brulin B, Cocquerel L, et al. (2004) Regulation of hepatitis C virus polyprotein processing by signal peptidase involves structural determinants at the p7 sequence junctions. J Biol Chem 279: 41384-41392.

91. Cocquerel L, Meunier JC, Pillez A, Wychowski C, Dubuisson J (1998) A retention signal necessary and sufficient for endoplasmic reticulum localization maps to the transmembrane domain of hepatitis C virus glycoprotein E2. J Virol 72: 2183-2191.

92. Cocquerel L, Duvet S, Meunier JC, Pillez A, Cacan R, et al. (1999) The transmembrane domain of hepatitis C virus glycoprotein E1 is a signal for static retention in the endoplasmic reticulum. J Virol 73: 2641-2649.

93. Cocquerel L, Meunier JC, Op de Beeck A, Bonte D, Wychowski C, et al. (2001) Coexpression of hepatitis C virus envelope proteins E1 and E2 in cis improves the stability of membrane insertion of E2. J Gen Virol 82: 1629-1635.

94. Charloteaux B, Lins L, Moereels H, Brasseur R (2002) Analysis of the C-terminal membrane anchor domains of hepatitis C virus glycoproteins E1 and E2: toward a topological model. J Virol 76: 1944-1958.

95. Cocquerel L, Wychowski C, Minner F, Penin F, Dubuisson J (2000) Charged residues in the transmembrane domains of hepatitis C virus glycoproteins play a major role in the processing, subcellular localization, and assembly of these envelope proteins. J Virol 74: 3623-3633.

96. Op De Beeck A, Montserret R, Duvet S, Cocquerel L, Cacan R, et al. (2000) The transmembrane domains of hepatitis C virus envelope glycoproteins E1 and E2 play a major role in heterodimerization. J Biol Chem 275: 31428-31437.

97. Cocquerel L, Op de Beeck A, Lambot M, Roussel J, Delgrange D, et al. (2002) Topological changes in the transmembrane domains of hepatitis C virus envelope glycoproteins. EMBO J 21: 2893-2902.

98. Falkowska E, Kajumo F, Garcia E, Reinus J, Dragic T (2007) Hepatitis C virus envelope glycoprotein E2 glycans modulate entry, CD81 binding, and neutralization. J Virol 81: 8072-8079.

99. Wei X, Decker JM, Wang S, Hui H, Kappes JC, et al. (2003) Antibody neutralization and escape by HIV-1. Nature 422: 307-312.

100. Meunier JC, Fournillier A, Choukhi A, Cahour A, Cocquerel L, et al. (1999) Analysis of the glycosylation sites of hepatitis C virus (HCV) glycoprotein E1 and the influence of E1 glycans on the formation of the HCV glycoprotein complex. J Gen Virol 80 (Pt 4): 887-896.

101. Goffard A, Dubuisson J (2003) Glycosylation of hepatitis C virus envelope proteins. Biochimie 85: 295-301.

102. Zhang M, Gaschen B, Blay W, Foley B, Haigwood N, et al. (2004) Tracking global patterns of N-linked glycosylation site variation in highly variable viral glycoproteins: HIV, SIV, and HCV envelopes and influenza hemagglutinin. Glycobiology 14: 1229-1246.

103. Slater-Handshy T, Droll DA, Fan X, Di Bisceglie AM, Chambers TJ (2004) HCV E2 glycoprotein: mutagenesis of N-linked glycosylation sites and its effects on E2 expression and processing. Virology 319: 36-48.

104. Goffard A, Callens N, Bartosch B, Wychowski C, Cosset FL, et al. (2005) Role of N-linked glycans in the functions of hepatitis C virus envelope glycoproteins. J Virol 79: 8400-8409.

105. Deleersnyder V, Pillez A, Wychowski C, Blight K, Xu J, et al. (1997) Formation of native hepatitis C virus glycoprotein complexes. J Virol 71: 697-704.

106. Michalak JP, Wychowski C, Choukhi A, Meunier JC, Ung S, et al. (1997) Characterization of truncated forms of hepatitis C virus glycoproteins. J Gen Virol 78 (Pt 9): 2299-2306.

107. Patel J, Patel AH, McLauchlan J (2001) The transmembrane domain of the hepatitis C virus E2 glycoprotein is required for correct folding of the E1 glycoprotein and native complex formation. Virology 279: 58-68.

108. Cocquerel L, Kuo CC, Dubuisson J, Levy S (2003) CD81-dependent binding of hepatitis C virus E1E2 heterodimers. J Virol 77: 10677-10683.

109. Brazzoli M, Helenius A, Foung SK, Houghton M, Abrignani S, et al. (2005) Folding and dimerization of hepatitis C virus E1 and E2 glycoproteins in stably transfected CHO cells. Virology 332: 438-453.

110. Choukhi A, Ung S, Wychowski C, Dubuisson J (1998) Involvement of endoplasmic reticulum chaperones in the folding of hepatitis C virus glycoproteins. J Virol 72: 3851-3858.

111. Trombetta ES, Helenius A (1998) Lectins as chaperones in glycoprotein folding. Curr Opin Struct Biol 8: 587-592.

112. Flint M, Maidens C, Loomis-Price LD, Shotton C, Dubuisson J, et al. (1999) Characterization of hepatitis C virus E2 glycoprotein interaction with a putative cellular receptor, CD81. J Virol 73: 6235-6244.

113. Forns X, Allander T, Rohwer-Nutter P, Bukh J (2000) Characterization of modified hepatitis C virus E2 proteins expressed on the cell surface. Virology 274: 75-85.

114. Yagnik AT, Lahm A, Meola A, Roccasecca RM, Ercole BB, et al. (2000) A model for the hepatitis C virus envelope glycoprotein E2. Proteins 40: 355-366.

115. Clayton RF, Owsianka A, Aitken J, Graham S, Bhella D, et al. (2002) Analysis of antigenicity and topology of E2 glycoprotein present on recombinant hepatitis C virus-like particles. J Virol 76: 7672-7682.

116. Weiner AJ, Christopherson C, Hall JE, Bonino F, Saracco G, et al. (1991) Sequence variation in hepatitis C viral isolates. J Hepatol 13 Suppl 4: S6-14.

117. Farci P, Shimoda A, Wong D, Cabezon T, De Gioannis D, et al. (1996) Prevention of hepatitis C virus infection in chimpanzees by hyperimmune serum against the

hypervariable region 1 of the envelope 2 protein. Proc Natl Acad Sci U S A 93: 15394-15399.

118. Kato N, Sekiya H, Ootsuyama Y, Nakazawa T, Hijikata M, et al. (1993) Humoral immune response to hypervariable region 1 of the putative envelope glycoprotein (gp70) of hepatitis C virus. J Virol 67: 3923-3930.

119. Forns X, Thimme R, Govindarajan S, Emerson SU, Purcell RH, et al. (2000) Hepatitis C virus lacking the hypervariable region 1 of the second envelope protein is infectious and causes acute resolving or persistent infection in chimpanzees. Proc Natl Acad Sci U S A 97: 13318-13323.

120. Keck ZY, Sung VM, Perkins S, Rowe J, Paul S, et al. (2004) Human monoclonal antibody to hepatitis C virus E1 glycoprotein that blocks virus attachment and viral infectivity. J Virol 78: 7257-7263.

121. Keck ZY, Op De Beeck A, Hadlock KG, Xia J, Li TK, et al. (2004) Hepatitis C virus E2 has three immunogenic domains containing conformational epitopes with distinct properties and biological functions. J Virol 78: 9224-9232.

122. Whidby J, Mateu G, Scarborough H, Demeler B, Grakoui A, et al. (2009) Blocking hepatitis C virus infection with recombinant form of envelope protein 2 ectodomain. J Virol 83: 11078-11089.

123. Dubuisson J (2000) Folding, assembly and subcellular localization of hepatitis C virus glycoproteins. Curr Top Microbiol Immunol 242: 135-148.

124. Flint M, Thomas JM, Maidens CM, Shotton C, Levy S, et al. (1999) Functional analysis of cell surface-expressed hepatitis C virus E2 glycoprotein. J Virol 73: 6782-6790.

125. Garry RF, Dash S (2003) Proteomics computational analyses suggest that hepatitis C virus E1 and pestivirus E2 envelope glycoproteins are truncated class II fusion proteins. Virology 307: 255-265.

126. Earp LJ, Delos SE, Park HE, White JM (2005) The many mechanisms of viral membrane fusion proteins. Curr Top Microbiol Immunol 285: 25-66.

127. Colman PM, Lawrence MC (2003) The structural biology of type I viral membrane fusion. Nat Rev Mol Cell Biol 4: 309-319.

128. Op De Beeck A, Voisset C, Bartosch B, Ciczora Y, Cocquerel L, et al. (2004) Characterization of functional hepatitis C virus envelope glycoproteins. J Virol 78: 2994-3002.

129. Carrere-Kremer S, Montpellier-Pala C, Cocquerel L, Wychowski C, Penin F, et al. (2002) Subcellular localization and topology of the p7 polypeptide of hepatitis C virus. J Virol 76: 3720-3730.

130. Sakai A, Claire MS, Faulk K, Govindarajan S, Emerson SU, et al. (2003) The p7 polypeptide of hepatitis C virus is critical for infectivity and contains functionally important genotype-specific sequences. Proc Natl Acad Sci U S A 100: 11646-11651.

131. Griffin SD, Beales LP, Clarke DS, Worsfold O, Evans SD, et al. (2003) The p7 protein of hepatitis C virus forms an ion channel that is blocked by the antiviral drug, Amantadine. FEBS Lett 535: 34-38.

132. Pavlovic D, Neville DC, Argaud O, Blumberg B, Dwek RA, et al. (2003) The hepatitis C virus p7 protein forms an ion channel that is inhibited by long-alkyl-chain iminosugar derivatives. Proc Natl Acad Sci U S A 100: 6104-6108.

133. Grakoui A, McCourt DW, Wychowski C, Feinstone SM, Rice CM (1993) A second hepatitis C virus-encoded proteinase. Proc Natl Acad Sci U S A 90: 10583-10587.

134. Hijikata M, Mizushima H, Akagi T, Mori S, Kakiuchi N, et al. (1993) Two distinct proteinase activities required for the processing of a putative nonstructural precursor protein of hepatitis C virus. J Virol 67: 4665-4675.

135. Lorenz IC, Marcotrigiano J, Dentzer TG, Rice CM (2006) Structure of the catalytic domain of the hepatitis C virus NS2-3 protease. Nature 442: 831-835.

136. Pallaoro M, Lahm A, Biasiol G, Brunetti M, Nardella C, et al. (2001) Characterization of the hepatitis C virus NS2/3 processing reaction by using a purified precursor protein. J Virol 75: 9939-9946.

137. Thibeault D, Maurice R, Pilote L, Lamarre D, Pause A (2001) *In vitro* characterization of a purified NS2/3 protease variant of hepatitis C virus. J Biol Chem 276: 46678-46684.

138. Kolykhalov AA, Mihalik K, Feinstone SM, Rice CM (2000) Hepatitis C virus-encoded enzymatic activities and conserved RNA elements in the 3' nontranslated region are essential for virus replication *in vivo*. J Virol 74: 2046-2051.

139. Pietschmann T, Kaul A, Koutsoudakis G, Shavinskaya A, Kallis S, et al. (2006) Construction and characterization of infectious intragenotypic and intergenotypic hepatitis C virus chimeras. Proc Natl Acad Sci U S A 103: 7408-7413.

140. Kalinina O, Norder H, Mukomolov S, Magnius LO (2002) A natural intergenotypic recombinant of hepatitis C virus identified in St. Petersburg. J Virol 76: 4034-4043.

141. Noppornpanth S, Lien TX, Poovorawan Y, Smits SL, Osterhaus AD, et al. (2006) Identification of a naturally occurring recombinant genotype 2/6 hepatitis C virus. J Virol 80: 7569-7577.

142. Wolk B, Sansonno D, Krausslich HG, Dammacco F, Rice CM, et al. (2000) Subcellular localization, stability, and trans-cleavage competence of the hepatitis C virus NS3-NS4A complex expressed in tetracycline-regulated cell lines. J Virol 74: 2293-2304.

143. Pause A, Kukolj G, Bailey M, Brault M, Do F, et al. (2003) An NS3 serine protease inhibitor abrogates replication of subgenomic hepatitis C virus RNA. J Biol Chem 278: 20374-20380.

144. Lamarre D, Anderson PC, Bailey M, Beaulieu P, Bolger G, et al. (2003) An NS3 protease inhibitor with antiviral effects in humans infected with hepatitis C virus. Nature 426: 186-189.

145. Serebrov V, Pyle AM (2004) Periodic cycles of RNA unwinding and pausing by hepatitis C virus NS3 helicase. Nature 430: 476-480.

146. Levin MK, Gurjar M, Patel SS (2005) A Brownian motor mechanism of translocation and strand separation by hepatitis C virus helicase. Nat Struct Mol Biol 12: 429-435.

147. Dumont S, Cheng W, Serebrov V, Beran RK, Tinoco I, Jr., et al. (2006) RNA translocation and unwinding mechanism of HCV NS3 helicase and its coordination by ATP. Nature 439: 105-108.

148. Frick DN, Rypma RS, Lam AM, Gu B (2004) The nonstructural protein 3 protease/helicase requires an intact protease domain to unwind duplex RNA efficiently. J Biol Chem 279: 1269-1280.

149. Yu GY, Lee KJ, Gao L, Lai MM (2006) Palmitoylation and polymerization of hepatitis C virus NS4B protein. J Virol 80: 6013-6023.

150. Egger D, Wolk B, Gosert R, Bianchi L, Blum HE, et al. (2002) Expression of hepatitis C virus proteins induces distinct membrane alterations including a candidate viral replication complex. J Virol 76: 5974-5984.

151. Tellinghuisen TL, Marcotrigiano J, Gorbalenya AE, Rice CM (2004) The NS5A protein of hepatitis C virus is a zinc metalloprotein. J Biol Chem 279: 48576-48587.

152. Penin F, Brass V, Appel N, Ramboarina S, Montserret R, et al. (2004) Structure and function of the membrane anchor domain of hepatitis C virus nonstructural protein 5A. J Biol Chem 279: 40835-40843.

153. Tellinghuisen TL, Marcotrigiano J, Rice CM (2005) Structure of the zinc-binding domain of an essential component of the hepatitis C virus replicase. Nature 435: 374-379.

154. Huang L, Hwang J, Sharma SD, Hargittai MR, Chen Y, et al. (2005) Hepatitis C virus nonstructural protein 5A (NS5A) is an RNA-binding protein. J Biol Chem 280: 36417-36428.

155. Quinkert D, Bartenschlager R, Lohmann V (2005) Quantitative analysis of the hepatitis C virus replication complex. J Virol 79: 13594-13605.

156. Miyanari Y, Hijikata M, Yamaji M, Hosaka M, Takahashi H, et al. (2003) Hepatitis C virus non-structural proteins in the probable membranous compartment function in viral genome replication. J Biol Chem 278: 50301-50308.

157. Wang QM, Hockman MA, Staschke K, Johnson RB, Case KA, et al. (2002) Oligomerization and cooperative RNA synthesis activity of hepatitis C virus RNA-dependent RNA polymerase. J Virol 76: 3865-3872.

158. Ago H, Adachi T, Yoshida A, Yamamoto M, Habuka N, et al. (1999) Crystal structure of the RNA-dependent RNA polymerase of hepatitis C virus. Structure 7: 1417-1426.

159. Lesburg CA, Cable MB, Ferrari E, Hong Z, Mannarino AF, et al. (1999) Crystal structure of the RNA-dependent RNA polymerase from hepatitis C virus reveals a fully encircled active site. Nat Struct Biol 6: 937-943.

160. Bressanelli S, Tomei L, Rey FA, De Francesco R (2002) Structural analysis of the hepatitis C virus RNA polymerase in complex with ribonucleotides. J Virol 76: 3482-3492.

161. Butcher SJ, Grimes JM, Makeyev EV, Bamford DH, Stuart DI (2001) A mechanism for initiating RNA-dependent RNA polymerization. Nature 410: 235-240.

162. Schwartz M, Chen J, Janda M, Sullivan M, den Boon J, et al. (2002) A positive-strand RNA virus replication complex parallels form and function of retrovirus capsids. Mol Cell 9: 505-514.

163. Lyle JM, Bullitt E, Bienz K, Kirkegaard K (2002) Visualization and functional analysis of RNA-dependent RNA polymerase lattices. Science 296: 2218-2222.

164. Watashi K, Ishii N, Hijikata M, Inoue D, Murata T, et al. (2005) Cyclophilin B is a functional regulator of hepatitis C virus RNA polymerase. Mol Cell 19: 111-122.

165. Okamoto T, Nishimura Y, Ichimura T, Suzuki K, Miyamura T, et al. (2006) Hepatitis C virus RNA replication is regulated by FKBP8 and Hsp90. EMBO J 25: 5015-5025.

166. Mateu G, Donis RO, Wakita T, Bukh J, Grakoui A (2008) Intragenotypic JFH1 based recombinant hepatitis C virus produces high levels of infectious particles but causes increased cell death. Virology 376: 397-407.

167. Bartenschlager R, Pietschmann T (2005) Efficient hepatitis C virus cell culture system: what a difference the host cell makes. Proc Natl Acad Sci U S A 102: 9739-9740.

168. Huang H, Sun F, Owen DM, Li W, Chen Y, et al. (2007) Hepatitis C virus production by human hepatocytes dependent on assembly and secretion of very low-density lipoproteins. Proc Natl Acad Sci U S A 104: 5848-5853.

169. Gastaminza P, Kapadia SB, Chisari FV (2006) Differential biophysical properties of infectious intracellular and secreted hepatitis C virus particles. J Virol 80: 11074-11081.

170. Lai CK, Jeng KS, Machida K, Lai MM (2010) Hepatitis C virus egress and release depend on endosomal trafficking of core protein. J Virol 84: 11590-11598.

171. Hoofnagle JH, Mullen KD, Jones DB, Rustgi V, Di Bisceglie A, et al. (1986) Treatment of chronic non-A,non-B hepatitis with recombinant human alpha interferon. A preliminary report. N Engl J Med 315: 1575-1578.

172. Lau DT, Kleiner DE, Ghany MG, Park Y, Schmid P, et al. (1998) 10-Year follow-up after interferon-alpha therapy for chronic hepatitis C. Hepatology 28: 1121-1127.

173. de Veer MJ, Holko M, Frevel M, Walker E, Der S, et al. (2001) Functional classification of interferon-stimulated genes identified using microarrays. J Leukoc Biol 69: 912-920.

174. Bekisz J, Schmeisser H, Hernandez J, Goldman ND, Zoon KC (2004) Human interferons alpha, beta and omega. Growth Factors 22: 243-251.

175. Sen GC (2001) Viruses and interferons. Annu Rev Microbiol 55: 255-281.

176. Di Bisceglie AM, Hoofnagle JH (2002) Optimal therapy of hepatitis C. Hepatology 36: S121-127.

177. McHutchison JG, Poynard T (1999) Combination therapy with interferon plus ribavirin for the initial treatment of chronic hepatitis C. Semin Liver Dis 19 Suppl 1: 57-65.

178. Feld JJ, Hoofnagle JH (2005) Mechanism of action of interferon and ribavirin in treatment of hepatitis C. Nature 436: 967-972.

179. Maag D, Castro C, Hong Z, Cameron CE (2001) Hepatitis C virus RNA-dependent RNA polymerase (NS5B) as a mediator of the antiviral activity of ribavirin. J Biol Chem 276: 46094-46098.

180. Crotty S, Maag D, Arnold JJ, Zhong W, Lau JY, et al. (2000) The broad-spectrum antiviral ribonucleoside ribavirin is an RNA virus mutagen. Nat Med 6: 1375-1379.

181. Crotty S, Cameron CE, Andino R (2001) RNA virus error catastrophe: direct molecular test by using ribavirin. Proc Natl Acad Sci U S A 98: 6895-6900.

182. Zhou S, Liu R, Baroudy BM, Malcolm BA, Reyes GR (2003) The effect of ribavirin and IMPDH inhibitors on hepatitis C virus subgenomic replicon RNA. Virology 310: 333-342.

183. Tam RC, Pai B, Bard J, Lim C, Averett DR, et al. (1999) Ribavirin polarizes human T cell responses towards a Type 1 cytokine profile. J Hepatol 30: 376-382.

184. Zhang Y, Jamaluddin M, Wang S, Tian B, Garofalo RP, et al. (2003) Ribavirin treatment up-regulates antiviral gene expression via the interferon-stimulated response element in respiratory syncytial virus-infected epithelial cells. J Virol 77: 5933-5947.

185. Glue P, Fang JW, Rouzier-Panis R, Raffanel C, Sabo R, et al. (2000) Pegylated interferon-alpha2b: pharmacokinetics, pharmacodynamics, safety, and preliminary efficacy data. Hepatitis C Intervention Therapy Group. Clin Pharmacol Ther 68: 556-567.

186. Zeuzem S, Feinman SV, Rasenack J, Heathcote EJ, Lai MY, et al. (2000) Peginterferon alfa-2a in patients with chronic hepatitis C. N Engl J Med 343: 1666-1672.

187. Heathcote EJ, Shiffman ML, Cooksley WG, Dusheiko GM, Lee SS, et al. (2000) Peginterferon alfa-2a in patients with chronic hepatitis C and cirrhosis. N Engl J Med 343: 1673-1680.

188. Lindsay KL, Trepo C, Heintges T, Shiffman ML, Gordon SC, et al. (2001) A randomized, double-blind trial comparing pegylated interferon alfa-2b to interferon alfa-2b as initial treatment for chronic hepatitis C. Hepatology 34: 395-403.

189. Manns MP, McHutchison JG, Gordon SC, Rustgi VK, Shiffman M, et al. (2001) Peginterferon alfa-2b plus ribavirin compared with interferon alfa-2b plus ribavirin for initial treatment of chronic hepatitis C: a randomised trial. Lancet 358: 958-965.

190. Hadziyannis SJ, Sette H, Jr., Morgan TR, Balan V, Diago M, et al. (2004) Peginterferon-alpha2a and ribavirin combination therapy in chronic hepatitis C: a randomized study of treatment duration and ribavirin dose. Ann Intern Med 140: 346-355.

191. Fried MW, Shiffman ML, Reddy KR, Smith C, Marinos G, et al. (2002) Peginterferon alfa-2a plus ribavirin for chronic hepatitis C virus infection. N Engl J Med 347: 975-982.

192. Strader DB (2002) Understudied populations with hepatitis C. Hepatology 36: S226-236.

193. Hinrichsen H, Benhamou Y, Wedemeyer H, Reiser M, Sentjens RE, et al. (2004) Short-term antiviral efficacy of BILN 2061, a hepatitis C virus serine protease inhibitor, in hepatitis C genotype 1 patients. Gastroenterology 127: 1347-1355.

194. Reiser M, Hinrichsen H, Benhamou Y, Reesink HW, Wedemeyer H, et al. (2005) Antiviral efficacy of NS3-serine protease inhibitor BILN-2061 in patients with chronic genotype 2 and 3 hepatitis C. Hepatology 41: 832-835.

195. Lin C, Lin K, Luong YP, Rao BG, Wei YY, et al. (2004) *In vitro* resistance studies of hepatitis C virus serine protease inhibitors, VX-950 and BILN 2061: structural analysis indicates different resistance mechanisms. J Biol Chem 279: 17508-17514.

196. Beaulieu PL, Tsantrizos YS (2004) Inhibitors of the HCV NS5B polymerase: new hope for the treatment of hepatitis C infections. Curr Opin Investig Drugs 5: 838-850.

197. Foster GR (2004) Past, present, and future hepatitis C treatments. Semin Liver Dis 24 Suppl 2: 97-104.

198. Yokota T, Sakamoto N, Enomoto N, Tanabe Y, Miyagishi M, et al. (2003) Inhibition of intracellular hepatitis C virus replication by synthetic and vector-derived small interfering RNAs. EMBO Rep 4: 602-608.

199. Wilson JA, Jayasena S, Khvorova A, Sabatinos S, Rodrigue-Gervais IG, et al. (2003) RNA interference blocks gene expression and RNA synthesis from hepatitis C replicons propagated in human liver cells. Proc Natl Acad Sci U S A 100: 2783-2788.

200. Kronke J, Kittler R, Buchholz F, Windisch MP, Pietschmann T, et al. (2004) Alternative approaches for efficient inhibition of hepatitis C virus RNA replication by small interfering RNAs. J Virol 78: 3436-3446.

201. Kapadia SB, Brideau-Andersen A, Chisari FV (2003) Interference of hepatitis C virus RNA replication by short interfering RNAs. Proc Natl Acad Sci U S A 100: 2014-2018.

202. Randall G, Grakoui A, Rice CM (2003) Clearance of replicating hepatitis C virus replicon RNAs in cell culture by small interfering RNAs. Proc Natl Acad Sci U S A 100: 235-240.

203. Wilson JA, Richardson CD (2005) Hepatitis C virus replicons escape RNA interference induced by a short interfering RNA directed against the NS5b coding region. J Virol 79: 7050-7058.

204. McKenna K, Beignon AS, Bhardwaj N (2005) Plasmacytoid dendritic cells: linking innate and adaptive immunity. J Virol 79: 17-27.

205. Hahn YS (2003) Subversion of immune responses by hepatitis C virus: immunomodulatory strategies beyond evasion? Curr Opin Immunol 15: 443-449.

206. Lemon SM, McKeating JA, Pietschmann T, Frick DN, Glenn JS, et al. (2010) Development of novel therapies for hepatitis C. Antiviral Res 86: 79-92.

207. Sakamoto N, Watanabe M (2009) New therapeutic approaches to hepatitis C virus. J Gastroenterol 44: 643-649.

208. Kolykhalov AA, Agapov EV, Blight KJ, Mihalik K, Feinstone SM, et al. (1997) Transmission of hepatitis C by intrahepatic inoculation with transcribed RNA. Science 277: 570-574.

209. Lohmann V, Korner F, Koch J, Herian U, Theilmann L, et al. (1999) Replication of subgenomic hepatitis C virus RNAs in a hepatoma cell line. Science 285: 110-113.

210. Sumpter R, Jr., Loo YM, Foy E, Li K, Yoneyama M, et al. (2005) Regulating intracellular antiviral defense and permissiveness to hepatitis C virus RNA replication through a cellular RNA helicase, RIG-I. J Virol 79: 2689-2699.

211. Bartenschlager R, Frese M, Pietschmann T (2004) Novel insights into hepatitis C virus replication and persistence. Adv Virus Res 63: 71-180.

212. Blight KJ, Kolykhalov AA, Rice CM (2000) Efficient initiation of HCV RNA replication in cell culture. Science 290: 1972-1974.

213. Blight KJ, McKeating JA, Marcotrigiano J, Rice CM (2003) Efficient replication of hepatitis C virus genotype 1a RNAs in cell culture. J Virol 77: 3181-3190.

214. Moradpour D, Evans MJ, Gosert R, Yuan Z, Blum HE, et al. (2004) Insertion of green fluorescent protein into nonstructural protein 5A allows direct visualization of functional hepatitis C virus replication complexes. J Virol 78: 7400-7409.

215. Ikeda M, Yi M, Li K, Lemon SM (2002) Selectable subgenomic and genome-length dicistronic RNAs derived from an infectious molecular clone of the HCV-N strain of hepatitis C virus replicate efficiently in cultured Huh7 cells. J Virol 76: 2997-3006.

216. Pietschmann T, Lohmann V, Kaul A, Krieger N, Rinck G, et al. (2002) Persistent and transient replication of full-length hepatitis C virus genomes in cell culture. J Virol 76: 4008-4021.

217. Lagging LM, Meyer K, Owens RJ, Ray R (1998) Functional role of hepatitis C virus chimeric glycoproteins in the infectivity of pseudotyped virus. J Virol 72: 3539-3546.

218. Buonocore L, Blight KJ, Rice CM, Rose JK (2002) Characterization of vesicular stomatitis virus recombinants that express and incorporate high levels of hepatitis C virus glycoproteins. J Virol 76: 6865-6872.

219. Matsuura Y, Tani H, Suzuki K, Kimura-Someya T, Suzuki R, et al. (2001) Characterization of pseudotype VSV possessing HCV envelope proteins. Virology 286: 263-275.

220. Triyatni M, Saunier B, Maruvada P, Davis AR, Ulianich L, et al. (2002) Interaction of hepatitis C virus-like particles and cells: a model system for studying viral binding and entry. J Virol 76: 9335-9344.

221. Wellnitz S, Klumpp B, Barth H, Ito S, Depla E, et al. (2002) Binding of hepatitis C virus-like particles derived from infectious clone H77C to defined human cell lines. J Virol 76: 1181-1193.

222. Appel N, Pietschmann T, Bartenschlager R (2005) Mutational analysis of hepatitis C virus nonstructural protein 5A: potential role of differential phosphorylation in RNA replication and identification of a genetically flexible domain. J Virol 79: 3187-3194.

223. Evans MJ, Rice CM, Goff SP (2004) Phosphorylation of hepatitis C virus nonstructural protein 5A modulates its protein interactions and viral RNA replication. Proc Natl Acad Sci U S A 101: 13038-13043.

224. Huang Y, Staschke K, De Francesco R, Tan SL (2007) Phosphorylation of hepatitis C virus NS5A nonstructural protein: a new paradigm for phosphorylation-dependent viral RNA replication? Virology 364: 1-9.

225. Bukh J, Pietschmann T, Lohmann V, Krieger N, Faulk K, et al. (2002) Mutations that permit efficient replication of hepatitis C virus RNA in Huh-7 cells prevent productive replication in chimpanzees. Proc Natl Acad Sci U S A 99: 14416-14421.

226. Kato T, Date T, Miyamoto M, Furusaka A, Tokushige K, et al. (2003) Efficient replication of the genotype 2a hepatitis C virus subgenomic replicon. Gastroenterology 125: 1808-1817.

227. Date T, Kato T, Miyamoto M, Zhao Z, Yasui K, et al. (2004) Genotype 2a hepatitis C virus subgenomic replicon can replicate in HepG2 and IMY-N9 cells. J Biol Chem 279: 22371-22376.

228. Kato T, Date T, Miyamoto M, Zhao Z, Mizokami M, et al. (2005) Nonhepatic cell lines HeLa and 293 support efficient replication of the hepatitis C virus genotype 2a subgenomic replicon. J Virol 79: 592-596.

229. Lindenbach BD, Meuleman P, Ploss A, Vanwolleghem T, Syder AJ, et al. (2006) Cell culture-grown hepatitis C virus is infectious *in vivo* and can be recultured *in vitro*. Proc Natl Acad Sci U S A 103: 3805-3809.

230. Yi M, Lemon SM (2004) Adaptive mutations producing efficient replication of genotype 1a hepatitis C virus RNA in normal Huh7 cells. J Virol 78: 7904-7915.

231. Yi M, Villanueva RA, Thomas DL, Wakita T, Lemon SM (2006) Production of infectious genotype 1a hepatitis C virus (Hutchinson strain) in cultured human hepatoma cells. Proc Natl Acad Sci U S A 103: 2310-2315.

232. Cai Z, Zhang C, Chang KS, Jiang J, Ahn BC, et al. (2005) Robust production of infectious hepatitis C virus (HCV) from stably HCV cDNA-transfected human hepatoma cells. J Virol 79: 13963-13973.

233. Kato T, Matsumura T, Heller T, Saito S, Sapp RK, et al. (2007) Production of infectious hepatitis C virus of various genotypes in cell cultures. J Virol 81: 4405-4411.

234. Bitzegeio J, Bankwitz D, Hueging K, Haid S, Brohm C, et al. (2010) Adaptation of hepatitis C virus to mouse CD81 permits infection of mouse cells in the absence of human entry factors. PLoS Pathog 6: e1000978.

235. McCaffrey AP, Ohashi K, Meuse L, Shen S, Lancaster AM, et al. (2002) Determinants of hepatitis C translational initiation *in vitro*, in cultured cells and mice. Mol Ther 5: 676-684.

236. Uprichard SL, Chung J, Chisari FV, Wakita T (2006) Replication of a hepatitis C virus replicon clone in mouse cells. Virol J 3: 89.

237. Heckel JL, Sandgren EP, Degen JL, Palmiter RD, Brinster RL (1990) Neonatal bleeding in transgenic mice expressing urokinase-type plasminogen activator. Cell 62: 447-456.

238. Meuleman P, Leroux-Roels G (2008) The human liver-uPA-SCID mouse: a model for the evaluation of antiviral compounds against HBV and HCV. Antiviral Res 80: 231-238.

239. Mercer DF, Schiller DE, Elliott JF, Douglas DN, Hao C, et al. (2001) Hepatitis C virus replication in mice with chimeric human livers. Nat Med 7: 927-933.

240. Meuleman P, Libbrecht L, De Vos R, de Hemptinne B, Gevaert K, et al. (2005) Morphological and biochemical characterization of a human liver in a uPA-SCID mouse chimera. Hepatology 41: 847-856.

241. Legrand N, Ploss A, Balling R, Becker PD, Borsotti C, et al. (2009) Humanized mice for modeling human infectious disease: challenges, progress, and outlook. Cell Host Microbe 6: 5-9.

242. Strowig T, Gurer C, Ploss A, Liu YF, Arrey F, et al. (2009) Priming of protective T cell responses against virus-induced tumors in mice with human immune system components. J Exp Med 206: 1423-1434.

243. Masciopinto F, Freer G, Burgio VL, Levy S, Galli-Stampino L, et al. (2002) Expression of human CD81 in transgenic mice does not confer susceptibility to hepatitis C virus infection. Virology 304: 187-196.

244. Bowen DG, Walker CM (2005) The origin of quasispecies: cause or consequence of chronic hepatitis C viral infection? J Hepatol 42: 408-417.

245. Rehermann B (2009) Hepatitis C virus versus innate and adaptive immune responses: a tale of coevolution and coexistence. J Clin Invest 119: 1745-1754.

246. Negro F, Pacchioni D, Shimizu Y, Miller RH, Bussolati G, et al. (1992) Detection of intrahepatic replication of hepatitis C virus RNA by in situ hybridization and comparison with histopathology. Proc Natl Acad Sci U S A 89: 2247-2251.

247. Dahari H, Major M, Zhang X, Mihalik K, Rice CM, et al. (2005) Mathematical modeling of primary hepatitis C infection: noncytolytic clearance and early blockage of virion production. Gastroenterology 128: 1056-1066.

248. Heller T, Rehermann B (2005) Acute hepatitis C: a multifaceted disease. Semin Liver Dis 25: 7-17.

249. Pal S, Shuhart MC, Thomassen L, Emerson SS, Su T, et al. (2006) Intrahepatic hepatitis C virus replication correlates with chronic hepatitis C disease severity *in vivo*. J Virol 80: 2280-2290.

250. Bigger CB, Brasky KM, Lanford RE (2001) DNA microarray analysis of chimpanzee liver during acute resolving hepatitis C virus infection. J Virol 75: 7059-7066.

251. Su AI, Pezacki JP, Wodicka L, Brideau AD, Supekova L, et al. (2002) Genomic analysis of the host response to hepatitis C virus infection. Proc Natl Acad Sci U S A 99: 15669-15674.

252. Saito T, Owen DM, Jiang F, Marcotrigiano J, Gale M, Jr. (2008) Innate immunity induced by composition-dependent RIG-I recognition of hepatitis C virus RNA. Nature 454: 523-527.

253. Kawai T, Akira S (2008) Toll-like receptor and RIG-I-like receptor signaling. Ann N Y Acad Sci 1143: 1-20.

254. Guo JT, Sohn JA, Zhu Q, Seeger C (2004) Mechanism of the interferon alpha response against hepatitis C virus replicons. Virology 325: 71-81.

255. Hui DJ, Bhasker CR, Merrick WC, Sen GC (2003) Viral stress-inducible protein p56 inhibits translation by blocking the interaction of eIF3 with the ternary complex eIF2.GTP.Met-tRNAi. J Biol Chem 278: 39477-39482.

256. Pflugheber J, Fredericksen B, Sumpter R, Jr., Wang C, Ware F, et al. (2002) Regulation of PKR and IRF-1 during hepatitis C virus RNA replication. Proc Natl Acad Sci U S A 99: 4650-4655.

257. Lin W, Kim SS, Yeung E, Kamegaya Y, Blackard JT, et al. (2006) Hepatitis C virus core protein blocks interferon signaling by interaction with the STAT1 SH2 domain. J Virol 80: 9226-9235.

258. Bode JG, Ludwig S, Ehrhardt C, Albrecht U, Erhardt A, et al. (2003) IFN-alpha antagonistic activity of HCV core protein involves induction of suppressor of cytokine signaling-3. FASEB J 17: 488-490.

259. Heim MH, Moradpour D, Blum HE (1999) Expression of hepatitis C virus proteins inhibits signal transduction through the Jak-STAT pathway. J Virol 73: 8469-8475.

260. Polyak SJ, Khabar KS, Paschal DM, Ezelle HJ, Duverlie G, et al. (2001) Hepatitis C virus nonstructural 5A protein induces interleukin-8, leading to partial inhibition of the interferon-induced antiviral response. J Virol 75: 6095-6106.

261. Gale MJ, Jr., Korth MJ, Tang NM, Tan SL, Hopkins DA, et al. (1997) Evidence that hepatitis C virus resistance to interferon is mediated through repression of the PKR protein kinase by the nonstructural 5A protein. Virology 230: 217-227.

262. Taylor DR, Shi ST, Romano PR, Barber GN, Lai MM (1999) Inhibition of the interferon-inducible protein kinase PKR by HCV E2 protein. Science 285: 107-110.

263. Li XD, Sun L, Seth RB, Pineda G, Chen ZJ (2005) Hepatitis C virus protease NS3/4A cleaves mitochondrial antiviral signaling protein off the mitochondria to evade innate immunity. Proc Natl Acad Sci U S A 102: 17717-17722.

264. Meylan E, Curran J, Hofmann K, Moradpour D, Binder M, et al. (2005) Cardif is an adaptor protein in the RIG-I antiviral pathway and is targeted by hepatitis C virus. Nature 437: 1167-1172.

265. Foy E, Li K, Wang C, Sumpter R, Jr., Ikeda M, et al. (2003) Regulation of interferon regulatory factor-3 by the hepatitis C virus serine protease. Science 300: 1145-1148.

266. Decalf J, Fernandes S, Longman R, Ahloulay M, Audat F, et al. (2007) Plasmacytoid dendritic cells initiate a complex chemokine and cytokine network and are a viable drug target in chronic HCV patients. J Exp Med 204: 2423-2437.

267. Dolganiuc A, Chang S, Kodys K, Mandrekar P, Bakis G, et al. (2006) Hepatitis C virus (HCV) core protein-induced, monocyte-mediated mechanisms of reduced IFN-alpha and plasmacytoid dendritic cell loss in chronic HCV infection. J Immunol 177: 6758-6768.

268. Marukian S, Jones CT, Andrus L, Evans MJ, Ritola KD, et al. (2008) Cell culture-produced hepatitis C virus does not infect peripheral blood mononuclear cells. Hepatology 48: 1843-1850.

269. Yoon JC, Shiina M, Ahlenstiel G, Rehermann B (2009) Natural killer cell function is intact after direct exposure to infectious hepatitis C virions. Hepatology 49: 12-21.

270. Auffermann-Gretzinger S, Keeffe EB, Levy S (2001) Impaired dendritic cell maturation in patients with chronic, but not resolved, hepatitis C virus infection. Blood 97: 3171-3176.

271. Dolganiuc A, Kodys K, Kopasz A, Marshall C, Do T, et al. (2003) Hepatitis C virus core and nonstructural protein 3 proteins induce pro- and anti-inflammatory cytokines and inhibit dendritic cell differentiation. J Immunol 170: 5615-5624.

272. Eisen-Vandervelde AL, Waggoner SN, Yao ZQ, Cale EM, Hahn CS, et al. (2004) Hepatitis C virus core selectively suppresses interleukin-12 synthesis in human macrophages by interfering with AP-1 activation. J Biol Chem 279: 43479-43486.

273. Khakoo SI, Thio CL, Martin MP, Brooks CR, Gao X, et al. (2004) HLA and NK cell inhibitory receptor genes in resolving hepatitis C virus infection. Science 305: 872-874.

274. Ahlenstiel G, Martin MP, Gao X, Carrington M, Rehermann B (2008) Distinct KIR/HLA compound genotypes affect the kinetics of human antiviral natural killer cell responses. J Clin Invest 118: 1017-1026.

275. Jinushi M, Takehara T, Tatsumi T, Kanto T, Miyagi T, et al. (2004) Negative regulation of NK cell activities by inhibitory receptor CD94/NKG2A leads to altered NK cell-induced modulation of dendritic cell functions in chronic hepatitis C virus infection. J Immunol 173: 6072-6081.

276. Tseng CT, Klimpel GR (2002) Binding of the hepatitis C virus envelope protein E2 to CD81 inhibits natural killer cell functions. J Exp Med 195: 43-49.

277. Crotta S, Stilla A, Wack A, D'Andrea A, Nuti S, et al. (2002) Inhibition of natural killer cells through engagement of CD81 by the major hepatitis C virus envelope protein. J Exp Med 195: 35-41.

278. Abe K, Inchauspe G, Shikata T, Prince AM (1992) Three different patterns of hepatitis C virus infection in chimpanzees. Hepatology 15: 690-695.

279. Cooper S, Erickson AL, Adams EJ, Kansopon J, Weiner AJ, et al. (1999) Analysis of a successful immune response against hepatitis C virus. Immunity 10: 439-449.

280. Missale G, Bertoni R, Lamonaca V, Valli A, Massari M, et al. (1996) Different clinical behaviors of acute hepatitis C virus infection are associated with different vigor of the anti-viral cell-mediated immune response. J Clin Invest 98: 706-714.

281. Diepolder HM, Zachoval R, Hoffmann RM, Wierenga EA, Santantonio T, et al. (1995) Possible mechanism involving T-lymphocyte response to non-structural protein 3 in viral clearance in acute hepatitis C virus infection. Lancet 346: 1006-1007.

282. Gerlach JT, Diepolder HM, Jung MC, Gruener NH, Schraut WW, et al. (1999) Recurrence of hepatitis C virus after loss of virus-specific CD4(+) T-cell response in acute hepatitis C. Gastroenterology 117: 933-941.

283. Thimme R, Oldach D, Chang KM, Steiger C, Ray SC, et al. (2001) Determinants of viral clearance and persistence during acute hepatitis C virus infection. J Exp Med 194: 1395-1406.

284. Barrera JM, Francis B, Ercilla G, Nelles M, Achord D, et al. (1995) Improved detection of anti-HCV in post-transfusion hepatitis by a third-generation ELISA. Vox Sang 68: 15-18.

285. Chien DY, Choo QL, Tabrizi A, Kuo C, McFarland J, et al. (1992) Diagnosis of hepatitis C virus (HCV) infection using an immunodominant chimeric polyprotein to capture circulating antibodies: reevaluation of the role of HCV in liver disease. Proc Natl Acad Sci U S A 89: 10011-10015.

286. Courouce AM, Le Marrec N, Girault A, Ducamp S, Simon N (1994) Anti-hepatitis C virus (anti-HCV) seroconversion in patients undergoing hemodialysis: comparison of second- and third-generation anti-HCV assays. Transfusion 34: 790-795.

287. Farci P, Alter HJ, Wong D, Miller RH, Shih JW, et al. (1991) A long-term study of hepatitis C virus replication in non-A, non-B hepatitis. N Engl J Med 325: 98-104.

288. Prince AM, Brotman B, Inchauspe G, Pascual D, Nasoff M, et al. (1993) Patterns and prevalence of hepatitis C virus infection in posttransfusion non-A, non-B hepatitis. J Infect Dis 167: 1296-1301.

289. Thimme R, Bukh J, Spangenberg HC, Wieland S, Pemberton J, et al. (2002) Viral and immunological determinants of hepatitis C virus clearance, persistence, and disease. Proc Natl Acad Sci U S A 99: 15661-15668.

290. Semmo N, Lucas M, Krashias G, Lauer G, Chapel H, et al. (2006) Maintenance of HCV-specific T-cell responses in antibody-deficient patients a decade after early therapy. Blood 107: 4570-4571.

291. Lavillette D, Morice Y, Germanidis G, Donot P, Soulier A, et al. (2005) Human serum facilitates hepatitis C virus infection, and neutralizing responses inversely correlate with viral replication kinetics at the acute phase of hepatitis C virus infection. J Virol 79: 6023-6034.

292. Logvinoff C, Major ME, Oldach D, Heyward S, Talal A, et al. (2004) Neutralizing antibody response during acute and chronic hepatitis C virus infection. Proc Natl Acad Sci U S A 101: 10149-10154.

293. Farci P, Alter HJ, Wong DC, Miller RH, Govindarajan S, et al. (1994) Prevention of hepatitis C virus infection in chimpanzees after antibody-mediated *in vitro* neutralization. Proc Natl Acad Sci U S A 91: 7792-7796.

294. Yu MY, Bartosch B, Zhang P, Guo ZP, Renzi PM, et al. (2004) Neutralizing antibodies to hepatitis C virus (HCV) in immune globulins derived from anti-HCV-positive plasma. Proc Natl Acad Sci U S A 101: 7705-7710.

295. Farci P, Alter HJ, Govindarajan S, Wong DC, Engle R, et al. (1992) Lack of protective immunity against reinfection with hepatitis C virus. Science 258: 135-140.

296. Lai ME, Mazzoleni AP, Argiolu F, De Virgilis S, Balestrieri A, et al. (1994) Hepatitis C virus in multiple episodes of acute hepatitis in polytransfused thalassaemic children. Lancet 343: 388-390.

297. Post JJ, Pan Y, Freeman AJ, Harvey CE, White PA, et al. (2004) Clearance of hepatitis C viremia associated with cellular immunity in the absence of seroconversion in the hepatitis C incidence and transmission in prisons study cohort. J Infect Dis 189: 1846-1855.

298. Netski DM, Mosbruger T, Depla E, Maertens G, Ray SC, et al. (2005) Humoral immune response in acute hepatitis C virus infection. Clin Infect Dis 41: 667-675.

299. Farci P, Shimoda A, Coiana A, Diaz G, Peddis G, et al. (2000) The outcome of acute hepatitis C predicted by the evolution of the viral quasispecies. Science 288: 339-344.

300. von Hahn T, Yoon JC, Alter H, Rice CM, Rehermann B, et al. (2007) Hepatitis C virus continuously escapes from neutralizing antibody and T-cell responses during chronic infection *in vivo*. Gastroenterology 132: 667-678.

301. Lechner F, Wong DK, Dunbar PR, Chapman R, Chung RT, et al. (2000) Analysis of successful immune responses in persons infected with hepatitis C virus. J Exp Med 191: 1499-1512.

302. Shoukry NH, Grakoui A, Houghton M, Chien DY, Ghrayeb J, et al. (2003) Memory CD8+ T cells are required for protection from persistent hepatitis C virus infection. J Exp Med 197: 1645-1655.

303. Urbani S, Amadei B, Fisicaro P, Pilli M, Missale G, et al. (2005) Heterologous T cell immunity in severe hepatitis C virus infection. J Exp Med 201: 675-680.

304. Nascimbeni M, Mizukoshi E, Bosmann M, Major ME, Mihalik K, et al. (2003) Kinetics of CD4+ and CD8+ memory T-cell responses during hepatitis C virus rechallenge of previously recovered chimpanzees. J Virol 77: 4781-4793.

305. Schulze zur Wiesch J, Lauer GM, Day CL, Kim AY, Ouchi K, et al. (2005) Broad repertoire of the CD4+ Th cell response in spontaneously controlled hepatitis C virus infection includes dominant and highly promiscuous epitopes. J Immunol 175: 3603-3613.

306. Shoukry NH, Sidney J, Sette A, Walker CM (2004) Conserved hierarchy of helper T cell responses in a chimpanzee during primary and secondary hepatitis C virus infections. J Immunol 172: 483-492.

307. Shoukry NH, Cawthon AG, Walker CM (2004) Cell-mediated immunity and the outcome of hepatitis C virus infection. Annu Rev Microbiol 58: 391-424.

308. Harcourt GC, Lucas M, Sheridan I, Barnes E, Phillips R, et al. (2004) Longitudinal mapping of protective CD4+ T cell responses against HCV: analysis of

fluctuating dominant and subdominant HLA-DR11 restricted epitopes. J Viral Hepat 11: 324-331.

309. Accapezzato D, Francavilla V, Rawson P, Cerino A, Cividini A, et al. (2004) Subversion of effector CD8+ T cell differentiation in acute hepatitis C virus infection: the role of the virus. Eur J Immunol 34: 438-446.

310. Francavilla V, Accapezzato D, De Salvo M, Rawson P, Cosimi O, et al. (2004) Subversion of effector CD8+ T cell differentiation in acute hepatitis C virus infection: exploring the immunological mechanisms. Eur J Immunol 34: 427-437.

311. Gruener NH, Lechner F, Jung MC, Diepolder H, Gerlach T, et al. (2001) Sustained dysfunction of antiviral CD8+ T lymphocytes after infection with hepatitis C virus. J Virol 75: 5550-5558.

312. Lechner F, Gruener NH, Urbani S, Uggeri J, Santantonio T, et al. (2000) CD8+ T lymphocyte responses are induced during acute hepatitis C virus infection but are not sustained. Eur J Immunol 30: 2479-2487.

313. Urbani S, Boni C, Missale G, Elia G, Cavallo C, et al. (2002) Virus-specific CD8+ lymphocytes share the same effector-memory phenotype but exhibit functional differences in acute hepatitis B and C. J Virol 76: 12423-12434.

314. Major ME, Dahari H, Mihalik K, Puig M, Rice CM, et al. (2004) Hepatitis C virus kinetics and host responses associated with disease and outcome of infection in chimpanzees. Hepatology 39: 1709-1720.

315. Ward S, Lauer G, Isba R, Walker B, Klenerman P (2002) Cellular immune responses against hepatitis C virus: the evidence base 2002. Clin Exp Immunol 128: 195-203.

316. Wedemeyer H, Mizukoshi E, Davis AR, Bennink JR, Rehermann B (2001) Cross-reactivity between hepatitis C virus and Influenza A virus determinant-specific cytotoxic T cells. J Virol 75: 11392-11400.

317. Cox AL, Mosbruger T, Lauer GM, Pardoll D, Thomas DL, et al. (2005) Comprehensive analyses of CD8+ T cell responses during longitudinal study of acute human hepatitis C. Hepatology 42: 104-112.

318. Prince AM, Pawlotsky JM, Soulier A, Tobler L, Brotman B, et al. (2004) Hepatitis C virus replication kinetics in chimpanzees with self-limited and chronic infections. J Viral Hepat 11: 236-242.

319. Folgori A, Spada E, Pezzanera M, Ruggeri L, Mele A, et al. (2006) Early impairment of hepatitis C virus specific T cell proliferation during acute infection leads to failure of viral clearance. Gut 55: 1012-1019.

320. Semmo N, Day CL, Ward SM, Lucas M, Harcourt G, et al. (2005) Preferential loss of IL-2-secreting CD4+ T helper cells in chronic HCV infection. Hepatology 41: 1019-1028.

321. Grakoui A, Shoukry NH, Woollard DJ, Han JH, Hanson HL, et al. (2003) HCV persistence and immune evasion in the absence of memory T cell help. Science 302: 659-662.

322. Lauer GM, Lucas M, Timm J, Ouchi K, Kim AY, et al. (2005) Full-breadth analysis of CD8+ T-cell responses in acute hepatitis C virus infection and early therapy. J Virol 79: 12979-12988.

323. Bassett SE, Guerra B, Brasky K, Miskovsky E, Houghton M, et al. (2001) Protective immune response to hepatitis C virus in chimpanzees rechallenged following clearance of primary infection. Hepatology 33: 1479-1487.

324. Major ME, Mihalik K, Puig M, Rehermann B, Nascimbeni M, et al. (2002) Previously infected and recovered chimpanzees exhibit rapid responses that control hepatitis C virus replication upon rechallenge. J Virol 76: 6586-6595.

325. Al-Sherbiny M, Osman A, Mohamed N, Shata MT, Abdel-Aziz F, et al. (2005) Exposure to hepatitis C virus induces cellular immune responses without detectable viremia or seroconversion. Am J Trop Med Hyg 73: 44-49.

326. Kamal SM, Amin A, Madwar M, Graham CS, He Q, et al. (2004) Cellular immune responses in seronegative sexual contacts of acute hepatitis C patients. J Virol 78: 12252-12258.

327. Koziel MJ, Wong DK, Dudley D, Houghton M, Walker BD (1997) Hepatitis C virus-specific cytolytic T lymphocyte and T helper cell responses in seronegative persons. J Infect Dis 176: 859-866.

328. Scognamiglio P, Accapezzato D, Casciaro MA, Cacciani A, Artini M, et al. (1999) Presence of effector CD8+ T cells in hepatitis C virus-exposed healthy seronegative donors. J Immunol 162: 6681-6689.

329. Mehta SH, Cox A, Hoover DR, Wang XH, Mao Q, et al. (2002) Protection against persistence of hepatitis C. Lancet 359: 1478-1483.

330. Rehermann B, Chang KM, McHutchison JG, Kokka R, Houghton M, et al. (1996) Quantitative analysis of the peripheral blood cytotoxic T lymphocyte response in patients with chronic hepatitis C virus infection. J Clin Invest 98: 1432-1440.

331. Nelson DR, Marousis CG, Davis GL, Rice CM, Wong J, et al. (1997) The role of hepatitis C virus-specific cytotoxic T lymphocytes in chronic hepatitis C. J Immunol 158: 1473-1481.

332. Wong DK, Dudley DD, Afdhal NH, Dienstag J, Rice CM, et al. (1998) Liver-derived CTL in hepatitis C virus infection: breadth and specificity of responses in a cohort of persons with chronic infection. J Immunol 160: 1479-1488.

333. Freeman AJ, Pan Y, Harvey CE, Post JJ, Law MG, et al. (2003) The presence of an intrahepatic cytotoxic T lymphocyte response is associated with low viral load in patients with chronic hepatitis C virus infection. J Hepatol 38: 349-356.

334. Erickson AL, Houghton M, Choo QL, Weiner AJ, Ralston R, et al. (1993) Hepatitis C virus-specific CTL responses in the liver of chimpanzees with acute and chronic hepatitis C. J Immunol 151: 4189-4199.

335. Grabowska AM, Lechner F, Klenerman P, Tighe PJ, Ryder S, et al. (2001) Direct *ex vivo* comparison of the breadth and specificity of the T cells in the liver and peripheral blood of patients with chronic HCV infection. Eur J Immunol 31: 2388-2394.

336. Koziel MJ, Dudley D, Wong JT, Dienstag J, Houghton M, et al. (1992) Intrahepatic cytotoxic T lymphocytes specific for hepatitis C virus in persons with chronic hepatitis. J Immunol 149: 3339-3344.

337. Spangenberg HC, Viazov S, Kersting N, Neumann-Haefelin C, McKinney D, et al. (2005) Intrahepatic CD8+ T-cell failure during chronic hepatitis C virus infection. Hepatology 42: 828-837.

338. Meyer-Olson D, Shoukry NH, Brady KW, Kim H, Olson DP, et al. (2004) Limited T cell receptor diversity of HCV-specific T cell responses is associated with CTL escape. J Exp Med 200: 307-319.

339. Appay V, Dunbar PR, Callan M, Klenerman P, Gillespie GM, et al. (2002) Memory CD8+ T cells vary in differentiation phenotype in different persistent virus infections. Nat Med 8: 379-385.

340. Lucas M, Vargas-Cuero AL, Lauer GM, Barnes E, Willberg CB, et al. (2004) Pervasive influence of hepatitis C virus on the phenotype of antiviral CD8+ T cells. J Immunol 172: 1744-1753.

341. Wedemeyer H, He XS, Nascimbeni M, Davis AR, Greenberg HB, et al. (2002) Impaired effector function of hepatitis C virus-specific CD8+ T cells in chronic hepatitis C virus infection. J Immunol 169: 3447-3458.

342. Urbani S, Amadei B, Fisicaro P, Tola D, Orlandini A, et al. (2006) Outcome of acute hepatitis C is related to virus-specific CD4 function and maturation of antiviral memory CD8 responses. Hepatology 44: 126-139.

343. Golden-Mason L, Castelblanco N, O'Farrelly C, Rosen HR (2007) Phenotypic and functional changes of cytotoxic CD56pos natural T cells determine outcome of acute hepatitis C virus infection. J Virol 81: 9292-9298.

344. Golden-Mason L, Palmer B, Klarquist J, Mengshol JA, Castelblanco N, et al. (2007) Upregulation of PD-1 expression on circulating and intrahepatic hepatitis C virus-specific CD8+ T cells associated with reversible immune dysfunction. J Virol 81: 9249-9258.

345. Radziewicz H, Ibegbu CC, Fernandez ML, Workowski KA, Obideen K, et al. (2007) Liver-infiltrating lymphocytes in chronic human hepatitis C virus infection display an exhausted phenotype with high levels of PD-1 and low levels of CD127 expression. J Virol 81: 2545-2553.

346. Radziewicz H, Ibegbu CC, Hon H, Osborn MK, Obideen K, et al. (2008) Impaired hepatitis C virus (HCV)-specific effector CD8+ T cells undergo massive apoptosis in the peripheral blood during acute HCV infection and in the liver during the chronic phase of infection. J Virol 82: 9808-9822.

347. Barber DL, Wherry EJ, Masopust D, Zhu B, Allison JP, et al. (2006) Restoring function in exhausted CD8 T cells during chronic viral infection. Nature 439: 682-687.

348. Urbani S, Amadei B, Tola D, Massari M, Schivazappa S, et al. (2006) PD-1 expression in acute hepatitis C virus (HCV) infection is associated with HCV-specific CD8 exhaustion. J Virol 80: 11398-11403.

349. Nakamoto N, Kaplan DE, Coleclough J, Li Y, Valiga ME, et al. (2008) Functional restoration of HCV-specific CD8 T cells by PD-1 blockade is defined by PD-1 expression and compartmentalization. Gastroenterology 134: 1927-1937, 1937 e1921-1922.

350. Nakamoto N, Cho H, Shaked A, Olthoff K, Valiga ME, et al. (2009) Synergistic reversal of intrahepatic HCV-specific CD8 T cell exhaustion by combined PD-1/CTLA-4 blockade. PLoS Pathog 5: e1000313.

351. Moore KW, de Waal Malefyt R, Coffman RL, O'Garra A (2001) Interleukin-10 and the interleukin-10 receptor. Annu Rev Immunol 19: 683-765.

352. Koziel MJ, Dudley D, Afdhal N, Grakoui A, Rice CM, et al. (1995) HLA class I-restricted cytotoxic T lymphocytes specific for hepatitis C virus. Identification of multiple epitopes and characterization of patterns of cytokine release. J Clin Invest 96: 2311-2321.

353. Accapezzato D, Francavilla V, Paroli M, Casciaro M, Chircu LV, et al. (2004) Hepatic expansion of a virus-specific regulatory CD8(+) T cell population in chronic hepatitis C virus infection. J Clin Invest 113: 963-972.

354. Abel M, Sene D, Pol S, Bourliere M, Poynard T, et al. (2006) Intrahepatic virus-specific IL-10-producing CD8 T cells prevent liver damage during chronic hepatitis C virus infection. Hepatology 44: 1607-1616.

355. Sugimoto K, Ikeda F, Stadanlick J, Nunes FA, Alter HJ, et al. (2003) Suppression of HCV-specific T cells without differential hierarchy demonstrated *ex vivo* in persistent HCV infection. Hepatology 38: 1437-1448.

356. Cabrera R, Tu Z, Xu Y, Firpi RJ, Rosen HR, et al. (2004) An immunomodulatory role for CD4(+)CD25(+) regulatory T lymphocytes in hepatitis C virus infection. Hepatology 40: 1062-1071.

357. Boettler T, Spangenberg HC, Neumann-Haefelin C, Panther E, Urbani S, et al. (2005) T cells with a CD4+CD25+ regulatory phenotype suppress *in vitro* proliferation of virus-specific CD8+ T cells during chronic hepatitis C virus infection. J Virol 79: 7860-7867.

358. Rushbrook SM, Ward SM, Unitt E, Vowler SL, Lucas M, et al. (2005) Regulatory T cells suppress *in vitro* proliferation of virus-specific CD8+ T cells during persistent hepatitis C virus infection. J Virol 79: 7852-7859.

359. Manigold T, Shin EC, Mizukoshi E, Mihalik K, Murthy KK, et al. (2006) Foxp3+CD4+CD25+ T cells control virus-specific memory T cells in chimpanzees that recovered from hepatitis C. Blood 107: 4424-4432.

360. Smyk-Pearson S, Golden-Mason L, Klarquist J, Burton JR, Jr., Tester IA, et al. (2008) Functional suppression by FoxP3+CD4+CD25(high) regulatory T cells during acute hepatitis C virus infection. J Infect Dis 197: 46-57.

361. Penna A, Missale G, Lamonaca V, Pilli M, Mori C, et al. (2002) Intrahepatic and circulating HLA class II-restricted, hepatitis C virus-specific T cells: functional characterization in patients with chronic hepatitis C. Hepatology 35: 1225-1236.

362. Puig M, Mihalik K, Tilton JC, Williams O, Merchlinsky M, et al. (2006) CD4+ immune escape and subsequent T-cell failure following chimpanzee immunization against hepatitis C virus. Hepatology 44: 736-745.

363. Wang JH, Layden TJ, Eckels DD (2003) Modulation of the peripheral T-Cell response by CD4 mutants of hepatitis C virus: transition from a Th1 to a Th2 response. Hum Immunol 64: 662-673.

364. Wang H, Bian T, Merrill SJ, Eckels DD (2002) Sequence variation in the gene encoding the nonstructural 3 protein of hepatitis C virus: evidence for immune selection. J Mol Evol 54: 465-473.

365. Fuller MJ, Shoukry NH, Gushima T, Bowen DG, Callendret B, et al. (2010) Selection-driven immune escape is not a significant factor in the failure of CD4 T cell responses in persistent hepatitis C virus infection. Hepatology 51: 378-387.

366. Bowen DG, Walker CM (2005) Mutational escape from CD8+ T cell immunity: HCV evolution, from chimpanzees to man. J Exp Med 201: 1709-1714.

367. Chang KM, Rehermann B, McHutchison JG, Pasquinelli C, Southwood S, et al. (1997) Immunological significance of cytotoxic T lymphocyte epitope variants in patients chronically infected by the hepatitis C virus. J Clin Invest 100: 2376-2385.

368. Wolfl M, Rutebemberwa A, Mosbruger T, Mao Q, Li HM, et al. (2008) Hepatitis C virus immune escape via exploitation of a hole in the T cell repertoire. J Immunol 181: 6435-6446.

369. Erickson AL, Kimura Y, Igarashi S, Eichelberger J, Houghton M, et al. (2001) The outcome of hepatitis C virus infection is predicted by escape mutations in epitopes targeted by cytotoxic T lymphocytes. Immunity 15: 883-895.

370. Cox AL, Mosbruger T, Mao Q, Liu Z, Wang XH, et al. (2005) Cellular immune selection with hepatitis C virus persistence in humans. J Exp Med 201: 1741-1752.

371. Tester I, Smyk-Pearson S, Wang P, Wertheimer A, Yao E, et al. (2005) Immune evasion versus recovery after acute hepatitis C virus infection from a shared source. J Exp Med 201: 1725-1731.

372. Timm J, Lauer GM, Kavanagh DG, Sheridan I, Kim AY, et al. (2004) CD8 epitope escape and reversion in acute HCV infection. J Exp Med 200: 1593-1604.

373. Ray SC, Fanning L, Wang XH, Netski DM, Kenny-Walsh E, et al. (2005) Divergent and convergent evolution after a common-source outbreak of hepatitis C virus. J Exp Med 201: 1753-1759.

374. Leslie AJ, Pfafferott KJ, Chetty P, Draenert R, Addo MM, et al. (2004) HIV evolution: CTL escape mutation and reversion after transmission. Nat Med 10: 282-289.

375. Friedrich TC, Dodds EJ, Yant LJ, Vojnov L, Rudersdorf R, et al. (2004) Reversion of CTL escape-variant immunodeficiency viruses *in vivo*. Nat Med 10: 275-281.

376. Uebelhoer L, Han JH, Callendret B, Mateu G, Shoukry NH, et al. (2008) Stable cytotoxic T cell escape mutation in hepatitis C virus is linked to maintenance of viral fitness. PLoS Pathog 4: e1000143.

377. Dazert E, Neumann-Haefelin C, Bressanelli S, Fitzmaurice K, Kort J, et al. (2009) Loss of viral fitness and cross-recognition by CD8+ T cells limit HCV escape from a protective HLA-B27-restricted human immune response. J Clin Invest 119: 376-386.

378. Moore CB, John M, James IR, Christiansen FT, Witt CS, et al. (2002) Evidence of HIV-1 adaptation to HLA-restricted immune responses at a population level. Science 296: 1439-1443.

379. Leslie A, Kavanagh D, Honeyborne I, Pfafferott K, Edwards C, et al. (2005) Transmission and accumulation of CTL escape variants drive negative associations between HIV polymorphisms and HLA. J Exp Med 201: 891-902.

380. Buchmeier MJ, de la Torre, J-C, Peters, C.J. (2007) Arenaviridae: the viruses and their replication. Fields Virology 5th Ed.: 1791-1827.

381. Jahrling PB, Peters CJ (1992) Lymphocytic choriomeningitis virus. A neglected pathogen of man. Arch Pathol Lab Med 116: 486-488.

382. Fischer SA, Graham MB, Kuehnert MJ, Kotton CN, Srinivasan A, et al. (2006) Transmission of lymphocytic choriomeningitis virus by organ transplantation. N Engl J Med 354: 2235-2249.

383. Parker JC, Igel HJ, Reynolds RK, Lewis AM, Jr., Rowe WP (1976) Lymphocytic choriomeningitis virus infection in fetal, newborn, and young adult Syrian hamsters (Mesocricetus auratus). Infect Immun 13: 967-981.

384. Enders G, Varho-Gobel M, Lohler J, Terletskaia-Ladwig E, Eggers M (1999) Congenital lymphocytic choriomeningitis virus infection: an underdiagnosed disease. Pediatr Infect Dis J 18: 652-655.

385. Barton LL, Peters CJ, Ksiazek TG (1995) Lymphocytic choriomeningitis virus: an unrecognized teratogenic pathogen. Emerg Infect Dis 1: 152-153.

386. Wright R, Johnson D, Neumann M, Ksiazek TG, Rollin P, et al. (1997) Congenital lymphocytic choriomeningitis virus syndrome: a disease that mimics congenital toxoplasmosis or Cytomegalovirus infection. Pediatrics 100: E9.

387. Chastel C, Bosshard S, Le Goff F, Quillien MC, Gilly R, et al. (1978) [Transplacental infection by lymphocytic choriomeningitis virus. Results of a retrospective serological study in France (author's transl)]. Nouv Presse Med 7: 1089-1092.

388. Sheinbergas MM (1976) Hydrocephalus due to prenatal infection with the lymphocytic choriomeningitis virus. Infection 4: 185-191.

389. Ackermann R, Korver G, Turss R, Wonne R, Hochgesand P (1974) [Prenatal infection with the virus of lymphocytic choriomeningitis: report of two cases (author's transl)]. Dtsch Med Wochenschr 99: 629-632.

390. Lehmann-Grube F, Kallay M, Ibscher B, Schwartz R (1979) Serologic diagnosis of human infections with lymphocytic choriomeningitis virus: comparative evaluation of seven methods. J Med Virol 4: 125-136.

391. Lewis VJ, Walter PD, Thacker WL, Winkler WG (1975) Comparison of three tests for the serological diagnosis of lymphocytic choriomeningitis virus infection. J Clin Microbiol 2: 193-197.

392. Park JY, Peters CJ, Rollin PE, Ksiazek TG, Gray B, et al. (1997) Development of a reverse transcription-polymerase chain reaction assay for diagnosis of lymphocytic choriomeningitis virus infection and its use in a prospective surveillance study. J Med Virol 51: 107-114.

393. Ackermann R, Jansen L (1958) [Epidemiology of infection with the virus of lymphocytic choriomeningitis]. Z Klin Med 155: 277-287.

394. Singh MK, Fuller-Pace FV, Buchmeier MJ, Southern PJ (1987) Analysis of the genomic L RNA segment from lymphocytic choriomeningitis virus. Virology 161: 448-456.

395. Riviere Y, Ahmed R, Southern PJ, Buchmeier MJ, Dutko FJ, et al. (1985) The S RNA segment of lymphocytic choriomeningitis virus codes for the nucleoprotein and glycoproteins 1 and 2. J Virol 53: 966-968.

396. Buchmeier MJ, Elder JH, Oldstone MB (1978) Protein structure of lymphocytic choriomeningitis virus: identification of the virus structural and cell associated polypeptides. Virology 89: 133-145.

397. Buchmeier MJ, Oldstone MB (1979) Protein structure of lymphocytic choriomeningitis virus: evidence for a cell-associated precursor of the virion glycopeptides. Virology 99: 111-120.

398. Salvato M, Shimomaye E, Oldstone MB (1989) The primary structure of the lymphocytic choriomeningitis virus L gene encodes a putative RNA polymerase. Virology 169: 377-384.

399. Lee KJ, Novella IS, Teng MN, Oldstone MB, de La Torre JC (2000) NP and L proteins of lymphocytic choriomeningitis virus (LCMV) are sufficient for efficient transcription and replication of LCMV genomic RNA analogs. J Virol 74: 3470-3477.

400. Ahmed R, Salmi A, Butler LD, Chiller JM, Oldstone MB (1984) Selection of genetic variants of lymphocytic choriomeningitis virus in spleens of persistently infected mice. Role in suppression of cytotoxic T lymphocyte response and viral persistence. J Exp Med 160: 521-540.

401. Ahmed R, Simon RS, Matloubian M, Kolhekar SR, Southern PJ, et al. (1988) Genetic analysis of *in vivo*-selected viral variants causing chronic infection: importance of mutation in the L RNA segment of lymphocytic choriomeningitis virus. J Virol 62: 3301-3308.

402. Evans CF, Borrow P, de la Torre JC, Oldstone MB (1994) Virus-induced immunosuppression: kinetic analysis of the selection of a mutation associated with viral persistence. J Virol 68: 7367-7373.

403. Ahmed R, Hahn CS, Somasundaram T, Villarete L, Matloubian M, et al. (1991) Molecular basis of organ-specific selection of viral variants during chronic infection. J Virol 65: 4242-4247.

404. Salvato MS, Shimomaye EM (1989) The completed sequence of lymphocytic choriomeningitis virus reveals a unique RNA structure and a gene for a zinc finger protein. Virology 173: 1-10.

405. Salvato M, Borrow P, Shimomaye E, Oldstone MB (1991) Molecular basis of viral persistence: a single amino acid change in the glycoprotein of lymphocytic choriomeningitis virus is associated with suppression of the antiviral cytotoxic T-lymphocyte response and establishment of persistence. J Virol 65: 1863-1869.

406. Cao W, Henry MD, Borrow P, Yamada H, Elder JH, et al. (1998) Identification of alpha-dystroglycan as a receptor for lymphocytic choriomeningitis virus and Lassa fever virus. Science 282: 2079-2081.

407. Sevilla N, Kunz S, Holz A, Lewicki H, Homann D, et al. (2000) Immunosuppression and resultant viral persistence by specific viral targeting of dendritic cells. J Exp Med 192: 1249-1260.

408. Smelt SC, Borrow P, Kunz S, Cao W, Tishon A, et al. (2001) Differences in affinity of binding of lymphocytic choriomeningitis virus strains to the cellular receptor alpha-dystroglycan correlate with viral tropism and disease kinetics. J Virol 75: 448-457.

409. Zinkernagel RM (2002) Lymphocytic choriomeningitis virus and immunology. Curr Top Microbiol Immunol 263: 1-5.

410. Mims CA, Blanden RV (1972) Antiviral action of immune lymphocytes in mice infected with lymphocytic choriomeningitis virus. Infect Immun 6: 695-698.

411. Moskophidis D, Laine E, Zinkernagel RM (1993) Peripheral clonal deletion of antiviral memory CD8+ T cells. Eur J Immunol 23: 3306-3311.

412. Moskophidis D, Lechner F, Pircher H, Zinkernagel RM (1993) Virus persistence in acutely infected immunocompetent mice by exhaustion of antiviral cytotoxic effector T cells. Nature 362: 758-761.

413. Kagi D, Ledermann B, Burki K, Seiler P, Odermatt B, et al. (1994) Cytotoxicity mediated by T cells and natural killer cells is greatly impaired in perforin-deficient mice. Nature 369: 31-37.

414. Oxenius A, Bachmann MF, Zinkernagel RM, Hengartner H (1998) Virus-specific MHC-class II-restricted TCR-transgenic mice: effects on humoral and cellular immune responses after viral infection. Eur J Immunol 28: 390-400.

415. Battegay M, Moskophidis D, Rahemtulla A, Hengartner H, Mak TW, et al. (1994) Enhanced establishment of a virus carrier state in adult CD4+ T-cell-deficient mice. J Virol 68: 4700-4704.

416. Muller D, Koller BH, Whitton JL, LaPan KE, Brigman KK, et al. (1992) LCMV-specific, class II-restricted cytotoxic T cells in beta 2-microglobulin-deficient mice. Science 255: 1576-1578.

417. Zajac AJ, Quinn DG, Cohen PL, Frelinger JA (1996) Fas-dependent CD4+ cytotoxic T-cell-mediated pathogenesis during virus infection. Proc Natl Acad Sci U S A 93: 14730-14735.

418. La Posta VJ, Auperin DD, Kamin-Lewis R, Cole GA (1993) Cross-protection against lymphocytic choriomeningitis virus mediated by a CD4+ T-cell clone specific for an envelope glycoprotein epitope of Lassa virus. J Virol 67: 3497-3506.

419. Matloubian M, Concepcion RJ, Ahmed R (1994) CD4+ T cells are required to sustain CD8+ cytotoxic T-cell responses during chronic viral infection. J Virol 68: 8056-8063.

420. Thomsen AR, Johansen J, Marker O, Christensen JP (1996) Exhaustion of CTL memory and recrudescence of viremia in lymphocytic choriomeningitis virus-infected MHC class II-deficient mice and B cell-deficient mice. J Immunol 157: 3074-3080.

421. Planz O, Ehl S, Furrer E, Horvath E, Brundler MA, et al. (1997) A critical role for neutralizing-antibody-producing B cells, CD4(+) T cells, and interferons in persistent and acute infections of mice with lymphocytic choriomeningitis virus: implications for adoptive immunotherapy of virus carriers. Proc Natl Acad Sci U S A 94: 6874-6879.

422. Moskophidis D, Lehmann-Grube F (1984) The immune response of the mouse to lymphocytic choriomeningitis virus. IV. Enumeration of antibody-producing cells in spleens during acute and persistent infection. J Immunol 133: 3366-3370.

423. Ahmed R, Butler LD, Bhatti L (1988) T4+ T helper cell function *in vivo*: differential requirement for induction of antiviral cytotoxic T-cell and antibody responses. J Virol 62: 2102-2106.

424. Brundler MA, Aichele P, Bachmann M, Kitamura D, Rajewsky K, et al. (1996) Immunity to viruses in B cell-deficient mice: influence of antibodies on virus persistence and on T cell memory. Eur J Immunol 26: 2257-2262.

425. Cerny A, Sutter S, Bazin H, Hengartner H, Zinkernagel RM (1988) Clearance of lymphocytic choriomeningitis virus in antibody- and B-cell-deprived mice. J Virol 62: 1803-1807.

426. Hangartner L, Zellweger RM, Giobbi M, Weber J, Eschli B, et al. (2006) Nonneutralizing antibodies binding to the surface glycoprotein of lymphocytic choriomeningitis virus reduce early virus spread. J Exp Med 203: 2033-2042.

427. Battegay M, Moskophidis D, Waldner H, Brundler MA, Fung-Leung WP, et al. (1993) Impairment and delay of neutralizing antiviral antibody responses by virus-specific cytotoxic T cells. J Immunol 151: 5408-5415.

428. Kyburz D, Aichele P, Speiser DE, Hengartner H, Zinkernagel RM, et al. (1993) T cell immunity after a viral infection versus T cell tolerance induced by soluble viral peptides. Eur J Immunol 23: 1956-1962.

429. Nguyen LT, Bachmann MF, Ohashi PS (2002) Contribution of LCMV transgenic models to understanding T lymphocyte development, activation, tolerance, and autoimmunity. Curr Top Microbiol Immunol 263: 119-143.

430. Zimmerman C, Brduscha-Riem K, Blaser C, Zinkernagel RM, Pircher H (1996) Visualization, characterization, and turnover of CD8+ memory T cells in virus-infected hosts. J Exp Med 183: 1367-1375.

431. Bachmann MF, Barner M, Viola A, Kopf M (1999) Distinct kinetics of cytokine production and cytolysis in effector and memory T cells after viral infection. Eur J Immunol 29: 291-299.

432. Zimmermann C, Prevost-Blondel A, Blaser C, Pircher H (1999) Kinetics of the response of naive and memory CD8 T cells to antigen: similarities and differences. Eur J Immunol 29: 284-290.

433. Bachmann MF, Gallimore A, Linkert S, Cerundolo V, Lanzavecchia A, et al. (1999) Developmental regulation of Lck targeting to the CD8 coreceptor controls signaling in naive and memory T cells. J Exp Med 189: 1521-1530.

434. Moskophidis D, Assmann-Wischer U, Simon MM, Lehmann-Grube F (1987) The immune response of the mouse to lymphocytic choriomeningitis virus. V. High numbers of cytolytic T lymphocytes are generated in the spleen during acute infection. Eur J Immunol 17: 937-942.

435. Christensen JP, Marker O, Thomsen AR (1994) The role of CD4+ T cells in cell-mediated immunity to LCMV: studies in MHC class I and class II deficient mice. Scand J Immunol 40: 373-382.

436. Oxenius A, Zinkernagel RM, Hengartner H (1998) Comparison of activation versus induction of unresponsiveness of virus-specific CD4+ and CD8+ T cells upon acute versus persistent viral infection. Immunity 9: 449-457.

437. Maloy KJ, Burkhart C, Junt TM, Odermatt B, Oxenius A, et al. (2000) CD4(+) T cell subsets during virus infection. Protective capacity depends on effector cytokine secretion and on migratory capability. J Exp Med 191: 2159-2170.

438. Masopust D, Kaech SM, Wherry EJ, Ahmed R (2004) The role of programming in memory T-cell development. Curr Opin Immunol 16: 217-225.

439. Bourgeois C, Rocha B, Tanchot C (2002) A role for CD40 expression on CD8+ T cells in the generation of CD8+ T cell memory. Science 297: 2060-2063.

440. Bourgeois C, Veiga-Fernandes H, Joret AM, Rocha B, Tanchot C (2002) CD8 lethargy in the absence of CD4 help. Eur J Immunol 32: 2199-2207.

441. Sun JC, Bevan MJ (2003) Defective CD8 T cell memory following acute infection without CD4 T cell help. Science 300: 339-342.

442. Sun JC, Williams MA, Bevan MJ (2004) CD4+ T cells are required for the maintenance, not programming, of memory CD8+ T cells after acute infection. Nat Immunol 5: 927-933.

443. Janssen EM, Lemmens EE, Wolfe T, Christen U, von Herrath MG, et al. (2003) CD4+ T cells are required for secondary expansion and memory in CD8+ T lymphocytes. Nature 421: 852-856.

444. Shedlock DJ, Shen H (2003) Requirement for CD4 T cell help in generating functional CD8 T cell memory. Science 300: 337-339.

445. Schultze JL, Michalak S, Seamon MJ, Dranoff G, Jung K, et al. (1997) CD40-activated human B cells: an alternative source of highly efficient antigen presenting cells to generate autologous antigen-specific T cells for adoptive immunotherapy. J Clin Invest 100: 2757-2765.

446. Hsu FJ, Benike C, Fagnoni F, Liles TM, Czerwinski D, et al. (1996) Vaccination of patients with B-cell lymphoma using autologous antigen-pulsed dendritic cells. Nat Med 2: 52-58.

447. Schultze JL, Grabbe S, von Bergwelt-Baildon MS (2004) DCs and CD40-activated B cells: current and future avenues to cellular cancer immunotherapy. Trends Immunol 25: 659-664.

448. Cassell DJ, Schwartz RH (1994) A quantitative analysis of antigen-presenting cell function: activated B cells stimulate naive CD4 T cells but are inferior to dendritic cells in providing costimulation. J Exp Med 180: 1829-1840.

449. Papanicolaou GA, Latouche JB, Tan C, Dupont J, Stiles J, et al. (2003) Rapid expansion of cytomegalovirus-specific cytotoxic T lymphocytes by artificial antigen-presenting cells expressing a single HLA allele. Blood 102: 2498-2505.

450. Latouche JB, Sadelain M (2000) Induction of human cytotoxic T lymphocytes by artificial antigen-presenting cells. Nat Biotechnol 18: 405-409.

451. Maus MV, Thomas AK, Leonard DG, Allman D, Addya K, et al. (2002) *Ex vivo* expansion of polyclonal and antigen-specific cytotoxic T lymphocytes by artificial APCs expressing ligands for the T-cell receptor, CD28 and 4-1BB. Nat Biotechnol 20: 143-148.

452. Thomas AK, Maus MV, Shalaby WS, June CH, Riley JL (2002) A cell-based artificial antigen-presenting cell coated with anti-CD3 and CD28 antibodies enables rapid expansion and long-term growth of CD4 T lymphocytes. Clin Immunol 105: 259-272.

453. Romani N, Gruner S, Brang D, Kampgen E, Lenz A, et al. (1994) Proliferating dendritic cell progenitors in human blood. J Exp Med 180: 83-93.

454. Girolomoni G, Ricciardi-Castagnoli P (1997) Dendritic cells hold promise for immunotherapy. Immunol Today 18: 102-104.

455. MartIn-Fontecha A, Sebastiani S, Hopken UE, Uguccioni M, Lipp M, et al. (2003) Regulation of dendritic cell migration to the draining lymph node: impact on T lymphocyte traffic and priming. J Exp Med 198: 615-621.

456. Fu YX, Chaplin DD (1999) Development and maturation of secondary lymphoid tissues. Annu Rev Immunol 17: 399-433.

457. Siemasko K, Clark MR (2001) The control and facilitation of MHC class II antigen processing by the BCR. Curr Opin Immunol 13: 32-36.

458. Zentz C, Wiesner M, Man S, Frankenberger B, Wollenberg B, et al. (2007) Activated B cells mediate efficient expansion of rare antigen-specific T cells. Hum Immunol 68: 75-85.

459. von Bergwelt-Baildon MS, Vonderheide RH, Maecker B, Hirano N, Anderson KS, et al. (2002) Human primary and memory cytotoxic T lymphocyte responses are efficiently induced by means of CD40-activated B cells as antigen-presenting cells: potential for clinical application. Blood 99: 3319-3325.

460. von Bergwelt-Baildon M, Maecker B, Schultze J, Gribben JG (2004) CD40 activation: potential for specific immunotherapy in B-CLL. Ann Oncol 15: 853-857.

461. Kondo E, Topp MS, Kiem HP, Obata Y, Morishima Y, et al. (2002) Efficient generation of antigen-specific cytotoxic T cells using retrovirally transduced CD40-activated B cells. J Immunol 169: 2164-2171.

462. Trojan A, Schultze JL, Witzens M, Vonderheide RH, Ladetto M, et al. (2000) Immunoglobulin framework-derived peptides function as cytotoxic T-cell epitopes commonly expressed in B-cell malignancies. Nat Med 6: 667-672.

463. Constant S, Schweitzer N, West J, Ranney P, Bottomly K (1995) B lymphocytes can be competent antigen-presenting cells for priming CD4+ T cells to protein antigens *in vivo*. J Immunol 155: 3734-3741.

464. Lapointe R, Bellemare-Pelletier A, Housseau F, Thibodeau J, Hwu P (2003) CD40-stimulated B lymphocytes pulsed with tumor antigens are effective antigen-presenting cells that can generate specific T cells. Cancer Res 63: 2836-2843.

465. Eynon EE, Parker DC (1992) Small B cells as antigen-presenting cells in the induction of tolerance to soluble protein antigens. J Exp Med 175: 131-138.

466. Qin Z, Richter G, Schuler T, Ibe S, Cao X, et al. (1998) B cells inhibit induction of T cell-dependent tumor immunity. Nat Med 4: 627-630.

467. Bennett SR, Carbone FR, Karamalis F, Flavell RA, Miller JF, et al. (1998) Help for cytotoxic-T-cell responses is mediated by CD40 signalling. Nature 393: 478-480.

468. Ke Y, Kapp JA (1996) Exogenous antigens gain access to the major histocompatibility complex class I processing pathway in B cells by receptor-mediated uptake. J Exp Med 184: 1179-1184.

469. Barnaba V, Franco A, Alberti A, Benvenuto R, Balsano F (1990) Selective killing of hepatitis B envelope antigen-specific B cells by class I-restricted, exogenous antigen-specific T lymphocytes. Nature 345: 258-260.

470. Yefenof E, Zehavi-Feferman R, Guy R (1990) Control of primary and secondary antibody responses by cytotoxic T lymphocytes specific for a soluble antigen. Eur J Immunol 20: 1849-1853.

471. Fuchs EJ, Matzinger P (1992) B cells turn off virgin but not memory T cells. Science 258: 1156-1159.

472. Lees A, Morris SC, Thyphronitis G, Holmes JM, Inman JK, et al. (1990) Rapid stimulation of large specific antibody responses with conjugates of antigen and anti-IgD antibody. J Immunol 145: 3594-3600.

473. Saoudi A, Simmonds S, Huitinga I, Mason D (1995) Prevention of experimental allergic encephalomyelitis in rats by targeting autoantigen to B cells: evidence that the protective mechanism depends on changes in the cytokine response and migratory properties of the autoantigen-specific T cells. J Exp Med 182: 335-344.

474. Snider DP, Segal DM (1989) Efficiency of antigen presentation after antigen targeting to surface IgD, IgM, MHC, Fc gamma RII, and B220 molecules on murine splenic B cells. J Immunol 143: 59-65.

475. Zaghouani H, Kuzo Y, Kuzo H, Mann N, Daian C, et al. (1993) Engineered immunoglobulin molecules as vehicles for T cell epitopes. Int Rev Immunol 10: 265-278.

476. Zaghouani H, Steinman R, Nonacs R, Shah H, Gerhard W, et al. (1993) Presentation of a viral T cell epitope expressed in the CDR3 region of a self immunoglobulin molecule. Science 259: 224-227.

477. Eidem JK, Rasmussen IB, Lunde E, Gregers TF, Rees AR, et al. (2000) Recombinant antibodies as carrier proteins for sub-unit vaccines: influence of mode of fusion on protein production and T-cell activation. J Immunol Methods 245: 119-131.

478. Zaghouani H, Kuzu Y, Kuzu H, Brumeanu TD, Swiggard WJ, et al. (1993) Contrasting efficacy of presentation by major histocompatibility complex class I

and class II products when peptides are administered within a common protein carrier, self immunoglobulin. Eur J Immunol 23: 2746-2750.

479. Lunde E, Bogen B, Sandlie I (1997) Immunoglobulin as a vehicle for foreign antigenic peptides immunogenic to T cells. Mol Immunol 34: 1167-1176.

480. Lunde E, Munthe LA, Vabo A, Sandlie I, Bogen B (1999) Antibodies engineered with IgD specificity efficiently deliver integrated T-cell epitopes for antigen presentation by B cells. Nat Biotechnol 17: 670-675.

481. Lunde E, Rasmussen IB, Eidem JK, Gregers TF, Western KH, et al. (2001) 'Troy-bodies': antibodies as vector proteins for T cell epitopes. Biomol Eng 18: 109-116.

482. Lunde E, Western KH, Rasmussen IB, Sandlie I, Bogen B (2002) Efficient delivery of T cell epitopes to APC by use of MHC class II-specific Troybodies. J Immunol 168: 2154-2162.

483. Lunde E, Lauvrak V, Rasmussen IB, Schjetne KW, Thompson KM, et al. (2002) Troybodies and pepbodies. Biochem Soc Trans 30: 500-506.

484. Norderhaug L, Olafsen T, Michaelsen TE, Sandlie I (1997) Versatile vectors for transient and stable expression of recombinant antibody molecules in mammalian cells. J Immunol Methods 204: 77-87.

CHAPTER 2

Stable cytotoxic T cell escape mutation in hepatitis C virus is linked to maintenance of viral fitness

Luke Uebelhoer[1], Jin-Hwan Han[2], Benoit Callendret[3,4], Guaniri Mateu[1], Naglaa H. Shoukry[5], Holly L. Hanson[1], Charles M. Rice[2], Christopher M. Walker[3,4] and Arash Grakoui[1*]

[1]Department of Medicine, Division of Infectious Diseases, Microbiology and Immunology, Emory Vaccine Center, Emory University School of Medicine, Atlanta, GA 30329; [2]Laboratory of Virology and Infectious Disease, Center for the Study of Hepatitis C, The Rockefeller University, New York, NY 10021; [3]The Center for Vaccines and Immunity, Nationwide Children's Hospital and [4]Deparment of Pediatrics, The Ohio State University, OH, 43205; [5]Department of Medicine, University of Montreal and Centre de Recherche du Centre Hospitalier de l'Université de Montréal (CR-CHUM), Montréal, Québec, Canada; *Corresponding author

Running title: T cell escape mutation and viral fitness

This chapter consists of a manuscript that was published in *PLoS Pathog. 2008 Sep 5;4(9):e1000143*.

Abstract

Mechanisms by which hepatitis C virus (HCV) evades cellular immunity to establish persistence in chronically infected individuals are not clear. Mutations in human leukocyte antigen (HLA) class I-restricted epitopes targeted by CD8+ T cells are associated with persistence, but the extent to which these mutations affect viral fitness is not fully understood. Previous work showed that the HCV quasispecies in a persistently infected chimpanzee accumulated multiple mutations in numerous class I epitopes over a period of 7 years. During the acute phase of infection one representative epitope in the C-terminal region of the NS3/4A helicase, $NS3_{1629\text{-}1637}$, displayed multiple serial amino acid substitutions in major histocompatibility complex (MHC) anchor and T cell receptor (TCR) contact residues. Only one of these amino acid substitutions at position 9 (P9) of the epitope was stable in the quasispecies. We therefore assessed the effect of each mutation observed during *in vivo* infection on viral fitness and T cell responses using an HCV subgenomic replicon system and a recently developed *in vitro* infectious virus cell culture model. Mutation of a position seven (P7) TCR-contact residue, I1635T, expectedly ablated the T cell response without affecting viral RNA replication or virion production. In contrast, two mutations at the P9 MHC-anchor residue abrogated antigen-specific T cell responses, but additionally decreased viral RNA replication and virion production. The first escape mutation, L1637P, detected *in vivo* only transiently at three months after infection, decreased viral production and reverted to the parental sequence *in vitro*. The second P9 variant, L1637S, which was stable *in vivo* through seven years of follow-up, evaded the antigen-specific T cell response and did not revert *in vitro* despite being less optimal in virion production compared to the parental virus. These studies

suggest that HCV escape mutants emerging early in infection are not necessarily stable, but are eventually replaced with variants that achieve a balance between immune evasion and fitness for replication.

Introduction

Hepatitis C virus (HCV) currently infects an estimated 3% of the world's population (~170 million people) [1,2], causing a myriad of health problems including fibrosis and cirrhosis of the liver [3,4]. Infection considerably increases the probability of hepatocellular carcinoma, and HCV-related hepatic disease has become the leading cause of orthotopic liver transplantation in the United States [5]. The majority of those infected with the virus are unable to spontaneously resolve the infection despite the presence of humoral and cellular immune responses that are at least occasionally robust [6-8]. There have been many reasons proposed as to why the immune system fails in the face of chronic HCV infection, including early T cell exhaustion, particularly of the CD4+ helper subset [9,10], dendritic cell (DC) dysfunction [11,12], impairment of effector cells [6,13,14], and cytotoxic T lymphocyte (CTL) viral epitope escape [15-18]. Like most small RNA viruses, HCV has an extremely high replication rate (~10^{10}-10^{12} virions/day, [19]), and the highly error prone NS5B polymerase allows for robust production of minor viral variants that may outpace cellular immune responses [6,20,21]. These variants are under constant immune pressure in the infected host, and Darwinian selection processes lead to domination of the viral quasispecies by the most fit virus that can also evade immune recognition.

Viremia varies widely in individuals with chronic HCV infection with steady state values that range from a few thousand to several million genomes per milliliter of plasma. Factors that regulate virus load in persistent HCV infection are not known but could conceivably influence the rate and severity of progressive liver disease. CTL mutational

escape could have positive or negative effects on virus replication depending on the site and nature of the amino acid substitution(s) within structural or non-structural HCV proteins. Some substitutions might be expected to result in loss of immune control and thus higher levels of virus production, but it is also plausible that mutations facilitating CTL escape have negative consequences for replication if they impair production, assembly, or release of virions. Impaired replicative fitness as a result of escape mutation has been associated with reduced viremia and slower disease progression in HIV-1-infected humans and SIV-infected rhesus macaques [22-25]. Despite the importance of CTL epitope viral mutation for immune evasion, in HCV infection many highly targeted epitopes have a low mutation frequency. Epitopes such as HLA-A2 restricted $NS3_{1073-1081}$ are consistently targeted by CD8+ T cells, but amino acid mutations facilitating immune evasion are rarely observed [26,27]. Since the NS3 protein shares both protease and NTPase-dependent helicase functions, it has been proposed that mutations in these epitopes may be lethal to the virus [28]. However, few studies have examined how CTL escape directly correlates with HCV fitness. Cell culture models of HCV replication utilizing viral replicons have been valuable in identifying adaptive mutations that facilitate robust replication in hepatocytes *in vitro* [29,30]. Using this tool along with recently developed systems allowing actual infection rather than just replication [31-34], we extend these models to study the impact of CTL escape mutation on virus replication and virion production. In this report, we assessed the evolution of a dominant MHC class I epitope during the acute and chronic phases of infection in a chimpanzee studied through seven years of follow-up. A C-terminal epitope of the NS3 protein, $NS3_{1629-1637}$, restricted by the chimpanzee Patr-B1701 molecule, has previously been shown to serially

acquire several distinct mutations in amino acid residues that impair MHC binding or TCR recognition [15,35,36]. The availability of longitudinal samples from this chimpanzee facilitated a careful examination of epitope evolution and an integrated assessment of the fitness of viral variants that arose *in vivo*, as well as the host immune response directed against these variants. Our results indicate that genomes encoding CTL escape mutations that emerge early in infection are not necessarily optimized for replication and are eventually replaced by variants that successfully balance escape from cellular immune pressure and replicative fitness in the chronic phase of infection. We predict that this could be an important factor influencing virus load in HCV-infected chimpanzees and humans, with as yet unknown consequences for liver disease progression.

Materials and Methods

Patr-B1701 plasmid, subgenomic replicon, and full-length chimeric genome construction

Patr-B1701 plasmid. The Patr-B1701 sequence was cloned into the pcDNA3.1Zeo(-) plasmid (Invitrogen, Carlsbad, CA). Briefly, the Patr-B1701 sequence was cloned from an EBV-transformed B cell line generated from chimpanzee CH503, linearized using SalI-EcoRI (1337 bp), and ligated to the multiple cloning site (MCS) of pcDNA3.1Zeo(-) cut with XhoI-EcoRI. Ligations were transformed into DH5α cells (Invitrogen, Carlsbad, CA), plated, and colonies picked and sequenced using the T7 forward and BGH reverse priming sequences (Macrogen, Korea).

Subgenomic replicons. Subgenomic replicons have been previously described [29,30]. The original BB7 replicon backbone containing a neomycin cassette under the control of the 5' HCV internal ribosomal entry site (IRES) and the NS3-NS5B genes under the control of an EMCV IRES was modified using site-directed PCR mutagenesis and standard cloning procedures, as described below.

JFHxJ6 Cp7 NS3 mutants. Plasmids pJFH1 (JFH) and pGND (GND) have been previously described [33], and plasmid pJ6CF (J6) is an autologous genotype 2a full-length clone that has been shown to be infectious in chimpanzees [37]. Sequence homology for NS3 between the infecting HCV 1/910 strain and BB7 is 92.2% and between HCV 1/910 and JFH/J6 is 80%. Proper controls to assess the effects of these differences at the epitope level were engineered into the backbones of BB7 and Cp7, respectively. To create the full-length chimeric JFHxJ6 Cp7 (Cp7) construct, two PCR products were produced and fused to create junction points between Core-p7 of J6 and

p7-NS5B of JFH, resulting in the JFHxJ6 Cp7 full-length clone (described in [34]). $NS3_{1629-1637}$ mutations were introduced in the Cp7 clone as follows, using standard cloning procedures. A single forward primer "039NS3Epi Forward" (5'-GATTCCCCTATCCTGCATCAAG-3') was used with four reverse primers "040NS3EpiGAVQNEITL" (5'-GTCAGCTTGCATGCATGTGGCGATGTACTTCGTCCCAGGGTGTGTGAGGGTAATCTCATTTTGTACAGCGCCCAAACGGTACAGGAGAGG-3'), "041NS3EpiGAVQNEITP" (5'-GTCAGCTTGCATGCATGTGGCGATGTACTTCGTCCCAGGGTGTGTAGGGGTAATCTCATTTTGTACAGCGCCCAAACGGTACAGGAGAGG-3'), "042NS3EpiGAVQNEITS" (5'-GTCAGCTTGCATGCATGTGGCGATGTACTTCGTCCCAGGGTGTGTGCTGGTAATCTCATTTTGTACAGCGCCCAAACGGTACAGGAGAGG-3'), and "043NS3EpiGAVQNETTL" (5'-GTCAGCTTGCATGCATGTGGCGATGTACTTCGTCCCAGGGTGTGTGAGGGTGGTCTCATTTTGTACAGCGCCCAAACGGTACAGGAGAGG-3'), to amplify mutated $NS3_{1629-1637}$ epitopes from the Cp7 full-length genome. PCR fragments were gel purified, NsiI-SacI digested (819 bp fragment cut to a 737 bp fragment), and a three-piece ligation performed; NsiI-SacI epitope fragment + NsiI-AvrII Cp7 + AvrII-SacI-BbvCI Cp7. All fragments generated by PCR were verified by sequencing (Macrogen, Korea).

Peptides

Wild-type (GAVQNEITL) and mutant (GAVQNEITP, GAVQNEITS, GAVQNETTL) $NS3_{1629-1637}$ peptides were synthesized by Genemed Biosynthesis (San Francisco, CA) and purified by high-performance liquid chromatography (HPLC). All peptides were stored at a concentration of 1 mg/ml at –20ºC.

Cell lines and cell culture

Huh-7.5 cells were maintained in Dulbecco's modified Eagle's medium supplemented with 10% fetal bovine serum (FBS, Hyclone, Logan, UT) at 37°C in 5% CO_2. The Huh-7.5/B1701 cell line was generated as follows. Huh-7.5 cells were trypsinized, washed with DMEM-10 media, and $4x10^6$ cells electroporated with 2.5 μg pcDNA3.1Zeo(-)B1701 plasmid using the AMAXA T-028 program (AMAXA, Gaithersburg, MD). Cells were resuspended in DMEM-10, plated in a p100 petri dish, and allowed to rest for 24 h before addition of 300 μg/ml zeocin (Invitrogen, Carlsbad, CA). Cell foci surviving selection were trypsinized, transferred to a 24-well plate, and allowed to grow under selection up to a p150 petri dish. Huh-7.5/B1701 cells were stained with 20 μl of anti-human pan-HLA-A, B, C FITC-conjugated antibody (BD Biosciences, San Jose, CA) in FACS buffer (0.5% (w/v) bovine serum albumin + 1% (v/v) of 10% sodium azide in PBS) in parallel with untransfected Huh-7.5 cells, and visualized on a Becton Dickinson FACScalibur flow cytometer. Huh-7.5 and Huh-7.5/B1701 were transfected with replicons harboring wild-type or mutated $NS3_{1629-1637}$ epitopes as previously described [29,30]. The $NS3_{1629-1637}$-specific CD8+ T cell clone has been previously described [15], and was stimulated using αCD3 mAb (Immunotech, Beckman Coulter, Fullerton, CA) in a ratio of $1x10^6$ CD8+ clone to $2x10^6$ irradiated peripheral blood mononuclear feeder

cells (PBMC) and maintained in RPMI media supplemented with 10% FBS, Gentamicin (Gibco, Invitrogen, Carlsbad, CA), Penicillin/Streptomycin (Lonza, Walkersville, MD), T-stim culture supplement (human-no PHA, BD Biosciences, San Jose, CA) and human recombinant IL-2 (rIL-2, Roche, Indianapolis, IN). Autologous chimpanzee B cells were EBV-transformed following established protocols using whole blood and conditioned medium from the marmoset cell line B95-8 [38].

Western blots for intracellular HCV protein

Huh-7.5 cells and Huh-7.5/B1701 cells with or without subgenomic replicons were lysed directly on 6-well plates using 150 μl lysis buffer (100 mM Tris pH 6.8, 20 mM dithiothreitol, 4% (w/v) sodium dodecyl sulfate, 20% (v/v) glycerol, 0.2% (w/v) bromophenol blue) and passed through a $27^{1/2}$ gauge needle 3-5 times before being stored at –80°C. Lysates were denatured at 92°C for 10 min, run on 5% stacking/8% resolving SDS-polyacrylamide gels, and transferred to Immobilon-P membranes (Millipore Corporation, Bedford, MA). Membranes were blocked with TBS-T (20 mM Tris pH 7.4, 150 mM NaCl, 0.1% (v/v) Tween-20 (polyoxyethylene sorbitan monolaurate) plus 5% (w/v) non-fat dry milk, and probed with antibodies against NS3 and NS5 (Virostat, Portland, ME), or β-actin in the same buffer overnight at 4°C. Membranes were washed 5 times with TBS-T, probed with HRP-conjugated secondary antibodies for 1 h at room temperature, washed 5 times, and detected using ECL Western detection reagents (Amersham Biosciences, Piscataway, NJ).

Quantification of HCV RNA by Real Time qRT-PCR

Total RNA from $1x10^6$ infected Huh-7.5 cells was isolated using an RNeasy Mini Kit (QIAGEN, Valencia, CA). 80 ng of total cellular RNA was used to perform Real-Time Quantitative Reverse Transcription PCR using Taqman® One Step RT-PCR Master Mix Reagents (Applied Biosystems, New Jersey, USA), primers specific for the HCV 5' NTR (forward, 10 μM: 5'-CTTCACGCAGAAAGCGCCTA-3' and reverse, 10μM: 5'-CAAGCGCCCTATCAGGCAGT-3'), and a probe (10 μM: 6-FAM-TATGAGTGTCGTACAGCCTC-MGB NFQ). Thermal cycling conditions were designed as follows: 48°C for 30 min, 95 °C for 10 min, and 40 cycles of 15 sec at 95°C, followed by 1 min at 60°C. All amplification reactions were carried out in duplicate. A standard curve was similarly generated using 10-fold dilutions of pJFH1 RNA transcripts generated by *in vitro* transcription, DNAse treatment, purification by RNeasy Mini Kit and quantification by spectrophotometry.

^{51}Cr-release assay

To determine lysis capability of the $NS3_{1629-1637}$-specific CD8+ T cell clone, Huh-7.5/B1701 cells with or without subgenomic replicons and EBV-transformed autologous B cells were spun at 1500 rpm for 5 min in a Beckman Coulter Allegra X-15R centrifuge, media aspirated, and tubes vortexed to resuspend the pellet. Cells were pulsed with ^{51}Cr per standard protocol (NEN Radiochemicals, Perkin Elmer, Waltham, MA) for 1 h, and cells not harboring subgenomic replicons were simultaneously pulsed with 1 μg/ml wild-type $NS3_{1629-1637}$ peptide resuspended in a total volume of 100 μl RPMI-10. Pulsed cells were washed 5 times to eliminate residual radiation and exogenous peptide, and mixed at different effector ($NS3_{1629-1637}$-specific CD8+ T cell clone) to target ratios in 200 μl

RPMI-10 in a 96-well round-bottom plate. Lysis was allowed to occur for 4 h at 37°C in 5% CO_2 before transferring 100 μl of supernatant to a flat-bottom 96-well plate. Supernatants were frozen at –80°C for at least 1 h to eliminate cellular carryover before being counted using a 1450 Microbeta Wallac Trilux liquid scintillation counter (Perkin Elmer, Waltham, MA).

Transfection and infection of human hepatoma cell lines

To transfect viral RNA, 20 μg of full-length JFHxJ6 Cp7 genomes with or without $NS3_{1629\text{-}1637}$ mutations were linearized by 4 h digestion with XbaI and subsequently blunt end-digested with Mung Bean Nuclease (New England Biolabs, Ipswich, MA). Linearized DNA was extracted twice with 25:24:1 phenol:choroform:isoamyl alcohol pH5.2±0.2 and once with chloroform, quantified by spectrophotometry, and 2 μg of purified product was RNA transcribed using a MEGAscript T7 High Yield Transcription Kit (Ambion, Austin, TX). RNA was purified again using phenol:chloroform:isoamyl alcohol followed by chloroform, and integrity was checked on an agarose gel. After RNA quantification by spectrophotometry, Huh-7.5 or Huh-7.5/B1701 cells were trypsinized for exactly 3 min, washed twice with ice cold PBS, and resuspended at $2x10^7$ cells/ml. 10 μg of purified RNA was electroporated into $8x10^6$ cells with 5 pulses of 99 μsec at 820 V over 1.1 sec in an ECM 830 electroporator using a 2 mm-gap electroporation cuvette (BTX Genomics, Harvard Apparatus, Holliston, MA). Cells were resuspended in DMEM-10 and plated in 6-well plates. To infect Huh-7.5 or Huh-7.5/B1701 cells using whole virus, cells were plated at 10-20% confluency in six-well plates. Media was aspirated, and viral supernatants harvested from transfected cells were added to the plates

in a volume of at least 200 µl. Plates were placed on a rocker at 37°C and 5% CO_2 for 4 hours before readdition of media.

Huh-7.5/B1701 cells as APCs and intracellular IFNγ release assay

Huh-7.5 and Huh-7.5/B1701 that had not been electroporated (either with subgenomic replicons or full-length viral RNA) or infected with whole virus were pulsed for 1 hour with wild-type or mutated $NS3_{1629-1637}$ peptides at decreasing concentrations as in the ^{51}Cr-release experiments. Cells harboring sugenomic replicons were harvested and used directly. Cells that had been transfected with full-length viral RNA were harvested 4 d post-transfection, and cells that had been infected with whole virus were harvested 5 d post-infection. Cocultures were established in a 24-well plate using a 1:1 ratio of $NS3_{1629-1637}$-specific CD8+ T cells to APCs, and allowed to incubate overnight at 37°C in 5% CO_2 in the presence of GolgiStop (BD Pharmingen, San Jose, CA) at a concentration of 1 µl/ml. After incubation, cells were harvested, washed once in FACS buffer, and permeabilized using BD FACS Permeabilizing Solution 2 (BD Biosciences, San Jose, CA). Cells were stained with mouse anti-human monoclonal antibodies to CD3 (APC-conjugated, BD Pharmingen, San Jose, CA), CD8 (PerCP-conjugated, BD Biosciences, San Jose, CA), and IFNγ (FITC-conjugated, BD Pharmingen, San Jose, CA), and visualized on a Becton Dickinson FACScalibur flow cytometer. Data were analyzed using FlowJo software (Tree Star, Inc).

Viral titration and immunohistochemical staining

96-well plates were coated with collagen for 1 h and allowed to dry before plating $6x10^3$ naïve Huh-7.5 cells/well. Viral supernatants from transfected or infected Huh-7.5 or Huh-7.5/B1701 cells were collected, passaged through a 0.22 μm filter, and used to inoculate cells at 10-fold dilutions. Three days post-infection, cells were immunostained for NS5A as previously described [32]. Briefly, the inoculum was removed, and cells were washed twice with PBS before fixation with methanol at –20°C. Cells were then washed twice with PBS, once with PBS + 0.1% (v/v) Tween-20 (PBS-T) (normal wash), and blocked for 30 min at room temperature with PBS-T + 1% (w/v) BSA + 0.2% non-fat dry milk, followed by an endogenous peroxidase blocking step (3% H_2O_2 (v/v) in PBS) for 5 min at room temperature. Cells were washed normally and stained overnight at 4°C with an anti-NS5A antibody (9E10). Cells were washed normally, and incubated for 30 min at room temperature with a 1:3 dilution of ImmPRESS goat anti-mouse HRP-conjugated antibody (Vector Laboratories, Burlingame, CA). Cells were washed normally once more before being developed using DAB substrate (Vector Laboratories, Burlingame, CA). Titers were determined by calculating the tissue culture infection dose at which 50% of wells were positive for NS5A antigen [39].

Sequencing of viral clones

Huh-7.5/B1701 cells were infected using viral supernatants from day 4 transfected cells. Post-infection, media was aspirated, cells were washed twice with PBS and lysed using Buffer RLT (QIAGEN, Valencia, CA) + 1% 2-mercaptoethanol (Fisher Scientific, Pittsburgh, PA). Lysates were placed directly onto QIAshredder columns, and total RNA isolated and purified using an RNeasy kit (QIAGEN, Valencia, CA). RNA integrity was

quantified using a spectrophotometer, checked on an agarose gel, and 2μg used in a first-strand cDNA synthesis reaction as follows. Briefly, RNA was incubated with random hexamer primers and 10mM dNTPs at 65°C for 5 minutes, then placed on ice. First-strand reverse transcriptase buffer, 0.1mM DTT and RNase H (Invitrogen, Carlsbad, CA) were added to each reaction and allowed to incubate at room temperature for 2 minutes before the addition of superscript II reverse transcriptase (Invitrogen, Carlsbad, CA). The reaction was allowed to proceed at 42°C for 2 hours, and first-strand cDNA was used directly in an $NS3_{1629-1637}$ epitope-specific PCR reaction using primers "211NS3EpiSeqInF" (5'-TCGCGTACCTAGTAGCCTACCAAGC-3') and "212NS3EpiSeqInR" (5'-GCTGGTTGACGTGCAAGCGGCCGA-3') to generate a 323bp fragment containing the epitope. PCR products were cleaned using a PCR cleanup kit (QIAGEN, Valencia, CA), cloned into Top10 chemically competent cells using a TOPO TA kit (Invitrogen, Carlsbad, CA), and individual clones were sent for sequencing (Macrogen, Rockville, MD).

Polyclonal antigen-specific expansion of T cells and intracellular cytokine staining

CD8+ T cells were positively isolated from frozen PBMC using the Dynal CD8+ Positive Isolation Kit (Invitrogen Dynal AS, Oslo, Norway) according to manufacturer instructions. Approximately 360,000 CD8+ T cells were plated in one well of a 24-well plate in 1 ml complete medium (RPMI 1640 containing 10% AB human serum and 1% penicillin/streptomycin). To serve as APCs, 6 million irradiated autologous PBMC were pulsed for 2 h with 5 μg/ml of the GAVQNETTL peptide. After three washes, APCs were resuspended in 1 ml complete medium and mixed with the CD8+ T cells. Cells were

incubated at 37°C in 7% CO_2. Every 3 days, 1 ml of the culture medium was replaced with 1 ml of complete medium containing 50 U/ml rIL-2. On day 20, CD8+ T cells were plated in a 96-well plate in AIM-V medium (Aim-V (Invitrogen, Carlsbad, CA) supplemented with 2% AB human serum) and allowed to rest for 8 h. Irradiated EBV-transformed autologous B cells were pulsed for 2 h with 10 μg/ml of peptide for use as APCs. After three washes, APCs were resuspended in Aim-V medium and mixed with CD8+ T cells at a 1:1 ratio with 1 μg/ml of anti-CD28 and anti-CD49d antibodies (BD Pharmingen, San Jose, CA). After one hour, GolgiStop (BD Pharmingen, San Jose, CA) was added at a concentration of 1 μl/ml and cells were further incubated 16 h at 37°C in 7% CO_2. After incubation, cells were harvested and washed once in FACS buffer. Cells were blocked with PBS-20% human serum and then stained with mouse monoclonal antibodies to CD8 (APC-conjugated, BD Pharmingen, San Jose, CA) and CD4 (Pacific Blue-conjugated, BioLegend). After two washes with FACS buffer, cells were stained with Live/Dead Fixable Blue Stain Kit (Invitrogen, Carlsbad, CA). Cells were washed twice with FACS buffer and permeabilized using BD Cytofix/Cytoperm solution (BD Biosciences, San Jose, CA). Cells were then stained with mouse monoclonal antibodies to CD3 (PerCP-conjugated, BD Pharmingen, San Jose, CA) and IFNγ (PE-conjugated, BD Pharmingen, San Jose, CA) and visualized on a Becton Dickinson LSR flow cytometer. Data were analyzed using FlowJo software (Tree Star, Inc).

Results

CTL escape mutations affect subgenomic transduction efficiency

It is well established that the Patr-B1701 restricted $NS3_{1629–1637}$ epitope is a dominant target of CD8+ T cells during HCV infection in chimpanzees [15,36]. This epitope displayed a complex pattern of evolution throughout the acute and chronic phases of infection in the chimpanzee, and thus is valuable for the study of viral epitope escape and fitness costs associated with increased immune pressure. In chimpanzee CH503 infected with a known inoculum of HCV1/910, sequence analysis over seven years showed three distinct mutations at three separate timepoints tested in the $NS3_{1629–1637}$ epitope [15]. The wild-type amino acid sequence of this epitope in the input HCV1/910 inoculum was GAVQNEITL (and from here on referred to as the "parent" epitope, $NS3_{1629–1637}$), and three months post-infection a L1637P variant was found in the animal. Ten months post-infection, this variant had been replaced by two dominant species, I1635T and L1637S, at P7 and P9 respectively. Eventually, L1637S became fixed in this chimpanzee, and was the only variant recovered up to 82 months post-infection (Figure 1A). There is one nucleotide change from leucine to proline and one nucleotide change from proline to serine and hence two changes to occur to change leucine to serine; this perhaps provides mechanistic insight into the early appearance of L1637P and its later replacement by L1637S. We set out to test directly the fitness cost associated with the mutating $NS3_{1629–1637}$ variants by modeling the *in vivo* infection using the HCV subgenomic replicon system [29,30]. Using site-directed PCR mutagenesis, we engineered the mutants in the $NS3_{1629–1637}$ region that had previously been observed in chimpanzees, starting with the original HCV1/910 parental epitope sequence. The mutated replicons on the BB7 backbone were

transfected into Huh-7.5 cells, which were then plated under neomycin selection at decreasing cell numbers to determine transduction efficiency (Figure 1A). It is important to note that the original amino acid sequence of $NS3_{1629–1637}$ epitope present in the BB7 subgenomic replicon is GAVQNEVTT, and was modified to insert the parental $NS3_{1629–1637}$ epitope of HCV1/910. Substitution of the parental HCV1/910 $NS3_{1629–1637}$ epitope resulted in a slight decrease of transduction efficiency in this replicon. The P9 mutations GAVQNEITP (L1637P) and GAVQNEITS (L1637S), which show a 400-fold decrease in B1701 binding capacity [15], showed increased susceptibility to neomycin, with L1637P growing the least efficiently. The P7 GAVQNETTL (I1635T) mutation was more resistant to selection than the HCV1/910 parental GAVQNEITL $NS3_{1629–1637}$ sequence. These results suggest that mutations in this epitope at P9 severely hinder the replicative capacity of the virus, while an isoleucine to threonine substitution at P7 (I1635T) has no apparent effect. Additionally, a GND clone containing a mutation in the NS5B RNA-dependent RNA polymerase GDD motif thus ablating HCV RNA replication was used as a negative control. A real-time quantitative RT-PCR assay was used to quantify the level of HCV RNA replication 6 d post-transfection of Huh-7.5 cells using relevant transcribed RNAs. As shown in Figure 1B, levels of viral RNA replication correlated identically with the transduction efficiencies observed between the different constructs shown in Figure 1A. NS3 and NS5A protein expression for all constructs, including the original HCV replicon BB7 epitope GAVQNEVTT, was similar when assayed by Western blot (Figure 1C). Similar non-structural protein expression suggests that the $NS3_{1629–1637}$ mutations may affect initiation of replication, with a steady-state accumulation of protein expression occurring once replication has been established. It has been shown that replicons under

drug-induced selective pressure, such as G418, display high levels of HCV replication (1000–5000 positive strand RNA molecules), and therefore may show similar levels of protein expression [40]. However, under non-selective conditions, replicons having lower transduction efficiencies are lost more rapidly than those with high transduction efficiencies, and these differences may be reflected in viral protein levels. Although the P9 L1637S mutation resulted in partially reduced replicative capacity, the intermediate phenotype (between L1637P and I1635T) suggests that this mutation represents a balance between replicative fitness and CTL escape. This observation is interesting as the P9 L1637S mutation became a fixed quasispecies through 7 years of persistent replication in animal CH503. It is also important to note that cells harboring HCV replicons were additionally sequenced to ensure fidelity of previously inserted mutations. Sequencing of at least six clones from each subgenomic-bearing Huh-7.5/B1701 cell line (six, nine, ten, and six clones for $NS3_{1629–1637}$, L1637P, L1637S, and I1635T, respectively) showed no variation from expected amino acid sequences. This sequencing was carried out on PCR fragments spanning the inserted $NS3_{1629–1637}$ epitope from total cellular RNA.

Wild-type but not mutant $NS3_{1629–1637}$ epitope is presented to $NS3_{1629–1637}$-specific CTL on class I MHC Patr-B1701

We next sought to determine the ability of parental or mutated $NS3_{1629–1637}$ epitope to be presented by a cell line expressing the appropriate chimpanzee MHC molecule. Patr-B1701 is a MHC class I molecule expressed in CH503, and previous data demonstrated that mutations at critical anchor residues in the $NS3_{1629–1637}$ epitope (including P9) hindered peptide binding to Patr-B1701 [15]. We first examined pan-class I surface

expression on Huh-7.5 cells, and compared those levels to Huh-7.5 cells that had been transfected with a plasmid containing Patr-B1701 under zeocin selection (Huh-7.5/B1701, Figure 2A). It is important to note that we are not able to specifically stain for the Patr-B1701 molecule since specific antibodies to this protein do not currently exist. However, overall class I expression was similar in both cell types when compared to the isotype control, which led us to test the ability of Patr-B1701 expression to mediate wild-type $NS3_{1629–1637}$ epitope-directed killing by a B1701-restricted CTL clone, 4A, that had been previously isolated from CH503 11 weeks post-infection with the HCV-1/910 virus stock [15]. When EBV-transformed autologous B cells (B1701T) or Huh-7.5/B1701 cells were pulsed with exogenous wild-type $NS3_{1629–1637}$ peptide (1 μg/ml) in a standard ^{51}Cr-release assay, the $NS3_{1629–1637}$-specific CTL clone was able to lyse both antigen presenting target cell populations with similar efficiency (Figure 2B). In contrast, peptide-pulsed Huh-7.5 cells lacking the Patr-B1701 molecule were not recognized by the CTL clone. In addition, we further determined the magnitude of the T cell interferon response to both the wild-type and mutated epitopes. To do so, we performed an intracellular IFNγ FACS analysis on the CTL clone cocultured with various APCs that had been pulsed with various peptide concentrations (Figure 2C). Huh-7.5/B1701 cells that had been pulsed for 1 h with wild-type $NS3_{1629–1637}$ peptide elicited a robust IFNγ response from the CTL clone. This response was not elicited by the three mutant epitopes at concentrations up to 0.5 μg/ml. Responses to each epitope could be seen at very high concentrations indicating that the CD8+ T cell clone could be stimulated to produce IFNγ even with mutants that had previously been shown to have lowered MHC-binding capacity [15] if the mutant was present at high (but not biologically significant) concentrations. These data

collectively show that Huh-7.5 cells stably transfected with the Patr-B1701 molecule efficiently present exogenous wild-type peptide *in vitro*, and that an antigen-specific T cell clone is able to respond by secreting IFNγ and exerting its cytotoxic effect. Conversely, this CTL clone is unable to efficiently respond when Huh-7.5/B1701 cells present mutated exogenous $NS3_{1629–1637}$ peptides reflective of *in vivo* viral species, containing a threonine substitution at P7 or a proline or serine substitution at P9, at physiologically relevant concentrations.

Huh-7.5/B1701 cells harboring subgenomic HCV replicons present the $NS3_{1629–1637}$ epitope to $NS3_{1629–1637}$-specific CTL

To determine whether Huh-7.5 cells expressing the Patr-B1701 expressed in CH503 could adequately process and present the $NS3_{1629–1637}$ epitope during active viral replication for T cell recognition, Huh-7.5/B1701 cells were stably transfected with various HCV replicons containing the appropriate mutations under neomycin selection as before (see Figure 1A). Cells exhibiting zeocin resistance (confirming Patr-B1701 expression) and neomycin resistance (confirming presence of replicons) were used to determine protein expression as well as $NS3_{1629–1637}$-specific CTL lysis and IFNγ production. Huh-7.5/B1701 cells harboring HCV replicons showed relatively similar levels of protein expression post-transfection and G418 selection (Figure 3A). Small differences in HCV protein expression were likely due to the stringency of dual selection (zeocin and G418) placed on these cells to maintain both the Patr-B1701 plasmid and the subgenomic construct. Protein expression was monitored to ensure that the replicons containing the parental HCV 1/910 $NS3_{1629–1637}$ epitope and the mutants were able to produce, process and present similar levels of viral peptides to the CTL clone. Huh-

7.5/B1701 cells harboring subgenomic HCV replicons were labeled with ^{51}Cr, and cocultured with the $NS3_{1629–1637}$-specific CTL clone to determine the ability of these cells to elicit epitope-directed lysis. Cells replicating the wild-type $NS3_{1629–1637}$ replicon were lysed by the CTL clone, with ~3-fold less efficiency than that seen using Huh-7.5/B1701 cells loaded with exogenous peptide (Figure 3B), reflective of lower levels of physiologic peptide generated in the replicon system. Cells harboring mutated $NS3_{1629–1637}$ replicons elicited very low to undetectable levels of lysis, even at the highest effector to target ratios. Additionally, we assessed whether Huh-7.5/B1701 subgenomic cell lines replicating HCV RNA could elicit an IFNγ response from the $NS3_{1629–1637}$-specific CTL clone. Similar to the pulsing experiment using low amounts of exogenous peptide shown in Figure 2C, only Huh-7.5/B1701 harboring the wild-type subgenomic replicon stimulated the CTL clone to produce IFNγ (Figure 3C).

Infectious HCV harboring the wild-type $NS3_{1629–1637}$ epitope but not escape mutants stimulate a functional T cell response

To test the replication fitness and infectivity costs associated with the mutations observed in the *in vivo* chimpanzee infection, we utilized the Huh-7.5/B1701 cell lines in both transfection and infection studies using full-length HCV constructs capable of producing infectious virus. The full-length genotype 2a JFH isolate has previously been shown to both replicate RNA and produce infectious virus in Huh-7 cells without acquiring adaptive mutations [33,40]. To study robust replication and virion production *in vitro*, a recombinant clone was created by exchanging the core to p7 region of the genotype 2a JFH virus with the genotype 2a J6 virus, and the resulting JFHxJ6 Cp7 (Cp7) recombinant genome produces high titers of virus when used to transfect naïve Huh-7.5

cells (Figure 4C). As in the BB7 replicon system, the corresponding $NS3_{1629–1637}$ epitope present in the JFH sequence of Cp7 was exchanged (using single-site PCR mutagenesis) with that of the parental HCV1/910, as well as the respective mutations seen in CH503 at 3, 10, and 82 months post-infection (Figure 5A). When RNA from parental $NS3_{1629–1637}$ epitope and mutant viruses was transfected into Huh-7.5/B1701 cells, no major difference in protein expression was seen after 4 d as compared to the Cp7 backbone recombinant construct (Figure 5B). The GND transfected RNA expectedly did not produce any protein. These results are consistent with other experiments performed in both Huh-7.5/B1701 cells and Huh-7.5 cells in that these mutations do not affect overall expression of NS3 protein, but may affect initiation of replication (Figure 1C, 3A, 4A, 5B). To determine the efficiency of viral epitope processing and presentation by cells replicating full-length infectious HCV, the $NS3_{1629–1637}$-specific CD8+ T cell clone was co-cultured with Huh-7.5/B1701 cells transfected with the Cp7 backbone, parental HCV1/910 $NS3_{1629–1637}$, and individual mutant infectious clones. These T cells were then analyzed by flow cytometry to determine levels of IFNγ produced by the CD8+ T cell clone 4A. CD8+ T cells that had been stimulated by Huh-7.5/B1701 cells transfected with full-length infectious virus containing the wild-type $NS3_{1629–1637}$ epitope had a robust intracellular IFNγ response, while those containing infectious virus with mutant epitopes were unable to elicit a T cell response (Figure 5C). To determine the level of $NS3_{1629–1637}$ epitope presentation during actual viral infection, supernatants from transfected Huh-7.5/B1701 cells were harvested after 4 d, passed through a 0.22 μm filter, and used to infect naïve Huh-7.5/B1701 cells for 5 d. These cells were then cocultured with the $NS3_{1629–1637}$-specific CD8+ T cell clone overnight, and examined via flow cytometry for

IFNγ release. As previously shown with transfected cells, only Huh-7.5/B1701 cells infected with virus containing the wild-type $NS3_{1629–1637}$ epitope were able to stimulate a response from the CD8+ T cell clone (Figure 5D).

L1637P and L1637S mutations in the P9 anchor residue of $NS3_{1629–1637}$ epitope impair viral fitness

Having previously established that mutations in the P7 and P9 residues of HCV $NS3_{1629–1637}$ epitope ablate CD8+ T cell responses, we sought to determine the effect of each mutation on virion production. Cp7 backbone virus along with the parental HCV1/910 $NS3_{1629–1637}$ and mutant viruses were transfected into Huh-7.5 cells, and protein expression assessed via Western blotting and virion production assessed using a TCID50/ml reinfection assay up to 4 d post-tranfection. There was little difference in protein expression between mutant, HCV1/910 $NS3_{1629–1637}$, and Cp7 backbone infectious viruses (Figure 4A). At the level of RNA replication, as detected by a sensitive qRT-PCR Taqman assay, the viral variant L1637P replicated 1–1.5 logs less efficiently than parental virus (Figure 4B). Interestingly, L1637S replicated with similar efficiency to parental virus, indicating that this variant was competent in replication. However, several differences in virion production were observed. The leucine to proline switch in P9 of $NS3_{1629–1637}$ epitope (L1637P) had a marked effect on the amount of virus secreted into the supernatant. This virus consistently produced 1.5–2 logs less virus than parental HCV1/910 $NS3_{1629–1637}$ and Cp7 backbone virus (Figure 4C). The P7 isoleucine to threonine substitution (I1635T) produced similar levels of virus to the wild-type and Cp7 backbone, all secreting approximately 10^5 TCID50/ml. However, the leucine to serine P9 substitution (L1637S) displayed increased virion production compared to the L1637P

mutation, producing approximately 10^4 TCID50/ml. The L1637S substitution of the parental HCV1/910 $NS3_{1629–1637}$ epitope was found fixed in CH503 from month 10 post-infection up to 82 months post-infection (Figure 1A), and the recovered virion production phenotype seen *in vitro* suggests that L1637S is a more fit clone than L1637P, able to survive with intermediate fitness but efficient escape from immune elimination.

L1637P reverts to the parental $NS3_{1629–1637}$ epitope sequence while L1637S is stable in the absence of CD8+ T cell pressure

Having established the relative fitness of each full-length viral clone, we wanted to determine what, if any, mutations arise in the $NS3_{1629–1637}$ epitope during prolonged *in vitro* viral infection and replication. Huh-7.5/B1701 cells were infected with parental HCV1/910 $NS3_{1629–1637}$ and mutant viruses, and cell lysates were used to obtain total cellular RNA up to 1 month post-infection. After first-strand cDNA synthesis and viral epitope-specific PCR, individual clones were sequenced. In the absence of CD8+ T cell selection pressure, we observed several amino acid mutations in the $NS3_{1629–1637}$ epitope 3 d post-infection. For the parental $NS3_{1629–1637}$ virus, one out of eight clones possessed a glutamic acid to glycine (E1634G) mutation at position 6 (Figure 6). This identical mutation was also found in the L1637S mutant virus 3 d post-infection. However, the E1634G mutation was absent in both the parental and L1637S viruses 23 d post-infection, indicating that this clone perhaps was not dominant or stable (Figure 6). Four out of eleven parental $NS3_{1629–1637}$ clones harbored an A1630D mutation 23 d post-infection, which was unusual given the absence of CD8+ T cell pressure and the fitness of this virus in both the replicon (Figure 1A) and cell culture (Figure 4B,C) models. The I1635T mutant virus was stable over the infection course, exhibiting no mutations on both 3 and

23 d post-infection. Similarly, the L1637S mutant virus remained fixed 23 d post-infection, demonstrating the stability of this viral variant in our *in vitro* cell culture model. The stability of the L1637S mutant virus *in vitro* mirrors that which was observed *in vivo* with a serine at P9 stable 7 years post infection. Interestingly, the L1637P mutant virus was unchanged 3 d post-infection, but two variants were found 23 d post-infection (Figure 6). One variant, V1631A, was present at low frequency (1/15), while the other, P1637L, represented a significant fraction of the total population (5/15 clones). The P1637L mutation is particularly interesting because it represents reversion at position 9 in an unstable *in vivo* variant to the parental $NS3_{1629–1637}$ epitope sequence in the absence of *in vitro* CD8+ T cell selection pressure. These results demonstrate that *in vitro* mutation of a CD8+ T cell epitope in hepatitis C virus can occur, that particular amino acid substitutions are not maintained over the course of *in vitro* infection, and that reversion of less fit viral variants to parental HCV sequence can occur when CD8+ T cell pressure is absent.

An antigen-specific memory CD8+ T cell response prevents I1635T from becoming fixed in the viral population

Variant I1635T was replication competent, escaped CTL recognition, and did not revert to the parental $NS3_{1629–1637}$ sequence in the absence of selective pressure. Because the I1635T variant possesses a mutation in a TCR-contact residue (P7) and not an MHC-binding residue, we hypothesized that it may have stimulated a novel CD8+ T cell response *in vivo*, resulting in immune pressure preventing I1635T from becoming fixed in the viral population. To test this hypothesis, CD8+ T cells were isolated from frozen CH503 PBMC samples taken more than 7 years post-infection and stimulated with the

I1635T peptide. Upon stimulation with autologous EBV-transformed B cells pulsed with I1635T peptide, CD8+ T cells secreted IFNγ (Figure 7). The I1635T antigen-specific CD8+ T cells did not respond to an irrelevant (SIINFEKL) control peptide, or the parental $NS3_{1629–1637}$ peptide (Figure 7). These results support the hypothesis that although the I1635T variant replicated efficiently and escaped from $NS3_{1629–1637}$-specific T cells, its persistence was hindered by a de novo T cell response.

Discussion

Growing evidence has shown that CD8+ T cell epitope mutation and subsequent viral escape are associated with persistence of viruses like HIV, SIV, and HCV [17,18,26,41–47]. Indeed, the rate of non-synonymous mutation leading to amino acid substitutions is statistically higher in MHC class I restricted epitopes than in non-restricted epitopes or flanking regions, indicating that they are subject to Darwinian selection pressure by CD8+ T cells [18,26,45,48–53]. With the development of cell culture models that support HCV infection and replication, it is now possible to model how changes to the genome influence the rate of viral reproduction. In this study we have exploited these *in vitro* replication models to better understand how the potentially oppositional forces of immune evasion and efficient viral replication shaped evolution of a well-characterized dominant MHC class I epitope that displayed iterative adaptive mutations during establishment of HCV persistence in a chimpanzee. Mutational analyses in the currently available *in vitro* systems are limited by the necessity to study viral fitness and virion production in the context of genotype 1b and 2a backbones, respectively. However, even with the caveat that unpredictable coordinated effects of introducing epitopes from varying isolates may occur, the ability to study the consequences of single epitope serial sequence mutation on viral fitness and virion production is extremely valuable.

Generation of Huh-7.5 cells harboring subgenomic replicons allowed for primary analysis of viral RNA replication, and helped establish the initial fitness characteristics of each NS3 mutation that had been observed *in vivo* (Figure 1A and 1B). Even single

amino acid changes in this epitope hindered transduction efficiency, with functional consequences of mutation on specific T cell responses. Interestingly, these changes did not seem to greatly affect protein expression, either in the replicon system or in the cell culture model (Figures 1C, 3A, 4A, and 5B). Similar non-structural protein expression implies that the $NS3_{1629–1637}$ mutations may affect initiation of replication (fewer G418 resistant colonies per μg of RNA), but that once replication has been established similar levels of steady-state replication/protein accumulation would be observed. Similar protein expression levels should result in similar levels of viral peptide production.

The inability of P9 mutations to generate a T cell response could be overcome by high amounts of exogenous peptide but not by more physiologic concentrations generated by replicating subgenomic or full-length infectious viruses (Figures 3 and 5). By engineering the $NS3_{1629–1637}$ epitope mutations into both a subgenomic replicon system and a recombinant full-length clone of Cp7 capable of robust virion production, a correlation between viral fitness and immune escape was established. CD8+ T cell recognition in transfected and infected Huh-7.5/B1701 cells occurred only with HCV1/910 parental $NS3_{1629–1637}$ epitope (Figures 3B, 3C, 5C, and 5D), indicating that single amino acid changes in this epitope abrogate T cell recognition. Each of the single substitutions at P9 decreased virion production while the virus containing the observed mutation at P7 (I1635T) was unimpaired in virus production. Together with the observation that mutant L1637S was maintained over 7 years despite I1635T having better viral fitness, these results suggest a balance between efficient immune escape and virion production attained by L1637S mutant virus. That is, since the mutant epitope I1635T, with a threonine at T

cell receptor contact residue P7, was detected at month 10 but not later in infection it is possible that its higher fitness and virion production allowed an additional T cell response to be generated against the new epitope. The I1635T mutation has been shown to bind well to Patr-B1701 [15], so that generation of novel CD8+ T cell clones targeting the I1635T epitope *in vivo* is plausible. In contrast, mutant L1637S, which abrogates MHC binding [15], may not select for a new T cell response to develop while still producing sufficient levels of virions. In fact in this study, using frozen PBMCs from CH503 from more than seven years after infection, we were able to isolate T cells specific for I1635T indicating that indeed, this otherwise "perfect" mutation was subject to new immune pressure *in vivo* (Figure 7). This de novo T cell response most likely prevented the I1635T variant from becoming stable in the population. Additionally, it is also possible that the P7 I1635T mutant isolated *in vivo* had fewer compensatory mutations in other highly targeted epitopes, allowing for recognition of the other epitopes by CD8+ T cells. Our data are consistent with a previous human study demonstrating that the variability of HCV sequences within immunological epitopes is limited by viral fitness [28], but extend these observations by assessing the long-term longitudinal evolutionary pattern of an immunologically and virologically important NS3 epitope.

It is noteworthy that the L1637P variant that appeared within 3 months of infection was least fit for replication in our cell culture models and was replaced in the plasma of the chimpanzee seven months later by two more fit variants. These results indicate that escaped viruses (like L1637P) may readily revert to a more fit sequence when transmitted from a recently infected donor to an HLA-mismatched recipient. In HIV-1, a CD8+ T

cell-mediated escape mutation in the dominant HLA-B57 TW10 epitope (TSTLQEQIGW) within the capsid protein p24 has been shown to impair viral replication *in vitro* [23]. Reversion of this mutation following transmission to an HLA-mismatched host provided evidence for the impaired fitness cost that was incurred *in vivo* while escaping from CTL pressure [54]. Another study utilizing a clonal SIV virus (SIV_{mac239}) harboring CTL escape mutations showed that escape can exact a severe replicative fitness cost, and that many of these variant sequences would be unlikely to propagate in HLA-diverse populations [51]. To date there are only two published examples of apparent reversion of escaped HCV epitopes in human subjects, and both involved viruses transmitted from donors during the acute phase of infection [18,46]. Ray et al. followed a group of women infected with a common virus from a single acutely infected donor. When HCV genomes from the recipients were compared with a consensus HCV genome assembled from published sequences, mutations trending away from consensus were observed in HLA-restricted epitopes (representing possible emergence of recipient escape variants) and toward consensus in non-restricted epitopes (representing possible reversion of donor escape variants) [46]. That acute phase escape variants might revert to a more fit sequence is also supported by a second detailed study of CD8+ T cell immunity in a donor-recipient pair [18]. A CD8+ T cell escape mutation that arose during the acute phase of infection in the virus donor was quickly lost from the quasispecies upon transmission to an HLA class I disparate recipient [18]. Our results suggest that this reversion may be less common when mutations are optimized for immune escape and replication over long periods of chronic infection. We hypothesize that variants like L1637S that have been fine tuned by a process of iterative mutation

during months of persistent replication might be considerably more stable upon transmission. We predict that these amino acid substitutions will not readily revert upon infection of a new host once escape from immunity has been carefully balanced against replicative fitness, particularly if HCV has a wide (though not limitless) tolerance for substitutions that alter replication. *In vitro*, we infected naïve Huh-7.5/B1701 cells with parental $NS3_{1629–1637}$ and mutant viruses, and studied the epitope evolution of individual clones. Interestingly, we found mutations in numerous (5/15) clones of L1637P 23 d post-infection, with the P9 proline mutating back to the parental leucine (Figure 6). These results strengthen the hypothesis that the L1637P mutant virus has diminished replicative fitness *in vitro* as well as *in vivo*. Additionally, the absence of CD8+ T cell pressure in these experiments suggests that transiently less fit viruses may trend towards input parental sequence in HLA-diverse populations or upon transmission to HLA-mismatched hosts. Importantly, the L1637S and I1635T viruses were relatively stable, confirming replication and virion production data (Figures 1A, 1B, 4B, and 4C). The stability of L1637S suggests that this virus has indeed struck a balance between replicative fitness and immune pressure, and would not likely revert back to the parental sequence upon transmission to a new host. These data correlate with long term $NS3_{1629–1637}$ epitope evolution in chimpanzees with L1637S stable over a 7-year period, and demonstrate that mutants arising *in vivo* can be recapitulated *in vitro*. We predict that the L1637S sequence represents a viral variant that has achieved balance between replicative capacity and immune evasion and would be stable upon transfer to naïve hosts regardless of whether they express MHC molecules required for presentation to CD8+ T cells.

The work reported here highlights the competing forces influencing the interplay between the virus and the immune system and the multiple varied effects of a single amino acid change on T cell function and virus production. These observations elucidate potential mechanisms by which viral persistence is established. Consequences of stable integration of escape mutations into viral genomes are not clear, but it is formally possible that epitopes presented by the most prevalent MHC class I molecules in human populations will eventually be lost or become less dominant, an outcome that could have implications for vaccine development. In light of the knowledge that HCV mutates nearly one nucleotide per replication cycle, this work provides sobering evidence that the anti-HCV CD8+ T cell response faces daunting challenges for efficient and lasting control of HCV.

Acknowledgments

The authors would like to thank the Grakoui lab members for helpful discussions, and Christopher Ibegbu for technical expertise and reagent support. The authors would like to acknowledge the support from the Canadian Institutes of Health Research (NHS); the Greenberg Medical Research Institute, the Starr Foundation, and the Ellison Medical Foundation (CMR); EVC/CFAR Flow Cytometry Core (P30 AI050409), Cancer Research Institute Investigator Award, Woodruff Health Sciences Fund, the Yerkes Research Center Base Grant RR-00165 (AG) and the US Public Health Service grants {CA85883 (CMR), AI40034 (CMR), U19 AI48231 (CMW), R37 AI47367 (CMW) and AI070101 (AG)}.

Figures

Figure 1

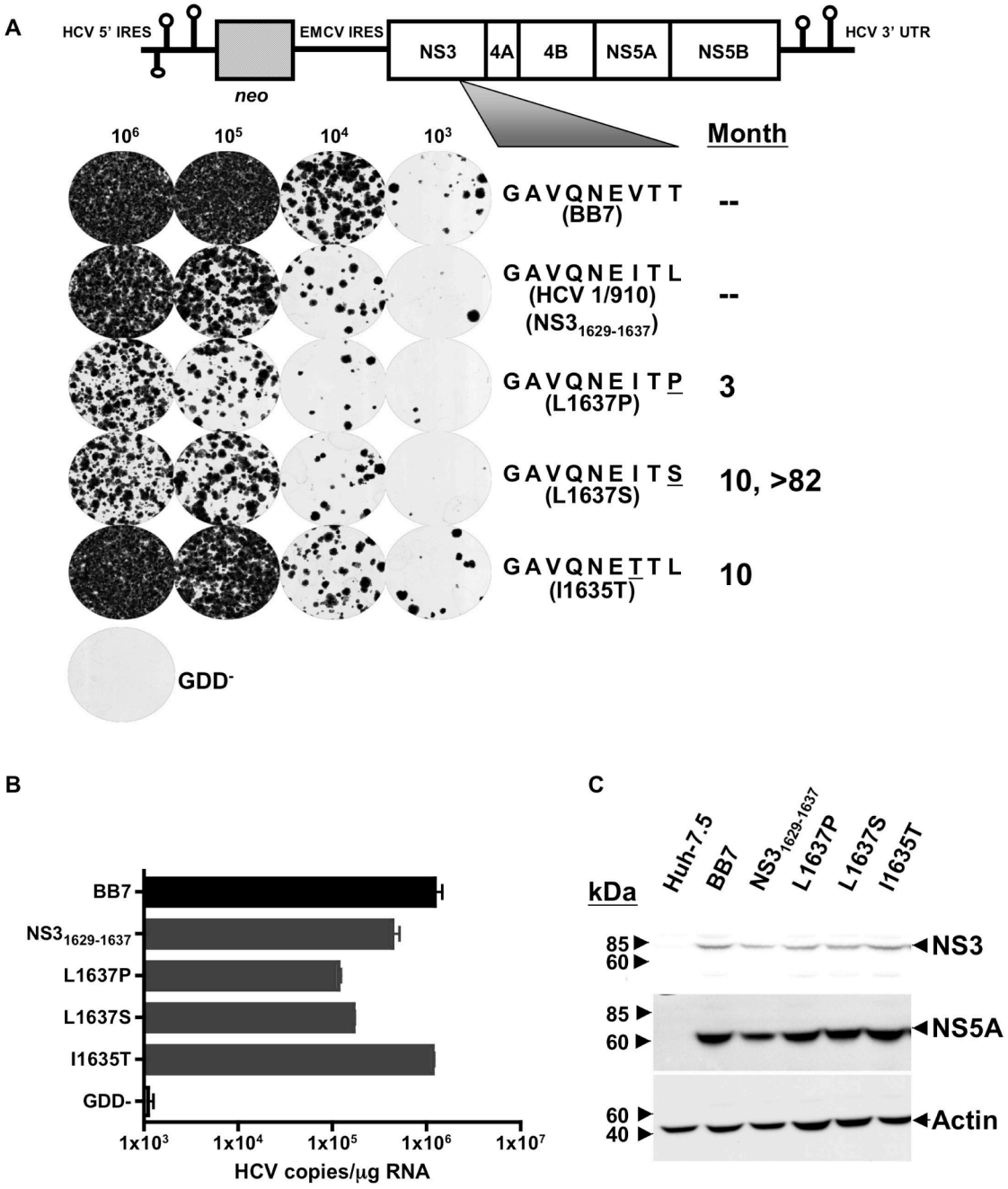

Figure 2

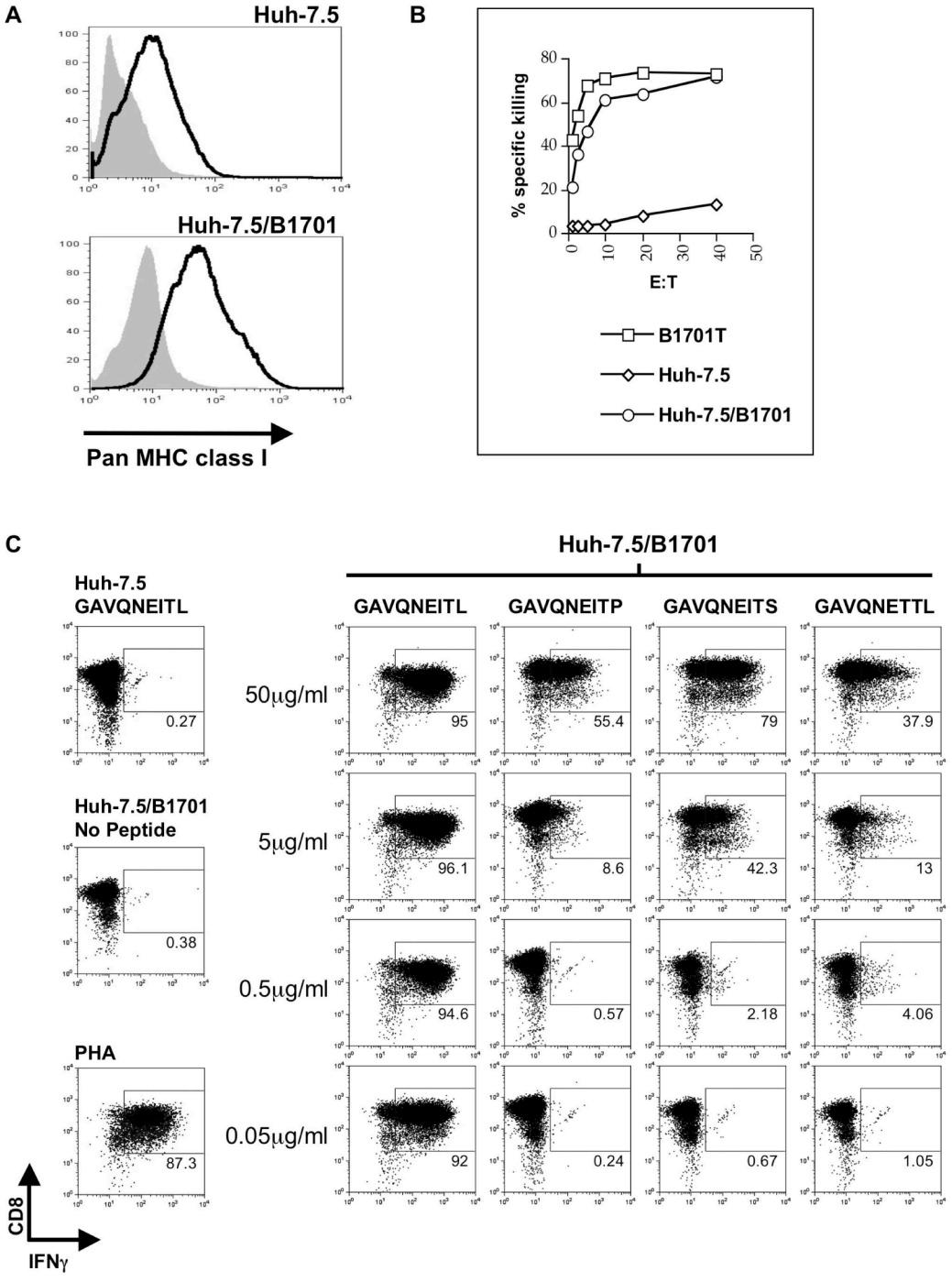
A
Huh-7.5
Huh-7.5/B1701
Pan MHC class I
B
% specific killing
E:T
B1701T
Huh-7.5
Huh-7.5/B1701
C
Huh-7.5/B1701
GAVQNEITL
GAVQNEITP
GAVQNEITS
GAVQNETTL
Huh-7.5
GAVQNEITL
Huh-7.5/B1701
No Peptide
PHA
50μg/ml
5μg/ml
0.5μg/ml
0.05μg/ml
0.27
95
55.4
79
37.9
96.1
8.6
42.3
13
0.38
94.6
0.57
2.18
4.06
87.3
92
0.24
0.67
1.05
CD8
IFNγ

Figure 3

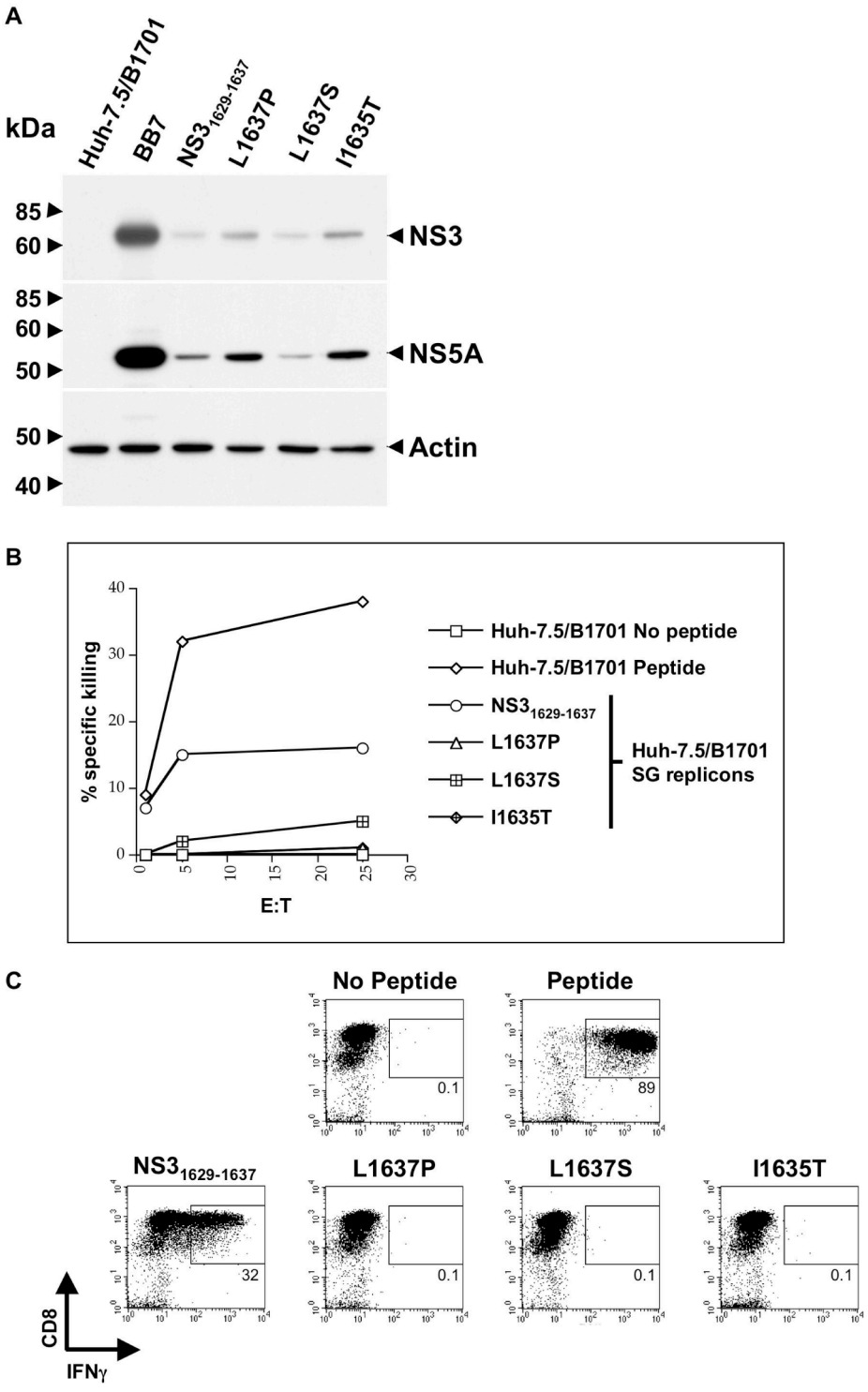
A
kDa
Huh-7.5/B1701
BB7
NS3 1629-1637
L1637P
L1637S
I1635T
85
60
NS3
85
60
50
NS5A
50
Actin
40
B
% specific killing
E:T
Huh-7.5/B1701 No peptide
Huh-7.5/B1701 Peptide
NS3 1629-1637
L1637P
L1637S
I1635T
Huh-7.5/B1701 SG replicons
C
No Peptide
Peptide
0.1
89
NS3 1629-1637
L1637P
L1637S
I1635T
32
0.1
0.1
0.1
CD8
IFNγ

Figure 4

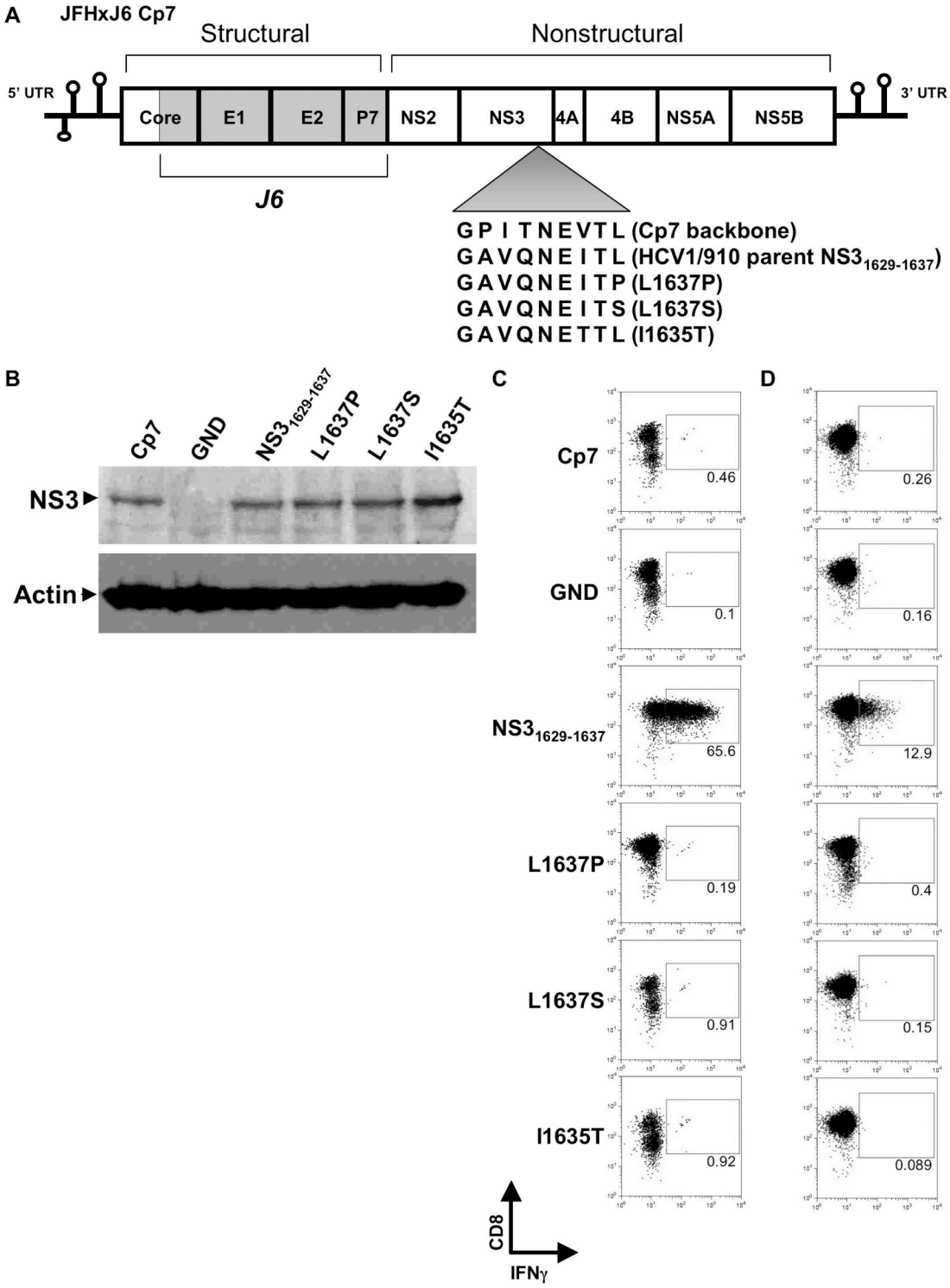
A
JFHxJ6 Cp7
Structural
Nonstructural
5' UTR
Core
E1
E2
P7
NS2
NS3
4A
4B
NS5A
NS5B
3' UTR
J6
G P I T N E V T L (Cp7 backbone)
G A V Q N E I T L (HCV1/910 parent NS3 1629-1637)
G A V Q N E I T P (L1637P)
G A V Q N E I T S (L1637S)
G A V Q N E T T L (I1635T)
B
Cp7
GND
NS3 1629-1637
L1637P
L1637S
I1635T
NS3
Actin
C
D
Cp7
GND
NS3 1629-1637
L1637P
L1637S
I1635T
0.46
0.26
0.1
0.16
65.6
12.9
0.19
0.4
0.91
0.15
0.92
0.089
CD8
IFNγ

Figure 5

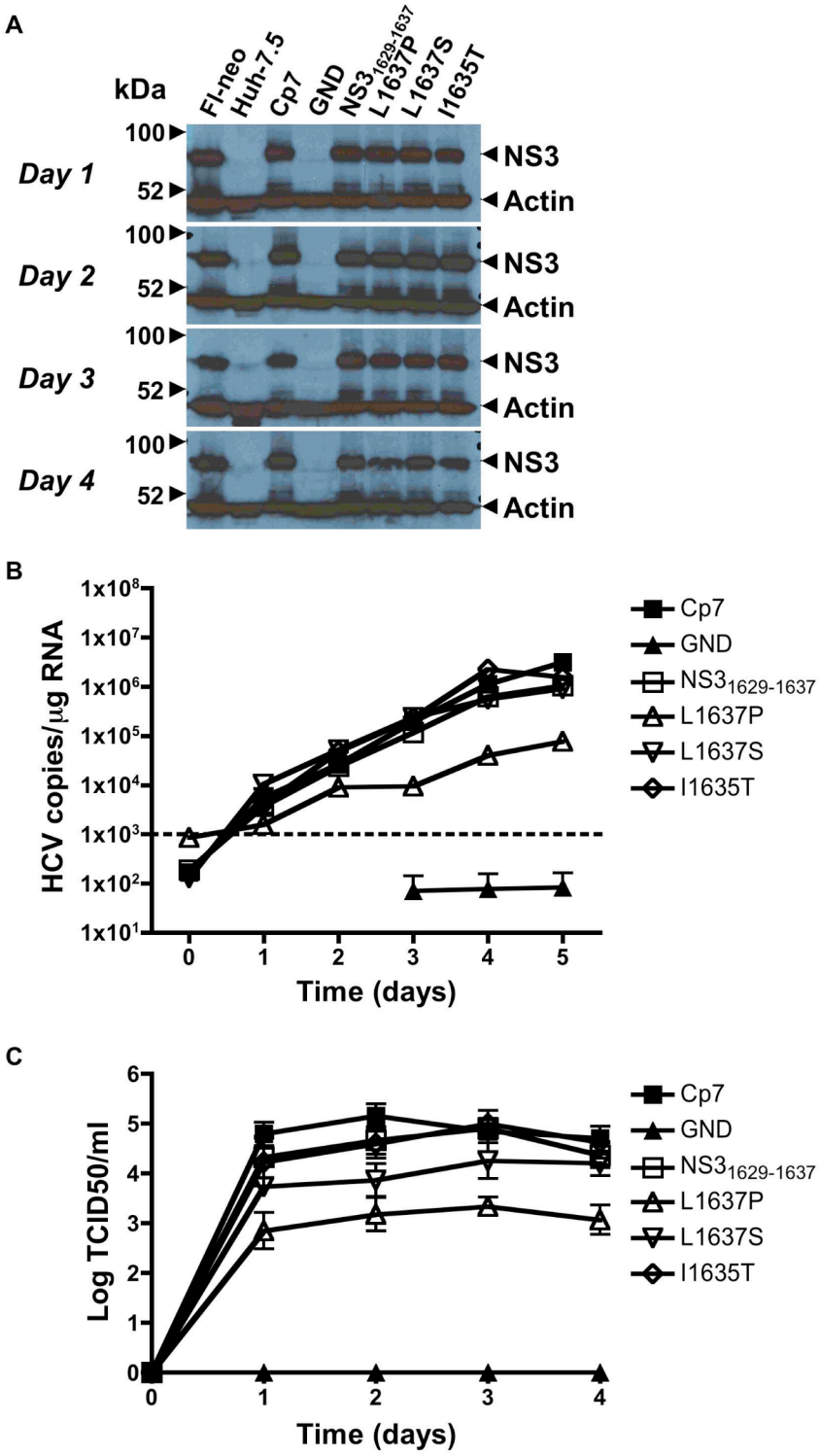
A
kDa
Fl-neo
Huh-7.5
Cp7
GND
NS3 1629-1637
L1637P
L1637S
I1635T
100
52
Day 1
Day 2
Day 3
Day 4
NS3
Actin
B
HCV copies/μg RNA
1x10^8
1x10^7
1x10^6
1x10^5
1x10^4
1x10^3
1x10^2
1x10^1
0
1
2
3
4
5
Time (days)
Cp7
GND
NS3 1629-1637
L1637P
L1637S
I1635T
C
Log TCID50/ml
6
5
4
3
2
1
0
0
1
2
3
4
Time (days)
Cp7
GND
NS3 1629-1637
L1637P
L1637S
I1635T

Figure 6

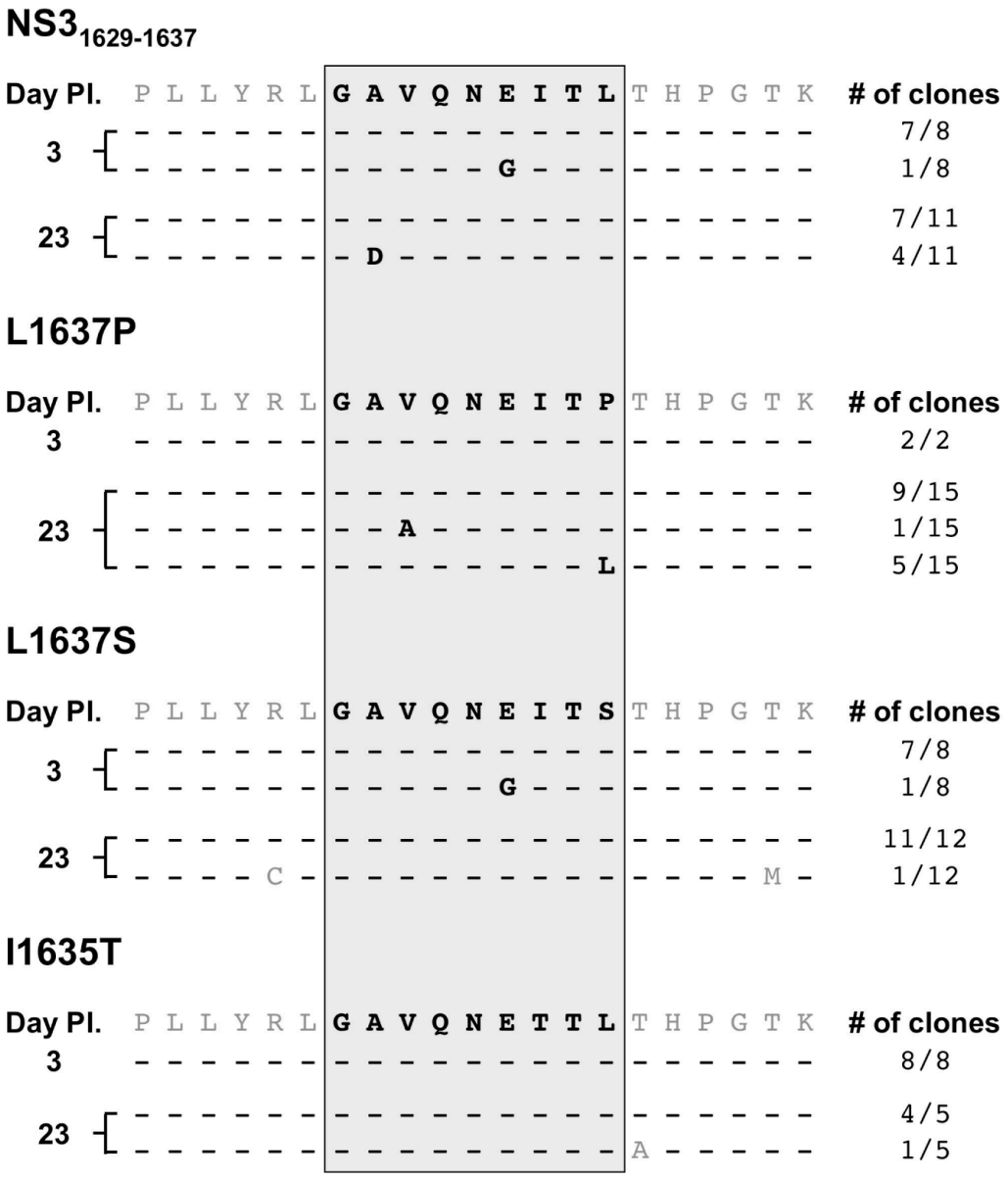
NS3 1629-1637
Day PI. P L L Y R L G A V Q N E I T L T H P G T K # of clones
3 - 7/8
- - - - - - - - - - - - G - - - - - - - - - - - 1/8
23 - 7/11
- - - - - - - - D - - - - - - - - - - - - - - - 4/11
L1637P
Day PI. P L L Y R L G A V Q N E I T P T H P G T K # of clones
3 - 2/2
23 - 9/15
- - - - - - - - - A - - - - - - - - - - - - - - 1/15
- - - - - - - - - - - - - - - - L - - - - - - - 5/15
L1637S
Day PI. P L L Y R L G A V Q N E I T S T H P G T K # of clones
3 - 7/8
- - - - - - - - - - - - G - - - - - - - - - - - 1/8
23 - 11/12
- - - - C - - - - - - - - - - - - - - - - M - 1/12
I1635T
Day PI. P L L Y R L G A V Q N E T T L T H P G T K # of clones
3 - 8/8
23 - 4/5
- - - - - - - - - - - - - - - - A - - - - - - 1/5

Figure 7

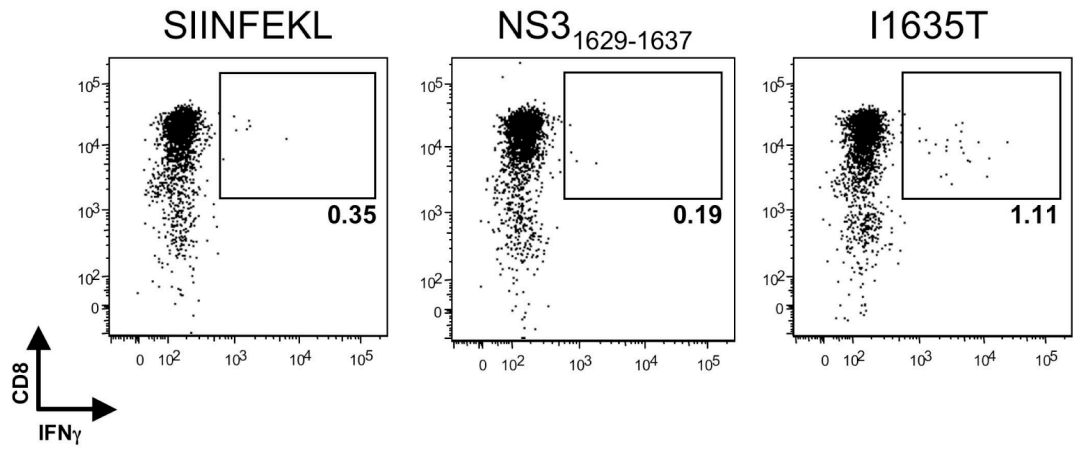

Figure Legends

Figure 1. Construction of subgenomic replicons and HCV protein expression in transfected Huh-7.5 cells. (A) Schematic representation of subgenomic (SG) replicons and their replication efficiency. Huh-7.5 cells were transfected with the indicated constructs and plated at decreasing cell number concentrations under neomycin selection to determine transduction efficiency of each construct, with GDD^- serving as a negative control. $NS3_{1629\text{-}1637}$ epitopes are listed by month(s) first detected in an *in vivo* chimpanzee CH503 infection model. (B) Replication of SG HCV RNA inside Huh-7.5 cells. Huh-7.5 cells were transfected with subgenomic replicons as in (A), and assayed for RNA replication six days post-transfection using a real time qRT-PCR Taqman assay as described in Materials and Methods. The minimum sensitivity of detection was 1000 HCV copies/μg RNA). (C) Western blot of replicon-transfected Huh-7.5 cell lysates. The expression of HCV proteins NS3 and NS5A were detected post-transfection using anti-NS3/anti-NS5A monoclonal Abs. Lysates from Huh-7.5 cells transfected with replicons containing the BB7 epitope served as a positive control, untransfected Huh-7.5 cells were used as a negative control, and β-actin served as a positive control for input protein.

Figure 2. Expression and recognition of the chimpanzee Patr-B1701 molecule on the surface of Huh-7.5 cells. (A) Surface expression of MHC class I on Huh-7.5 cells transfected with a plasmid containing the Patr-B1701 molecule and zeocin selection marker. No difference in surface expression was observed when compared to untransfected Huh-7.5 cells. Isotype control is depicted in grey. (B) CTL lysis of transfected Huh-7.5 cells. Huh-7.5 cells expressing the Patr-B1701 (Huh-7.5/B1701)

molecule were pulsed with wild-type peptide and incubated with increasing amounts of CTL clone 4A specific for the $NS3_{1629-1637}$ wild-type epitope. Cells presenting this peptide on the Patr-B1701 molecule are lysed by CTLs as efficiently as EBV-transformed autologous B cells presenting peptide (B1701T). Untransfected Huh-7.5 cells served as a negative control. (C) CD8+ T cell clone IFNγ response to Huh-7.5/B1701 cells presenting exogenous peptide. Huh-7.5/B1701 cells were loaded with parent HCV1/910 $NS3_{1629-1637}$ or mutant $NS3_{1629-1637}$ peptide as in (B) and cocultured with a CD8+ T cell clone targeting the $NS3_{1629-1637}$ epitope. Huh-7.5/B1701 cells presenting parent HCV1/910 $NS3_{1629-1637}$ but not mutant peptide at concentrations of 0.5 μg/ml and lower could elicit an IFNγ response from the CD8+ T clone. Cocultures were stimulated with PHA as a positive control, and unpulsed Huh-7.5/B1701 cells or Huh-7.5 cells pulsed with parent HCV1/910 $NS3_{1629-1637}$ peptide served as negative controls. Plots depicted are gated on CD3+ T cells.

Figure 3. Mutations in the $NS3_{1629-1637}$ epitope abrogate CTL recognition in the replicon system. (A) Western blots of replicon-transfected Patr-B1701-expressing Huh-7.5 cells. The expression of HCV proteins NS3 and NS5A were detected in Huh-7.5/B1701 cells harboring subgenomic replicons. Lysates from Huh-7.5/B1701 cells transfected with replicons containing the BB7 epitope served as a positive control, untransfected Huh-7.5/B1701 cells were used as a negative control, and β-actin served as a positive control for input protein. (B) CTLs are unable to lyse Huh-7.5/B1701 cells transfected with subgenomic mutant replicons with the same efficiency as the parent HCV1/910 $NS3_{1629-1637}$ subgenomic replicon. Huh-7.5/B1701 cells with or without parent

HCV1/910 $NS3_{1629\text{-}1637}$ peptide were used as a positive and negative control, respectively. (C) CD8+ T cell IFNγ response to the mutated $NS3_{1629\text{-}1637}$ epitope in the subgenomic system. CD8+ T cells specific for the wild-type $NS3_{1629\text{-}1637}$ epitope were incubated with Huh-7.5/B1701 cells transfected with either the parent HCV1/910 $NS3_{1629\text{-}1637}$ subgenomic replicon or the mutant subgenomic replicons, stained for CD8 and IFNγ, and analyzed by flow cytometry. CD8+ T cells secrete IFNγ in response to the parent HCV1/910 $NS3_{1629\text{-}1637}$ subgenomic-transfected Huh-7.5/B1701 cells, but are unable to secrete IFNγ when incubated with Huh-7.5/B1701 cells harboring the subgenomic mutant replicons. Huh-7.5/B1701 cells were incubated with or without the parent HCV1/910 $NS3_{1629\text{-}1637}$ peptide as a positive and negative control, respectively.

Figure 4. CD8+ T cell response to the mutated $NS3_{1629\text{-}1637}$ epitope in an infectious system. (A) Schematic representation of the full-length HCV genome used to produce infectious virus *in vitro*. The core to p7 region of the JFH backbone was replaced by the corresponding region of the autologous genotype 2a J6 strain to create JFHxJ6 Cp7 (Cp7), and single-site PCR mutagenesis used to alter the $NS3_{1629\text{-}1637}$ epitope. (B) Western blot confirmation of NS3 protein expression four days post-transfection in the Huh-7.5/B1701 cell line. β-actin served as a control for input protein. (C) Transfection and recognition of Huh-7.5/B1701 cells by 4A CD8+ T cell clone. Huh-7.5/B1701 cells were transfected with parent HCV1/910 $NS3_{1629\text{-}1637}$ or mutant full-length constructs, and cocultured (as in Figures 2C and 3C) with the $NS3_{1629\text{-}1637}$ epitope-specific CD8+ T cell clone. The CD8+ clone was only able to secrete IFNγ in response to Huh-7.5/B1701 cells transfected with the parent HCV1/910 $NS3_{1629\text{-}1637}$ construct. Huh-7.5/B1701 cells pulsed

with parent HCV1/910 $NS3_{1629-1637}$ peptide served as a positive control (not shown). (D) Infection of naïve Huh-7.5/B1701 cells with parent HCV1/910 $NS3_{1629-1637}$ but not mutant full-length constructs elicits an IFNγ response. Supernatants were harvested from Huh-7.5/B1701 cells that had been transfected four days earlier and used to infect naïve Huh-7.5/B1701 cells. Five days post-infection, cells were harvested and cocultured with the CD8+ T cell clone to determine level of IFNγ production produced by 4A CD8+ T cell clone.

Figure 5. *In vitro* analysis of the mutated $NS3_{1629-1637}$ epitope in a full-length viral genome system. (A) Short-term transfection Western blots. Expression of NS3 protein in transfected Huh-7.5 cells is similar among the mutant constructs. Fl-neo cell lysates harboring full-length HCV genotype 1b replicon were used as a positive control, along with lysates from Huh-7.5 cells transfected with the Cp7 backbone construct. Untransfected Huh-7.5 cells and Huh-7.5 cells transfected with the replication-defective GND construct were used as negative controls. (B) Infection of naïve Huh-7.5 cells and quantitation of HCV RNA replication. Supernatants of transfected Huh-7.5 cells were harvested and normalized to infect naïve Huh-7.5 cells over a five-day period with identical multiplicity of infection doses. Every 24 hours, total RNA was harvested from cells and HCV RNA levels were measured using a qRT-PCR Taqman assay. Results are displayed as HCV copies/μg input RNA. The minimum sensitivity of detection (1000 HCV copies/μg RNA) is displayed as a dashed line. (C) Short-term transfection viral titers. Supernatants of transfected Huh-7.5 cells were harvested up to four days post-transfection, and used to infect naïve Huh-7.5 cells. NS5A monoclonal antibody (9E10)

was used in an immunohistochemical assay to determine TCID50/mL viral titers. Mean standard error bars from four separate experiments are displayed.

Figure 6. $NS3_{1629-1637}$ epitope evolution during *in vitro* viral infection. At indicated times post-infection, cells were harvested and the nucleotide sequence of the viral $NS3_{1629-1637}$ epitope was cloned and examined. Input sequence is listed above each timepoint, and "# of clones" denotes the number of individual colonies with the displayed sequence. Dashes represent no amino acid change from the listed input sequence.

Figure 7. I1635T-specific CD8+ T cells are present in PBMC from CH503 more than seven years post-infection. 20 days post-expansion, $5x10^4$ CD8+ T cells were cultured with $5x10^4$ autologous EBV-transformed B cells pulsed with the indicated peptide, and the presence of peptide-specific IFNγ-secreting CD8+ T cells was assessed by intracellular cytokine staining. Cells are gated on live, CD3+ lymphocytes. The percent of CD8+ T cells that stained positively for intracellular IFNγ is displayed.

References

1. Wasley A, Alter MJ (2000) Epidemiology of hepatitis C: geographic differences and temporal trends. Semin Liver Dis 20: 1-16.

2. (1999) Global surveillance and control of hepatitis C. Report of a WHO Consultation organized in collaboration with the Viral Hepatitis Prevention Board, Antwerp, Belgium. J Viral Hepat 6: 35-47.

3. Alter MJ, Kruszon-Moran D, Nainan OV, McQuillan GM, Gao F, et al. (1999) The prevalence of hepatitis C virus infection in the United States, 1988 through 1994. N Engl J Med 341: 556-562.

4. Alter MJ, Margolis HS, Krawczynski K, Judson FN, Mares A, et al. (1992) The natural history of community-acquired hepatitis C in the United States. The Sentinel Counties Chronic non-A, non-B Hepatitis Study Team. N Engl J Med 327: 1899-1905.

5. Fishman JA, Rubin RH, Koziel MJ, Periera BJ (1996) Hepatitis C virus and organ transplantation. Transplantation 62: 147-154.

6. Thimme R, Oldach D, Chang KM, Steiger C, Ray SC, et al. (2001) Determinants of viral clearance and persistence during acute hepatitis C virus infection. J Exp Med 194: 1395-1406.

7. Lechner F, Wong DK, Dunbar PR, Chapman R, Chung RT, et al. (2000) Analysis of successful immune responses in persons infected with hepatitis C virus. J Exp Med 191: 1499-1512.

8. Diepolder HM, Zachoval R, Hoffmann RM, Wierenga EA, Santantonio T, et al. (1995) Possible mechanism involving T-lymphocyte response to non-structural protein 3 in viral clearance in acute hepatitis C virus infection. Lancet 346: 1006-1007.

9. Kantzanou M, Lucas M, Barnes E, Komatsu H, Dusheiko G, et al. (2003) Viral escape and T cell exhaustion in hepatitis C virus infection analysed using Class I peptide tetramers. Immunol Lett 85: 165-171.

10. Radziewicz H, Uebelhoer L, Bengsch B, Grakoui A (2007) Memory CD8+ T cell differentiation in viral infection: a cell for all seasons. World J Gastroenterol 13: 4848-4857.

11. Bain C, Fatmi A, Zoulim F, Zarski JP, Trepo C, et al. (2001) Impaired allostimulatory function of dendritic cells in chronic hepatitis C infection. Gastroenterology 120: 512-524.

12. Kanto T, Hayashi N, Takehara T, Tatsumi T, Kuzushita N, et al. (1999) Impaired allostimulatory capacity of peripheral blood dendritic cells recovered from hepatitis C virus-infected individuals. J Immunol 162: 5584-5591.

13. Wedemeyer H, He XS, Nascimbeni M, Davis AR, Greenberg HB, et al. (2002) Impaired effector function of hepatitis C virus-specific CD8+ T cells in chronic hepatitis C virus infection. J Immunol 169: 3447-3458.

14. Urbani S, Boni C, Missale G, Elia G, Cavallo C, et al. (2002) Virus-specific CD8+ lymphocytes share the same effector-memory phenotype but exhibit functional differences in acute hepatitis B and C. J Virol 76: 12423-12434.

15. Erickson AL, Kimura Y, Igarashi S, Eichelberger J, Houghton M, et al. (2001) The outcome of hepatitis C virus infection is predicted by escape mutations in epitopes targeted by cytotoxic T lymphocytes. Immunity 15: 883-895.

16. Guglietta S, Garbuglia AR, Pacciani V, Scotta C, Perrone MP, et al. (2005) Positive selection of cytotoxic T lymphocyte escape variants during acute hepatitis C virus infection. Eur J Immunol 35: 2627-2637.

17. Tester I, Smyk-Pearson S, Wang P, Wertheimer A, Yao E, et al. (2005) Immune evasion versus recovery after acute hepatitis C virus infection from a shared source. J Exp Med 201: 1725-1731.

18. Timm J, Lauer GM, Kavanagh DG, Sheridan I, Kim AY, et al. (2004) CD8 epitope escape and reversion in acute HCV infection. J Exp Med 200: 1593-1604.

19. Neumann AU, Lam NP, Dahari H, Gretch DR, Wiley TE, et al. (1998) Hepatitis C viral dynamics *in vivo* and the antiviral efficacy of interferon-alpha therapy. Science 282: 103-107.

20. Bukh J, Miller RH, Purcell RH (1995) Genetic heterogeneity of hepatitis C virus: quasispecies and genotypes. Semin Liver Dis 15: 41-63.

21. Thimme R, Bukh J, Spangenberg HC, Wieland S, Pemberton J, et al. (2002) Viral and immunological determinants of hepatitis C virus clearance, persistence, and disease. Proc Natl Acad Sci U S A 99: 15661-15668.

22. Brockman MA, Schneidewind A, Lahaie M, Schmidt A, Miura T, et al. (2007) Escape and compensation from early HLA-B57-mediated cytotoxic T-lymphocyte pressure on human immunodeficiency virus type 1 Gag alter capsid interactions with cyclophilin A. J Virol 81: 12608-12618.

23. Martinez-Picado J, Prado JG, Fry EE, Pfafferott K, Leslie A, et al. (2006) Fitness cost of escape mutations in p24 Gag in association with control of human immunodeficiency virus type 1. J Virol 80: 3617-3623.

24. Friedrich TC, Frye CA, Yant LJ, O'Connor DH, Kriewaldt NA, et al. (2004) Extraepitopic compensatory substitutions partially restore fitness to simian immunodeficiency virus variants that escape from an immunodominant cytotoxic-T-lymphocyte response. J Virol 78: 2581-2585.

25. Peyerl FW, Bazick HS, Newberg MH, Barouch DH, Sodroski J, et al. (2004) Fitness costs limit viral escape from cytotoxic T lymphocytes at a structurally constrained epitope. J Virol 78: 13901-13910.

26. Chang KM, Rehermann B, McHutchison JG, Pasquinelli C, Southwood S, et al. (1997) Immunological significance of cytotoxic T lymphocyte epitope variants in patients chronically infected by the hepatitis C virus. J Clin Invest 100: 2376-2385.

27. Seifert U, Liermann H, Racanelli V, Halenius A, Wiese M, et al. (2004) Hepatitis C virus mutation affects proteasomal epitope processing. J Clin Invest 114: 250-259.

28. Soderholm J, Ahlen G, Kaul A, Frelin L, Alheim M, et al. (2006) Relation between viral fitness and immune escape within the hepatitis C virus protease. Gut 55: 266-274.

29. Blight KJ, Kolykhalov AA, Rice CM (2000) Efficient initiation of HCV RNA replication in cell culture. Science 290: 1972-1974.

30. Lohmann V, Korner F, Koch J, Herian U, Theilmann L, et al. (1999) Replication of subgenomic hepatitis C virus RNAs in a hepatoma cell line. Science 285: 110-113.

31. Zhong J, Gastaminza P, Cheng G, Kapadia S, Kato T, et al. (2005) Robust hepatitis C virus infection *in vitro*. Proc Natl Acad Sci U S A 102: 9294-9299.

32. Lindenbach BD, Evans MJ, Syder AJ, Wolk B, Tellinghuisen TL, et al. (2005) Complete replication of hepatitis C virus in cell culture. Science 309: 623-626.

33. Wakita T, Pietschmann T, Kato T, Date T, Miyamoto M, et al. (2005) Production of infectious hepatitis C virus in tissue culture from a cloned viral genome. Nat Med 11: 791-796.

34. Mateu G, Donis RO, Wakita T, Bukh J, Grakoui A (2008) Intragenotypic JFH1 based recombinant hepatitis C virus produces high levels of infectious particles but causes increased cell death. Virology 376: 397-407.

35. Choo QL, Kuo G, Ralston R, Weiner A, Chien D, et al. (1994) Vaccination of chimpanzees against infection by the hepatitis C virus. Proc Natl Acad Sci U S A 91: 1294-1298.

36. Cooper S, Erickson AL, Adams EJ, Kansopon J, Weiner AJ, et al. (1999) Analysis of a successful immune response against hepatitis C virus. Immunity 10: 439-449.

37. Yanagi M, Purcell RH, Emerson SU, Bukh J (1999) Hepatitis C virus: an infectious molecular clone of a second major genotype (2a) and lack of viability of intertypic 1a and 2a chimeras. Virology 262: 250-263.

38. Darlington G (2006) Epstein-Barr Virus Transformation of Lymphoblasts.

39. Reed L, Muench H (1938) A simple method of estimating fifty percent end points. Am J Hyg: 493–497.

40. Kato T, Date T, Miyamoto M, Furusaka A, Tokushige K, et al. (2003) Efficient replication of the genotype 2a hepatitis C virus subgenomic replicon. Gastroenterology 125: 1808-1817.

41. Evans DT, O'Connor DH, Jing P, Dzuris JL, Sidney J, et al. (1999) Virus-specific cytotoxic T-lymphocyte responses select for amino-acid variation in simian immunodeficiency virus Env and Nef. Nat Med 5: 1270-1276.

42. Phillips RE, Rowland-Jones S, Nixon DF, Gotch FM, Edwards JP, et al. (1991) Human immunodeficiency virus genetic variation that can escape cytotoxic T cell recognition. Nature 354: 453-459.

43. Borrow P, Lewicki H, Wei X, Horwitz MS, Peffer N, et al. (1997) Antiviral pressure exerted by HIV-1-specific cytotoxic T lymphocytes (CTLs) during primary infection demonstrated by rapid selection of CTL escape virus. Nat Med 3: 205-211.

44. Allen TM, O'Connor DH, Jing P, Dzuris JL, Mothe BR, et al. (2000) Tat-specific cytotoxic T lymphocytes select for SIV escape variants during resolution of primary viraemia. Nature 407: 386-390.

45. Cox AL, Mosbruger T, Mao Q, Liu Z, Wang XH, et al. (2005) Cellular immune selection with hepatitis C virus persistence in humans. J Exp Med 201: 1741-1752.

46. Ray SC, Fanning L, Wang XH, Netski DM, Kenny-Walsh E, et al. (2005) Divergent and convergent evolution after a common-source outbreak of hepatitis C virus. J Exp Med 201: 1753-1759.

47. Grakoui A (2004) Hepatitis C virus infection. How does the host respond? Minerva Gastroenterol Dietol 50: 21-28.

48. Jones NA, Wei X, Flower DR, Wong M, Michor F, et al. (2004) Determinants of human immunodeficiency virus type 1 escape from the primary CD8+ cytotoxic T lymphocyte response. J Exp Med 200: 1243-1256.

49. Karlsson AC, Deeks SG, Barbour JD, Heiken BD, Younger SR, et al. (2003) Dual pressure from antiretroviral therapy and cell-mediated immune response on the human immunodeficiency virus type 1 protease gene. J Virol 77: 6743-6752.

50. Yang OO, Sarkis PT, Ali A, Harlow JD, Brander C, et al. (2003) Determinant of HIV-1 mutational escape from cytotoxic T lymphocytes. J Exp Med 197: 1365-1375.

51. Friedrich TC, Dodds EJ, Yant LJ, Vojnov L, Rudersdorf R, et al. (2004) Reversion of CTL escape-variant immunodeficiency viruses *in vivo*. Nat Med 10: 275-281.

52. Farci P, Shimoda A, Coiana A, Diaz G, Peddis G, et al. (2000) The outcome of acute hepatitis C predicted by the evolution of the viral quasispecies. Science 288: 339-344.

53. Tsai SL, Chen YM, Chen MH, Huang CY, Sheen IS, et al. (1998) Hepatitis C virus variants circumventing cytotoxic T lymphocyte activity as a mechanism of chronicity. Gastroenterology 115: 954-965.

54. Leslie AJ, Pfafferott KJ, Chetty P, Draenert R, Addo MM, et al. (2004) HIV evolution: CTL escape mutation and reversion after transmission. Nat Med 10: 282-289.

CHAPTER 3

Disruption of a conserved disulfide bond in HCV E2 protein impacts CD81 binding and abrogates infectivity

Guaniri Mateu[1#], Luke Uebelhoer[1#], Jillian Whidby Freund[2#], Daniel Claiborne[1], Joseph Marcotrigiano[2*] and Arash Grakoui[1*]

[1]Department of Medicine, Division of Infectious Diseases, Microbiology and Immunology, Emory Vaccine Center, Emory University School of Medicine, Atlanta, GA 30329; [2] Center for Advanced Biotechnology and Medicine, Dept of Chemistry and Chemical Biology, Rutgers University, Piscataway, NJ 08854; *Corresponding author

[#]These authors have contributed equally to the manuscript

Conceived and designed the experiments: GM JM AG

Performed the experiments: GM (Fig1-4) LU (Fig1-4) JWF (Fig5) DC (Fig2)

Analyzed the data: GM JM AG

Contributed reagents/materials/analysis tools: JM AG

Wrote the paper: GM LU AG

Running title: Impact of HCV E2 disulfide bond disruption

This chapter consists of a manuscript that is currently in submission to *PLoS Pathogens* (March 11, 2011).

Abstract

The high sequence variability in the hepatitis C virus genome is a major contributor to the development of inefficient humoral and adaptive immune responses in chronically infected patients. While the ectodomain of the HCV envelope glycoprotein 2 (eE2) contains some of the most variable regions of the entire genome, its encoded eighteen cysteine residues are absolutely conserved across all genotypes. In this study we assessed the importance of these cysteine residues with respect to HCV viral replication, virion production, and infectivity. Using a mutagenesis approach, all eighteen cysteines were dispensable for HCV replication in cell culture. Each E2 cysteine mutant was characterized for virion production and classified into one of three categories based on phenotype: (i) absent to low production of non-infectious particles, (ii) low production of particles with limited infectivity ($C_{429}A$ and $C_{585}A$), and (iii) high production of non-infectious particles ($C_{505}A$). The lack of infectivity for the $C_{505}A$ mutant corresponded with its inability to bind HCV co-receptor, CD81. Further mutagenesis in the highly conserved sequence adjacent to $C_{505}A$ revealed a novel region involved in CD81 binding within HCV eE2. Our results highlight the potential importance of conserved cysteines found within this region for proper folding, virion assembly, receptor binding, and infectivity.

Introduction

The surface of enveloped viruses is composed of glycoproteins that have important roles in receptor attachment, fusion with the host cell membrane, particle formation, and egress. Accordingly, the envelope of the hepatitis C virus (HCV) is composed of two glycoproteins, E1 and E2 [1,2]. E1 has been proposed to participate in viral fusion but its role in viral entry is not known [3,4,5]. E2 is primarily involved in receptor-binding interactions and internalization into host cells [6,7]. HCV E2 is a heavily glycolsylated type I transmembrane protein which has been shown to bind to glycosaminoglycans [8], CD81 [9], and SR-B1 [10].

While the HCV genomic segment encoding E2 contains multiple hypervariable regions, E2 also contains twenty cysteines that are one hundred percent conserved both intra- and inter-genotypically. For simplicity, we annotated each of the cysteine residues in E2 based on its position relative to the N-terminal amino acid position of E2 (Cysteines 1-18, Figure 1A). Two of these cysteines are in the transmembrane region and are not involved in disulfide bond formation, while the remaining eighteen have been shown to form disulfide bonds [11,12]. Of these eighteen, seventeen are present in the ectodomain of E2 (eE2), and one is present in the stem region [13]. Recently, a model for the tertiary structure of E2 was proposed based on a) the connectivity of the nine disulfide bonds, b) functional data on deletion mutants, c) CD81 binding, and d) secondary structure predictions. This model divides HCV E2 into three distinct physical domains (I, II, and III) that contain CD81 binding residues (domains I and III) and a candidate viral fusion

peptide (domain II) [12], highlighting the potential importance of disulfide bonds in maintaining the structure and functional integrity of the protein.

Disulfide bonds are considered essential for the folding and structural maintenance of mature proteins, which accounts for the fact that the disulfide-bonded structure of proteins is usually conserved across species and within protein families. Disulfide bonding helps to mediate folding of nascent proteins [14], while additionally stabilizing and protecting mature viral proteins from degradation [15] and presentation to the host immune response [16]. For viral envelope proteins involved in receptor binding and fusion, disulfide bonds can provide a trigger mechanism that enables the structural changes necessary for viral entry [17,18,19,20,21]. Importantly, disulfide bridges have been shown to stabilize large covalent complexes formed by E1 and E2 in extracellular HCV virions [22].

As one might expect, manipulation of the oxidation state often leads to misfolded and aggregated proteins that do not leave the endoplasmic reticulum [23]. For viruses like human immunodeficiency virus type 1 (HIV-1) and HCV, disulfide bond disruption might have numerous downstream effects on receptor binding, infectivity, and replication. However, a recent study of the Env protein (gp120 and gp160) of HIV-1 found that this protein was remarkably tolerant of substitutions at cysteine residues known to form disulfide bonds even though they were strictly conserved [24]. This plasticity was unexpected due to their strict conservation in the context of such a variable glycoprotein. Similarly, the E2 protein of HCV contains some of the most variable

regions of the entire genome as well as strictly conserved disulfide bond-forming cysteine residues. However, the importance of these disulfide bonds for the HCV life cycle has not yet been studied.

In this study we utilized the HCVcc system to assess the role of HCV E2 disulfide bonds on viral particle formation, secretion, receptor binding, and infectivity. To this end, site-directed mutagenesis was used to disrupt the individual disulfide bonds of E2 by substituting an alanine for each conserved cysteine residue. The more phenotypically interesting mutants were created in the recombinant HCV E2 ectodomain (eE2) to study the effect of disulfide bond disruption on CD81 binding. Mutating the eighteen individual cysteine residues present in the ectodomain of E2 resulted in three distinct phenotypic effects. The first type represented the majority of the cysteine mutants, where elimination of disulfide bonding resulted in low to undetectable levels of viral particle release and a lack of infectivity, suggesting that these bonds were necessary for oxidative folding in the ER and subsequent egress from the cell. For mutants C1A and C11A, elimination of disulfide bonding yielded low levels of secreted viral particles that correlated with low or no infectivity. Finally, a unique phenotype was associated with the C6A mutant, which produced high levels of non-infectious viral particles. Recombinant eE2 with the C6A mutation failed to bind CD81 *in vitro*, although the protein retained an overall secondary structure that was similar to wild type eE2. C6 is located in a proposed viral fusion peptide and is thought to bond to an adjacent cysteine residue, C7 [12]. Importantly, subsequent mutations in amino acid residues adjacent to C6 (residues $V_{504}A$, $C_{505}A$ (C6A), $G_{506}A$, $V_{508}A$, $Y_{509}A$, $C_{510}A$ (C7A), $F_{511}A$) suggested that these highly conserved

residues are involved in CD81 binding. This work provides new information on how the disulfide bonding of E2 influences HCV assembly, egress, and infectivity. Moreover, identification of a novel region within HCV E2 that impacts CD81 binding offers insight into the biology of HCV and may provide an additional target for therapeutic intervention in chronic HCV infection.

Materials and Methods

Cell culture

Huh-7.5 cells were maintained in Dulbecco's Modified Eagle Medium (DMEM, Hyclone, Logan, UT) supplemented with 10% fetal bovine serum (FBS, Hyclone, Logan, UT) and penicillin/streptomycin (100 μg/ml, BioWhittaker Inc., Walkersville, Maryland, USA). Unless otherwise noted, cells were incubated at 37ºC and 5% CO_2.

Intergenotypic HCV E2 glycoprotein sequence analysis

To determine the degree of cysteine conservation across all known HCV genotypes, the European HCV (euHCVdb, http://euhcvdb.ibcp.fr/euHCVdb/) and Los Alamos HCV (http://hcv.lanl.gov/content/index) sequence databases were queried using all known E2 entries as a primary filter, followed by the genotype of interest, and limited to confirmed data sets. Individual sequences from both databases were compiled in FASTA format and were first compared intragenotypically with CLC Bio Sequence Viewer™ software and subsequently intergenotypically.

Plasmids

The full-length J6/JFH genotype 2a Cp7 virus has been previously described [25]. Generation of full-length virus containing a *Renilla* Luciferase gene was generated by introducing an *Mlu*I restriction site between the p7 and NS2 coding sequence of the CNS2 infectious clone by PCR. The *Mlu*I restriction site was subsequently used to insert the *Renilla* luciferase gene fused to a sequence encoding the foot and mouth disease virus (FMDV) 2A peptide (amplified from the plasmid FL-J6/JFH-C19'Rluc2AUbi, [26]).

The ΔE1E2 clone was constructed by performing an in-frame deletion of E1 and E2 (from nucleotide 943 to 2560) coding sequence in the Cp7 backbone using PCR deletion mutagenesis.

Site-directed cysteine mutagenesis of HCV E2 glycoprotein

Mutation of the eighteen conserved cysteine residues and individual amino acid residues found within the putative fusion peptide of the E2 glycoprotein were carried out using a QuikChange Site-Directed Mutagenesis Kit according to the manufacturer's instructions (Stratagene, La Jolla, California). The following primers and their reverse complement were used for the site directed mutagenesis:

E2_C1A: (F) 5' CGCACCGCCCTGAACGCCAATGACTCCTTGC 3' ; E2_C2A: (F) 5' GCTTCAACTCGTCAGGAGCTCCCGAACGCATGTCCG 3' ; E2_C3A: (F) 5' CCCGAACGCATGTCCGCCGCCCGCAGTATCGAGGCC 3' ;

E2_C4A: (F) 5' GGATATGAGACCCTATGCCTGGCACTACCCACCAAGG 3';

E2_C5A: (F) 5' GGCACTACCCACCAAGGCAGGCTGGCGTGGTCTCCGCG 3';

E2_C6A: (F) 5' CTCCGCGAAGACTGTGGCTGGCCCAGTGTACTG 3'; E2_C7A: (F) 5' GTGTGGCCCAGTGTACGCTTTCACCCCCAGCCC 3';

E2_C8A: (F) 5' GGGGTCATGGTTCGGCGCCACGTGGATGAACTC 3' ;

E2_C9A: (F) 5' CTGGCTACACCAAGACTGCCGGCGCACCACCCTGCC 3'

E2_C10A: (F) 5' CTTGCGGCGCACCACCCGCCCGTACTAGAGCTGAC 3';

E2_C11A: (F) 5' CCAGCACGGACCTGTTGGCCCCCACGGACTGTTTTAGG 3'

E2_C12A: (F) 5' CTGTTGTGCCCCACGGACGCTTTTAGGAAGCATCCTG 3'

E2_C13A: (F) 5' GATACCACTTACCTCAAAGCCGGCTCTGGGCCCTGGC 3'

E2_C14A: (F) 5’ CCTGGCTCACGCCAAGGGCCCTGATCGACTACCCC 3’ and E2_C15A: (F) 5’ GCTCTGGCATTACCCCGCCACAGTTAACTATACC 3’ E2_C16A: (F) 5’ CACAGGCTCACGGCTGCAGCCAATTTCACTCGTGGGG 3’ E2_C17A: (F) 5’ CACTCGTGGGGATCGTGCCAACTTGGAGGACAG 3’

E2_C18A: (F) 5’ GGAATGGGCCATTTTACCTGCCTCTTACTCGGACCTGC 3’

V504A: (F) 5’ GTCTCCGCGAAGACTGCATGCGGCCCAGTGTACTGTTTCACC

G506A: (F) 5’ CGAAGACTGTGTGTGCCCCAGTATACTGTTTCACCCCC 3’

V508A: (F) 5’ CGCGAAGACTGTGTGCGGACCGGCGTACTGTTTCACCCC 3’

Y509A: (F) 5’ CTGTGTGTGGCCCAGTGGCATGCTTCACCCCCAGCCCAG 3’

F511A: (F) 5’ CTGTGTGTGGCCCAGTATACTGTGCCACCCCCAGCCCAGTGG 3’

F511A: (F) 5’

TGTGTGTGGCCCCAGTATACTGTTTCGCCCCCAGCCCAGTGGTAG 3’

Plasmid DNA clones with the correct mutation sequence were cloned into the CNS2Rluc HCV backbone plasmid using an EcoRI/BsaBI double digest or into the Cp7 HCV backbone plasmid using an EcoRI/NotI double digest.

RNA transcription and transfection

Purified plasmid DNA containing full-length viral sequences was linearized and the remaining 3’ or 5’ overhanging nucleotides were eliminated by Mung Bean Nuclease digestion (New England Biolabs, Ipswich, MA). Blunt-end DNA was extracted twice with phenol and once with chloroform, and precipitated with 100% ethanol and 3M sodium acetate (pH 5.2). 2 μg of the linear template DNA was transcribed using a MEGAscript® High Yield T7 Transcription Kit (Ambion, Austin, TX) according to

manufacturer's instructions. RNA was extracted with the RNeasy Kit (QIAGEN, Valencia, CA) and subjected to a second DNase treatment (RNase-Free DNase Set, QIAGEN, Valencia, CA) for samples later analyzed by RT-qPCR. The integrity and quantity of the transcribed RNA was verified using a nanodrop machine (ThermoScientific, Wilmington, DE) and by standard agarose gel electrophoresis.

Transfection of Huh-7.5 cells was performed as previously described [25]. Briefly, Huh-7.5 cells were trypsinized, washed once in cold PBS, and resuspended at a concentration of $2x10^7$ cells/ml. $8x10^6$ cells were mixed with 10 μg of HCV RNA and electroporated using an ECM 830 apparatus (BTX Genetronics) with five pulses of 99 μsec at 820 V over 1.1sec. Cells were resuspended in 20 ml of complete growth medium, plated and incubated at 37°C with 5% CO_2 and 100% relative humidity.

Western blots

Huh-7.5 cells were transfected with HCVcc Cp7, GND, or mutant E2 RNA as previously described. Two days post-transfection, cells were washed twice with PBS, and lysed directly in 6-well plates with western lysis buffer (100 mM Tris, pH6.8; 20mM dithiothreitol; 4%(w/v) SDS; 20% glycerol; 0.2%(w/v) bromophenol blue). Lysates were passed through a $27^{1/2}$ gauge syringe and boiled at 90ºC for 5 minutes prior to use. For E2 detection, samples were run on an 8% sodium dodecyl sulfate polyacrylamide gel and transferred to an Immobilon-P membrane (Millipore Corporation, Bedford, MA). The membrane was first blocked for 1 hour using a 5%(w/v) solution of non-fat dry milk dissolved in tris-buffered saline tween-20 (TBST, 20mM Tris, pH 7.4; 150mM NaCl;

0.1%(v/v) Tween-20) prior to overnight incubation at 4°C with a mouse monoclonal antibody to HVR1 region of E2 (2C1) (H. Scarborough, J. Whidby, J. Marcotrigiano, and A. Grakoui, unpublished results) or β-actin (SIGMA, St. Louis, MO). The following day, the membrane was probed with a goat anti-mouse horseradish peroxidase (HRP) - conjugated secondary antibody (Pierce, Rockford, IL) and developed using ECL Western detection reagents (Amersham Biosciences, Piscataway, NJ).

Concentration of viral supernatants and sucrose gradient analysis

Supernatants were layered on an 8 ml cushion of 20%(w/v) sucrose dissolved in TNE buffer (100mM NaCl; 10mM Tris-HCl, pH 8.0; 1mM EDTA). Virions were pelleted at 27,000 rpm for 4 hours at 4ºC in a Beckman Coulter SW28 rotor. After centrifugation, concentrated virus was applied to a 20-60% sucrose gradient that was continuously poured using a Gradient Master 107 machine (New Brunswick, Canada). Concentrated viral supernatants were spun through these gradients at 40,000 rpm for 16 hours at 4ºC with no brake in a Beckman Coulter swing-bucket SW41 rotor. 500 µl fractions were collected post-centrifugation from the top-down, analyzed for density using a refractometer (Master Refractometer, ATAGO, Tokyo, Japan), and stored at -80ºC until further use.

HCV core ELISA

Quantitative levels of core protein in transfected cell supernatants or individual sucrose gradient fractions were determined using an Ortho™ HCV Antigen core-specific ELISA (Wako Chemicals, Richmond, VA) according to the manufacturer's instructions. Briefly,

100 µl of sample was incubated with the pretreatment solution at 60ºC for 30 minutes, and then added to a 96-well microplate coated with mouse monoclonal anti-HCV core for 6 hours at room temperature. Plates were developed with an HRP-labeled mouse monoclonal anti-HCV core antibody and *o*-phenylenediamine (OPD) substrate. The optical density of each well was measured using Softmax Pro Software, and the amount of core in each sample was calculated against a standard curve generated with recombinant HCV core antigen.

Quantitative RT-PCR

Total RNA from cells and cell supernatants were isolated using an RNeasy Mini Kit and a QIAMP Viral RNA Extraction Kit (QIAGEN, Valencia, CA), respectively, according to the manufacturer's instructions. Real-Time Quantitative Reverse Transcription (RT-QPCR) reactions were performed by using Taqman® One Step RT-PCR Master Mix Reagents (Applied Biosystems, New Jersey, USA), primers specific for the HCV 5' NTR (forward, 10 µM: 5'-CTT CAC GCA GAA AGC GCC TA-3' and reverse, 10 µM: 5'-CAA GCG CCC TAT CAG GCA GT-3') and a probe (10 µM: 6-FAM-TAT GAG TGT CGT ACA GCC TC-MGB NFQ). The thermal cycling conditions were: 48°C for 30 minutes, 95°C for 2 minutes, and 40 cycles of 15 seconds at 95°C and 1 minute at 60°C. All amplification reactions were carried out in duplicate. A standard curve was generated using pJFH1 RNA transcripts generated by *in vitro* transcription.

Immunohistochemistry

Huh-7.5 cells were grown in collagen-coated 96-well plates and inoculated with HCVcc samples (diluted when appropriate) in complete growth medium. After 3 days of incubation, cells were fixed with ice-cold methanol, washed twice with PBS, and permeabilized with PBS plus 0.1% Tween-20 (PBST). Cells were then blocked for 30 minutes at room temperature with PBST containing 1%(w/v) bovine serum albumin (BSA) and 0.2% (w/v) dry skim milk, followed by blockage of endogenous peroxidase using 3% H_2O_2. Cells were washed twice with PBS, once with PBST, and incubated for 1 hour at room temperature with the 2C1 monoclonal antibody to E2. After washing twice with PBS and once with PBST, cells were incubated with goat anti-mouse HRP (ImmPRESS™ , Vector Labs), washed, and developed using DAB substrate (Vector Laboratories). Viral titers were determined by using 10-fold dilutions and calculating the tissue culture infectious dose at which 50% of the wells were positive for viral antigen ($TCID_{50}$) [27].

Inhibition of HCVcc infection by recombinant eE2 proteins

Huh-7.5 cells were seeded in a collagen-coated 96-well plate. Approximately 100 $TCID_{50}$s of HCVcc Cp7 [25] virus was incubated with 50 ng/ml of purified recombinant eE2, eE2-C17S, eE2-C11A, eE2-C6A, glutathione S-transferase (GST), or GST-human CD81-LEL. This concentration of eE2 protein has previously been shown to inhibit 55-85% HCVcc infectivity, as assessed by immunohistochemistry (IHC) [11].

Purification of eE2-WT, eE2-C6A, and eE2-C11A

Purification of soluble eE2 mutants was performed as previously described [11]. Briefly,

HEK293T stable cell lines were created to express each of the eE2 variants under the control of a CMV promoter. Each of the eE2 variants included both an amino-terminal prolactin signal sequence and a carboxyl-terminal Fc tag. A hygromycin resistance gene enabled stable clone selection. Supernatants from each of the stable cell lines were harvested, centrifuged to remove cellular debris, and filtered through a 0.22 μm membrane. The supernatants were then applied to protein A-conjugated resin (GE Healthcare, Piscataway, NJ) overnight for eE2 immobilization via Fc binding. Following extensive washing, the resin was incubated with thrombin protease for Fc tag removal. The protein eluates were then consolidated and the concentration determined by BioRad Protein Assay.

Circular Dichroism

Purified protein samples were desalted into 20mM sodium phosphate pH 7.0 and 50mM KCl. The CD spectra in the wavelength range of 195-260 nm were measured at 0.5 nm intervals on an Aviv spectropolarimeter model 400 (Lakewood, NJ) at 25ºC at the Robert Wood Johnson Medical School Core Facility. A quartz cell with a path length of 0.1 cm was used. The data are presented in degree cm^2 $dmol^{-1}$ [11].

CD81 Binding Assay

The protocol used for this assay was originally described by Flint et al. [28]. GST-human CD81-LEL was expressed and purified as described previously [11]. 96-well plates (Nalgene Nunc, Thermo Fisher Scientific, Rochester, NY) were coated with 50 μg/ml of GST-CD81-LEL overnight at 4°C. Plates were washed 3x with PBST and blocked with

3% BSA in PBST for 1 hour at room temperature. 100 µl of supernatant from cells stably expressing eE2-WT, eE2-C6A, and eE2-C11A was added to appropriate wells and incubated overnight at 4°C. Following supernatant incubation, plates were washed 5x with PBST and developed with TMB substrate (Pierce, Rockford, IL).

Results

Construction and expression of HCV E2 mutations in a full-length viral genome

Previous studies on HCV E2 have proposed that disulfide bonds formed by the 18 conserved cysteines in its ectodomain and stem serve as a scaffold for the protein's conformation [12], however reduction of up to half of the nine disulfide bonds has no significant effect on receptor binding [29]. In addition, disulfide bonds have been shown to stabilize large covalent complexes formed by E1 and E2 in extracellular HCV viral particles [22]. In this study, we assessed the physiological relevance of the individual cysteine residues of E2 in the HCV life cycle. Analysis of HCV E2 sequences was first carried out using the Los Alamos and European (euHCVdb) HCV databases (Figure 1A). The E2 protein is composed of four hyperconserved regions (HCR1-4) and three hypervariable regions (HVR1-3) [30,31]. Of the eighteen conserved cysteine residues, nine are in HCRs (C4, C5, C6, C7, C8, C9, C13, C14, C15), eight are in regions of intermediate variability (C1, C2, C3, C10, C12, C16, C17, C18) and only one (C11) is in an HVR. In order to study the effect of HCV E2 glycoprotein disulfide bond disruption on viral replication and virion production, we individually substituted the eighteen conserved ectodomain cysteine residues with alanine. Substitutions were generated in a previously reported infectious HCV clone termed Cp7, in which the structural proteins of the JFH-1 strain (core through p7) are replaced by the J6 genotype 2a sequence (Figure 1B, top panel) [25]. To assess the viability of the cysteine mutant genomes and the integrity of the E2 protein, Huh-7.5 cells were electroporated with the *in vitro* generated transcripts and E2 protein expression was examined by Western blot (Figure 1B). As shown in Figure 1B (bottom panel), mutations did not affect protein migration, and the

overall amount of protein produced by each mutant was comparable to that generated by wild type Cp7. To facilitate the detection of viral replication, individual cysteine substitutions were also engineered into an HCV reporter genome, termed CNS2Rluc. In this clone, the JFH-1 genomic sequence spanning from core to NS2 was replaced with the corresponding sequence of HCV J6, with the *Renilla* luciferase reporter gene inserted between the p7 and NS2 genes. The CNS2Rluc clone is equivalent to the J6/JFH (p7-Rluc2A) genome reported by Jones et al., 2007, and has been shown to produce high levels of infectious viral particles when transfected into Huh-7.5 cells [32].

HCV E2 disulfide bonds are dispensable for RNA replication but necessary for infectivity

To examine the importance of specific cysteines for viral fitness, we analyzed the replication of HCV E2 mutants in cell culture using CNS2Rluc and a *Renilla* luciferase reporter assay. First, *in vitro* transcribed RNA from each of the eighteen E2 mutants as well as wild type CNS2Rluc and replication-defective GND controls were transfected into Huh-7.5 cells. Cells were then passaged over 40 days and lysates used to measure HCV RNA replication by quantification of luciferase activity (Figure 2A). Four independent experiments showed that each of the E2 mutants replicated at levels similar to wild type on days 1-4, but declined over time to reach levels similar to replication-defective GND (Figure 2A). While the CNS2Rluc-transfected cells maintained a high production of *Renilla*, cells transfected with each of the E2 mutants had diminishing quantities of *Renilla*-positive cells over time indicating a lack of viral spread for all cysteine mutants.

To test whether individual cysteine mutations affected the production of infectious virus, supernatants from Huh-7.5 cells transfected with CNS2Rluc and the individual E2 mutants were used to infect freshly plated Huh-7.5 cells at various time points and a *Renilla* luciferase reporter assay was performed (Figure 2B). In contrast to the robust level of infectious virus produced by the wild type CNS2Rluc clone, almost none of the E2 cysteine mutants produced detectable levels of infectious virus at any time point, despite high levels of RNA replication early on (Figure 2B). It should be noted that cell supernatants following transfection with the C11A clone did contain infectious particles on days 2-4, but the production of infectious virus by C11A was not sustained (Figure 2B, middle panel).

Disruption of E2 disulfide bonds abrogates core release for the majority of E2 mutants

We hypothesized that the lack of infectivity might have been due to the destabilization of the E2 protein by individual cysteine to alanine substitutions. This destabilization could potentially lead to lack of viral particle formation, the production of viral particles that fail to egress, or the production of viral particles that are non-infectious due to lack of receptor binding or defects in fusion with the host cell membrane.

In order to determine the ability of the replicating E2 mutant genomes to secrete viral particles, the level of HCV core protein released into the supernatant following Huh-7.5 transfection with either wild-type Cp7, individual E2 mutants or a clone lacking the

E1/E2 glycoprotein (ΔE1E2) as a negative control clone was measured using the Ortho™ HCV antigen core-specific ELISA (Figure 2C, black bars). Cell lysates were simultaneously assayed for HCV replication by RT-qPCR to ensure an equivalent level of replication between each of the HCVcc clones (Figure 2C, white bars). As predicted, wild type Cp7 released high levels of core protein in the supernatant ($1.147x10^5$ fmol/ml) following transfection, while substantially less core protein was detected following transfection with each of the mutants: C6A produced $7.4x10^3$ fmol/ml, followed by C1A and C11A with $3.2x10^3$ and $3.9\ x10^3$ fmol/ml, respectively, and the rest of the mutants which did not release more than $1.5x10^3$ fmol/ml of core in the supernantants. Three of the eighteen mutants were noted for their production of extracellular core following transfection. Mutants C1A and C11A produced equivalent levels of core following transfection at 3,238 fmol/ml and 3,910 fmol/ml, respectively, but only C11A had previously demonstrated levels of infectivity that were detectable by the *Renilla* assay (Figure 2B). A third mutant, C6A, produced extracellular core at an approximately 2-fold higher level than either the C1A and C11A mutants and a 10-fold higher level than the ΔE1E2 negative control. The higher level of extracellular core produced by the C6A mutant was unexpected given that it did not produce infectious virus. These results indicate that the majority of these conserved cysteine residues, with the exception of mutants C1A, C11A and C6A, are crucial for the structure/assembly of the virions prior to release.

To determine whether any of the clones defective in secretion harbored intracellular infectious particles defective in egress, we also tested the infectivity of intracellular

material. Huh-7.5 cells transfected with cysteine mutant constructs were washed and lysed by freeze-thaw cycles. These lysates were applied to naïve Huh-7.5 cells and the infectivity was analyzed by immunohistochemistry 72 hours post-infection (data not shown). Similar to the levels of infectivity demonstrated by cell supernatants following transfection with each of the E2 mutants, only cell lysate from E2 mutant C11A was infectious, indicating that these mutants were impaired before infectious particle assembly and/or egress.

HCV C6A mutant viral particles have similar sedimentation characteristics to wild type virus

The above results indicate that with the exception of mutants C1A, C11A, and C6A, mutations in the cysteine residues of E2 had adverse effects on viral particle secretion. Density gradient analysis was employed to determine if the E2 mutants C1A, C11A, and C6A were secreting viral particles. This assay was also used to characterize potential differences in particle densities between these mutants and the wild type HCVcc Cp7. Supernatants from cells transfected with wild type Cp7, C1A, C11A, C6A, ΔE1E2, and GND were concentrated 300-fold over a 20% sucrose cushion and separated on a continuous 20-60% sucrose gradient by ultracentrifugation. Twenty-four fractions were collected and infectivity and RNA composition were assayed in fractions of equivalent densities for each mutant throughout the gradient.

As shown in Figure 3A, supernatants of cells transfected with mutants C1A, C11A, and C6A showed similar HCV RNA composition profiles compared to Cp7, with a peak

fraction of HCV RNA appearing between 1.17-1.20 g/ml. Additionally, the levels of RNA in supernatants coincided with levels of core detected by ELISA (Figure 2C): wild type Cp7 and C6A showed higher levels of HCV RNA ($6.46x10^5$ and $5x10^5$ HCV genomes/ml, respectively) compared to C1A and C11A ($2x10^4$ and $3x10^4$ genomes/ml, respectively) while no HCV RNA was detected for ΔE1E2 or GND negative controls. Because core protein was being secreted (Figure 2C) and the distribution of RNA in the gradient corresponded to the wild type Cp7 (Figure 3A), we concluded that intact virions were indeed present for the mutants C1A, C11A, and C6A.

We also tested the infectivity of the peak RNA fraction from each gradient by infecting naïve Huh-7.5 cells. Three days post-infection, cells were fixed and stained by immunohistochemistry. Consistent with our previous observations (Figure 2B), robust ($1x10^4$ FFU/ml) infectivity was detected for the peak fraction of wild type Cp7, barely detectable in the peak fraction of the C11A mutant (50 FFU/ml), and undetectable for the C1A and C6A peak fractions.

Disruption of the C6-C7 disulfide bond is responsible for the C6A mutant phenotype.

We next focused our attention on mutant C6A because our results suggested that this mutant produced the highest levels of viral particles that lacked infectivity. Sequence alignment of E2 from the six genotypes of HCV revealed that the residues neighboring C6 are 90-100% conserved across all genotypes (Figure 1A, 4A). To determine whether production of non-infectious viral particles by C6A was due to the disruption of the

disulfide bond or to local structural changes, we assessed the functional role of this region by introducing single amino acid mutations in the context of the HCVcc Cp7 clone and subsequently analyzed glycoprotein synthesis, virion release, and infectivity.

Huh-7.5 cells were transfected with RNA from E2 mutants $V_{504}A$, $G_{506}A$, $V_{508}A$, $Y_{509}A$, $F_{511}A$, and $T_{512}A$ in the context of the HCVcc Cp7 backbone (Figure 4A), as well as the previously described mutants C6A ($C_{505}A$) and C7A ($C_{510}A$). Wild-type HCVcc Cp7, ΔE1E2, and GND were included as controls. Three days post-transfection, E2 production and RNA replication were compared for each of the HCVcc clones by Western blot (Figure 4B) and RT-qPCR respectively (Figure 4D, white bars). Western blot analysis demonstrated that each of the mutants produced comparable levels of E2 protein that migrated similarly to the wild type Cp7 virus, suggesting that none of the mutations affected the expression of E2 (Figure 4B). Similarly, RT-qPCR of cell lysates demonstrated that all mutants replicate to similar levels (Figure 4D, white bars)

When secretion of viral particles was assessed by core ELISA, only wild type Cp7, mutant $T_{512}A$, and C6A released detectable levels of core into the supernatant. Cp7 produced 40,700 fmol/ml of core protein, while both $T_{512}A$ and C6A released 18,000 fmol/ml of core. The other mutations were defective in extracellular core production (Figure 4D, black bars). To simultaneously assess if substitutions of these conserved amino acids altered viral infectivity, viral titers of supernatants from the transfected cells were determined by IHC (Figure 4B). Mutants $V_{504}A$, $G_{506}A$, $V_{508}A$, and $Y_{509}A$ retained very low infectivity (between 2 and 10 FFU/ml), while $T_{512}A$ showed 10-fold less

infectivity than wild type Cp7 (1x 10^4 FFU/ml). Mutants $C_{505}A$ (C6A), $C_{510}A$ (C7A), and $F_{511}A$ were noninfectious (Figure 4C).

These results demonstrated that a correlation between extracellular core production and infectivity could be observed for each of the mutants except C6A. The majority of mutants secreted undetectable or very low levels of core and produced low levels of infectious viral particles. Mutant $T_{512}A$ secreted higher levels of core (18,000 fmol/ml, the same as C6A) and showed higher infectivity. Yet none of the mutations of amino acid residues in close proximity to C6 had an identical phenotype to the original C6 cysteine to alanine substitution. Because the C6A phenotype was unique, we hypothesized that the production of non-infectious viral particles by the C6A mutant may be due to disulfide bond disruption leading to impaired receptor binding rather than from a general alteration in the local architecture of that region.

HCV eE2-C6A and surrounding mutants influence hCD81 binding

To further investigate the role of C6 in HCV infection, we sought to determine the effect of this mutation and the nearby mutations described above on CD81 binding, using purified recombinant E2 and large extracellular loop (LEL) of human CD81. It has been previously shown that CD81 is necessary for HCVcc infectivity [33,34,35]. The soluble form of eE2 used here has previously been employed to characterize E2-CD81 interactions, and has been shown to mimic native E2 in human CD81 (hCD81) binding, blockage of HCVcc infection, and recognition by antibodies from patients chronically infected with HCV [11,12]. Since substitutions in the highly conserved region of amino

acids 483 to 513 were shown to impair infectivity, the hCD81 binding ability of each of these mutant recombinant eE2 proteins was analyzed *in vitro* as previously described [11]. As shown in figure 5A, $T_{512}A$ recombinant protein binds to hCD81 almost as well as wild type eE2, while mutants $V_{504}A$, $G_{506}A$, $V_{508}A$, $Y_{509}A$, C7A, and $F_{511}A$ bind at only 30% to 60% the capacity of wild type eE2. Interestingly, the recombinant mutant protein C6A showed the weakest interaction with CD81, with less than 20% binding capacity compared to wild type eE2.

In order to distinguish if the lack of CD81 binding was due to changes in secondary structure, circular dichroism (CD) analysis was performed on eE2-wt and eE2-C6A. The results showed that the CD spectra of C6A was identical to that generated by wild type eE2, indicating that substitution of C6 by alanine did not generate gross changes in the secondary structure of eE2 (Figure 5B). These results suggest that this region likely harbors a CD81-binding domain, and provide compelling evidence that the C6A mutant was unable to establish productive infection in cell culture due to a defect in CD81 coreceptor binding.

eE2-C6A is defective in blocking HCV infection

To determine whether the recombinant mutant protein C6A mimicked the function of wild type eE2 *in vitro*, we first compared the ability of these two proteins to block HCVcc infection [11,12]. Naïve Huh-7.5 cells were incubated for three days with 100 TCID50 (tissue culture infectious dose 50) of Cp7 virus mixed with 50 μg/ml of purified eE2, eE2-C17S, eE2-C6A, hCD81, or GST. eE2-C17S was included as a control since we previously showed that this recombinant protein was able to be recognized by antibodies

from patients infected with HCV, block HCVcc infectivity, and bind hCD81 [11]. As shown in Figure 5C, control proteins eE2, eE2-C17S, and hCD81 blocked 60-70% virus infectivity while C6A blocked 25%.

Discussion

It is well known that disulfide bonding is critical for the structure and function of mature viral proteins, providing an explanation for the conservation of such bonding across HCV viral genotypes. In this study, we have shown that mutagenesis of conserved cysteine residues elucidated the importance of disulfide bonding at various stages of the HCV replication life cycle. While others have shown that the HIV envelope glycoprotein can accommodate certain changes in strictly conserved disulfide bonds and still be infectious [24], we observed that disulfide bond disruption within HCV E2 profoundly decreased HCV virion production and infectivity. This block in infectivity was at the step of egress for most mutants, suggesting that there is no plasticity regarding changes in the disulfide connectivity pattern or restoration of structural integrity. Although we could not rule out the reshuffling of disulfide bonds in the envelope of any of the cysteine mutants, there is evidence that it does not take place in this system [36]. Importantly, it has been previously shown using HCVpp, in which half of the disulfide bonds have been cleaved, that reshuffling mediated by oxidoreductase activity does not take place during entry [36]. Additionally, it has been shown that Env, the only viral protein present on the surface of the HIV virions, does not undergo alternative cysteine pairing when disulfide bond disruption occurs [24].

In our study, we did not see an increased level of viral replication with time for any of the mutants. This reduction in replication with serial passages was attributed to the lack of viral spread, suggesting that these mutants either failed to revert or failed to generate compensating mutations to produce infectious virus.

The results gathered from intracellular replication, infectivity and core release allowed us to distinguish between three types of mutants. Type I, which comprised the majority of the mutants, replicated and synthesized E2 while releasing very low to undetectable levels of core protein in supernatants. These mutants likely had a defect in E1 and E2 incorporation into the viral particle. Because of the conservation of the cysteines in the E2 protein sequence, we anticipated that the majority of these residues would be critical for folding since elimination of disulfide bonds often leads to misfolded and aggregated proteins that are unable to leave the endoplasmic reticulum. It has been shown that point mutations in the E2 protein can alter the incorporation of E1 and E2 in HCVpp even when these proteins seem to run similarly to the WT protein in western blots [4]. Type II, which included both C1A and C11A, produced undetectable or very low levels of infectious particles, respectively and very low levels of core. The lower levels of extracellular core seen in C11A (as compared to C6A) might represent a smaller but functionally competent subset of particles that retained their infectivity due to a continued ability to bind cellular receptors (data not shown). Also, C11 is the only cysteine that is contained in a region that has been described as hypervariable (HVR3, amino acids 575-587), and could possibly tolerate alterations better than other regions. The majority of the cysteine mutants comprised disulfide bonds whose elimination most likely led to severe folding deficiencies and subsequently failed quality control mechanisms necessary for proper exit from the endoplasmic reticulum (type I). For type II mutants, it is more difficult to relate misfolding with marginal viral infectivity. It is likely that a minority of these mutant E2 proteins managed to fold correctly, exit the endoplasmic reticulum, and

become incorporated into viral particles that were able to bind hCD81 (C11A, data not shown) and infect cells. The inefficient spread of these particles and the lack of selective pressure led to a loss of infectivity. These results are supported by the observation that disulfide bonds are necessary for proper folding of E2 in the ER, most likely maintaining the basic structure of the protein [12] instead of playing a role in fusion by mediating changes in the secondary structure upon exposure to low pH as shown for reoviruses [18], retroviruses [37,38,17,39,40], alphaviruses [20], herpesviruses [19], and paramyxoviruses [21].

Finally, for the type III mutant, comprised only by C6A, substitution of the cysteine residue for alanine led to production of viral particles that were not infectious, most likely due to a defect in their ability to bind hCD81 (Figure 5A). While this region (amino acids 502 to 520) has been proposed to be a fusion peptide on the basis of amino acid composition, sequence conservation and secondary structure prediction [12], a functional role in CD81 binding has never been described. In addition, according to the model of the tertiary structure of HCV E2 that has been recently proposed, C6 and C7 form a disulfide bond and both cysteines are in the putative fusion peptide [12]. Since C6 is in this highly conserved region, it was possible that the phenotype of C6A was due to alterations of this sequence and not due to disruption of the disulfide bond. In order to assess this possibility, some of the conserved amino acids of the putative fusion peptide were individually substituted by alanine and their phenotypes compared to C6A. Our results suggested that the disruption of this disulfide bond determined the phenotype of C6A since none of the mutations in the putative fusion peptide abolished infectivity without

affecting particle release. Since mutant $F_{509}A$ secreted very low to undetectable levels of core and lacked infectivity, it was classified as type I mutant. Mutants $V_{504}A$, $G_{506}A$, $V_{508}A$, and $Y_{509}A$ belonged to type II, since they showed very low levels of core release and therefore low infectivity, as described for C11A. Despite the fact that $T_{512}A$ showed comparable levels of core release as C6A, it could not be classified as type III like C6A on account of the observation that the levels of core were comparable to the levels of infectivity (Figure 5C, D). It has previously been shown in the HCVpp system that G_{506}, Y_{509}, T_{511}, and T_{512} (referred as G_{504}, Y_{507}, T_{509}, and T_{510} in reference [4]) alter E1 and E2 incorporation in viral particles. This lack of incorporation was attributed to differences in glycosylation patterns. For mutant $T_{512}A$ ($T_{510}A$ in reference [4]), incorporation of E1 and E2 in viral particles was affected to a lesser extent, and cell entry decreased by two and a half logs. This result correlates with our observation that in HCVcc, $T_{512}A$ showed comparable levels of core release to C6A and retained infectivity (Figure 4C, D). Additionally, we also showed that the levels of infectivity correlated with the hCD81 binding activity of $T_{512}A$ (Figure 5A).

An advantage of using *in vitro* cell culture over purified protein is the ability to determine at which step of the viral life cycle the disruption of individual disulfide bonds has an effect. The C11A mutation had no effect on CD81 receptor binding. However, using the *in vitro* HCVcc system, we demonstrated that the C11A mutation exerted its effects on the HCV replication life cycle at the level of cellular egress. After the physiological relevance of the mutations was established, we focused our attention on the most interesting phenotype, type III, and found that changes associated with this phenotype

impaired CD81 binding. Since this region has not been previously implicated in CD81 binding, we introduced the C6A mutation as well as mutations in the neighboring region in a novel expression system for the production of a secreted form of E2 ectodomain that enabled us to assess the ability of these eE2 variants of eE2 to bind hCD81 and block viral infection [11]. Here we showed that C6A and $V_{504}A$, $G_{506}A$, $V_{508}A$, and $Y_{509}A$ mutants were impaired in their ability to bind CD81. These results implicate domain II of E2 in CD81 binding. The lack of CD81 binding of C6A may be due to the fact that the 6^{th} cysteine is directly involved in CD81 binding. However, it is also possible that this mutation caused local minor changes undetectable by CD analysis, or that the resulting free cysteine that would normally form a disulfide bond with C6 yielded an E2 protein that is no longer able to bind CD81.

We then studied the ability of the C6A purified eE2 to block HCVcc. We did not assess the blocking capacity of mutations in the putative fusion peptide neighboring C6A as they did not secrete viral particles and, therefore were not physiologically relevant for these studies. We observed a reduction in the capacity of C6A to block viral infection. This blocking deficiency exhibited by C6A soluble protein is most likely due to the fact that this mutation impairs CD81 binding (Figure 5A) and not due to changes in the overall structure of the molecule (Figure 5C).

As stated before, in the current model for the tertiary structure of HCV E2, C6 and C7 form a disulfide bond [12]. However neither C7A nor any other cysteine mutant shared the unique C6A phenotype. It has been previously shown that virion-associated envelope

glycoprotein E1 and E2 form large covalent complexes stabilized by disulfide bonds [22]. Although we did not determine the oligomeric state of the E2 molecule in the virions of C6A, we hypothesize that the free cysteine of the C6A mutant protein might be forming disulfide bonds either with E1 or with another E2 molecule.

In summary, our results provided evidence that the majority of the conserved cysteines in the HCV E2 glycoprotein are necessary to maintain its structure. We have demonstrated that region 502-520 of the proposed domain II [12] has an effect on CD81-binding, a function previously unreported in the literature. Most importantly, we characterized mutant C6A, which has significant future implications in both HCV vaccine and therapeutic development. This mutant did not revert, was capable of assembling egress-competent particles, and was absolutely incapable of infecting naïve cells, making it an attractive platform upon which to design an attenuated vaccine.

Acknowledgments

The authors would like to thank the members of the Grakoui and Marcotrigiano laboratories for helpful discussions, especially Victoria Best and Holly L. Hanson for critical reading of the manuscript. The authors would like to acknowledge the support from the New Jersey Commission on Cancer Research 10-1962-CCR-EO (JM), EVC/CFAR Core P30 AI050409 (AG), the Yerkes Research Center Base Grant RR-00165 (AG), and the US Public Health Service grants [AI080659 (JM), DK083356 (AG), and AI070101 (AG)].

Figures

Figure 1

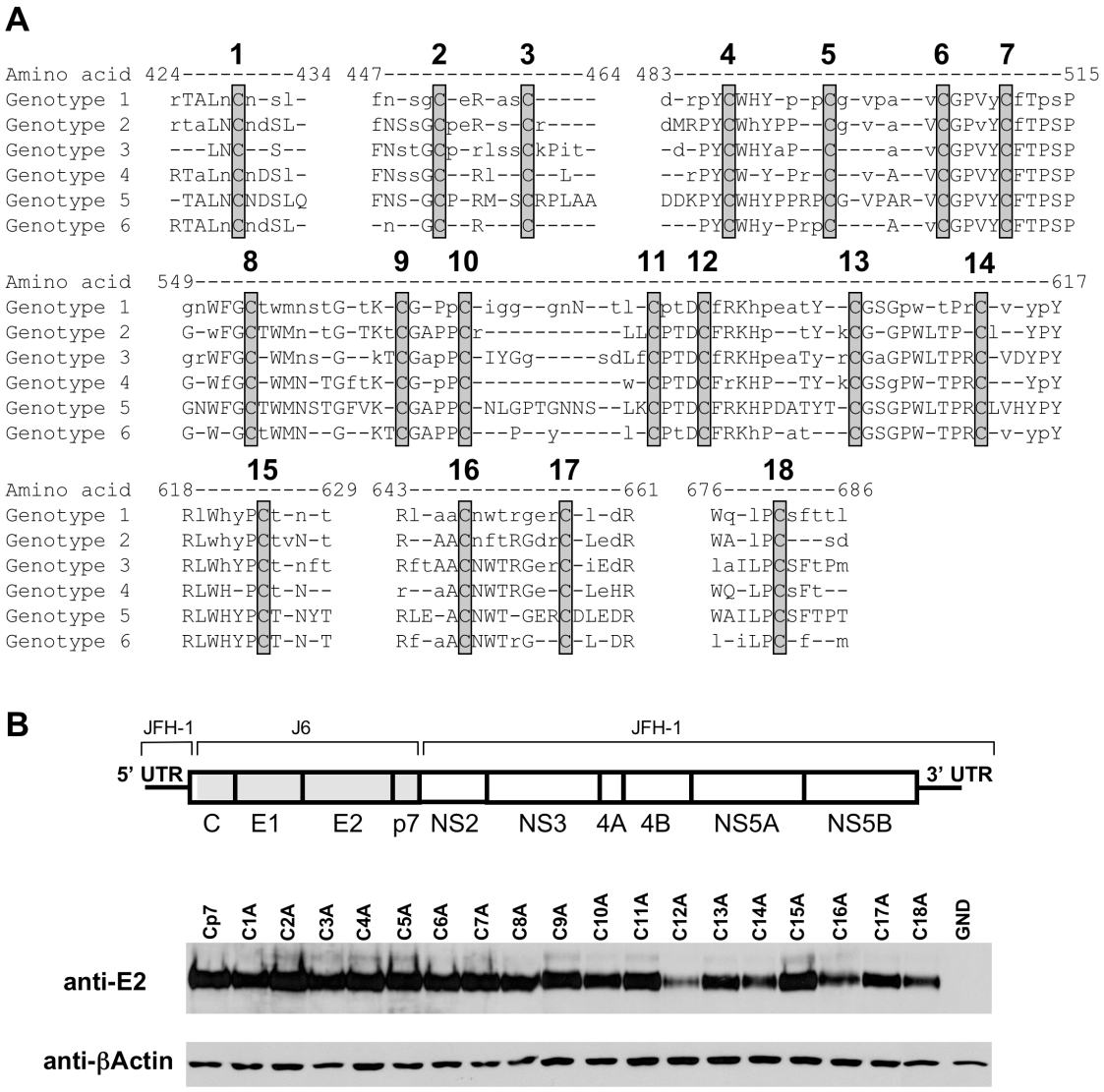

Figure 2

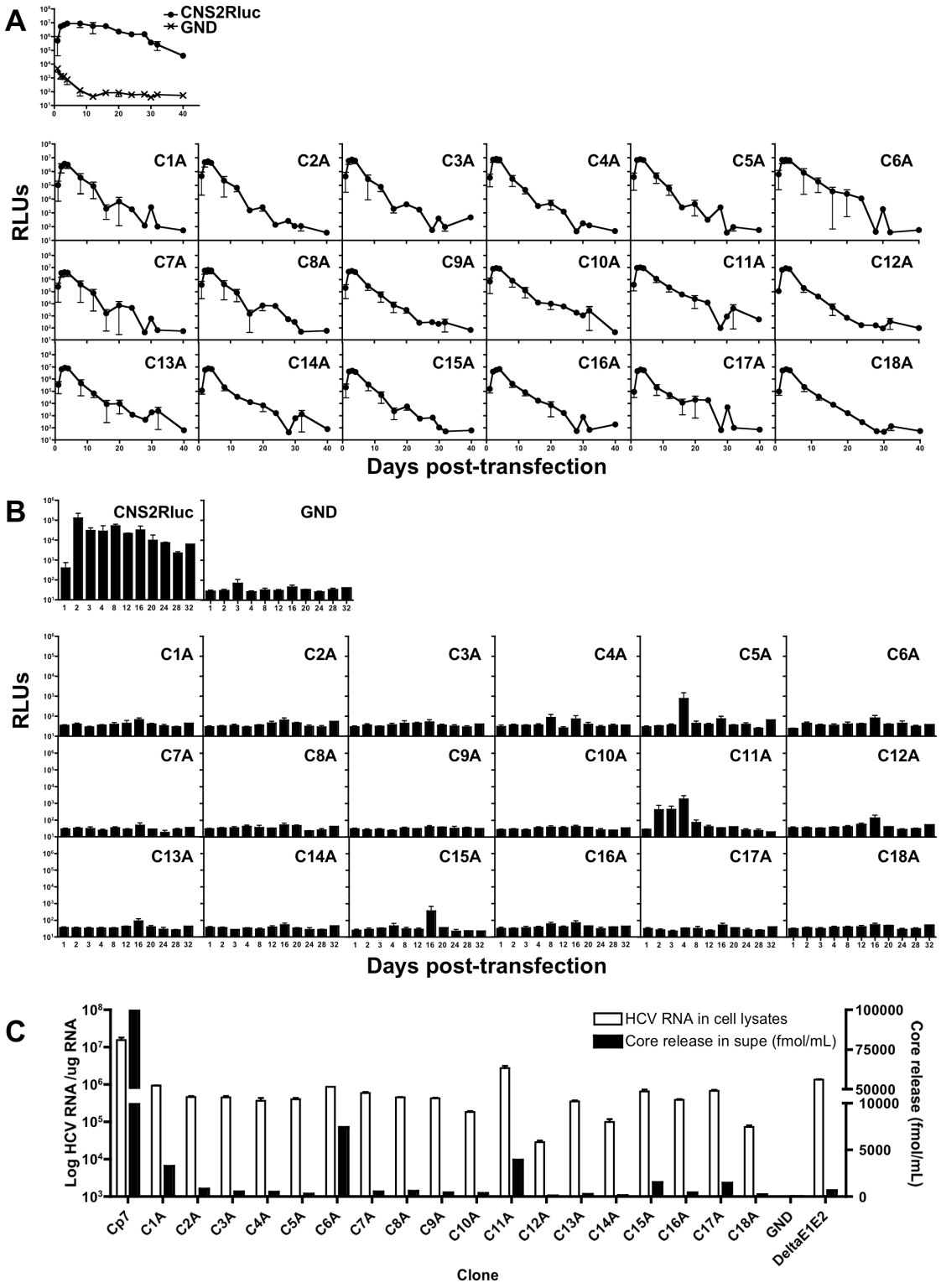
A
CNS2Rluc
GND
RLUs
C1A
C2A
C3A
C4A
C5A
C6A
C7A
C8A
C9A
C10A
C11A
C12A
C13A
C14A
C15A
C16A
C17A
C18A
Days post-transfection
B
CNS2Rluc
GND
RLUs
Days post-transfection
C
HCV RNA in cell lysates
Core release in supe (fmol/mL)
Log HCV RNA /ug RNA
Core release (fmol/mL)
Cp7
GND
DeltaE1E2
Clone

Figure 3

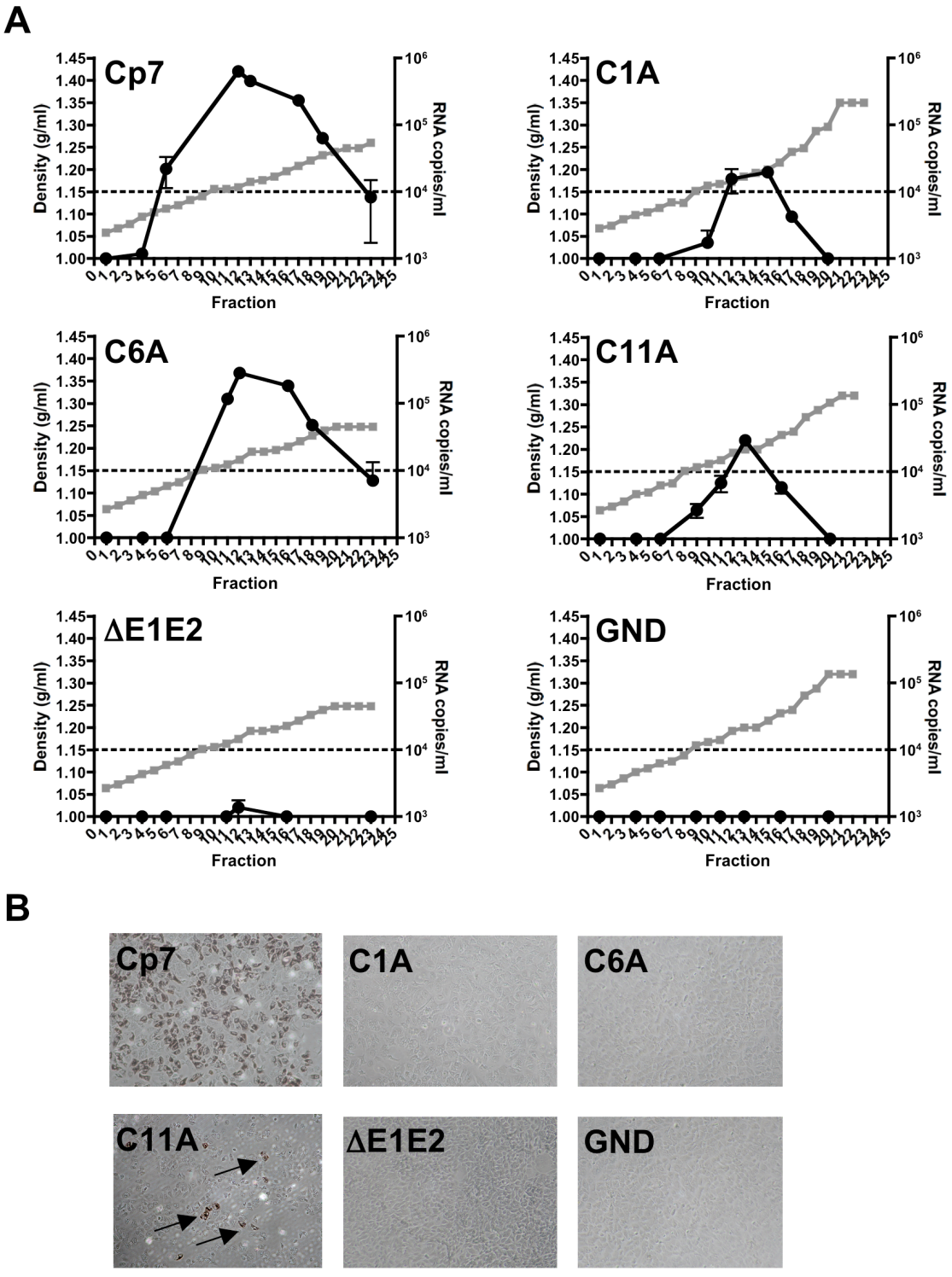
A
Cp7
C1A
C6A
C11A
ΔE1E2
GND
Density (g/ml)
RNA copies/ml
Fraction
B
Cp7
C1A
C6A
C11A
ΔE1E2
GND

Figure 4

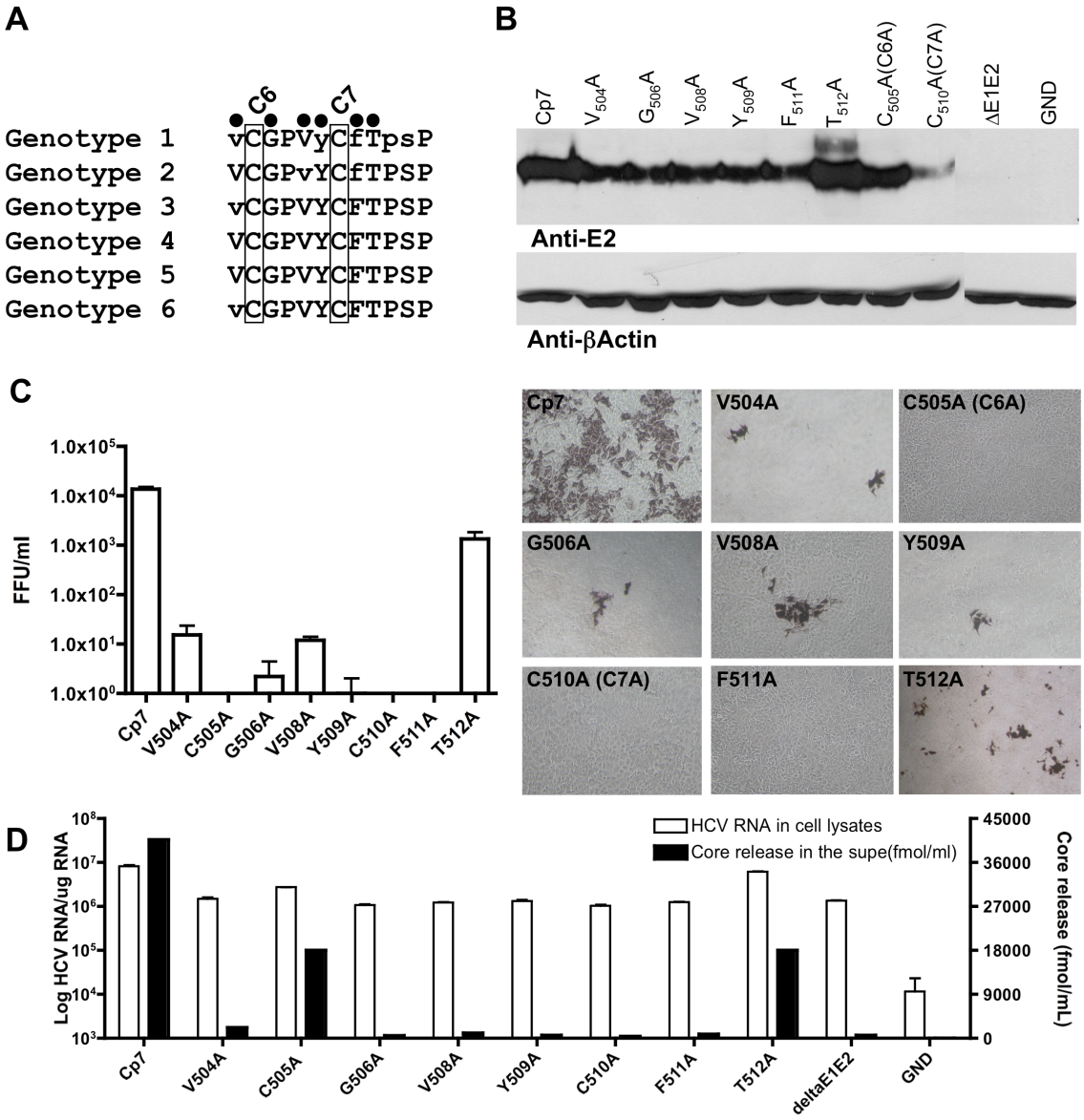
A
C6
C7
Genotype 1 vCGPVyCfTpsP
Genotype 2 VCGPvYCfTPSP
Genotype 3 vCGPVYCFTPSP
Genotype 4 VCGPVYCFTPSP
Genotype 5 VCGPVYCFTPSP
Genotype 6 vCGPVYCFTPSP
B
Cp7
V504A
G506A
V508A
Y509A
F511A
T512A
C505A(C6A)
C510A(C7A)
ΔE1E2
GND
Anti-E2
Anti-βActin
C
FFU/ml
1.0x10^5
1.0x10^4
1.0x10^3
1.0x10^2
1.0x10^1
1.0x10^0
Cp7
V504A
C505A
G506A
V508A
Y509A
C510A
F511A
T512A
Cp7
V504A
C505A (C6A)
G506A
V508A
Y509A
C510A (C7A)
F511A
T512A
D
Log HCV RNA/ug RNA
HCV RNA in cell lysates
Core release in the supe(fmol/ml)
Core release (fmol/mL)
45000
36000
27000
18000
9000
0
Cp7
V504A
C505A
G506A
V508A
Y509A
C510A
F511A
T512A
deltaE1E2
GND

Figure 5

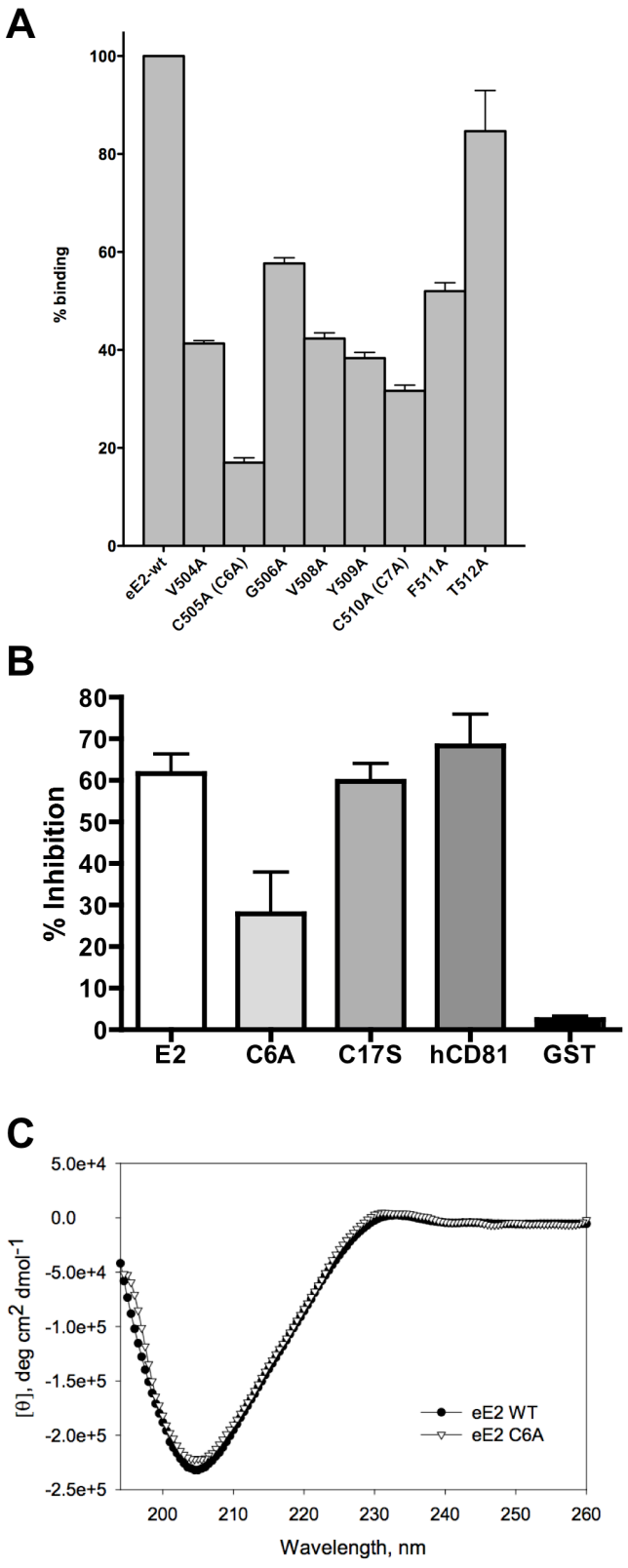
A
% binding
100
80
60
40
20
0
eE2-wt
V504A
C505A (C6A)
G506A
V508A
Y509A
C510A (C7A)
F511A
T512A
B
% Inhibition
80
70
60
50
40
30
20
10
0
E2
C6A
C17S
hCD81
GST
C
[θ], deg cm2 dmol-1
5.0e+4
0.0
-5.0e+4
-1.0e+5
-1.5e+5
-2.0e+5
-2.5e+5
200
210
220
230
240
250
260
Wavelength, nm
eE2 WT
eE2 C6A

Figure Legends

Figure 1. Mutations in conserved cysteines of the HCV eE2. A) Multiple alignments of HCV E2 proteins reveal the presence of 18 highly conserved cysteines (grey boxes). Cysteine residues are numbered according to their proximity to the amino terminus. Symbol "-" represents residues that are less than 90% conserved, lower case represents 90% conservation, and upper case represents 100% conservation across genotypes. The numbers above the grey boxes are a reference for the alternative nomenclature in the text. Sequences were aligned using clustal alignments (see Materials and Methods for reference). B) Top panel depicts a schematic representation of the viral chimera Cp7 used as a wild type control. The bottom panel depictsa Western blot for which anti-E2 and anti-βactin antibodies were used to detect replication and total protein input, respectively.

Figure 2. Mutations in conserved cysteines of HCV E2 impair infectivity for all mutants and ablate core release in all mutants except C6A. E2 cysteine mutations were introduced in the CNS2Rluc clone to facilitate detection of replication. GND is a nonreplicative control genome. A) Replication of individual cysteine mutants as assayed by relative light units (RLUs) in cell lysates up to 40 days post-transfection. B) Infectivity of the E2 cysteine mutants up to 32 days post-tranfection. Supernatants from transfected cells were harvested at the indicated time points and used to infect naïve Huh-7.5 cells. Three days post-infection cells were lysed and tested for Renilla expression. For A) and B), means and standard error of the means of four transfections and infections are shown. C) Replication (white bars) and total core release (black bars) of the E2 cysteine

mutants 48 hours post-transfection. Representative data from two separate experiments are shown.

Figure 3. Mutants C1A, C6A, and C11A produce viral particles. A) Density gradient analysis of cysteine mutant particles. Only mutants with detectable levels of core in the supernatants were tested. Concentrated supernatant from transfected cells were fractioned using a 20-60% sucrose density gradient. The density of each fraction (grey line) was assessed using a refractrometer, and the HCV RNA copies were quantified by real time RT-PCR (black line). B) Infectivity of the peak HCV RNA fraction from each gradient. Fractions were used to infect naïve Huh-7.5 cells and stained by IHC three days post-infection using an anti-E2 monoclonal antibody. Arrows denote small groups of stained cells.

Figure 4. C6A displays a unique phenotype. A) Mutations of conserved residues surrounding C6 were engineered into the Cp7 backbone. The dots indicate residues that were substituted by alanine. B) Western blot analysis of lysates from cells transfected with the controls Cp7 and GND, mutants C6A and C7A, and mutants containing alanine substitutions in conserved residues surrounding C6A ($V_{504}A$, $G_{506}A$, $V_{508}A$, $Y_{509}A$, $F_{511}A$ and $T_{512}A$). C) Infectivity of E2 mutants. Three days post-transfection, supernatants were harvested and used to infect naïve Huh-7.5 cells. Cells were stained three days post-infection by IHC. Means and SEM of three electroporations are shown. Right panel depicts representative images of graphed data. D) Replication (white bars) and total core release (black bars) of E2 conserved region mutants at 48 hours post-transfection.

Figure 5. Mutation of the 6th cysteine and conserved neighboring residues in HCV E2 affect hCD81 binding. A) ELISA for CD81-binding. Tissue culture supernatants of recombinant mutant proteins were incubated in plates coated with GST-hCD81LEL and, after washing, bound eE2 mutants were detected with anti-human-Fc. B) Inhibition of HCVcc infection by recombinant mutant proteins. Cells were incubated with 50 ng/ml of eE2-C6A and eE2-C11A plus Cp7 virus. Three days post-infection, cells were fixed, focus-forming units were determined, and the percentage of inhibition calculated. Error bars represent SEM for two independent experiments. Each experiment was performed in duplicate. C) CD spectroscopy of eE2 and eE2-C6A. CD spectra are shown as millidegrees versus wavelength (nm). Error bars for each data point are given.

References

1. Bartosch B, Cosset FL (2006) Cell entry of hepatitis C virus. Virology 348: 1-12.

2. Deleersnyder V, Pillez A, Wychowski C, Blight K, Xu J, et al. (1997) Formation of native hepatitis C virus glycoprotein complexes. J Virol 71: 697-704.

3. Drummer HE, Boo I, Poumbourios P (2007) Mutagenesis of a conserved fusion peptide-like motif and membrane-proximal heptad-repeat region of hepatitis C virus glycoprotein E1. J Gen Virol 88: 1144-1148.

4. Lavillette D, Pecheur EI, Donot P, Fresquet J, Molle J, et al. (2007) Characterization of fusion determinants points to the involvement of three discrete regions of both E1 and E2 glycoproteins in the membrane fusion process of hepatitis C virus. J Virol 81: 8752-8765.

5. Li HF, Huang CH, Ai LS, Chuang CK, Chen SS (2009) Mutagenesis of the fusion peptide-like domain of hepatitis C virus E1 glycoprotein: involvement in cell fusion and virus entry. J Biomed Sci 16: 89.

6. Dubuisson J (2007) Hepatitis C virus proteins. World J Gastroenterol 13: 2406-2415.

7. Falkowska E, Kajumo F, Garcia E, Reinus J, Dragic T (2007) Hepatitis C virus envelope glycoprotein E2 glycans modulate entry, CD81 binding, and neutralization. J Virol 81: 8072-8079.

8. Barth H, Schafer C, Adah MI, Zhang F, Linhardt RJ, et al. (2003) Cellular binding of hepatitis C virus envelope glycoprotein E2 requires cell surface heparan sulfate. J Biol Chem 278: 41003-41012.

9. Pileri P, Uematsu Y, Campagnoli S, Galli G, Falugi F, et al. (1998) Binding of hepatitis C virus to CD81. Science 282: 938-941.

10. Scarselli E, Ansuini H, Cerino R, Roccasecca RM, Acali S, et al. (2002) The human scavenger receptor class B type I is a novel candidate receptor for the hepatitis C virus. Embo J 21: 5017-5025.

11. Whidby J, Mateu G, Scarborough H, Demeler B, Grakoui A, et al. (2009) Blocking hepatitis C virus infection with recombinant form of envelope protein 2 ectodomain. J Virol 83: 11078-11089.

12. Krey T, d'Alayer J, Kikuti CM, Saulnier A, Damier-Piolle L, et al. The disulfide bonds in glycoprotein E2 of hepatitis C virus reveal the tertiary organization of the molecule. PLoS Pathog 6: e1000762.

13. Drummer HE, Poumbourios P (2004) Hepatitis C virus glycoprotein E2 contains a membrane-proximal heptad repeat sequence that is essential for E1E2 glycoprotein heterodimerization and viral entry. J Biol Chem 279: 30066-30072.

14. Benham AM (2005) Oxidative protein folding: an update. Antioxid Redox Signal 7: 835-838.

15. Betz SF (1993) Disulfide bonds and the stability of globular proteins. Protein Sci 2: 1551-1558.

16. Jensen PE (1995) Antigen unfolding and disulfide reduction in antigen presenting cells. Semin Immunol 7: 347-353.

17. Abrahamyan LG, Markosyan RM, Moore JP, Cohen FS, Melikyan GB (2003) Human immunodeficiency virus type 1 Env with an intersubunit disulfide bond engages coreceptors but requires bond reduction after engagement to induce fusion. J Virol 77: 5829-5836.

18. Barry C, Key T, Haddad R, Duncan R Features of a spatially constrained cystine loop in the p10 FAST protein ectodomain define a new class of viral fusion peptides. J Biol Chem 285: 16424-16433.

19. Cairns TM, Landsburg DJ, Whitbeck JC, Eisenberg RJ, Cohen GH (2005) Contribution of cysteine residues to the structure and function of herpes simplex virus gH/gL. Virology 332: 550-562.

20. Glomb-Reinmund S, Kielian M (1998) The role of low pH and disulfide shuffling in the entry and fusion of Semliki Forest virus and Sindbis virus. Virology 248: 372-381.

21. Jain S, McGinnes LW, Morrison TG (2008) Overexpression of thiol/disulfide isomerases enhances membrane fusion directed by the Newcastle disease virus fusion protein. J Virol 82: 12039-12048.

22. Vieyres G, Thomas X, Descamps V, Duverlie G, Patel AH, et al. Characterization of the envelope glycoproteins associated with infectious hepatitis C virus. J Virol 84: 10159-10168.

23. Mamathambika BS, Bardwell JC (2008) Disulfide-linked protein folding pathways. Annu Rev Cell Dev Biol 24: 211-235.

24. van Anken E, Sanders RW, Liscaljet IM, Land A, Bontjer I, et al. (2008) Only five of 10 strictly conserved disulfide bonds are essential for folding and eight for function of the HIV-1 envelope glycoprotein. Mol Biol Cell 19: 4298-4309.

25. Mateu G, Donis RO, Wakita T, Bukh J, Grakoui A (2008) Intragenotypic JFH1 based recombinant hepatitis C virus produces high levels of infectious particles but causes increased cell death. Virology 376: 397-407.

26. Tscherne DM, Jones CT, Evans MJ, Lindenbach BD, McKeating JA, et al. (2006) Time- and temperature-dependent activation of hepatitis C virus for low-pH-triggered entry. J Virol 80: 1734-1741.

27. Reed LJ, Muench, H. (1938) A simple method of estimating fifty percent endpoints. American Journal of Hygiene 27: 493-497.

28. Flint M, von Hahn T, Zhang J, Farquhar M, Jones CT, et al. (2006) Diverse CD81 proteins support hepatitis C virus infection. J Virol 80: 11331-11342.

29. Fenouillet E, Lavillette D, Loureiro S, Krashias G, Maurin G, et al. (2008) Contribution of redox status to hepatitis C virus E2 envelope protein function and antigenicity. J Biol Chem 283: 26340-26348.

30. Hijikata M, Kato N, Ootsuyama Y, Nakagawa M, Ohkoshi S, et al. (1991) Hypervariable regions in the putative glycoprotein of hepatitis C virus. Biochem Biophys Res Commun 175: 220-228.

31. Kato N, Ootsuyama Y, Tanaka T, Nakagawa M, Nakazawa T, et al. (1992) Marked sequence diversity in the putative envelope proteins of hepatitis C viruses. Virus Res 22: 107-123.

32. Jones CT, Murray CL, Eastman DK, Tassello J, Rice CM (2007) Hepatitis C virus p7 and NS2 proteins are essential for production of infectious virus. J Virol 81: 8374-8383.

33. Lindenbach BD, Evans MJ, Syder AJ, Wolk B, Tellinghuisen TL, et al. (2005) Complete replication of hepatitis C virus in cell culture. Science 309: 623-626.

34. Zhong J, Gastaminza P, Cheng G, Kapadia S, Kato T, et al. (2005) Robust hepatitis C virus infection *in vitro*. Proc Natl Acad Sci U S A 102: 9294-9299.

35. Wakita T, Pietschmann T, Kato T, Date T, Miyamoto M, et al. (2005) Production of infectious hepatitis C virus in tissue culture from a cloned viral genome. Nat Med 11: 791-796.

36. Fenouillet E, Barbouche R, Jones IM (2007) Cell entry by enveloped viruses: redox considerations for HIV and SARS-coronavirus. Antioxid Redox Signal 9: 1009-1034.

37. Sjoberg M, Wallin M, Lindqvist B, Garoff H (2006) Furin cleavage potentiates the membrane fusion-controlling intersubunit disulfide bond isomerization activity of leukemia virus Env. J Virol 80: 5540-5551.

38. Ou W, Silver J (2006) Role of protein disulfide isomerase and other thiol-reactive proteins in HIV-1 envelope protein-mediated fusion. Virology 350: 406-417.

39. Sanders RW, Vesanen M, Schuelke N, Master A, Schiffner L, et al. (2002) Stabilization of the soluble, cleaved, trimeric form of the envelope glycoprotein complex of human immunodeficiency virus type 1. J Virol 76: 8875-8889.

40. Melder DC, Yin X, Delos SE, Federspiel MJ (2009) A charged second-site mutation in the fusion peptide rescues replication of a mutant avian sarcoma and leukosis virus lacking critical cysteine residues flanking the internal fusion domain. J Virol 83: 8575-8586.

CHAPTER 4

Binding and entry dynamics of hepatitis C virus and recombinant ectodomain E2 glycoprotein in human hepatoma cell lines

Luke Uebelhoer[1], Hannah Scarborough[1], Jillian Whidby Freund[2], Joseph Marcotrigiano[2] and Arash Grakoui[1*]

[1]Department of Medicine, Division of Infectious Diseases, Microbiology and Immunology, Emory Vaccine Center, Emory University School of Medicine, Atlanta, GA 30329; [2] Center for Advanced Biotechnology and Medicine, Dept of Chemistry and Chemical Biology, Rutgers University, Piscataway, NJ 08854; *Corresponding author

Running title: Binding and entry of hepatitis C virus

This chapter consists of a manuscript that is currently in preparation for submission.

Abstract

Hepatitis C virus (HCV) undergoes a highly coordinated binding and entry process in hepatocytes that is just now beginning to be understood. Identification of new HCV receptors and novel full-length infectious cell culture systems have provided a picture of early events where the virus undergoes stepwise receptor binding, culminating in tight cellular attachment and internalization via clathrin-mediated endocytosis. However, despite advances in the field, little is known about the specific interactions between an incoming virion and a target hepatocyte, and imaging of early binding events has been lacking. We describe here a system for generating large quantities of highly infectious unmodified HCV cell culture (HCVcc) -derived virus and visualizing initial binding events using temperature modification and centrifugal force. Additionally, we developed a system for studying the binding and internalization of mammalian cell-generated soluble HCV ectodomain E2 (eE2) protein and derivatives in human hepatoma cell lines. HCVcc can be found bound to the apical surface of liver-derived cells immediately post-spin-inoculation, and this initial binding event is dependent on host cytoskeletal rearrangment and viral glycan interactions with host cell surface molecules. Furthermore, quantification of early and late infection events in the HCVcc system suggests that cell surface binding of virions is an accurate predictor of future productive infection. eE2 protein interactions with hepatic cell lines, although not necessarily representative of native E1E2 heterodimers, may provide insight in the initial attachment, uncoating, and trafficking of HCV. This study represents a technical advance for imaging HCV binding, and may help identify unknown host cellular cofactors involved in early steps of the viral life cycle.

Introduction

Hepatitis C virus (HCV) infects hundreds of millions of people worldwide, and the current lack of a vaccine makes this virus a serious public health challenge [1]. The virus infects and replicates almost exclusively in hepatocytes, with consequence to the normal liver microenvironment and hepatic function [2]. HCV is a small, single-stranded RNA virus of positive polarity consisting of a lipid bilayer studded with two types of glycoproteins (E1 and E2) surrounding a capsid structure that contains the ~9600 base pair genome [3]. The life cycle of the virus can be broken down into four main phases: i) binding and entry, ii) fusion with host membranes, iii) genome translation and replication, and iv) packaging and egress of mature infectious particles. The first two of these phases represent an important fraction of the infectious cycle, and much work has been done to elucidate the receptor-driven mechanisms that govern these processes. Model systems to study these events include recombinant glycoproteins [4,5,6,7], viral pseudoparticles (HCVpp) [8,9], and most recently full-length infectious HCV cell culture clones (HCVcc) [10,11,12].

Circulating HCV is associated with serum lipoproteins, and initial virus-cell interactions most likely occur through low density lipoprotein (LDL) receptor-binding and a low-affinity interaction with glycosaminoglycans (GAGs) that serves to retain the viral particle at the cell surface and facilitate subsequent higher-affinity binding [13,14,15,16,17,18,19]. Following these transient interactions, a specific set of receptors are required for HCV to infect a cell, including scavenger receptor class B type 1 (SR-BI) [6], the tetraspanin CD81 [7], and the tight junction proteins claudin (CLDN) -1, -6, -9,

and occludin (OCLN) [20,21,22]. Because of HCV's late interaction with CLDN and OCLN, it has been hypothesized that virions may be shuttled on the surface of a hepatocyte to tight junctions prior to endocytosis. Clathrin is believed to be involved in this process, as HCVpp and HCVcc internalization are inhibited by targeting clathrin components with siRNA and the drug chlorpromazine [23,24,25]. However, HCV has never been found in a clathrin-coated vesicle, and visualization of viral internalization is just now becoming possible. Additionally, recent studies have shown that tight junctions are dispensable for *in vitro* infectivity, although this may be a unique feature of *in vitro* systems and not necessarily reflect *in vivo* conditions of primary polarized hepatocytes [26,27,28].

The proportion of infected hepatocytes in chronic HCV patients remains unknown, although sensitive *in situ* hybridziation methods indicate that up to 50% may contain viral RNA [29]. This number is likely variable, with fluctuations dependent on several factors including co-infection [29], cell-cell transmission [30], rates of virion output by single cells, and lysis of infected cells by intrahepatic CD8+ T cells. Similarly, the study of productive infection rates resulting from single particle attachment to hepatocytes has been hampered due to lack of individual HCV particle tracking systems. Coller *et al*. recently developed a single particle tracking system to examine HCV entry in hepatocytes, but did not link single particles to productive infection nor were these particles visible in clathrin-coated pits [26]. To study these aspects of the viral life cycle, we established a system to track HCV particles throughout the course of *in vitro* cell culture infection. We avoided technical difficulties with lipophilic-dye labeling by

concentrating large amounts of HCVcc particles and normalizing initial binding events through temperature manipulation and spin-inoculation. Initial binding and subsequent infection were probed using several monoclonal antibodies to different structural and nonstructural viral proteins, as well as drug-targeted inhibition of cellular processes, specific host cell compartment labeling, and randomized quantitative analysis of fluorescent signals. We provide evidence that HCVcc particles can be visualized immediately upon initial binding at the apex of human hepatoma cells, and associate in tightly clustered puncta with adjacent host cell actin. Furthermore, binding is dependent on CD81 expression and glycan interactions. Surprisingly, initial binding events in this system are a faithful predictor of future productive infection, and suggest that every hepatocyte that comes in contact with these HCV puncta will eventually become infected. This system will be useful for future studies correlating early and late events of the viral life cycle, as well as the study of how host cytoskeletal proteins and clathrin or clathrin-associated proteins rearrange during HCV infection.

Materials and Methods

Cell lines and cell culture

Human hepatoma cell lines Huh-7.5 and HepG2 were maintained in Dulbecco's modified Eagle's medium supplemented with 10% fetal bovine serum (DMEM-10) (FBS, Hyclone, Logan, UT) and penicillin/streptomycin at 37°C in 5% CO_2 plus 100% humidity. For microscopy assays, glass coverslips were coated with type 1 collagen (Sigma-Aldrich, St. Louis, MO) and subsequently washed with sterile dH_20 and allowed to dry before plating cells.

Protein production, purification, and binding assays

Stable HEK293T cell lines were used for the production and purification of proteins as previously described [31]. Where indicated, proteins were deglycosylated through expression in CHOLec3.2.8.1 cell lines followed by purification and Endo H_f treatment according to the manufacturer's protocol (New England Biolabs, Ipswich, MA). To analyze binding, cells were incubated with indicated concentrations of purified protein diluted in DMEM-10 before fixation and subsequent immunofluorescent staining. Proteins were also spin-inoculated onto cells as described below, but high levels of background were usually obtained using this protocol. All proteins were produced using a GST-tag, and as such purified GST protein was produced as previously described [32] and included as a control in these experiments.

Linearization and transfection of plasmids

The full-length J6/JFH genotype 2a Cp7 (Cp7) and pGND (GND) constructs have been previously described [33]. The ΔE1E2 clone was constructed by performing an in-frame deletion of E1 and E2 (from nucleotide 943 to 2560) coding sequence in the Cp7 backbone using PCR deletion mutagenesis. 20 μg of plasmid DNA was linearized by 4 h digestion with XbaI followed by treatment with Mung Bean Nuclease for blunt end digestion (New England Biolabs, Ipswich, MA). Digested plasmids were subsequently extracted twice with 25:24:1 phenol:choroform:isoamyl alcohol pH 5.2 +/- 0.2 and once with chloroform, quantified by spectrophotometry, and 2 μg transcribed using a MEGAscript T7 High Yield RNA Transcription Kit (Ambion, Austin, TX). Transcribed RNA was purified again as above and quality/yield assessed by spectrophotometry and agarose gel electrophoresis. Cells were washed with PBS, trypsinized for 3 min, and counted using a haemocytometer. Cells were then spun at 1500 rpm for 5 min at 4°C followed by one additional wash with 50 ml ice cold PBS before resuspension at $2x10^7$ cells/ml in ice cold PBS. 10 μg of purified RNA was electroporated into $8x10^6$ cells with 5 pulses of 99 ms at 820 V over 1.1 s in an ECM 830 electroporator using a 2 mm-gap electroporation cuvette (BTX Genomics, Harvard Apparatus, Holliston, MA). Cells were resupsended in 30 ml DMEM-10, split equally between 3 p100 plates, and incubated at 37°C with 5% CO_2 and 100% relative humidity.

Concentration of viral supernatant

24 h following electroporation, supernatants were aspirated and cells washed once with PBS before readdition of media to eliminate dead cell carryover from transfection. Cells were monitored for growth daily, and split to p150 plates when ~90% confluent.

Supernatants were harvested either at time of split or at four days after plating, whichever came first, using a sterile 20 ml syringe followed by passage through a 0.22 μm filter and stored at -80°C. Cells were not passaged more than three times during this procedure to limit cell culture adaptive mutations. To concentrate HCVcc virus, supernatants were thawed at room temperature and layered on an 8 ml cushion of 20%(w/v) sucrose dissolved in TNE buffer (100mM NaCl; 10mM Tris-HCl, pH 8.0; 1mM EDTA). Virions were pelleted at 27000 rpm for 4 hours at 4ºC in a Beckman Coulter SW28 rotor and stored at -80ºC until further use. Titration of concentrated viral stocks was performed as previously described [34] by infection of naïve Huh-7.5 cells followed by immunohistochemical staining with anti-E2 2C1 monoclonal antibody (described below).

Standard and high-speed centrifugal infection of human hepatoma cells

Naïve Huh-7.5 cells were infected either using a standard infection protocol or a spin-inoculation protocol. For standard infection, naïve cells were plated at 10-20% confluency and allowed to rest for at least 8 h before aspiration of media and addition of viral inoculum to cover the monolayer. Infection proceeded at 37°C with 5% CO_2 and 100% relative humidity for at least 4 h before either addition of media or aspiration of inoculum and addition of media. For spin-inoculation, cells were plated at varying densities on collagen-coated coverslips (for microscopy) in a 24-well plate and allowed to rest overnight. Depending on the assay, cells were inoculated with virus or protein either at room temperature or at 4°C diluted in a volume of no less than 300 μl of DMEM or DMEM-10. Plates were spun at 2095xg (~3000 rpm) for one hour, inoculum removed and fresh media added before transferring to 37°C with 5% CO_2 and 100% relative

humidity. For T=0 timepoints, inoculum was removed, cells were washed once with PBS, and fixed by indicated method.

Antibodies and immunofluroescence staining

For microscopy experiments, cells bound to coverslips were washed once in PBS, fixed for 20 min at room temperature in a buffer containing 4% formaldehyde, 320 mM sucrose, and cytoskeleton buffer (10 mM 2-(*N*-morpholino)ethanesulfonic acid, pH 6.1, 138 mM KCl, 3 mM $MgCl_2$, and 2 mM EGTA in ddH_20), and permeabilized using 0.1%(v/v) Triton X-100 (Triton wash) in PBS. Cells were blocked with 4% BSA in Triton wash for 1 h at room temperature or overnight at 4°C and stained with primary antibody at 37°C with 5% CO_2 and 100% relative humidity. The following primary mouse monoclonal antibodies and concentrations were used: 1 μg/ml antibody to HVR1 region of E2 (2C1) (H. Scarborough, J. Whidby, J. Marcotrigiano, and A. Grakoui, unpublished results), 1 μg/ml antibody to NS5A (9E10) [11], and 1 μg/ml anti-GST (26H1) (Cell Signaling Technology, Danvers, MA). After extensive washing, primary antibody binding was detected using anti-mouse secondary antibodies from Jackson ImmunoResearch Laboratories. In several experiments, eE2, GST, and ovalbumin proteins were directly labeled using Invitrogen protein-labeling kits per manufacturer's instructions. Nuclei were stained using 1 μg/ml DAPI (Sigma, St. Louis, MO), and actin was labeled using 1 μg/ml phalloidin-AF488, 546, or 594 (Molecular Probes/Invitrogen, Carlsbad, CA). For endosomal labeling, cells were pre-incubated for 2 h with 10-100 μg/ml Rhodamine Green-conjugated dextran (10,000 MW lysine fixable) or 20 μg/ml AF568-labeled human transferrin (Molecular Probes/Invitrogen, Carlsbad, CA)

and maintained as such throughout each experiment. Endoplasmic reticulum was stained using an anti-protein disulfide isomerase (PDI) antibody (Clone RL90, Abcam, Cambridge, MA). Post-staining, coverslips were washed in ddH_20 and mounted using ProLong® Gold Antifade Reagent (Molecular Probes/Invitrogen, Carlsbad, CA). Immunohistochemical analysis was performed as previously described, using anti-E2 2C1 [33,34]. Briefly, naïve cells were infected with appropriate dilutions of concentrated virus or unconcentrated supernatants and incubated for 72 h before fixation with ice-cold methanol. Primary antibody binding was detected using a 1:5 dilution of ImmPRESS goat anti-mouse HRP-conjugated antibody, and developed using DAB substrate (Vector Laboratories, Burlingame, CA). Titers were determined by calculating the tissue culture infection dose at which 50% of wells were positive for E2 antigen [35].

Microscopy

Images were acquired in collaboration with Dr. Daniel Kalman and Ruth Napier using a scientific-grade cooled charge-coupled device (Cool-Snap HQ with ORCA-ER chip) on a multi-wavelength wide-field three-dimensional Zeiss 200M inverted microscopy system (Intelligent Imaging Innovations). Immunofluorescent samples were analyzed at room temperature using 40x N.A. 1.3, 63x N.A. 1.4, or 100x oil 1.4 lenses (Zeiss). Acquisition parameters used for all images under all conditions were identical on a given day. To deconvolve images, a standard Sedat filter set (Chroma) was employed and out-of-focus light was removed from successive 0.20 μm focal planes using a constrained iterative deconvolution algorithm [36]. For spin-inoculation experiments, HCV was visible immediately post-centrifugation and up to 4 h using anti-E2 2C1 and from 1-8 h using

anti-NS5A 9E10 as tightly clustered puncta measuring between 1.5-3 μm (2C1) or 2-4 μm (NS5A) in diameter. Where indicated, colocalization was assessed by coincidence of fluorescent staining in the FITC, Cy3, or Cy5 channels. To ensure signal overlap was real, multicolored fluorescent beads were used to calibrate microscope filters for coincidence of signals to within 1 pixel (100 nm using the 63X or 100X lenses). Quantitative measurements of infection or protein binding were performed using the DAPI channel to image hundreds of nuclei in random locations on coverslips followed by analysis using the MASK function in the Intelligent Imaging Innovations software package (see [37] for reference). Briefly, contrast and intensity levels were adjusted to equivalent levels for all images to be analyzed. Control images were then used to define a threshold of signal for all channels of interest whereby objects of greater or lesser intensity were excluded, and these MASK parameters were applied to all images to determine true positive signal. Experiments were performed multiple times, and representative images and data from a single experiment are displayed in the figures. In most quantitative experiments, >400 nuclei over at least 12 images were analyzed per condition, and data is graphed as average % positive nuclei per field imaged.

Preliminary Results

A method to visualize unmodified HCVcc early binding events

We established a system to directly visualize HCVcc at early timepoints in the infection process to gain a better understanding of how HCV is internalized in liver-derived cell lines. Initial attempts at labeling virions using lipophilic dyes were unsuccessful due to non-specific binding and high background, and as such infection events could not be followed in real time (data not shown). We overcame this difficulty by concentrating the HCVcc clone Cp7 using sucrose cushions and high-speed ultracentrifugation. Tissue culture infectious dose (TCID) was significantly increased as assessed by standard infection assays and immunohistochemistry (Figure 1A). However, standard infection using these concentrated viral stocks did not allow for fluorescent microscopy visualization of early HCVcc binding to Huh-7.5 cells (in less than 40 min), presumably due to slow kinetics of infectious particle contact (data not shown). To increase the probability of particle-cell contact, we added concentrated viral inoculum and spun cells at 3000 rpm for 1 h to bring all virions to the cell surface. We reduced the temperature to 4°C before and during spin-inoculation to equalize virion binding, and cells were washed extensively with PBS post-spin to eliminate weak binding interactions. HCVcc were visible immediately after this wash as tightly clustered punctate bodies of approximately 1.5-3 μm (1500-3000 nm) in diameter when stained with anti-E2 2C1 monoclonal antibody (Figure 1B, first panel). These puncta could be found up to 4 h post-infection using 2C1, at which point larger diffuse structures of >3 μm were found. Puncta could also be found using anti-NS5A 9E10 monoclonal antibody, but no sooner than 1 h post-infection (Figure 1B, second panel). HCVcc was simultaneously spun onto coverslips

alone and identical washes performed to ensure that punctate structures were associated with cells and not glass-bound (data not shown). Additionally, Z-stacking and deconvolution analysis suggested that at early timepoints puncta were found primarily at the cell surface and were associated with cytoskeletal proteins as demonstrated by actin "ruffling" (Figure 1C, Figure 2).

HCVcc early binding events are not affected by translation inhibition but are dependent on glycosylation status

To ensure that puncta visible at early timepoints were intact HCVcc particles and not partial virion components, Huh-7.5 cells were treated with 100 μg/ml cycloheximide, a potent inhibitor of translation, for 30 minutes prior to and following spin-inoculation. Anti-E2 2C1-stained puncta were able to bind to Huh-7.5 cells under these conditions, but infection did not progress further than 2 h, with no structures visible at 4 h post-infection (Figure 3, third panel). Conversely, no puncta were visible by anti-NS5A 9E10 staining at any timepoints with cycloheximide, consistent with the idea that incoming virions were able to bind in the presence of the drug but incoming HCV RNA was not translated and replication complexes failed to form (Figure 3, fourth panel). Pre-incubation of Huh-7.5 cells with decreasing amounts of heparin sodium potently inhibited HCVcc, with a dramatic decrease in focus forming units (FFUs) seen using as low as 0.0001 U at 24 h post-infection by immunohistochemistry (Supplementary Figure 4B, right panel). Similar inhibition was seen using heparin sodium to block purified eE2 protein binding to Huh-7.5 cells (Supplementary Figure 4B, left panel), indicating that glycosylation of E2 plays a key role in both HCVcc and eE2 protein binding to human

hepatoma cells. This observation was confirmed by quantitative microscopy and flow cytometry using a deglycosylated form of eE2 (Supplementary Figure 4A, C), and CD spectroscopy additionally revealed that deglycosylation of the protein results in a misfolded, non-native conformation (data not shown). Additional purified proteins containing fewer occupied glycosylation sites did not bind to liver-derived cell lines with the affinity of eE2, lending further support to the direct involvement of glycosylation in the virus-host receptor relationship (Supplementary Figure 4D).

HCVcc early binding events result in productive infection in Huh-7.5 cells and are dependent on CD81 expression

Due to limitations in immunohistochemical analysis and the kinetics of viral protein translation, TCID assays do not necessarily reflect complete viral populations within a given HCVcc stock. It is conceivable that *in vitro* infection models may produce defective particles that are unable to complete the viral life cycle and are not detectable by such assays, similar to *in vivo* quasispecies that are unfit for propagation or are outcompeted by more dominant variants. Because spin-inoculation allows us to examine early attachment events, we used quantitative measurements of fluorescent signal at various times during infection to determine whether a 1:1 ratio of particle binding to productive infection existed in our system. Random counting experiments proved that similar percentages of nuclei were associated with positive signal at early (time zero) and late (24 and 48 h) timepoints (Figure 4A). Furthermore, passaging viral inoculum to a set of naïve Huh-7.5 cells and re-spin-inoculating three times following the primary spin yielded equivalent numbers of infected cells in all passages (Figure 4B). This result was

confirmed in parallel using immunohistochemistry (data not shown). Interestingly, quantitative analysis revealed that low numbers of cells were positive at all timepoints analyzed, reflecting the stringency of washing conditions and potentially the nature of binding interactions post-spin-inoculation (Figure 3). Productive infectivity was dependent on CD81 expression as expected, although some very rare examples of anti-E2 2C1-stained puncta on HepG2 cells were found at early timepoints, suggesting that initial binding is not CD81 dependent (data not shown). It must be noted that our system does not track a viral particle in real time, and as such any correlations drawn between early and late timepoints are indirect and based on repetitive observation over several experiments.

In contrast to HCVcc, HCV eE2 protein binding was completely independent of CD81 expression, as demonstrated by quantitative analysis of HepG2 binding and anti-CD81 blocking (Supplementary Figure 3B, C). Additionally, large quantities of purified eE2 protein efficiently and rapidly bound to a large percentage of human hepatoma cells (between 15-30% depending on the experiment) without the aid of spin-inoculation, and were quickly endocytosed in transferrin- or dextran-labeled endosomal compartments (Supplementary Figure 1, 2B). HCV is known to be internalized in early but not late endosomes [24], but an association with these compartments using spin-inoculation and transferrin- or dextran-labeling methods has yet to be found.

Discussion and Future Directions

In this study, we have developed an efficient method for visualization of early HCVcc binding and entry in human hepatoma cell lines. Our approach differs from others in that our concentrated virion preparations are unmodified by lipophilic dyes or integrated fluorescent proteins such as GFP or YFP. This limits the chance for live cell phototoxicity, as well as replication defects that may be a side effect of foreign sequence integration in the full-length HCV genome. Such defects have been well characterized in different chimeric strains of HCVcc, and even constructs stably expressing the *Renilla* luciferase gene produce less infectious particles than the wild type parent sequence (G. Mateu and L. Uebelhoer, unpublished results). A peculiar feature of our spin-inoculation system is the identification of 1.5-3 μm punctate structures when staining cell-bound HCVcc virions with a mouse monoclonal antibody raised against purified eE2 protein (Figures 1-3). We originally hypothesized that these structures may have been an artifact caused by multiple E2-bound primary antibodies per virion coupled with secondary antibody signal amplification, as their size far exceeds the predicted size of ~50 nm for HCVcc [10]. However, titration of both primary and secondary detection antibodies yielded the same punctate structures, suggesting that sucrose concentration of HCVcc may increase clumping of virions by an unknown mechanism. It is also possible that our concentration method does not eliminate serum lipoproteins. HCV is know to associate with these molecules [38,39,40], and the clustered puncta seen under the microscope may be multiple virions clinging to one or several lipoproteins. Refinement of our concentration technique through manipulation of a sucrose density interface may yield higher titers of unclustered virions, allowing for more efficient single particle tracking. In

addition to this, ongoing experiments using micro-filter particle size exclusion will help to elucidate the role of these clustered structures during infection.

Bulk concentration and spin-inoculation have thus far yielded similar conclusions previously shown by several groups studying binding and entry: HCVcc infectivity is CD81-dependent [7,41], actin plays a pivotal role immediately post-binding [26], and glycosylation status of E2 is important for initial virion-cell attachment [18,19]. Our work with deglycosylated envelope glycoproteins and heparin-based binding inhibition lends strength to the hypothesis that both viral and cell surface sugar moieties are responsible for initial virion attachment and sequestration to facilitate subsequent tight-binding events. Interestingly, initial experiments comparing viral and non-viral protein binding to Huh-7.5 cells have demonstrated that HCV glycoproteins are unique in their specificity for liver-derived cell types (Supplementary Figure 4D, L. Uebelhoer unpublished data). We are currently working to selectively deglycosylate HCV eE2 as well as examining other viral glycoproteins to determine whether this specificity is a function of the number of proteoglycans, or of the position and orientation of these sugars. Elucidation of HCV-specific glycan-based binding motifs may allow for novel therapies targeting the initial weak attachment that subsequently propagates infection.

The role of specific cytoskeletal or cytoskeletal-associated proteins in HCV infection is not well known. Our lab and others have shown the link between actin and incoming virions to be unmistakable, with large percentages of imaged virions rearranging or even colocalizing with stress fibers (Figure 1D, Figure 2) [26]. Coller and colleagues have

begun to characterize the viral relationship with the host cortical actin cytoskeleton, showing that actin nucleation and transport are key determinants of infection. Our experiments are similar to Coller *et al*. in that we do not see a breakdown of actin stress fibers as has been previously reported in other viruses [42,43], nor an increase of these fibers during infection, as has been thought to happen in HCV [44]. We have yet to examine actin-associated proteins in our infectious system, and clathrin is a likely candidate for future experimentation. HCV is internalized via clathrin-coated pits, but the virus has yet to be visualized in such a structure. Using multiple different monoclonal antibodies to both the heavy and light chains of clathrin combined with sophisticated wide-field deconvolution microscopy in this system may allow us to tease out the stepwise interactions that occur between viral envelope glycoproteins and host mediators of nascent pit formation. Furthermore, higher resolution imaging and conformational prediction of viral proteins bound to clathrin structures may give clues as to how HCV structural proteins mediate endosomal fusion for genomic interjection in the cytoplasm.

Finally, this new system of concentration and spin-inoculation of HCVcc has begun to shed light on the capabilities of single or tightly clumping virions to facilitate infection. Our initial quantification experiments at early and late stages of infection suggest that every particle binding to a cell results in that cell becoming infected, a finding that is previously unreported in the literature. It must be noted that the main limitation of unlabeled concentrated virus is the inability to track infectious particles in real time, and although directly labeled single particle analysis is an active area of HCV research, there currently exists no HCVcc system to reliably track a virion up to its fusion event. As

such, any correlations between early and later timepoints must be indirectly measured through repeated observation and experimentation. The *in vitro* HCVcc model does not precisely mimic the complex hepatic environment, but it does allow for normalized infection and quantitative analysis that may validate predictive models of *in vivo* infected hepatocyte percentages. This in turn may lead to a better understanding of how individual or clustered hepatocytes transmit virus or are cleared by CD8+ T cells *in vivo*, and could have important implications in the development of novel, liver-targeted therapies.

Figures

Figure 1

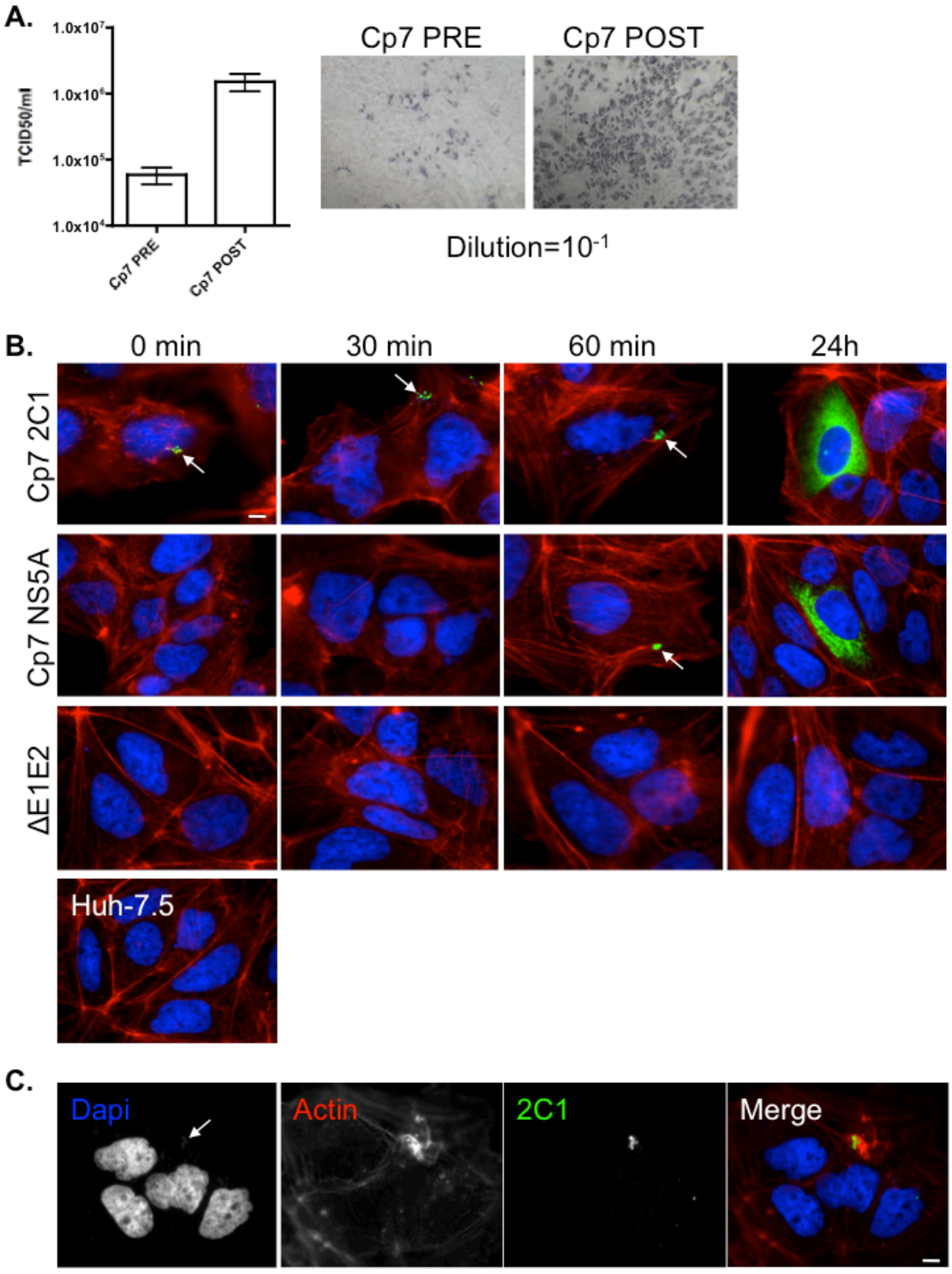

Figure 2

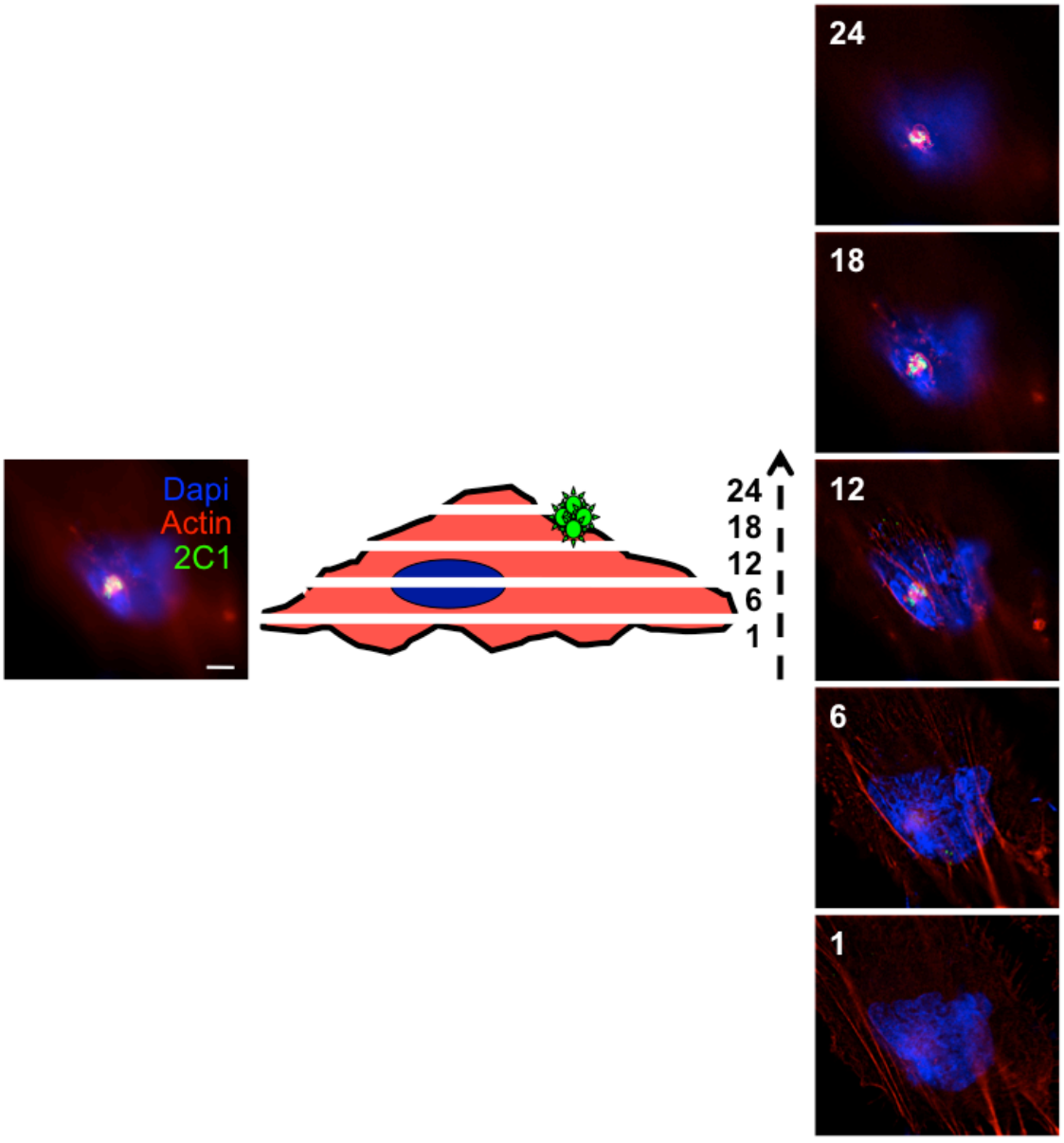

Figure 3

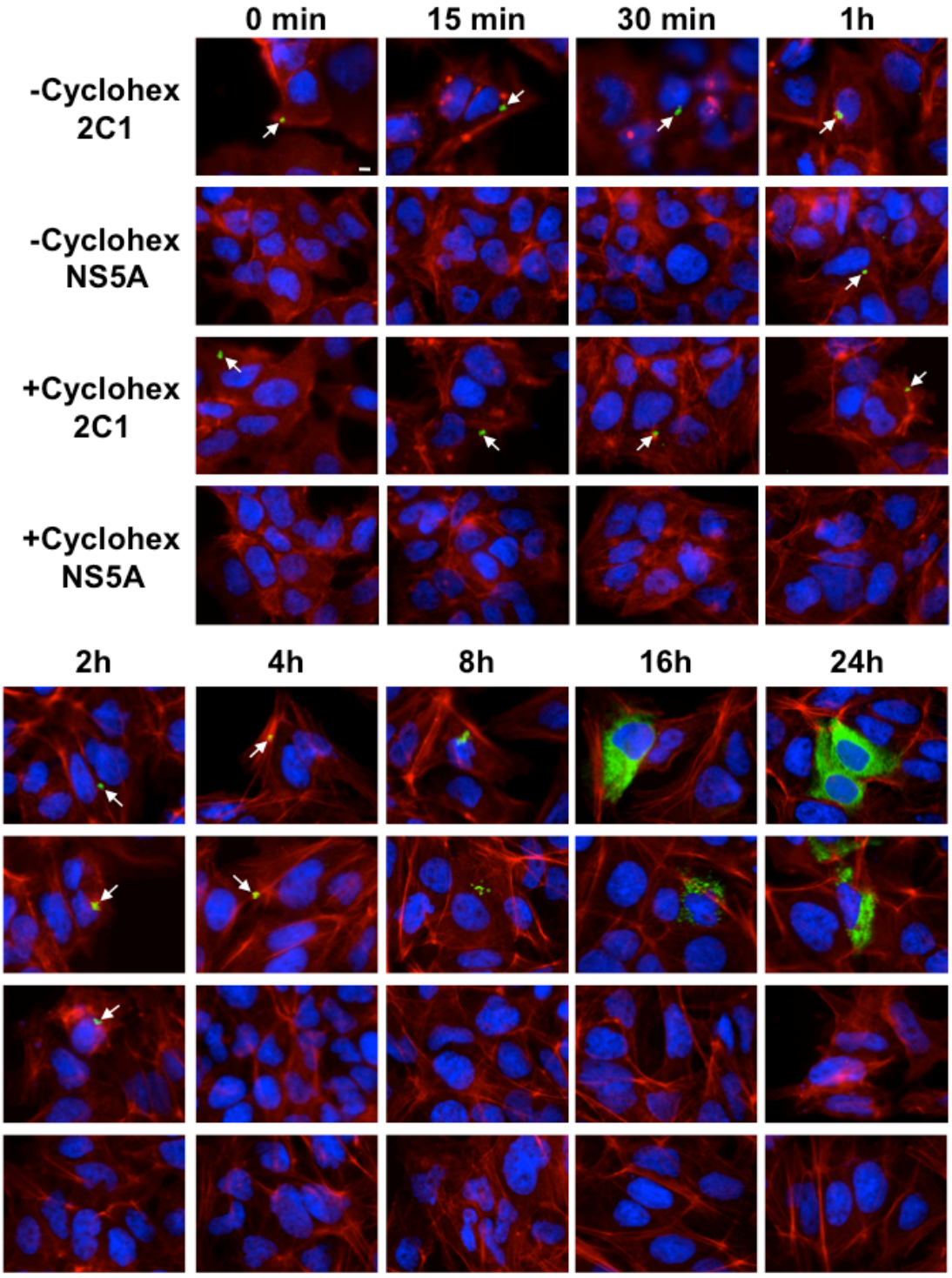
0 min
15 min
30 min
1h
-Cyclohex 2C1
-Cyclohex NS5A
+Cyclohex 2C1
+Cyclohex NS5A
2h
4h
8h
16h
24h

Figure 4

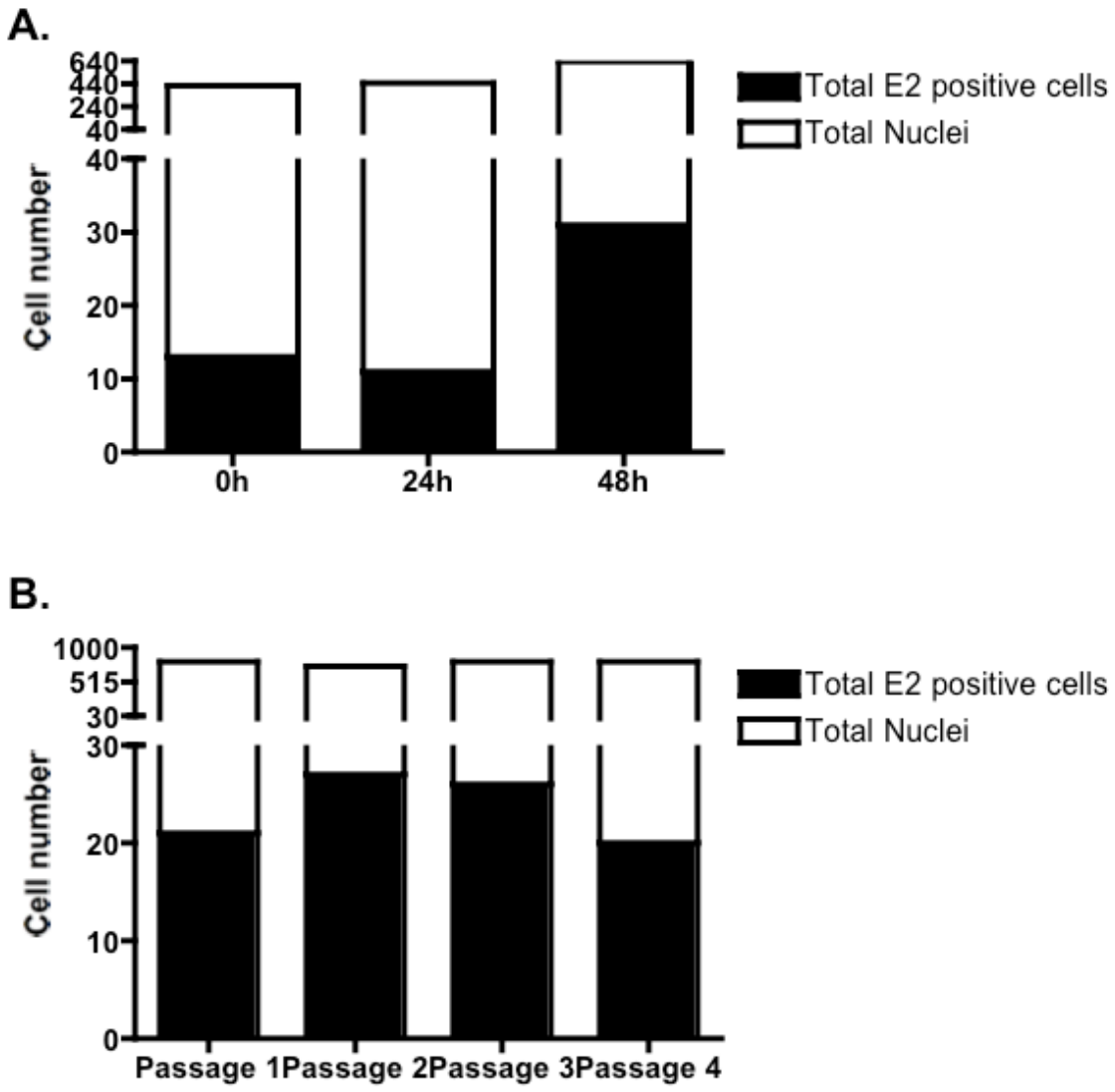
A.
640
440
240
40
40
30
20
10
0
Cell number
0h
24h
48h
Total E2 positive cells
Total Nuclei
B.
1000
515
30
30
20
10
0
Cell number
Passage 1
Passage 2
Passage 3
Passage 4
Total E2 positive cells
Total Nuclei

Supplementary Figure 1

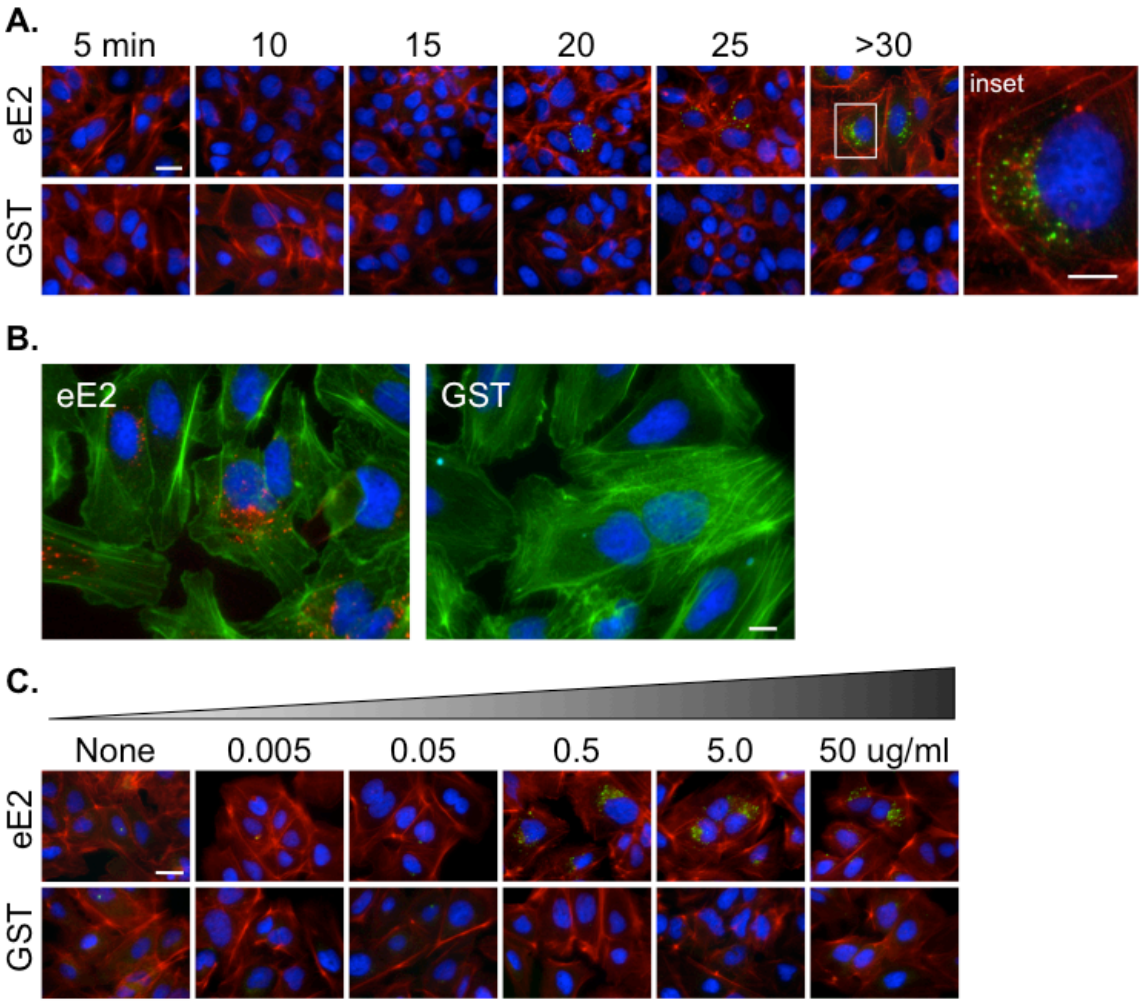

Supplementary Figure 2

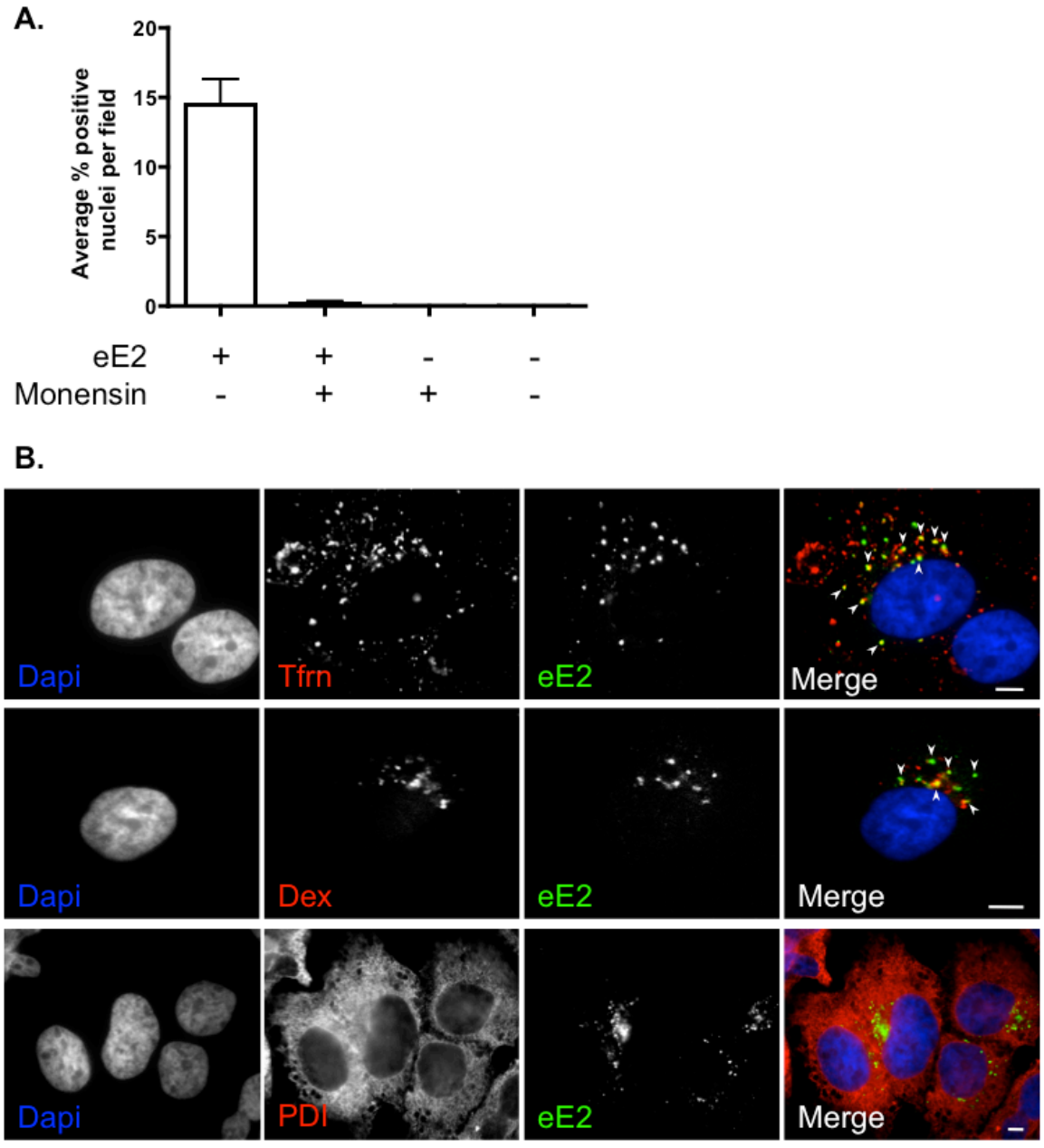

Supplementary Figure 3

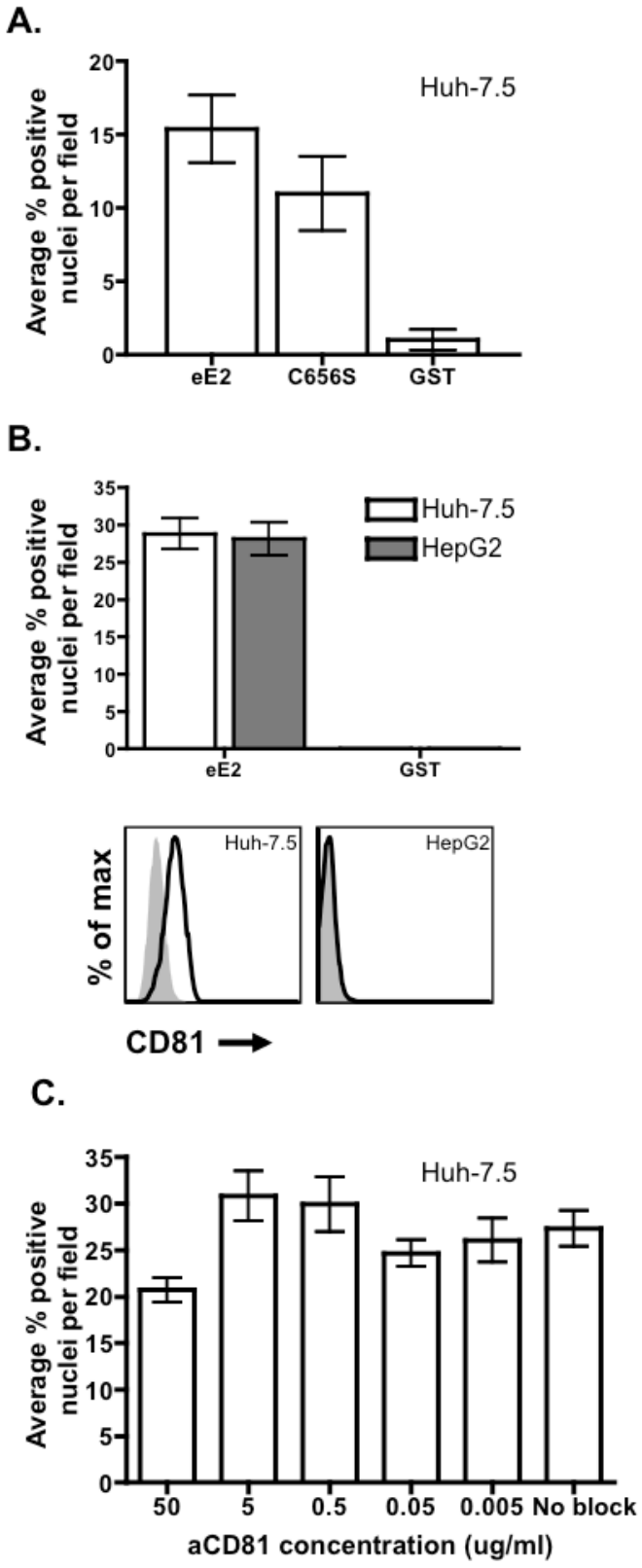

Supplementary Figure 4

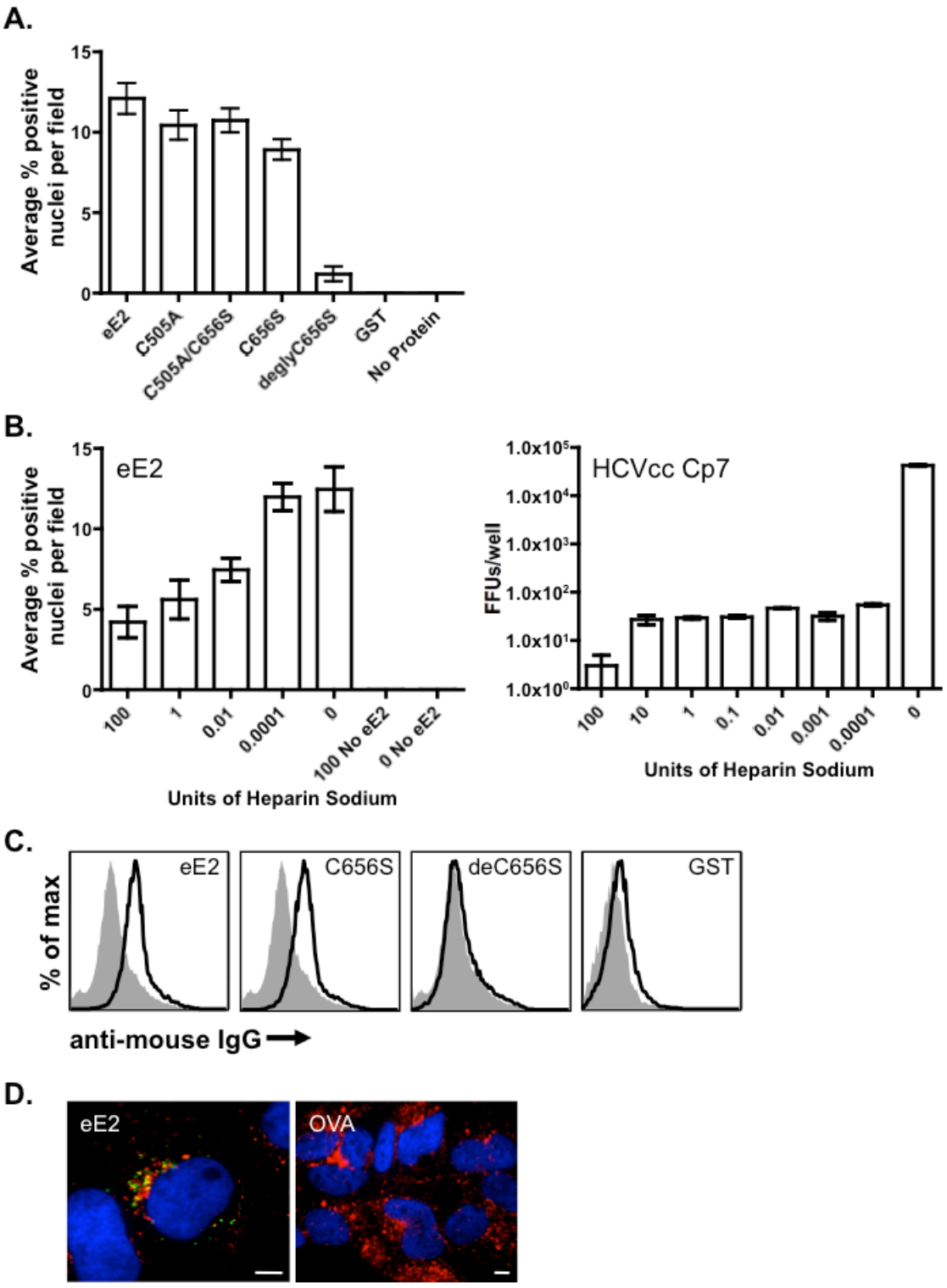

Figure Legends

Figure 1. HCVcc concentration and spin-inoculation in Huh-7.5 cells. (A) 300-fold concentration of supernatants from cells transfected with Cp7 full-length RNA. The average pre- and post-TCID50/ml of three separate concentration experiments is shown at left using anti-E2 2C1 monoclonal antibody to detect infected cells, with representative 10x images at right. (B) Concentrated Cp7 (TCID50/ml M.O.I. of 0.5) was spin-inoculated onto Huh-7.5 cells at 4ºC, washed with PBS, and infection allowed to proceed for 24 h at 37ºC. Arrows indicate punctate structures staining positive for indicated antigens. NS5A staining was never observed before 60 min post-infection. The "ΔE1E2" panel is representative of cells stained for either 2C1 or NS5A following spin-inoculation of this virus, and "Huh-7.5" is a no-inoculum control. (C) Representative image demonstrating "actin ruffling" in Huh-7.5 cells 4 h post-infection with concentrated Cp7. Individual channels are represented in black and white, with merged image at right. Note DAPI co-staining with anti-E2 2C1 antibody (white arrow), indicative of a replication complex. In both (B) and (C), white bar indicates a 3 μm scale, and staining is as follows: blue=DAPI, red=phalloidin-labeled actin, green=antibodies to HCV antigens.

Figure 2. Concentrated HCVcc can be found at early timepoints bound to the apical surface of human hepatoma cells. Huh-7.5 cells were spin-inoculated with concentrated Cp7 virus, fixed, and stained for indicated antigen. At left is a standard 2D confocal image with Cp7 puncta in focus. The same field was then imaged using 30 successive 0.2 μm focal planes and deconvolved as indicated in the center diagram (see Materials and Methods for details). At right are select images from the deconvolution analysis

labeled with the corresponding focal plane, with "0" being out of focus below all channels and "30" being out of focus above all channels. White bar indicates a 3 μm scale, and staining is as follows: blue=DAPI, red=phalloidin-labeled actin, green=antibodies to HCV antigens.

Figure 3. Concentrated HCVcc binds to Huh-7.5 cells in the presence of a protein translation inhibitor, but is unable to establish productive infection. Huh-7.5 cells were pre-incubated with 100 μg/ml cycloheximide, spin-inoculated at 4ºC with a Cp7 TCID50/ml M.O.I. of 0.5, washed with PBS, and infection allowed to proceed for 24 h at 37ºC. Arrows indicate punctate structures staining positive for indicated antigens with or without cycloheximide. NS5A-stained structures visible after 1 h are established replication complexes. White bar indicates a 3 μm scale, and staining is as follows: blue=DAPI, red=phalloidin-labeled actin, green=antibodies to HCV antigens.

Figure 4. Quantitative measurement of HCVcc fluorescence after spin-inoculation of Huh-7.5 cells. (A) Huh-7.5 cells were cooled to 4ºC and spin-inoculated with a TCID50/ml M.O.I. of 1. Post-spin-inoculation, cells were washed extensively with PBS and either fixed or allowed to incubate for the indicated times before fixation and staining with anti-E2 2C1. Random images were acquired and normalized using a MASK function to detect true positive signal per nuclei examined. Black bars indicate total Huh-7.5 nuclei staining positive for E2, and are inset on white bars depicting total number of nuclei counted. Data is representative of two separate experiments. (B) Huh-7.5 cells were cooled and spin-inoculated as in (A), but supernatants were passed to a new set of

naïve cells three successive times following initial infection. Regardless of the supernatant passage, cells were washed extensively with PBS and allowed to incubate for 24 h before fixation, staining, and counting as above.

Supplementary Figure 1. Binding kinetics of purified recombinant eE2 protein to Huh-7.5 cells. (A) Cells were plated overnight and media aspirated before addition of 2.5 μg/ml purified recombinant eE2 diluted in fresh media. Cells were allowed to incubate at 37ºC for indicated times before fixation and staining with anti-E2 2C1 for microscopy analysis. Purified GST was included in parallel as a control and stained using anti-GST and equivalent secondary antibodies. White bar at 0 min depicts 25 μm scale. White box at >30 depicts "inset" zoom, with a 10 μm scale bar. Representative images are displayed, and staining is as follows: blue=DAPI, red=phalloidin-labeled actin, green=antibodies to eE2 or GST. (B) The same experiment was performed as in (A), but eE2 and GST were directly labeled with AF647 dye prior to incubation. Representative images from 1 h post-incubation are displayed, white bar depicts 10 μm scale, and staining is as follows: blue=DAPI, green=phalloidin-labeled actin, red=AF647-labeled eE2 or GST. (C) Huh-7.5 cells were incubated with decreasing amounts of purified eE2 or GST for 1 h to determine effective binding concentrations. White bar depicts 25 μm scale, and staining method is identical to (A).

Supplementary Figure 2. Purified recombinant eE2 protein internalization in Huh-7.5 cells is dependent on endosomal trafficking but is not shuttled to the endoplasmic reticulum. (A) Huh-7.5 cells were pre-incubated with the protein transport

inhibitor BD Golgistop™ (containing monensin) diluted in media for 4 h before incubation with 2.5 μg/ml eE2. Cells were fixed at 1 h post-incubation and stained for eE2 before quantitative analysis. Data depicts average number of nuclei with positive signal in a field, with twelve fields analyzed per condition. (B) Huh-7.5 cells were serum-starved overnight in DMEM and subsequently incubated with a molar excess of either Rhodamine-green-conjugated 10000 MW dextran or AF568-conjugated human holo-transferrin for 2 h prior to eE2 binding. PDI staining for endoplasmic reticulum was carried out during secondary antibody step. Individual channels are represented in black and white, with merged image at right. Staining was visualized in the following channels; Tfrn=transferrin (Cy3, red), Dex=dextran (Cy3, red), PDI=protein disulfide isomerase (Cy3, red), eE2=2C1 stain or directly-conjugated eE2 (FITC, green). White arrows indicate coincidence of fluorescent signal in the Cy3 and FITC channels to within a pixel (100 nm). White bars depict 5 μm scale for all images.

Supplementary Figure 3. eE2 binding and internalization in Huh-7.5 cells is not dependent on CD81 expression. (A) Huh-7.5 cells were incubated with eE2, eE2 in which the carboxy-terminal cysteine had been substituted for serine (C656S), and GST for 1 h before fixation, staining with 2C1, and quantitative analysis. Data is representative of more than four independent experiments. (B) eE2 and GST binding were quantified in Huh-7.5 cells and HepG2 cells. Lower panel, flow cytometry analysis of CD81 surface expression Huh-7.5 and HepG2 cells. (C) Huh-7.5 cells were pre-incubated with decreasing concentrations of purified CD81 for 1 h prior to eE2 binding and

quantification. In all quantification experiments, signal from >300 nuclei were averaged across >12 images per condition.

Supplementary Figure 4. Binding of eE2 and HCVcc to Huh-7.5 cells is dependent on glycosylation. (A) Huh-7.5 cells were incubated with indicated purified proteins for 1 h before fixation and quantification using anti-E2 2C1. "C505A" is a form of eE2 in which the 6th cysteine from the amino-terminus has been replaced with alanine, "C505A/C656S" eE2 contains this mutation along with the previously mentioned carboxy-terminal serine mutation, and "deglyC656S" is a deglycosylated form of C656S produced in ChoLec3.2.8.1 and treated with Endo H_f. >500 nuclei were quantified for positive signal across 15 images per condition. (B) Decreasing concentrations of Heparin Sodium were added to Huh-7.5 cells, and purified eE2 was allowed to bind for 1 h before fixation and quantification (left panel, eE2). This experiment was performed in parallel with 100 TCID50/ml concentrated Cp7, and cells were infected for 72 h before methanol-fixation and quantification of focus forming units (FFUs) by immunohistochemistry (right panel, HCVcc Cp7). In both cases cells were detected using anti-eE2 2C1, and for eE2 binding, >400 nuclei were quantified for positive signal across 12 images per condition. (C) $5x10^5$ Huh-7.5 cells were trypsinized, washed, and incubated with 5 μg/ml of the indicated purified proteins for 30 min at room temperature. After binding, cells were fixed using a non-permeabilizing solution, stained with anti-E2 2C1, and analyzed by flow cytometry using a secondary anti-mouse IgG-FITC antibody. Data are displayed as % of max, and grey histograms represent control Huh-7.5 cells incubated in FACS buffer and stained with 2C1 and secondary antibody. (D) Huh-7.5 cells were serum-

starved for 24 h, labeled for 2 h with a molar excess of AF568-conjugated human holo-transferrin, and incubated with titrations of either eE2 or ovalbumin-FITC for 1 h. eE2 was detected using 2C1 and secondary antibody (left image), while ovalbumin was viewed directly in the FITC channel (right image). Representative images of 5 μg/ml purified protein are shown, and arrows depict coincidence of fluorescence within 100 nm as in Supplemental Figure 2. White scale bars depict 5 and 25 μm scale for eE2 and OVA, respectively.

References

1. Shepard CW, Finelli L, Alter MJ (2005) Global epidemiology of hepatitis C virus infection. Lancet Infect Dis 5: 558-567.

2. Lindenbach BD, Thiel, H.-J., and Rice, C.M. (2007) Flaviviridae: the viruses and their replication. Fields Virology 5th Ed.: 1101-1152.

3. Lindenbach BD, Rice CM (2005) Unravelling hepatitis C virus replication from genome to function. Nature 436: 933-938.

4. Michalak JP, Wychowski C, Choukhi A, Meunier JC, Ung S, et al. (1997) Characterization of truncated forms of hepatitis C virus glycoproteins. J Gen Virol 78 (Pt 9): 2299-2306.

5. Flint M, Maidens C, Loomis-Price LD, Shotton C, Dubuisson J, et al. (1999) Characterization of hepatitis C virus E2 glycoprotein interaction with a putative cellular receptor, CD81. J Virol 73: 6235-6244.

6. Scarselli E, Ansuini H, Cerino R, Roccasecca RM, Acali S, et al. (2002) The human scavenger receptor class B type I is a novel candidate receptor for the hepatitis C virus. EMBO J 21: 5017-5025.

7. Pileri P, Uematsu Y, Campagnoli S, Galli G, Falugi F, et al. (1998) Binding of hepatitis C virus to CD81. Science 282: 938-941.

8. Bartosch B, Dubuisson J, Cosset FL (2003) Infectious hepatitis C virus pseudo-particles containing functional E1-E2 envelope protein complexes. J Exp Med 197: 633-642.

9. Hsu M, Zhang J, Flint M, Logvinoff C, Cheng-Mayer C, et al. (2003) Hepatitis C virus glycoproteins mediate pH-dependent cell entry of pseudotyped retroviral particles. Proc Natl Acad Sci U S A 100: 7271-7276.

10. Wakita T, Pietschmann T, Kato T, Date T, Miyamoto M, et al. (2005) Production of infectious hepatitis C virus in tissue culture from a cloned viral genome. Nat Med 11: 791-796.

11. Lindenbach BD, Evans MJ, Syder AJ, Wolk B, Tellinghuisen TL, et al. (2005) Complete replication of hepatitis C virus in cell culture. Science 309: 623-626.

12. Zhong J, Gastaminza P, Cheng G, Kapadia S, Kato T, et al. (2005) Robust hepatitis C virus infection *in vitro*. Proc Natl Acad Sci U S A 102: 9294-9299.

13. Germi R, Crance JM, Garin D, Guimet J, Lortat-Jacob H, et al. (2002) Cellular glycosaminoglycans and low density lipoprotein receptor are involved in hepatitis C virus adsorption. J Med Virol 68: 206-215.

14. Agnello V, Abel G (1997) Localization of hepatitis C virus in cutaneous vasculitic lesions in patients with type II cryoglobulinemia. Arthritis Rheum 40: 2007-2015.

15. Monazahian M, Bohme I, Bonk S, Koch A, Scholz C, et al. (1999) Low density lipoprotein receptor as a candidate receptor for hepatitis C virus. J Med Virol 57: 223-229.

16. Agnello V, Abel G, Elfahal M, Knight GB, Zhang QX (1999) Hepatitis C virus and other flaviviridae viruses enter cells via low density lipoprotein receptor. Proc Natl Acad Sci U S A 96: 12766-12771.

17. Molina S, Castet V, Fournier-Wirth C, Pichard-Garcia L, Avner R, et al. (2007) The low-density lipoprotein receptor plays a role in the infection of primary human hepatocytes by hepatitis C virus. J Hepatol 46: 411-419.

18. Barth H, Schafer C, Adah MI, Zhang F, Linhardt RJ, et al. (2003) Cellular binding of hepatitis C virus envelope glycoprotein E2 requires cell surface heparan sulfate. J Biol Chem 278: 41003-41012.

19. Barth H, Schnober EK, Zhang F, Linhardt RJ, Depla E, et al. (2006) Viral and cellular determinants of the hepatitis C virus envelope-heparan sulfate interaction. J Virol 80: 10579-10590.

20. Evans MJ, von Hahn T, Tscherne DM, Syder AJ, Panis M, et al. (2007) Claudin-1 is a hepatitis C virus co-receptor required for a late step in entry. Nature 446: 801-805.

21. Liu S, Yang W, Shen L, Turner JR, Coyne CB, et al. (2009) Tight junction proteins claudin-1 and occludin control hepatitis C virus entry and are downregulated during infection to prevent superinfection. J Virol 83: 2011-2014.

22. Ploss A, Evans MJ, Gaysinskaya VA, Panis M, You H, et al. (2009) Human occludin is a hepatitis C virus entry factor required for infection of mouse cells. Nature 457: 882-886.

23. Blanchard E, Belouzard S, Goueslain L, Wakita T, Dubuisson J, et al. (2006) Hepatitis C virus entry depends on clathrin-mediated endocytosis. J Virol 80: 6964-6972.

24. Meertens L, Bertaux C, Dragic T (2006) Hepatitis C virus entry requires a critical postinternalization step and delivery to early endosomes via clathrin-coated vesicles. J Virol 80: 11571-11578.

25. Codran A, Royer C, Jaeck D, Bastien-Valle M, Baumert TF, et al. (2006) Entry of hepatitis C virus pseudotypes into primary human hepatocytes by clathrin-dependent endocytosis. J Gen Virol 87: 2583-2593.

26. Coller KE, Berger KL, Heaton NS, Cooper JD, Yoon R, et al. (2009) RNA interference and single particle tracking analysis of hepatitis C virus endocytosis. PLoS Pathog 5: e1000702.

27. Mee CJ, Grove J, Harris HJ, Hu K, Balfe P, et al. (2008) Effect of cell polarization on hepatitis C virus entry. J Virol 82: 461-470.

28. Mee CJ, Harris HJ, Farquhar MJ, Wilson G, Reynolds G, et al. (2009) Polarization restricts hepatitis C virus entry into HepG2 hepatoma cells. J Virol 83: 6211-6221.

29. Pal S, Shuhart MC, Thomassen L, Emerson SS, Su T, et al. (2006) Intrahepatic hepatitis C virus replication correlates with chronic hepatitis C disease severity *in vivo*. J Virol 80: 2280-2290.

30. Timpe JM, Stamataki Z, Jennings A, Hu K, Farquhar MJ, et al. (2008) Hepatitis C virus cell-cell transmission in hepatoma cells in the presence of neutralizing antibodies. Hepatology 47: 17-24.

31. Whidby J, Mateu G, Scarborough H, Demeler B, Grakoui A, et al. (2009) Blocking hepatitis C virus infection with recombinant form of envelope protein 2 ectodomain. J Virol 83: 11078-11089.

32. Flint M, von Hahn T, Zhang J, Farquhar M, Jones CT, et al. (2006) Diverse CD81 proteins support hepatitis C virus infection. J Virol 80: 11331-11342.

33. Mateu G, Donis RO, Wakita T, Bukh J, Grakoui A (2008) Intragenotypic JFH1 based recombinant hepatitis C virus produces high levels of infectious particles but causes increased cell death. Virology 376: 397-407.

34. Uebelhoer L, Han JH, Callendret B, Mateu G, Shoukry NH, et al. (2008) Stable cytotoxic T cell escape mutation in hepatitis C virus is linked to maintenance of viral fitness. PLoS Pathog 4: e1000143.

35. Reed LJ, Muench, H. (1938) A simple method of estimating fifty percent endpoints. American Journal of Hygiene 27: 493-497.

36. Swedlow JR, Sedat, J. W., and Agard, D. A. (1997) Deconvolution in Optical Microscopy. Deconvolution of Images and Spectra: 284-307.

37. Swimm AI, Kalman D (2008) Cytosolic extract induces Tir translocation and pedestals in EPEC-infected red blood cells. PLoS Pathog 4: e4.

38. Bartosch B, Verney G, Dreux M, Donot P, Morice Y, et al. (2005) An interplay between hypervariable region 1 of the hepatitis C virus E2 glycoprotein, the scavenger receptor BI, and high-density lipoprotein promotes both enhancement of infection and protection against neutralizing antibodies. J Virol 79: 8217-8229.

39. Voisset C, Callens N, Blanchard E, Op De Beeck A, Dubuisson J, et al. (2005) High density lipoproteins facilitate hepatitis C virus entry through the scavenger receptor class B type I. J Biol Chem 280: 7793-7799.

40. Voisset C, Op de Beeck A, Horellou P, Dreux M, Gustot T, et al. (2006) High-density lipoproteins reduce the neutralizing effect of hepatitis C virus (HCV)-infected patient antibodies by promoting HCV entry. J Gen Virol 87: 2577-2581.

41. Bartosch B, Vitelli A, Granier C, Goujon C, Dubuisson J, et al. (2003) Cell entry of hepatitis C virus requires a set of co-receptors that include the CD81 tetraspanin and the SR-B1 scavenger receptor. J Biol Chem 278: 41624-41630.

42. Pelkmans L, Puntener D, Helenius A (2002) Local actin polymerization and dynamin recruitment in SV40-induced internalization of caveolae. Science 296: 535-539.

43. Van Minnebruggen G, Van de Walle GR, Favoreel HW, Nauwynck HJ, Pensaert MB (2002) Temporary disturbance of actin stress fibers in swine kidney cells during pseudorabies virus infection. Vet Microbiol 86: 89-94.

44. Brazzoli M, Bianchi A, Filippini S, Weiner A, Zhu Q, et al. (2008) CD81 is a central regulator of cellular events required for hepatitis C virus infection of human hepatocytes. J Virol 82: 8316-8329.

CHAPTER 5

A novel recombinant chimeric antibody system to deliver CD4+ T cell epitopes to naïve B cells during chronic infection

Luke Uebelhoer[1], Brian Norris[1], Robert Mittler[1], Elin Lunde[2,3], Inger Sandlie[2,3], Holly Hanson[1], and Arash Grakoui[1*]

[1]Department of Medicine, Division of Infectious Diseases, Microbiology and Immunology, Emory Vaccine Center, Emory University School of Medicine, Atlanta, GA 30329; [2]Center for Immune Regulation and [3]Department of Molecular Biosciences, University of Oslo, Oslo 0316, Norway; *Corresponding author

This chapter consists of a manuscript that is currently in preparation for submission.

Abstract

The immune system relies on the interaction between professional antigen presenting cells (APC) such as dendritic cells, macrophages, or B cells and CD4+ T cells to efficiently control many types of pathogens. Much is known about the APC-T cell interaction in the context of dendritic cells and macrophages, but the interaction of naïve B cells with CD4+ T cells is less well understood. In this study we sought to facilitate this critical interaction by maximizing viral antigen delivery to B cells to further define their role as an APC subset. To this end, we developed recombinant anti-IgD antibody molecules (rAb) with an embedded immunogenic lymphocytic choriomeningitis virus (LCMV) -derived epitope that can be processed and presented by naïve B cells to responding CD4+ T cells. We demonstrate that these rAbs efficiently target naïve B cells, that efficient processing and presentation of the embedded epitope occurs, and that antigen-specific CD4+ T cells are stimulated to proliferate both *in vitro* and *in vivo*. Furthermore, we examine the phenotypes of both B cells and T cells targeted by this approach, and show that exogenous costimulation is necessary in the context of naïve B cells and rAb to drive antigen-specific CD4+ T cells to complete activation. These findings suggest that CD4+ T cell priming by naïve B cells through surface IgD-targeting is inadequate, resulting in short-lived effector T cells with poor memory potential. This approach has applications both in basic immunological study and in the development of potential vaccine candidates.

Introduction

CD4+ T cells are able to stimulate both humoral and cellular immunity through cytokine-driven responses, making them critical players in the host immune response [1]. This stimulation occurs after CD4+ T cell recognition of antigen presented by dendritic cells, macrophages, or B lymphoctyes. These three cell types, known as professional antigen presenting cells (APC), endocytose large antigenic peptides which undergo proteolytic breakdown by endosomal-associated enzymes. After initial processing, APCs are able to display short, antigenic peptide sequences bound to major histocompatibility (MHC) class II molecules on their cell surface which are later recognized by antigen-specific CD4+ T cells. Although dendritic cells are the only APC solely responsible for antigen presentation, both macrophages and B cells have been shown to be necessary for cell-mediated and humoral immunity. While dendritic cells have been shown to be potent activators of T cells, driving them to differentiate into TH1, TH2, TH17, or Treg cells [2], the fate of CD4+ T cells upon interaction with antigen-presenting B cells has not been well-defined. Initial work demonstrated that B cells could present antigen to T cell clones or hybridoma lines [3,4,5,6]. Fractionation experiments refined this hypothesis, suggesting that only highly activated “large” B cells were able to efficiently present antigen to clonal T cell lines [7,8]. Following these studies, adoptive transfers of APCs modified this idea by showing that only previously primed T cells were able to be stimulated by resting (naïve) B cells, and that initial priming of a naïve T cell by a naïve B cell resulted in T cell tolerance [9,10,11]. Interestingly, a study using small numbers of adoptively transferred transgenic T cells followed by adoptively transferred naïve or tolerant B cell receptor (BCR) transgenic B cells demonstrated that antigen-specific B

cells can efficiently activate rare T cell populations [12]. However, this study also demonstrated that all T cells activated in this manner possess a default mechanism for abortive proliferation, raising the question of whether B cells can sustain a prolonged, functional T cell response. More recent work using the Bpep IgG2a^{b} transgenic mouse model demonstrated that persistence of antigen presentation by B cells was a major determining factor in peripheral T cell tolerance, regardless of B cell activation state [13,14]. Taken together, the data suggest that B cells are efficient activators of T cells, but the long-term potential of these T cells is acutely dependent on the status of the B cell at time of activation.

In recent years, the targeting of antigen to specific molecules on antigen presenting cells has been utilized as a novel method to study APC-T cell interactions. Such targeting has been shown to augment the immune response by enhancement of peptide loading onto MHC class II molecules and stimulation of target CD4+ cells [15]. Immunoglobulin, or antibody, (Ig, Ab) molecules in particular have provided an attractive choice for antigen-targeting due to their long half-life and ability to be internalized via Fc or other receptors on APCs [16]. Initial targeting approaches employed antibodies or carrier proteins specific to APC surface molecules that were chemically conjugated to antigens of interest, and were shown to increase presentation and T cell activation [17,18,19,20,21]. However, these approaches suffered from limitations such as numbers of antigens able to complex with a single antibody, impaired serum half-life of complexes, and weak tissue penetration due to size exclusion. More recently, recombinant antibodies have been developed that genetically incorporate antigenic sequences into their tertiary structures

[22]. The complementarity determining regions (CDR) of Igs are loops that connect the various beta strands of these molecules, and are surprisingly plastic in their ability to accommodate foreign sequences without altering native Ab structure [23]. Several groups have shown that insertion of foreign peptides into these heavy chain regions resulted in efficient processing and presentation by APCs, and in some cases a 100-1000 fold increase in T cell activation both *in vitro* and *in vivo* over free synthetic peptide [16,24,25,26,27,28]. Additionally, sequences for these recombinant Abs (termed "troybodies", referred to here as "rAbs") can be cloned into expression cassettes, allowing for rapid epitope insertion mutations of the heavy chain and simultaneous expression of both light and heavy chains in permissive cells [29]. However, studies employing rAbs as antigen delivery vehicles have yet to assess their long-term effect on responding T cells, and whether such a strategy creates long-lived memory T cells or instead invokes a pathway of abortive proliferation.

In this study, we created rAb molecules with embedded antigen from lymphocytic choriomeningitis virus (LCMV) and variable regions that target IgD surface molecules on B cells to eliminate the possibility of passive uptake and examine the potential of specifically-targeted naïve B cells to activate small populations of CD4+ T cells. Using these rAb molecules, we determine the efficiency of B cell antigen presentation to both a T cell hybridoma and, more relevantly, non-immortalized murine CD4+ T cells. We further define the status of these B cells upon rAb targeting, as well as the phenotype and proliferative potential of responding CD4+ T cells upon stimulation. Taken together, the data suggest that CD4+ T cells primed by rAb-targeted naïve B cells differentiate into

short-lived effector cells that are rapidly cleared by either functional inactivation or activation-induced cell death.

Materials and methods

Plasmids, primers, and peptides

The pLNOH2 (heavy chain) and pLNOκ (light chain) vectors were a kind gift from Dr. Elin Lunde and Dr. Inger Sandlie, and have been previously described as expression vectors for human immunoglobulin G subclass 3 (hIgG3) heavy and light chains containing a variable region specific for the IgD antigen receptor on the surface of naïve B cells [25,28]. To incorporate our embedded epitope, PCR was performed using two opposing inner oligos with non-annealing overlapping tails containing the GP61-80 LCMV CD4+ T cell epitope and two outer oligos facing inward (MWG Biotech, High Point, NC) to mutagenize the 0.9kb region containing the hIgG3 heavy chain of pLNOH2. These specific primers were:

5'-outer cctcaggtgagttaacgtacg;

5'-inner attg**gtatac**tcctttgtaaatgtcgggtcccttaagaccgtgattcacgttgcaggtgt;

3'-outer ggaggtgtgtcacaagatttg;

3'-inner ttacaaagga**gtatac**caatttaagtcagtggagtttgataccaaggtggacaagagagt

(GP61-80 epitope underlined, silent site BstZ17I bold). The 0.9kb fragment was excised and cloned into a pUC19 shuttle vector to be sequenced for proper orientation (Macrogen, Korea). Recombinant LCMV GP61-80 peptide (GLKGPDIYKGVYQFKSVEFD) was obtained from Genmed Synthesis Inc. (San Francisco, CA), and prepared at a stock concentration of 2 mg/ml. Recombinant GP33-41 (KAVYNFATM), GP276-286 (SGVENPGGYCL), NP309-328 (SGEGWPYIACRTSVVGRAWE) and NP396-404 (FQPQNGQFI) peptides were obtained from the microchemical facility at Emory University, Atlanta, GA. These

peptides were stored at 1 mg/ml stock concentration. The original cysteine residue at position 41 in GP33-41 was modified to a methionine to prevent dimer formation.

Transfection and generation of crude rAb supernatant

The mutated pLNOH2 vector was cotransfected with pLNOκ as follows. 2 μg of each vector was transfected simultaneously, or the hIgG light chain was cloned into mutated pLNOH2 downstream of the CMV promoter to drive expression of both chains on one vector, and then transfected. NSO cells were cultured in RPMI (Cambrex, Biowhittaker) with 5% Low IgG FCS and 1% L-glutamine (Hyclone, Logan, UT) until ~80% confluent. $2x10^6$ cells per reaction were harvested, electroporated following the AMAXA T-27 protocol (AMAXA, Gaithersburg, MD), and allowed to rest for one day before selection with 0.5 mg/ml G418 (Mediatech, Herndon, VA). Surviving clones were subjected to limiting dilution cloning in 96-well plates to obtain clonal transfectants.

hIgG ELISA

Supernatants from G418-resistant transfected NSO clones were harvested and tested in a sandwich ELISA for the presence of anti-IgD hIgG3 molecules as follows. EIA/RIA 96-well plates (Corning, Corning, NY) were coated with 5 μg/ml of goat anti-human IgG specific for the Fcγ chain (Accurate Chemical and Scientific Corp., Westbury, NY), and allowed to bind supernatant protein overnight. Plates were washed twice with PBS-Tween 20 0.05% (Fisher Scientific, Pittsburgh, PA) and blocked for 1 hour with 0.5% nonfat dry milk in the same wash buffer. After additional washing, secondary goat anti-human IgG-BIOTIN (specific for the Fcγ chain, SIGMA, St. Louis, MO) was applied,

and streptavidin-HRP added as a final conjugate. TMB peroxidase substrate was used as a colorimetric readout to determine final concentration of secreted supernatant rAb (KPL, Gaithersburg, MD).

Purification of rAb

Clones secreting supernatant showing high IgG protein concentration and allotype-specific B cell staining were expanded in bioreactors and supernatant harvested after all producer cells died (between two and three weeks). Supernatant was spun briefly to eliminate cell debris, and further filtered over a 0.22 μm filter (Millipore, Billerica, MA) before concentration through a Pall Filtron Centramate stacked filtration system (Pall Corporation, East Hills, NY). Following concentration, supernatant was diluted with protein G binding buffer (Pierce Biotechnology, Rockford, IL) and affinity purified on a column using protein G sepharose (Amersham Biosciences, Uppsala, Sweden). Elution was performed using protein G elution buffer (Pierce Biotechnology), re-concentrated, sterile-filtered, and UV absorbance used to determine specific protein fraction.

Mice

C57BL/6J, B6.Cg-Igh^{a} Thy1^{a} Gpi1^{a}/J, and Balb/c mice were purchased from The Jackson Laboratory (Stock #000664, #001317 and #000651, Bar Harbor, ME). GP61-80-specific I-A^{b} SMARTA CD4+ transgenic mice were a generous gift from Dr. Rafi Ahmed, and have been previously described [29]. Both B6.Cg-Igh^{a} Thy1^{a} Gpi1^{a}/J and SMARTA strains were bred on different Thy markers in the C57BL/6J background according to standard husbandry practice, and age-matched at four to six weeks. For adoptive transfer

studies, SMARTA CD4+ T cell inputs were standardized and injected intravenously in volumes of no less than 300 μl PBS. In all *in vivo* experiments, littermate controls were used. Mice were housed in the Yerkes Vaccine Research Center vivarium in accordance with current IUCAC protocol.

Generation of a GP61-80-specific CD4+ T cell hybridoma

Naïve B6.Cg-Igh^a Thy1^a Gpi1^a/J mice were primed subcutaneously via footpad injection with 50 μg of recombinant GP61-80 peptide emulsified in complete Freund's adjuvant (CFA) H37 Ra (DIFCO Laboratories, Detroit, MI), for a total volume of 0.1ml. Seven days post-priming, popliteal lymph nodes were removed, single cell suspensions prepared, and bulk cultures established at $1x10^7$ cells/flask. Cultures were stimulated with 50 or 100 μg/ml of peptide, and parallel microcultures were pulsed with 1 μCi/well of thymidine (^{3}H, Perkin Elmer, Waltham, MA) in a 96-well plate three days post stimulation. Cells were harvested using a MachIII multiple automated sample harvester (MASH, TOMTEC, Hamden, CT) and counted using a 1450 Microbeta Wallac Trilux liquid scintillation counter to determine antigen-specific proliferative capacity. Bulk stimulation cultures were harvested four days post-stimulation, purified over Ficoll-Hypaque (GE Healthcare Biosciences, Uppsala, Sweden), and fused using polyethylene glycol with BW5147, a TCR-negative thymoma cell line that has been previously described [30,31].

IL-2 release assay

To measure antigen presentation, $1x10^5$ GP61-80-specific hybridoma cells were co-cultured with different numbers of APCs (i.e. whole splenocytes, purified B cells, etc.) in a 96-well round-bottom plate. These cultures were simultaneously provided with exogenous antigen (i.e. rAb, recombinant peptide, etc.), or in most cases had already been exposed to antigen by *in vivo* rAb stimulus. After 24 h, culture supernatants were harvested to a flat bottom plate at –80°C for at least 30 min to ensure no cellular carryover. Post-thaw, a CTLL-2 indicator cell line (ATCC, #TIB-214) was added at $5x10^3$/well and allowed to grow overnight. This cell line requires IL-2 for growth, and was pulsed with ^3H for 18 hours and counted as above to indirectly measure the stimulation of the hybridoma line by these different APC/antigen combinations.

Virus preparation

The Armstrong and Clone 13 variants of LCMV were originally a gift from Dr. Rafi Ahmed. Both variants were grown in BHK-21 cells (ATCC catalog #CCL-10), stored at –80ºC, and only freeze-thawed once after determining titers. In all cases, viral stock titers were checked by direct plaque assay or by infection of naïve C57BL/6J mice. $2x10^6$ pfu of either virus was delivered intravenously in 500 μl of RPMI-1640 without serum (Mediatech Inc., Herndon, VA), and mice were monitored for the appearance of a rough coat and hunching. Spleen, liver, kidney and serum were collected from all infected mice, and titered for LCMV using standard protocol [32]. Briefly, organs were homogenized, serial dilutions prepared, and confluent monolayers of Vero cells infected (ATCC, #CRL-1586). Cells were overlaid with a 1:1 mixture of 2X199 media:1% agarose (Gibco,

Invitrogen), rested for four days, fixed with 7% paraformaldehyde, and stained with 2% crystal violet.

Cell isolation

To obtain single-cell lymphocyte suspensions, various tissue-specific protocols were employed. For spleen and lymph node, gentle homogenization was employed, and cells were washed in RPMI-1640 plus 5% fetal bovine serum (FBS, Hyclone) before being forced through a 70 μm cell strainer (BD Biosciences, San Jose, CA). For liver lymphocytes, mice were anesthetized with Nembutal sodium pentobarbital according to weight, and the inferior vena cava used as an entry point for catheter insertion (Exelint International Co., USA). 50 ml of Hanks Balanced Salt Solution containing heparin (HBSS, Hyclone) was perfused through the liver using a GENIE Plus Infusion/Withdrawal Pump (Kent Scientific Co., Torrington, CT) and the hepatic vein nicked to allow exit of contaminating PBMC. After liver excision, single cell suspensions were prepared using a Medimachine (BD Biosciences) and centrifuged in 5 ml 44% Percoll layered on a 3 ml 66% Percoll cushion (Amersham Biosciences, Piscataway, NJ). All lymphocyte preparations were red blood cell-lysed using RBC lysis buffer (Cambrex, Baltimore, MD). To obtain purified naïve B cells for our antigen presentation studies, B6.Cg-Igh^{a} Thy1^{a} Gpi1^{a}/J splenocytes were isolated, and B cells positively selected using Miltenyi beads specific for the B220 surface molecule and a Miltenyi autoMACS cell sorter (Miltenyi Biotech, Auburn, CA).

Tetramer staining

I-A^b restricted tetramers bearing the truncated GP66-77 peptide from the GP61-80 LCMV CD4+ T cell epitope were folded and synthesized with the help of Dr. John Altman and Dr. John Shires at the Emory University Vaccine Center in conjunction with the NIH tetramer core facility. To test the binding efficacy of newly generated tetramer batches, $5x10^6$ hybridoma cells (either GP61-80-specific Clone 33 alone or a 1:1 ratio of GP61-80-specific:non-specific) were incubated with 2 or 4 μg/ml of tetramer in a total volume of 0.5 ml RPMI-5% serum at 37°C plus 5% CO_2 for three hours on a rotator. Cells were washed in FACS buffer (PBS 1X, 1% BSA, 0.01% NaN_3), stained for additional markers for 20 minutes at room temperature, and visualized via flow cytometry. The identical experiment was performed in parallel using I-A^b-restricted tetramers bearing either the OVA 323-339 or CLIP peptide as negative controls, and SMARTA CD4+ T cells as positive controls. Class I LCMV tetramers were stained according to standard surface staining protocol.

Antibodies, phenotyping, and *in vivo* reagents

The 3N7 monoclonal anti-CD28 antibody was a generous gift from Dr. Robert Mittler and was purified by the same column method as the rAbs. CpG ODN adjuvants (types B and C; for review, see [33]) were kindly provided by Dr. Bali Pulendran. For phenotypic T cell analysis, single cell suspensions were prepared as described above and stained for the following T cell markers: CD25, CD44, CD45RA/RO, CD62L, CD69, CD127, PD-1, PD-L1, PD-L2, and FoxP3 (ICC, Ebiosciences, San Diego, CA). With the exception of allophyocyanin-conjugated (APC) antibodies to FoxP3 and CD127, phenotypic antibodies conjugated to phycoerythrin (PE) were used (BD Biosciences; Ebiosciences,

San Diego, CA). CD4 and CD8 T cell antibodies conjugated to fluorescein isothiocyanate (FITC) or phycoerithrin (PE) were used depending on the specific phenotype panel (BD Biosciences, San Diego, CA), and live-dead analysis was performed using either Viaprobe 7-AAD (BD Biosciences, San Diego, CA) or AF430-Live/Dead dye (Molecular Probes, Invitrogen, Carlsbad, CA). B cells were similarly isolated from mice, live/dead discriminated as above, and stained with B220 or CD19 conjugated to FITC or APC depending on the phenotypic antibodies used; CD38-FITC, CD40-FITC, CD69-FITC or PE, CD80-FITC or PE, CD86-FITC or PE, CD95/Fas-PE, peanut agglutinin (PNA)-FITC, GL7 (Ly-77)-FITC, and IgD-PE (BD Biosciences; Ebiosciences, San Diego, CA; Vector Labs, Burlingame, CA). Carboxyfluorescein succinimidyl ester (CFSE) staining was carried out according to a standardized protocol [34]: varying numbers of cells were stained for seven minutes using CFSE at a final concentration of 5 μM (Molecular Probes, Invitrogen, Carlsbad, CA) and quenched with FBS. For adoptive transfer, cells were washed once with RPMI plus 10% FBS followed by PBS, and injected intravenously in 200 μl PBS. For long-term culture, stained cells were cultured for three days with 2 μg/ml of appropriate recombinant peptide and collected for surface staining. All staining was visualized on FACScalibur or LSR-II flow cytometers (BD Biosciences), and data analyzed using FlowJo (Tree Star Inc., Ashland, OR).

Results

Construction, expression, and proposed mechanism of action of anti-IgD rAb

Our work focuses on the well-characterized CD4+ T cell epitope GP61-80 of LCMV. This epitope has been previously shown to be immunodominant, and is presented on H-2^b I-A^b MHC molecules to responding CD4+ T cells [35]. To facilitate our studies on the presentation capacities of naïve B cells, we PCR amplified and cloned the protein-encoding portion of the Ig(5a)7.2 V-L and V-H domains into cassette vectors pLNOH2 and pLNOκ (kindly provided by E. Lunde and I. Sandlie). These vectors have been shown to yield IgD-targeting antibodies bearing integrated T cell epitopes that can be efficiently processed by antigen presenting cells [25]. The first vector, pLNOH2, encodes for the heavy chain of a human isotype IgG3 (hIgG3) antibody with a variable region specific to murine IgD of allotype a (IgD^a), while the second, pLNOκ, encodes the light chain of an isotype- and variable region-matched antibody [28,36]. Using an overlapping, nested primer set with complementary non-annealing tails, we replaced four amino acids (KPSN) of the L3 loop of the heavy chain genes with the immunogenic LCMV GP61-80 (reviewed in [26]) (Figure 1A). Both heavy and light chain vectors were transfected into NSO cells, and stable transfectants were obtained by limiting dilution analysis and selection with G418. These transfectants were initially screened using a hIgG3-specific sandwich ELISA to determine which clones were producing high levels of rAb (data not shown). Additionally, supernatants from stable transfectants were tested for functional naïve B cell targeting using flow cytometry. Splenocytes were isolated from C57BL/6J (IgD^b), Balb/c (IgD^a), or B6.Cg-Igh^a $Thy1^a$ $Gpi1^a$/J (IgD^a) mice and stained directly using transfected supernatants. B220+ cells from Balb/c or B6.Cg-Igh^a $Thy1^a$ $Gpi1^a$/J but not

C57BL/6J mice were detected using a biotin-conjugated secondary antibody to the Fc portion of hIgG3 (Figure 1B, left panel). Splenocytes were stained in parallel with IgD to determine percentages of naïve B cells, and the data indicate that similar percentages of B220+IgD+ cells can be stained with rAb (Figure 1B, right panel). The same results were seen with CD19+ gating (data not shown), indicating that supernatants from transfected cells contained rAbs that were folded properly and able to functionally bind allotype-specific naïve B cells. Furthermore, titration of supernatants into the same assay demonstrated that *in vitro* binding was dose-dependent (Figure 1C). rAbs not containing the GP61-80 epitope were also able to bind naïve B cells efficiently, and further concentration/purification of rAbs via protein G sepharose column chromatography and non-centrifugation techniques did not diminish *ex vivo* binding capability (data not shown). Intravenous injection of column-purified rAb with or without GP61-80 embedded epitope in B6.Cg-Igh^a Thy1^a Gpi1^a/J mice caused a downregulation of surface IgD on targeted B cells *in vivo* as early as 4 hours post-treatment, the earliest time point examined (Figure 1D). However, IgD gradually increases on these cells to baseline levels approximately 24 hours post-treatment, both in percentages of B cells and total cell numbers (data not shown).

GP61-80 rAb can be processed and presented by *ex vivo* isolated naïve splenic B cells to stimulate an antigen-specific CD4+ T cell hybridoma

Having shown that GP61-80 rAbs are properly folded and able to target naïve B cells, we sought to determine the CD4+ T cell activation potential of these rAbs. B6.Cg-Igh^a Thy1^a Gpi1^a/J mice were footpad-immunized with LCMV GP61-80 peptide emulsified in

complete Freund's adjuvant, draining lymph nodes were harvested seven days post-immunization, and bulk lymphocyte cultures stimulated and fused with an immortalized thymoma cell line. Of the 100 clones selected in this fusion, six were extremely sensitive to GP61-80 peptide presented by whole splenocytes, the best of which secreted enough IL-2 in response to 0.001-0.01 μg/ml (1-10 ng/ml) peptide to allow for CTLL-2 indicator cell proliferation (see Materials and Methods for description of indirect IL-2 proliferation assay). All hybridoma clones were found to be CD3+CD4+, and all could be detected using class II I-A^b tetramers bearing a shortened GP66-77 peptide (data not shown). Using this newly established fixed readout of CD4+ T cell activation, we determined the efficiency of GP61-80 rAb processing and presentation by naïve B cells. Splenocytes were isolated from B6.Cg-Igh^a $Thy1^a$ $Gpi1^a$/J or C57BL/6J mice, given decreasing concentrations of GP61-80 rAb or whole peptide, and co-cultured with the CD4+ T cell hybridoma. Although both splenocyte populations were able to present whole peptide, only B6.Cg-Igh^a $Thy1^a$ $Gpi1^a$/J splenocytes were able to process and present GP61-80 rAb supernatant to the hybridoma (Figure 2C). It should be noted that in all IL-2 proliferation assays, counts per minute (cpm) of thymidine-pulsed CTLLs varies from experiment to experiment (compare Figures 2A-C). These discrepancies can be attributed to a number of experimental variables such as the current growth state of CTLLs at time of assay, time allowed for thymidine incorporation (18 versus 24 hours), and exact plating numbers of both hybridoma cells and CTLLs. These results demonstrated that GP61-80 rAbs can be processed and presented to highly sensitive immortalized antigen-specific CD4+ T cells. Furthermore, because these two congenic mouse strains differ only at the Igh locus, we can conclude that this process is mediated by naïve B cells and

no other antigen presenting cells. To test the *in vivo* effects of GP61-80 rAb, column-purified rAb was injected directly into B6.Cg-Igh^{a} Thy1^{a} Gpi1^{a}/J mice via the intravenous route. Splenocytes were harvested four hours post-injection, and titrated into a fixed culture of CD4+ T cell hybridomas to determine if processing of rAb by naïve B cells could occur *in vivo*, followed by direct *ex vivo* presentation of GP61-80 peptide. Splenocytes from mice injected with GP61-80 rAb were able to present antigen to the hybridoma in a dose-dependent manner, while splenocytes from mice receiving rAb with no epitope could not (Figure 2A). 20 μg of GP61-80 rAb was the minimum dose sufficient to induce stimulation of the hybridoma by whole splenocytes (Figure 2A, upright triangle symbol). We then performed the same experiment using B220+ cell enriched or depleted fractions, and found that B cells are definitively targeted by GP61-80 rAb for *in vivo* processing (Figure 2B). It is important to note that a small amount of CD4+ T cell hybridoma stimulation occurred when using high numbers of the B cell depleted fraction (Figure 2B, X symbol). This was most likely due to incomplete depletion of the B cell compartment in our bead sorting analysis, which was confirmed by flow cytometry. B cell enriched fractions were also able to stimulate the hybridoma when CD16/32 Fc blocking antibodies were injected simultaneously with GP61-80 rAb and then added to post-injection cocultures, ruling out the possibility of passive uptake of GP61-80 rAb upon delivery (data not shown).

GP61-80 can be processed and presented *in vivo* by naïve B cells to stimulate antigen-specific CD4+ T cells

Injection of GP61-80 rAb into naïve B6.Cg-Igh^{a} Thy1^{a} Gpi1^{a}/J mice failed to generate a detectable antigen-specific CD4+ T cell response, which may have been due to inadequate dosage or insufficient costimulation. To circumvent this, we decided to use the SMARTA TCR transgenic mouse model to ask basic questions about the activation status and proliferative potential of non-immortalized antigen-specific CD4+ T cells. Depending on the experiment, between $5x10^{4}$ and $5x10^{6}$ Thy1.2+ SMARTA CD4+ T cells specific for the LCMV GP61-80 epitope were adoptively transferred into Thy1.1+ B6.Cg-Igh^{a} Thy1^{a} Gpi1^{a}/J mice, and allowed to rest for 24 hours. Intravenous administration of 200 μg GP61-80 rAb after cell transfer did not result in a marked increase in cell proliferation five days post-treatment compared to control mice receiving PBS (Figure 3B). Input cell numbers showed a modest proliferative increase with concurrent administration of the immune adjuvant deoxycytidyl-deoxyguanosine oligonucleotides (CpG ODN). We also labeled input SMARTA cells with CFSE before intravenous treatment to examine antigen-specific CD4+ T cell expansion *in vivo*. In mice treated with 200 μg GP61-80 rAb, transferred SMARTA cells were clearly able to divide, indicating that naïve B cells can process and present rAb to rare populations of antigen-specific T cells (Figure 3A). Division was dose-dependent and occurred within 2-3 days post-treatment, with an average of 4-6 total divisions. CpG ODN treatment again had little effect on transferred cells, with similar CFSE dilution as rAb treatment. Additionally, increasing input concentration of GP61-80 rAb (up to 1 mg) resulted in no further division when compared to 200 μg input, and transferred cells from mice treated with rAb containing no specific epitope showed no division beyond PBS controls (data not shown). For division experiments, CFSE dilution was controlled for by adoptively

transferring SMARTA CD4+ T cells into age-matched mice and infecting intraveneously with $2x10^6$ pfu LCMV Armstrong (acute variant, not shown) or Clone 13 (chronic variant). Upon infection with either variant, transferred cells showed a massive proliferation and terminally diluted CFSE, dividing greater than eight times over the course of five days (Figure 3A, B). It should be noted that the SMARTA CD4+ T cell adoptive transfer system established here is useful only in short-term experiments. Numerous attempts using GP61-80 rAb to develop long-term SMARTA CD4+ memory T cells failed, due to an inherent defect in the longevity of transferred SMARTA cells. Approximately 15 days post-transfer, SMARTA populations wane in both control and experimental groups, and examination of numerous compartments (blood, liver, lymph node, spleen) three weeks post-treatment yielded no long-lived memory CD4+ T cells.

SMARTA CD4+ T cells require GP61-80 rAb plus exogenous costimulatory signals to fully divide and differentiate into cells with an effector phenotype

Adoptively transferred SMARTA cells do not undergo full division and are not retained following stimulation by GP61-80 rAb. Having already tested antigen dose, we hypothesized that improper costimulation signals from rAb-targeted B cells resulted in inadequate priming of CD4+ T cells. We adoptively transferred CFSE-labeled SMARTA cells and treated mice with GP61-80 rAb plus varying doses of anti-CD40 or anti-CD28, hoping to provide adequate costimulation *in vivo* by aiding B cells or T cells, respectively. Concurrent CD40 stimulation on targeted B cells yielded no significant division of SMARTA cells five days post-treatment when compared to the GP61-80 rAb monotherapy (Figure 3C). Administration of GP61-80 rAb with concurrent CD28

stimulation using 20 ug of an anti-CD28 antibody allowed for full division of SMARTA cells, presumably by acting directly on CD4+ T cell populations (Figure 3C). Transferred cells from mice receiving anti-CD28 antibody alone failed to divide by five days, displaying a CFSE profile identical to cells receiving PBS or rAb with no integrated epitope. In addition, providing these cells with exogenous GP61-80 peptide alone allowed for division, albeit incomplete when compared to Clone 13-infected controls. These controls proved that both primary and secondary stimulation in our rAb system were necessary for full T cell division, suggesting that B cells targeted by rAbs do not provide adequate costimulation to CD4+ T cells. Phenotypic analysis of transferred SMARTA cells found several activation and memory markers differentially expressed between treatment groups. GP61-80 rAb administration induced downregulation of CD25 (IL-2 receptor) on CFSE-low cells, while concurrent anti-CD28 stimulation resulted in a large percentage of CFSE-low cells with decreased CD25 but an additional CD25-high population, mimicking Clone 13-infected groups (Figure 4, top row). This data suggests that rAb treatment pushes dividing cells towards an effector phenotype, and providing adequate costimulation in this setting reserves a small population for long-lived memory or even CD4+ regulatory T cell generation. rAb-treated cells also upregulated CD44, a common activation marker of T and B cells conferring functional hyaluronic acid-binding potential (Figure 4, second row from top) [37]. Upregulation of another activation marker, CD69, occurred within 24 hours of treatment but quickly decreased, while addition of exogenous anti-CD28 allowed for detection of this marker up to five days post-stimulation (Figure 4, fourth row from top). We also analyzed L-selectin (CD62L) expression on transferred cells, and again found a modest downregulation in the single

rAb-treated group compared to a two- to three-fold further downregulation in the rAb plus anti-CD28 group (Figure 4, third from top). This result further supports the notion that rAb treatment skews CD4+ T cells away from immune surveillance in secondary lymphoid organs (memory phenotype) and towards an effector cell phenotype capable of immediate response upon encountering antigen. CD127, the IL-7 receptor α chain, is markedly downregulated on CFSE-low cells upon treatment with GP61-80 rAb (Figure 4, fifth row from top), and multiple treatments had a synergistic affect (data not shown). High expression of this molecule is predictive of memory cell precursors, and the downregulation seen in this setting again suggests that these antigen-specific CD4+ T cells have become activated effectors. Interestingly, this phenotype was also seen in cells with simultaneous anti-CD28 at five days post-treatment, indicating that the kinetics of CD127 expression in the double-treated animals may be delayed. Furthermore, CD4+ T cells stimulated with rAb plus anti-CD28 showed an upregulation of PD-1 (Programmed Death 1) protein that was not seen in rAb monotreatment (Figure 4, bottom row). Upregulation of this negative regulator of immune responses suggests that rAb plus anti-CD28 treated cells have the potential to modulate their responses following T cell receptor signaling, similar to T cells during LCMV infection [38].

Priming transferred SMARTA CD4+ T cells with GP61-80 rAb before or during Armstrong or Clone 13 infection in B6.Cg-Igh^{a} Thy1^{a} Gpi1^{a}/J mice did not alter the course of infection, and viral load remained comparable to untreated mice in the spleen, liver, kidney and serum (data not shown). However, during the course of these experiments we found that mice with large numbers of transferred SMARTA cells

succumbed to Clone 13 infection eight days post-infection, presumably from hypercytokinemia. This observation was supported by experiments titrating the input number of SMARTA cells; the fewer cells transferred, the less likely mice were to have a lethal course of infection, with 100% of animals surviving with $5x10^4$ or less cells (data not shown). To determine the fate of GP61-80 rAb-treated CD4+ T cells, we transferred a lethal amount of CD4+ SMARTA cells ($5x10^6$) into B6.Cg-Igh^a Thy1^a Gpi1^a/J mice, treated with PBS, anti-CD28, or GP61-80 rAb with or without anti-CD28, and infected animals intravenously with $2x10^6$ pfu LCMV Clone 13. All groups lost similar amounts of weight over the course of infection (data not shown), but all mice receiving both rAb and anti-CD28 survived (Figure 5, X). Half of all animals treated with rAb alone succumbed to infection (Figure 5, ∇), compared to PBS or untreated controls. Interestingly, mice treated with anti-CD28 alone survived infection, suggesting that survival was not related to adequate priming of CD4+ T cells (Figure 5, Δ). This is consistent with our previous observation that priming with rAb in this manner fails to decrease viral load. Taken together, these results suggest that priming adoptively transferred SMARTA CD4+ T cells with GP61-80 rAb plus anti-CD28 through naïve B cells creates short-term effector cells that are unable to affect viral burden and are rapidly cleared from mice before they become immunopathological.

Discussion

In this study, we describe a system for activation of CD4+ T cells by maximizing antigen presentation through small resting B cells. We additionally define the relationship between these two cells during antigen presentation through phenotypic and functional analyses. Our recombinant antibodies were created by inserting a well-defined CD4+ T cell epitope of the LCMV glycoprotein, GP61-80, into a loop connecting the β-strands of the Ig constant domain of a humanized antibody targeting the mouse IgD molecule. This approach has previously been shown to deliver antigen to targeted cell types more efficiently than incomplete Fab fragments containing attached epitope tails, and to enhance T cell proliferation both *in vitro* and *in vivo* [25,39]. The plasticity of these interconnecting loops has been demonstrated to an extent [14,26], and we confirmed these results by demonstrating efficient production and targeting of our rAbs containing a 20 amino acid insertion. Proper folding of rAbs containing such large sequences lends support to their usage as vaccine delivery vehicles. One could potentially synthesize many rAb molecules, each with multiple insertions of epitopes from the same pathogen, in the hope of creating a multivalent vaccine strategy. Side by side experiments comparing B220+ (CD45R+) B cells staining for IgD or rAb-binding demonstrated that almost all naïve B cells are targeted by rAbs *in vitro*, and additional experiments showed that B220+IgD+ naïve B cells could be simultaneously stained with rAbs, indicating that rAbs do not occlude binding sites on these surface molecules (Figure 1B). We further defined the kinetics of IgD expression on *in vivo* rAb-targeted B cells. It had previously been shown that similar rAbs effectively stain CD45R+TcR- B cells, but the IgD expression status of these cells was not properly defined. With our treatment, naïve B

cells rapidly downregulated surface IgD, presumably through a contact-dependent internalization mechanism (Figure 1D). It is unknown whether the subsequent upregulation of this molecule occurs on B cells that have been targeted, or whether there is replenishment of new cells expressing IgD from another compartment, such as the bone marrow. Preliminary FACS data from our lab indicates that CD69 may be transiently upregulated on targeted B cells, suggesting that rAbs may be able to activate and differentiate naïve B cells. These B cells shows modest costimulatory molecule increase (CD80 and CD86), and small, discreet populations of CD95+GL7+ B cells arise in peripheral lymph nodes by 12 days with our GP61-80 monotreatment. GL7 is known to be a marker of peripheral germinal center B cells in the spleen, whereas upregulation of CD95 (also known as Fas or Apo-1) has been shown to regulate B cell numbers and control autoimmunity (reviewed in [40,41]). Additionally, small populations of CD38-CD80+ B cells and peanut agglutinin (PNA) positive B cells were found in the spleen between 48 hours and 13 days post-treatment. High expression of the PNA lectin increases the ability of a cell to bind Gal- β(1-3)-GalNAc carbohydrates, and is a hallmark of germinal center transformation [42,43,44]. Although the expression of CD38 on B cells is varied depending on the activation status (immature versus mature) or compartment (splenic versus tonsillar), it is generally accepted that there exist populations of long-lived, splenic germinal center B cells with a CD38-low phenotype [45,46,47]. However, the transient upregulation of B cell activation markers, coupled with the inconsistency of B cells targeted versus B cells activated (along with our T cell activation data), point to incomplete activation of these B cells. From these preliminary studies, we hypothesize that rAb targeting *in vivo* reaches a large fraction of naïve B

cells, but a low frequency of adequate IgD cross-linking events activates only a select number of targeted cells. Further studies are needed to address the question of whether populations of B cells receiving sufficient IgD-crosslinking from rAb treatment form actual germinal centers, and whether this incomplete priming of B cells by rAbs can be overcome by antigen dosage, alteration of priming kinetics, or addition of exogenous maturation factors such as those used in dendritic cell priming [48].

We hypothesized that the dose-response seen *in vitro* should be mirrored *in vivo*, due to both efficient naïve B cell-targeting and increased tissue penetration over larger antigen-antibody conjugates. This was indeed the case, as direct *ex vivo* priming of hybridoma cells by *in vivo* targeted naïve B cells was dependent on the amount of injected rAb as well as the amount of cells targeted by treatment (Figure 2). This result held true even when B cells were purified and excess amounts of Fc blocking antibodies were administered to mice, confirming naïve B cells as the culprit of *ex vivo* T cell priming and highlighting the fine specificity of this system. Our results suggest that rAb targeting eliminates the need for passive uptake, thereby equalizing all APC types and underscoring the efficiency of the processing and presentation machinery inherent to each particular APC. Although beyond the scope of this current work, similar experiments can be performed altering the rAb variable region to target various APC types with a fixed epitope for processing and presentation comparisons [23].

Much work has been done to characterize rAbs, including studies on epitope type and placement [15,22,26,28,49], IgG subtype [22], and stimulatory capacity [23,25,27]. We

chose instead to focus on the interaction of antigen-specific CD4+ T cells with naïve B cells that had been targeted by rAbs. Previous studies utilizing B cell-specific rAbs demonstrated that antigen-specific CD4+ T cells could be stimulated to proliferate, but the extent of this stimulation as well as the phenotype of responding T cells was not explored. We chose a simple adoptive transfer system employing small numbers of CD4+ SMARTA T cells and congenic mice whose naïve B cells are efficiently targeted by rAbs *in vivo*. A similar study has shown that this approach is desirable for tracking B-T cell interactions because it avoids disruption of the native lymphoid microenvironment, as is often seen in whole irradiated animals, as well as controls the abnormally high numbers of specific T cells seen in whole transgenic animals that can mask regulatory effects [11]. We extended previous B cell-rAb studies by demonstrating that adoptively transferred CD4+ T cells show a defect in both proliferation and division upon contact with rAb-targeted B cells (Figure 3A, B). Interestingly, this defect is only rescued upon direct treatment of T cells with anti-CD28 antibodies, and not with direct stimulation of B cells via CD40 stimulation or indirect danger signals such as an environment rich in CpG oligodeoxynucleotides (Figure 3C). It has previously been shown that B cells exposed to antigens coupled to CpG signals can stimulate a Th1 response through IL-12 production [50], so it is reasonable to hypothesize that coupling rAbs to CpGs may have a similar effect. These findings led us to hypothesize that an inherent defect exists in CD4+ T cells stimulated by processed rAb antigens, which was confirmed upon phenotypic analysis (Figure 4). GP61-80 rAb treatment coupled to direct T cell costimulation drives CD4+ T cells to differentiate along a short-term effector pathway that is commonly seen in cells during acute LCMV infection [51]. However, unlike LCMV-stimulated T cells, rAb-

stimulated T cells may not form long-lived memory cells. The default pathway for these cells seems to be rapid clearance from all compartments, most likely due to signal 2-deficient activation mechanisms. Systems with fewer constraints on the longevity of transferred T cells could better address the long-term potential of these cells. Additionally, our data suggests that rAbs with embedded epitopes specific for autoreactive T cells could be used to alleviate autoimmune conditions in systems such as experimental autoimmune encephalitis (EAE) and rheumatoid arthritis.

Our work further defines the role of naïve B cell surface Ig molecules in processing and presentation of antigen embedded in a novel delivery method. Although rAbs have been shown to efficiently stimulate antigen-specific T cells both *in vitro* and *in vivo*, our data suggests that the rAb approach may suffer from specific limitations when naïve B cells are the intended target. Based on the results presented here, we hypothesize that each specific pathogen (or antigenic entity) may necessitate a unique repertoire of rAbs coupled with a unique set of epitopes to achieve maximum T cell activation and long-lived memory responses.

Acknowledgments

The authors would like to thank members of the Grakoui lab for their helpful discussion, especially Raghavan Chinnadurai for experimental advice and Victoria Velazquez for critical reading of the manuscript. The authors would also like to thank Don Latner for input concerning LCMV viral stock preparation and SMARTA T cell analysis.

Figures

Figure 1

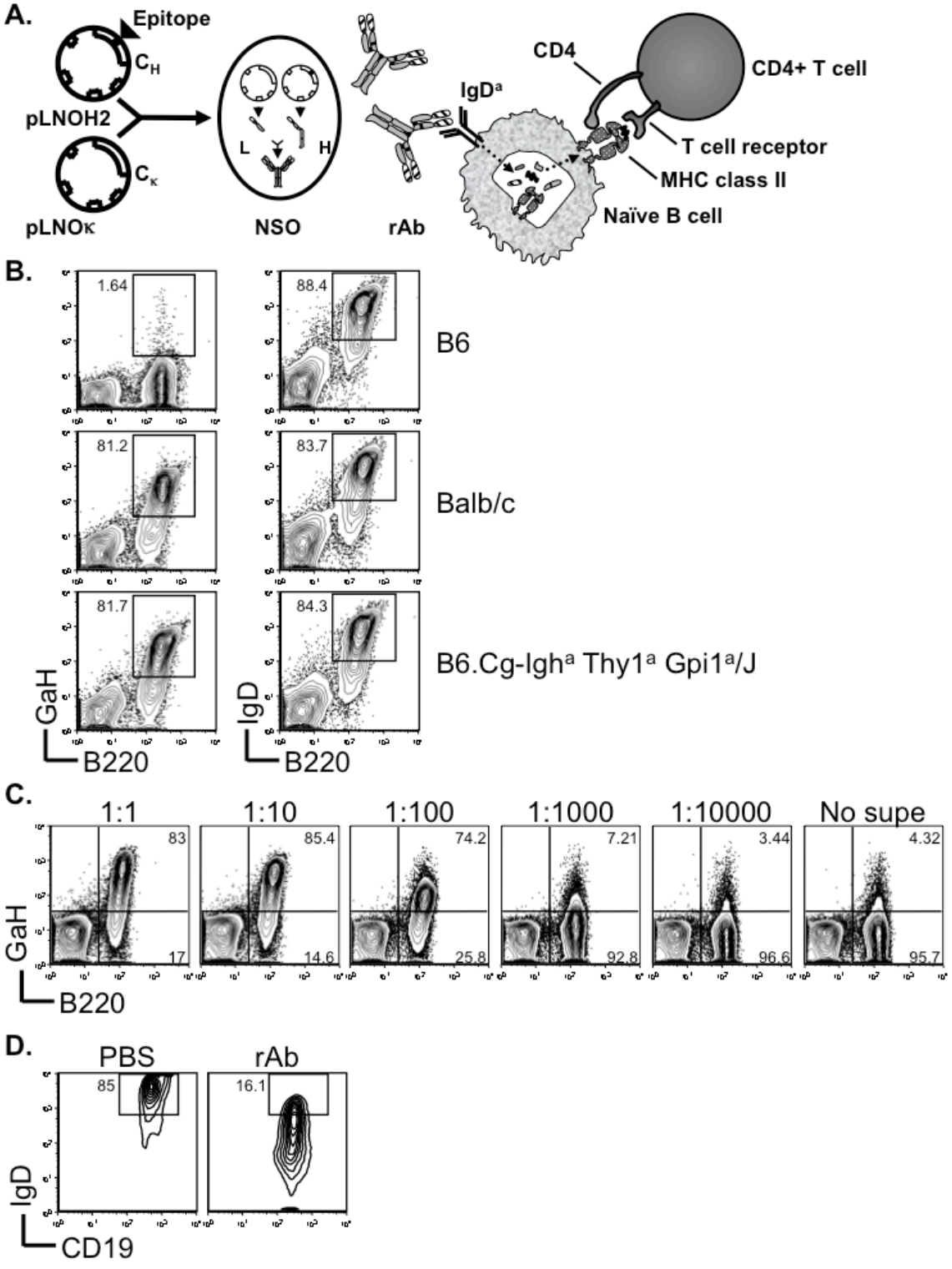

Figure 2

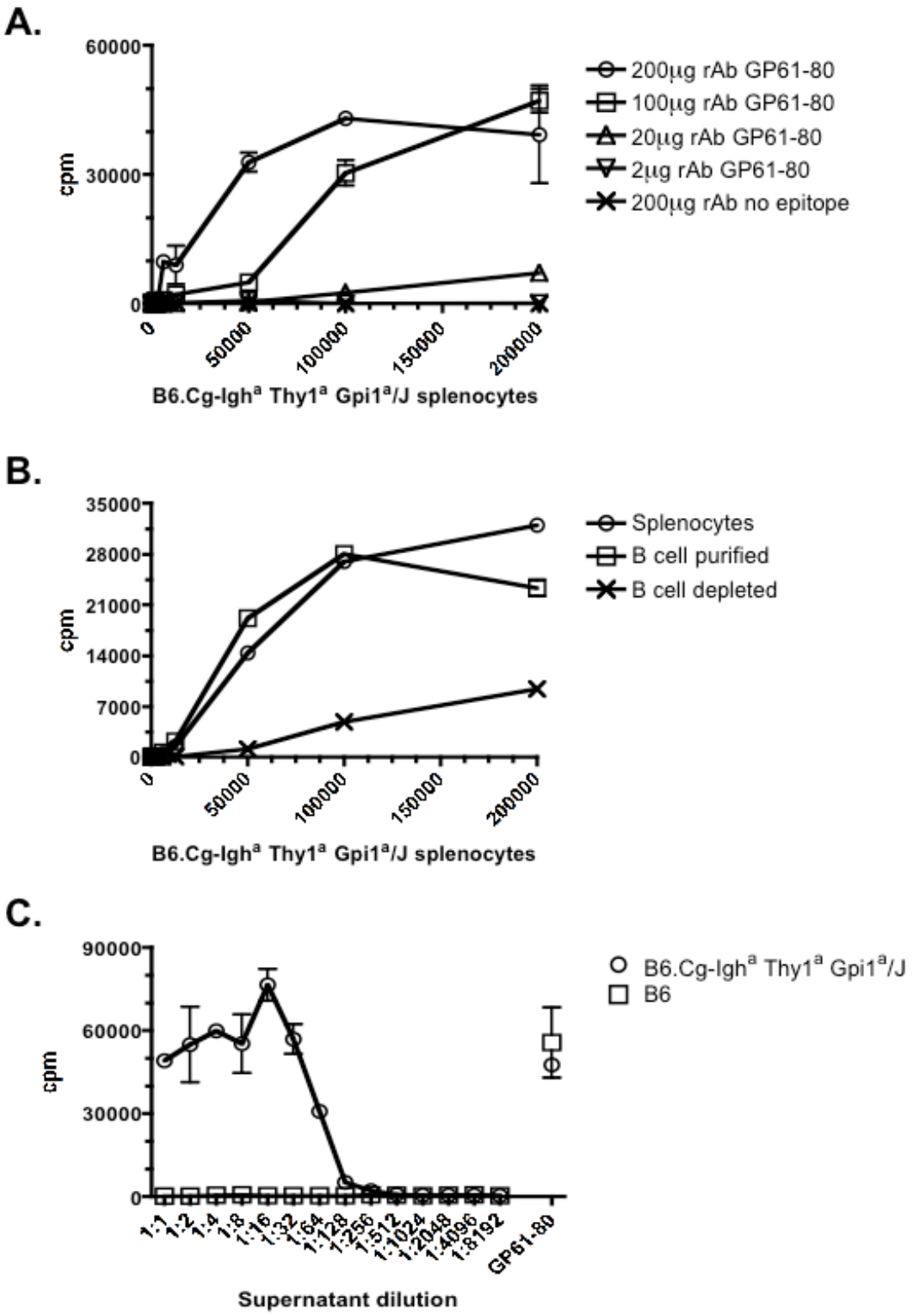
A.
60000
30000
0
cpm
0
50000
100000
150000
200000
B6.Cg-Igh^a Thy1^a Gpi1^a/J splenocytes
200µg rAb GP61-80
100µg rAb GP61-80
20µg rAb GP61-80
2µg rAb GP61-80
200µg rAb no epitope
B.
35000
28000
21000
14000
7000
0
cpm
0
50000
100000
150000
200000
B6.Cg-Igh^a Thy1^a Gpi1^a/J splenocytes
Splenocytes
B cell purified
B cell depleted
C.
90000
60000
30000
0
cpm
1:1
1:2
1:4
1:8
1:16
1:32
1:64
1:128
1:256
1:512
1:1024
1:2048
1:4096
1:8192
GP61-80
Supernatant dilution
B6.Cg-Igh^a Thy1^a Gpi1^a/J
B6

Figure 3

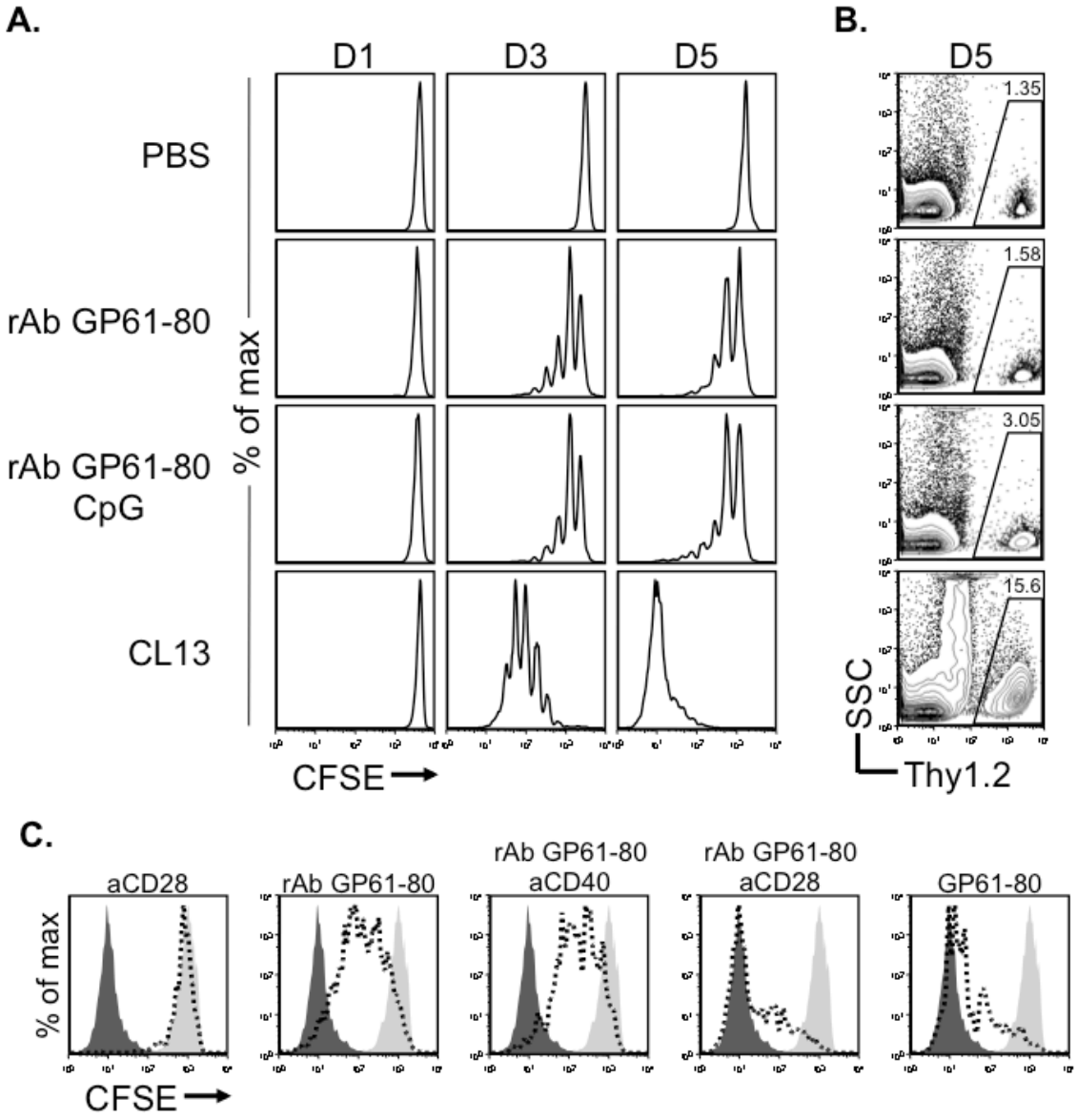
A.
D1
D3
D5
PBS
rAb GP61-80
rAb GP61-80
CpG
CL13
% of max
CFSE
B.
D5
1.35
1.58
3.05
15.6
SSC
Thy1.2
C.
aCD28
rAb GP61-80
rAb GP61-80
aCD40
rAb GP61-80
aCD28
GP61-80
% of max
CFSE

Figure 4

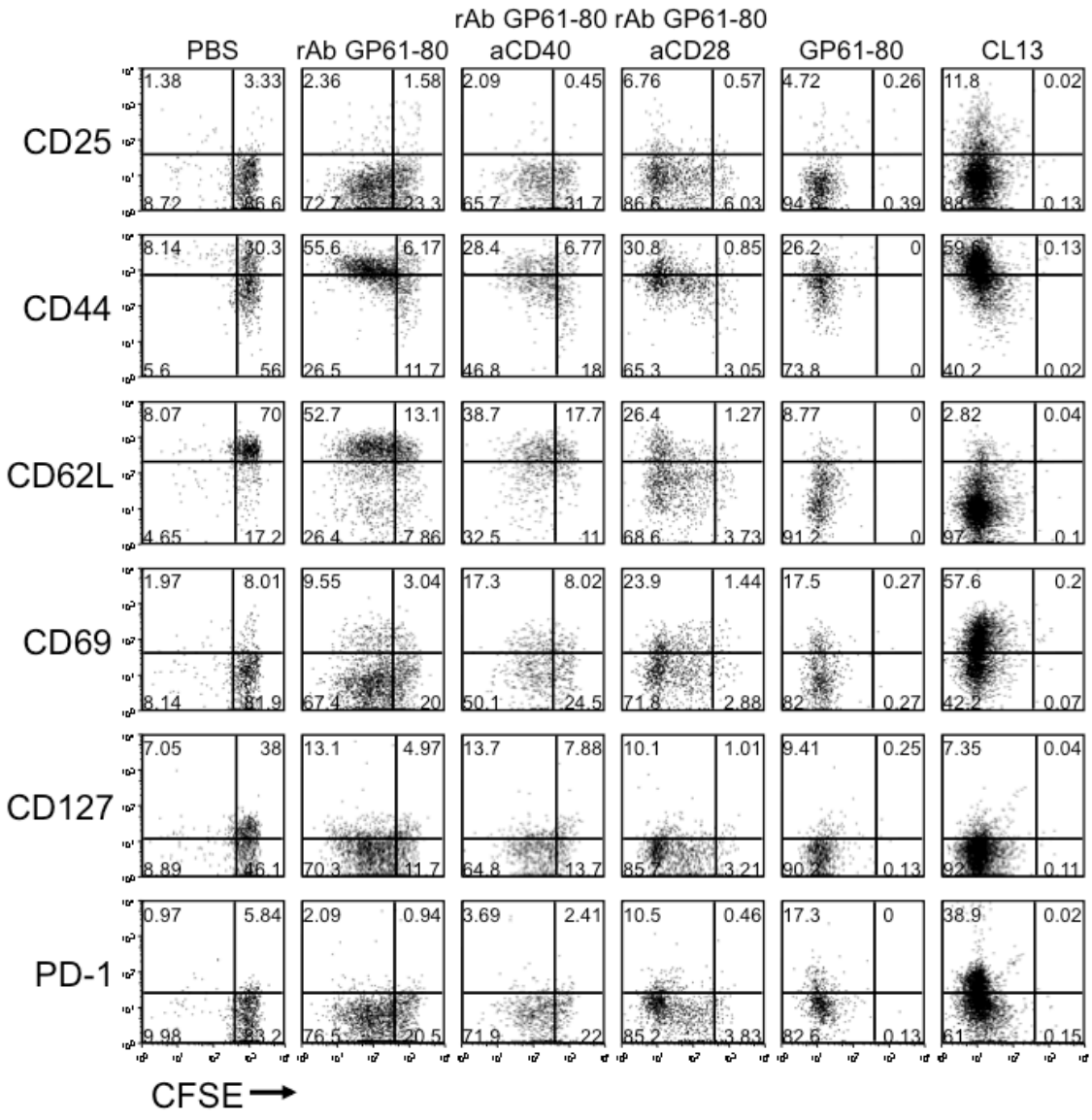
rAb GP61-80 rAb GP61-80
PBS
rAb GP61-80
aCD40
aCD28
GP61-80
CL13
CD25
CD44
CD62L
CD69
CD127
PD-1
CFSE

Figure 5

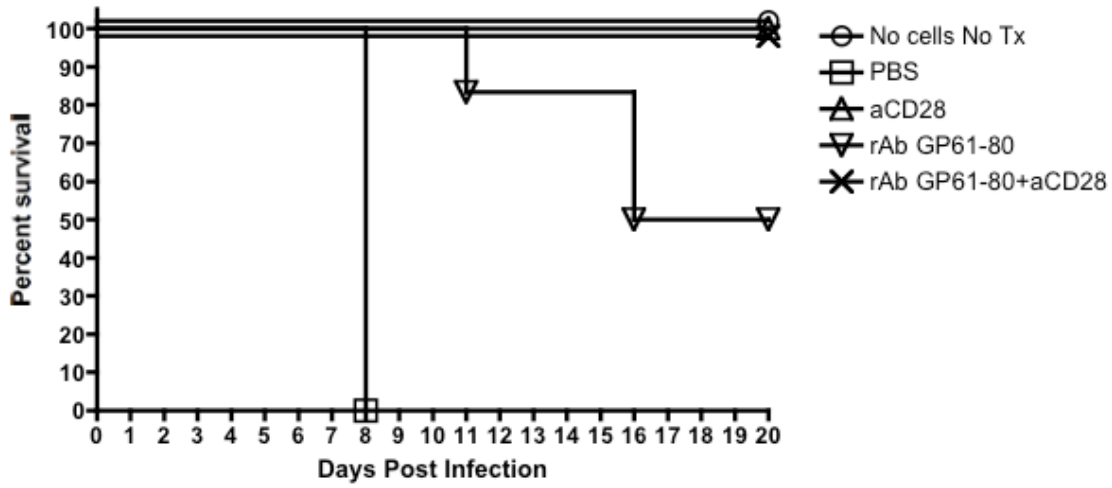
Percent survival
100
90
80
70
60
50
40
30
20
10
0
0 1 2 3 4 5 6 7 8 9 10 11 12 13 14 15 16 17 18 19 20
Days Post Infection
No cells No Tx
PBS
aCD28
rAb GP61-80
rAb GP61-80+aCD28

Figure legends

Figure 1. Proposed mechanism of action and *in vitro* targeting of rAb to splenic B cells. (A) The LCMV GP61-80 CD4+ T cell epitope was cloned into a specific region of a cassette encoding the human immunoglobulin 3 heavy chain (pLNOH2), and cotransfected with the matched light chain (pLNOκ) into an NSO producer cell line. Unlike previous approaches of antibody-antigen conjugates, this approach focuses on targeting naïve B cells via surface IgD of the a allotype. In doing so, bound rAb is internalized, followed by processing and presentation through the MHC class II pathway to antigen-specific CD4+ T cells. (B) Allotype-specific rAb staining of splenic B cells. Splenic B cells from mice with the a allotype (Balb/c or B6.Cg-Igh^a Thy1^a Gpi1^a/J) can be stained using rAb generated in NSO supernatant, whereas C57BL/6J (B6) b allotype splenocytes cannot (left panel). Whole splenocytes from all three strains show similar percentages of B220+IgD+ naïve B cells (right panel), and these numbers are similar to rAb-stained cell numbers. Gate percentages represent percent of live B220+ cells staining positive for indicated markers. (C) *In vitro* staining of allotype a splenic B cells is dose-dependent. Percentages were determined using a separate B220 gate (not shown). GaH, secondary goat anti-human IgG antibody conjugated to biotin, detected using strepatavidin conjugated to phycoerythrin (PE). Cells were gated on live lymphocytes. (D) Naïve B cells targeted by rAb downregulate surface IgD. B6.Cg-Igh^a Thy1^a Gpi1^a/J mice were injected intravenously with 200 μg purified rAb or PBS, and splenocytes harvested at various timepoints post-injection. IgD is downregulated on CD19+ B cells from rAb-treated mice as early as four hours post-injection. Representative plots of two separate experiments are shown.

Figure 2. Stimulation of an LCMV GP61-80-specific CD4+ T cell hybridoma by *in vivo* administration of rAb. (A) *Ex vivo* presentation of GP61-80 by rAb-targeted B cells is dose dependent. Indicated amounts of GP61-80 rAb were administered intravenously to B6.Cg-Igh^a Thy1^a Gpi1^a/J mice. Splenocytes from treated animals are able to stimulate GP61-80 hybridoma cells directly *ex vivo* dependent on number of input cells, while rAbs with no embedded epitope are not able to stimulate the antigen-specific hybridoma. (B) *Ex vivo* stimulation of GP61-80 hybridoma cells is B cell-dependent. 200 μg of GP61-80 rAb was administered intravenously, and splenocytes were enriched for B cells using B220-specific beads before addition to hybridoma cocultures. Only B cell enriched fractions were able to stimulate the GP61-80 CD4+ hybridoma. (C) Splenocytes harvested from C57BL/6J and B6.Cg-Igh^a Thy1^a Gpi1^a/J are both able to present GP61-80 peptide to the CD4+ hybridoma, but only B6.Cg-Igh^a Thy1^a Gpi1^a/J can process and present GP61-80 rAb in NSO-transfected supernatants. Presentation of this rAb occurs even at a 1:200 dilution of supernatant. Cpm, counts per minute.

Figure 3. Adoptively transferred antigen-specific CD4+ T cells divide upon treatment with rAb, but show a significant proliferation defect. (A) 1x10^6 GP61-80-specific SMARTA CD4+Thy1.2+ T cells were labeled with CFSE, transferred into B6.Cg-Igh^a Thy1^a Gpi1^a/J mice bred on a Thy1.1 background, and allowed to rest for 24 hours before intravenous treatments. At indicated time points, splenocytes were harvested and stained with CD4-PE, Thy1.2-APC, and a live dead marker to examine cell division. All histograms shown are gated on CD4+Thy1.2+ lymphocytes, and representative of

three animals in four separate experiments. (B) Proliferation defect of transferred SMARTA cells 5 days post-treatment. (C) The same experiment was performed and analyzed as in (A), but additional groups of mice received anti-CD40, anti-CD28 alone or in conjunction with GP61-80 rAb, or whole GP61-80 peptide. Light histogram, PBS treatment; dark histogram, Clone 13 treatment; dashed histogram, indicated treatment. Results are representative of three mice in two separate experiments.

Figure 4. Phenotypic profile and division of adoptively transferred antigen-specific CD4+ T cells treated with rAb in the presence or absence of exogenous costimulation. $1x10^6$ CD4+Thy1.2+ CFSE-labeled SMARTA cells were transferred into B6.Cg-Igh^a Thy1^a Gpi1^a/J mice, treatment administered intravenously, and splenocytes harvested five days post-treatment. As controls, mice were given GP61-80 peptide or infected with $2x10^6$ pfu LCMV Clone 13. Cells were stained with CD4-PerCP, Thy1.2-APC, and the indicated phenotypic markers in the PE channel. All plots are gated on CD4+Thy1.2+ cells.

Figure 5. Functionality of adoptively transferred antigen-specific CD4+ T cells treated with rAb in the presence or absence of exogenous costimulation affects survival of mice infected with LCMV. $5x10^6$ CD4+Thy1.2+ SMARTA cells were transferred into B6.Cg-Igh^a Thy1^a Gpi1^a/J mice, treatment administered intravenously, and survival of mice monitored for ~3 weeks. Data is representative of two separate experiments, with n=6 animals in each experiment.

References

1. Abbas AK, Lichtman, A. H., Pober, J. S. (2005) Cellular and Molecular Immunology 5th Ed.: 11-12, 17, 19.

2. Pulendran B, Tang H, Manicassamy S (2010) Programming dendritic cells to induce T(H)2 and tolerogenic responses. Nat Immunol 11: 647-655.

3. Rock KL, Benacerraf B, Abbas AK (1984) Antigen presentation by hapten-specific B lymphocytes. I. Role of surface immunoglobulin receptors. J Exp Med 160: 1102-1113.

4. Ashwell JD, DeFranco AL, Paul WE, Schwartz RH (1984) Antigen presentation by resting B cells. Radiosensitivity of the antigen-presentation function and two distinct pathways of T cell activation. J Exp Med 159: 881-905.

5. Chesnut RW, Grey HM (1981) Studies on the capacity of B cells to serve as antigen-presenting cells. J Immunol 126: 1075-1079.

6. Lanzavecchia A (1985) Antigen-specific interaction between T and B cells. Nature 314: 537-539.

7. Krieger JI, Grammer SF, Grey HM, Chesnut RW (1985) Antigen presentation by splenic B cells: resting B cells are ineffective, whereas activated B cells are effective accessory cells for T cell responses. J Immunol 135: 2937-2945.

8. Krieger JI, Chesnut RW, Grey HM (1986) Capacity of B cells to function as stimulators of a primary mixed leukocyte reaction. J Immunol 137: 3117-3123.

9. Lassila O, Vainio O, Matzinger P (1988) Can B cells turn on virgin T cells? Nature 334: 253-255.

10. Fuchs EJ, Matzinger P (1992) B cells turn off virgin but not memory T cells. Science 258: 1156-1159.

11. Ronchese F, Hausmann B (1993) B lymphocytes *in vivo* fail to prime naive T cells but can stimulate antigen-experienced T lymphocytes. J Exp Med 177: 679-690.

12. Townsend SE, Goodnow CC (1998) Abortive proliferation of rare T cells induced by direct or indirect antigen presentation by rare B cells *in vivo*. J Exp Med 187: 1611-1621.

13. Raimondi G, Zanoni I, Citterio S, Ricciardi-Castagnoli P, Granucci F (2006) Induction of peripheral T cell tolerance by antigen-presenting B cells. II. Chronic antigen presentation overrules antigen-presenting B cell activation. J Immunol 176: 4021-4028.

14. Raimondi G, Zanoni I, Citterio S, Ricciardi-Castagnoli P, Granucci F (2006) Induction of peripheral T cell tolerance by antigen-presenting B cells. I. Relevance of antigen presentation persistence. J Immunol 176: 4012-4020.

15. Tunheim G, Schjetne KW, Rasmussen IB, Sollid LM, Sandlie I, et al. (2008) Recombinant antibodies for delivery of antigen: a single loop between beta-strands in the constant region can accommodate long, complex and tandem T cell epitopes. Int Immunol 20: 295-306.

16. Zaghouani H, Steinman R, Nonacs R, Shah H, Gerhard W, et al. (1993) Presentation of a viral T cell epitope expressed in the CDR3 region of a self immunoglobulin molecule. Science 259: 224-227.

17. Kawamura H, Berzofsky JA (1986) Enhancement of antigenic potency *in vitro* and immunogenicity *in vivo* by coupling the antigen to anti-immunoglobulin. J Immunol 136: 58-65.

18. Casten LA, Pierce SK (1988) Receptor-mediated B cell antigen processing. Increased antigenicity of a globular protein covalently coupled to antibodies specific for B cell surface structures. J Immunol 140: 404-410.

19. Lees A, Morris SC, Thyphronitis G, Holmes JM, Inman JK, et al. (1990) Rapid stimulation of large specific antibody responses with conjugates of antigen and anti-IgD antibody. J Immunol 145: 3594-3600.

20. Snider DP, Segal DM (1987) Targeted antigen presentation using crosslinked antibody heteroaggregates. J Immunol 139: 1609-1616.

21. Baiu DC, Prechl J, Tchorbanov A, Molina HD, Erdei A, et al. (1999) Modulation of the humoral immune response by antibody-mediated antigen targeting to complement receptors and Fc receptors. J Immunol 162: 3125-3130.

22. Zanetti M (1992) Antigenized antibodies. Nature 355: 476-477.

23. Eidem JK, Rasmussen IB, Lunde E, Gregers TF, Rees AR, et al. (2000) Recombinant antibodies as carrier proteins for sub-unit vaccines: influence of mode of fusion on protein production and T-cell activation. J Immunol Methods 245: 119-131.

24. Lunde E, Western KH, Rasmussen IB, Sandlie I, Bogen B (2002) Efficient delivery of T cell epitopes to APC by use of MHC class II-specific Troybodies. J Immunol 168: 2154-2162.

25. Lunde E, Rasmussen IB, Eidem JK, Gregers TF, Western KH, et al. (2001) 'Troy-bodies': antibodies as vector proteins for T cell epitopes. Biomol Eng 18: 109-116.

26. Lunde E, Munthe LA, Vabo A, Sandlie I, Bogen B (1999) Antibodies engineered with IgD specificity efficiently deliver integrated T-cell epitopes for antigen presentation by B cells. Nat Biotechnol 17: 670-675.

27. Lunde E, Bogen B, Sandlie I (1997) Immunoglobulin as a vehicle for foreign antigenic peptides immunogenic to T cells. Mol Immunol 34: 1167-1176.

28. Lunde E, Lauvrak V, Rasmussen IB, Schjetne KW, Thompson KM, et al. (2002) Troybodies and pepbodies. Biochem Soc Trans 30: 500-506.

29. Norderhaug L, Olafsen T, Michaelsen TE, Sandlie I (1997) Versatile vectors for transient and stable expression of recombinant antibody molecules in mammalian cells. J Immunol Methods 204: 77-87.

30. Oxenius A, Zinkernagel RM, Hengartner H (1998) Comparison of activation versus induction of unresponsiveness of virus-specific CD4+ and CD8+ T cells upon acute versus persistent viral infection. Immunity 9: 449-457.

31. Allen PM, McKean DJ, Beck BN, Sheffield J, Glimcher LH (1985) Direct evidence that a class II molecule and a simple globular protein generate multiple determinants. J Exp Med 162: 1264-1274.

32. Kappler JW, Skidmore B, White J, Marrack P (1981) Antigen-inducible, H-2-restricted, interleukin-2-producing T cell hybridomas. Lack of independent antigen and H-2 recognition. J Exp Med 153: 1198-1214.

33. Wherry EJ, Blattman JN, Murali-Krishna K, van der Most R, Ahmed R (2003) Viral persistence alters CD8 T-cell immunodominance and tissue distribution and results in distinct stages of functional impairment. J Virol 77: 4911-4927.

34. Klinman DM (2006) Adjuvant activity of CpG oligodeoxynucleotides. Int Rev Immunol 25: 135-154.

35. Parish CR, Warren HS (2002) Use of the intracellular fluorescent dye CFSE to monitor lymphocyte migration and proliferation. Curr Protoc Immunol Chapter 4: Unit 4 9.

36. Kamperschroer C, Quinn DG (1999) Quantification of epitope-specific MHC class-II-restricted T cells following lymphocytic choriomeningitis virus infection. Cell Immunol 193: 134-146.

37. Huck S, Fort P, Crawford DH, Lefranc MP, Lefranc G (1986) Sequence of a human immunoglobulin gamma 3 heavy chain constant region gene: comparison with the other human C gamma genes. Nucleic Acids Res 14: 1779-1789.

38. Hathcock KS, Hirano H, Murakami S, Hodes RJ (1993) CD44 expression on activated B cells. Differential capacity for CD44-dependent binding to hyaluronic acid. J Immunol 151: 6712-6722.

39. Barber DL, Wherry EJ, Masopust D, Zhu B, Allison JP, et al. (2006) Restoring function in exhausted CD8 T cells during chronic viral infection. Nature 439: 682-687.

40. Baier G, Baier-Bitterlich G, Looney DJ, Altman A (1995) Immunogenic targeting of recombinant peptide vaccines to human antigen-presenting cells by chimeric anti-

HLA-DR and anti-surface immunoglobulin D antibody Fab fragments *in vitro*. J Virol 69: 2357-2365.

41. Cervenak L, Magyar A, Boja R, Laszlo G (2001) Differential expression of GL7 activation antigen on bone marrow B cell subpopulations and peripheral B cells. Immunol Lett 78: 89-96.

42. Ramaswamy M, Siegel RM (2007) A FAScinating receptor in self-tolerance. Immunity 26: 545-547.

43. Butcher EC, Rouse RV, Coffman RL, Nottenburg CN, Hardy RR, et al. (1982) Surface phenotype of Peyer's patch germinal center cells: implications for the role of germinal centers in B cell differentiation. J Immunol 129: 2698-2707.

44. Coico RF, Bhogal BS, Thorbecke GJ (1983) Relationship of germinal centers in lymphoid tissue to immunologic memory. VI. Transfer of B cell memory with lymph node cells fractionated according to their receptors for peanut agglutinin. J Immunol 131: 2254-2257.

45. Haberman AM, Shlomchik MJ (2003) Reassessing the function of immune-complex retention by follicular dendritic cells. Nat Rev Immunol 3: 757-764.

46. Deaglio S, Mehta K, Malavasi F (2001) Human CD38: a (r)evolutionary story of enzymes and receptors. Leuk Res 25: 1-12.

47. Kolar GR, Mehta D, Pelayo R, Capra JD (2007) A novel human B cell subpopulation representing the initial germinal center population to express AID. Blood 109: 2545-2552.

48. Rasmussen T, Lodahl M, Hancke S, Johnsen HE (2004) In multiple myeloma clonotypic CD38- /CD19+ / CD27+ memory B cells recirculate through bone marrow, peripheral blood and lymph nodes. Leuk Lymphoma 45: 1413-1417.

49. Fujii S, Liu K, Smith C, Bonito AJ, Steinman RM (2004) The linkage of innate to adaptive immunity via maturing dendritic cells *in vivo* requires CD40 ligation in addition to antigen presentation and CD80/86 costimulation. J Exp Med 199: 1607-1618.

50. Rasmussen IB, Lunde E, Michaelsen TE, Bogen B, Sandlie I (2001) The principle of delivery of T cell epitopes to antigen-presenting cells applied to peptides from influenza virus, ovalbumin, and hen egg lysozyme: implications for peptide vaccination. Proc Natl Acad Sci U S A 98: 10296-10301.

51. Shirota H, Sano K, Hirasawa N, Terui T, Ohuchi K, et al. (2002) B cells capturing antigen conjugated with CpG oligodeoxynucleotides induce Th1 cells by elaborating IL-12. J Immunol 169: 787-794.

52. Kaech SM, Wherry EJ, Ahmed R (2002) Effector and memory T-cell differentiation: implications for vaccine development. Nat Rev Immunol 2: 251-262.

CHAPTER 6

CONCLUSIONS AND FUTURE DIRECTIONS

Cytotoxic T lymphocyte escape mutations in hepatitis C virus

Escape from the CD8+ T cell arm of the immune response is a well-established phenomenon in both acute and chronic HCV infection [1,2,3]. The work presented in Chapter 2 is the first published study showing a direct link between CD8+ T cell pressure and the maintenance of HCV replicative fitness. The advent of a cell culture system for HCV propagation has opened up many new avenues for research, including reverse genetics approaches that allow for individual analysis of specific viral clones isolated in either humans or chimpanzees. This is a daunting task, as the staggering rates of replication and mutation in HCV make it virtually impossible to track all mutations in all regions of the genome at any given time [4,5,6,7]. It was previously known that non-synonymous mutation rates are higher in MHC class I-restricted HCV epitopes than in flanking or non-restricted regions [8], and as such well-defined epitopes represented an ideal starting point for *in vitro* reverse engineering. We took advantage of the *in vivo* chimpanzee infection model to select a well-sequenced HCV1/910 dominant class I epitope for further analysis. This epitope, $NS3_{1629\text{-}1637}$, is located in the C-terminus of NS3, and was found to acquire numerous mutations over the course of a seven-year long study [8,9,10]. Our initial findings using subgenomic replicons containing the observed *in vivo* mutations were surprising, in that single amino acid substitutions in known TCR- and MHC- contact residues had a significant effect on transduction efficiency (*Chapter 2, Figure 1A, B*). From these results and the knowledge that the C-terminus of NS3 has

RNA helicase function, it was clear that this epitope represented an important region for HCV replication.

To further probe the host-pathogen relationship, we created a basic assay to apply CD8+ T cell pressure to liver-derived cells presenting $NS3_{1629\text{-}1637}$ wild type or mutant antigens. Huh-7.5 cells were engineered to express the chimpanzee MHC Patr-B1701 molecule, and were allowed to present antigen through several methods to an $NS3_{1629\text{-}1637}$-restricted CD8+ T cell clone derived from the same experimental chimpanzee. These methods included peptide pulsing (*Chapter 2, Figure 2C*), subgenomic replicon transfection (*Chapter 2, Figure 3B, C*), and transfection or infection of full-length HCV RNA and whole virus, respectively (*Chapter 2, Figure 5C, D*). Regardless of the antigen delivery method, the CD8+ T cell clone could not function in response to Huh-7.5/B1701 cells presenting anything except wild type $NS3_{1629\text{-}1637}$ (*Chapter 2, Figure 2C, 3B, 3C, 5C, 5D*), indicative of successful escape from a highly focused immune response. Subsequent analysis of full-length HCV clones bearing wild type or mutated $NS3_{1629\text{-}1637}$ epitope established a hierarchy of RNA replication and virion production, with the early leucine to proline mutation at position 9 (L1637P) being the least fit in cell culture, and the leucine to serine mutation at position 9 (L1637S) displaying an intermediate phenotype between L1637P and the parental $NS3_{1629\text{-}1637}$ clone. These data corresponded well with previous replicon data, but the isoleucine to threonine switch at position 7 (I1635T) did not show a decrease in fitness in any assay, which did not make sense because of its apparently efficient escape from T cell pressure (*Chapter 2, Figure 4B, C*). Indeed, this clone did not revert to parental sequence in the absence of *in vitro* CD8+ T cells even

when passaged for weeks in culture (*Chapter 2, Figure 6*). Further analysis of PBMCs isolated seven years after initial infection demonstrated a de novo CD8+ T cell clone that was most likely responsible for limitation of the I1635T clone's success *in vivo* (*Chapter 2, Figure 7*). Upon several rounds of restimulation, this I1635T-specific T cell expanded to large numbers from bulk PBMC cultures (>7% of total cells, B. Callendret, unpublished results), suggesting that *in vivo* expansion of this clone was adequate to control this infectious variant.

Our study has left several open questions pertaining to structural impact of CTL escape mutations and the immune response during acute and chronic HCV infection. We demonstrated that single amino acid substitutions in a dominant MHC class I epitope can have a profound effect on replication, virion production, and T cell recognition. However, it is unlikely that every targeted class I epitope found during *in vivo* infection is as sensitive to sequence variation as the $NS3_{1629\text{-}1637}$ epitope. Shortly after our work was published, Dazert and colleagues published a report demonstrating a requirement for mutational clustering within an immunodominant HLA-B27-restricted NS5B epitope to escape T cell recognition [11]. One would predict that mutation of epitopes in the RdRp of HCV would have grave consequences to viral propagation. This is indeed the case, but only when those mutations occur in known positions of MHC contact (positions 2 or 9). $NS3_{1629\text{-}1637}$ variants that fall within the MHC binding residues (L1637P and L1637S) are certainly less fit than wild type $NS3_{1629\text{-}1637}$, but the persistence of a serine at position 9 suggests that this mutation is not so detrimental that it cannot exist for years. The nature of each individual's T cell responses may also dictate whether such mutants persist in the

host swarm. For example, circulating T cells to the wild type $NS3_{1629\text{-}1637}$ and other variants may have been present for long periods of time in the particular chimpanzee of our study, and the L1637S mutation may represent one of only a few viable options for successful immune escape. Additionally, structural analysis of the $NS3_{1629\text{-}1637}$ epitope was not performed, and the relative plasticity of this sequence may be correlated to its involvement in a less critical region of the NS3 helicase (as compared to the RdRp or other motifs in C-terminal NS3). Ultimately, each epitope may be selected for different positional mutations depending on its location in the genome, the particular MHC restriction, and the species in which it is propagated. Infection of naïve HLA-matched or -mismatched chimpanzees with the L1637S variant may provide interesting data as to the true *in vivo* reversion capacity of this variant.

A lingering question of this work is the impact of CD4+ T cell epitope escape mutation on viral fitness. Mutational escape does occur in these epitopes [12,13,14], albeit at a much lower frequency than CD8+ T cell epitopes (18% vs 75% of all CD4+ and CD8+ epitopes examined) [15]. This suggests that CD4+ T cell epitopes are relatively stable overall, and therefore make it difficult to analyze mutational impact on viral fitness. Significant mutations may occur early in the acute phase, but selection of these changes may be fleeting as CD4+ T cell responses rapidly wane and infection progresses to chronicity [1,7,16,17,18,19,20]. This presents a classic "chicken or the egg" question: does the virus abandon significant class II-restricted epitope mutations because of a diminishing CD4+ response, or are these variants actually selected for early on and subsequently responsible for a lessening of helper T cell pressure? The latter hypothesis

is an attractive mechanism for initial CD4+ dysfunction and transition into the chronic phase, but is likely not the only contributing factor. Clearly more in-depth longitudinal analysis of CD4+ epitope evolution in the acute phase will be needed to fully explain the contribution of this phenomenon to disease progression.

HCV E2 glycoprotein structure and involvement in the viral life cycle

The structure of the HCV E2 glycoprotein has been an area of intense research since its implication in binding to host cell receptors CD81 and SR-BI [21,22]. Although much effort has been devoted to determining the crystal structure of this protein, attempts thus far have been unsuccessful, owing to its complex mature form and intimate association with membranes and HCV E1. Biochemical analyses and deletion/mutagenesis studies have revealed that E2 is a highly glycosylated type 1 transmembrane protein containing an amphipathic helical stem region that connects the amino-terminal ectodomain and the carboxy-terminal membrane-spanning segment [23,24]. Recently, a comprehensive tertiary model of eE2 was proposed by incorporating the E2 polypeptide sequence along with CD81-binding data and disulfide connectivity patterns into a structure built upon consensus templates of alpha- and flaviviruses [25]. This model predicts eE2 to have three domains, with CD81-binding sites located in domain I, a putative fusion peptide located in domain II, and 18 cysteine residues throughout. The 18 cysteines of E2 located in the ectodomain (an additional 2 are located in the membrane-spanning segment) are highly conserved across HCV genotypes, and as such are hypothesized to form 9 disulfide bonds (*Chapter 3, Figure 1A*). However, the pattern of disulfide bonding proposed in the Krey *et al*. model is speculative, and has not yet been confirmed.

We built upon this study by determining the contribution of each disulfide bond of E2 to the viral life cycle. To achieve this, we performed a comprehensive site-directed alanine substitution of every cysteine in eE2, and cloned these mutations into the HCVcc backbones Cp7 and CNS2Rluc (*Chapter 3, Figure 1B, 2A, 2B*). Elimination of disulfide bonding in eE2 had no effect on initial replication or production of the protein (*Chapter 3, Figure 1B, 2A*), but severely crippled viral spread and core protein release in cell culture supernatants (*Chapter 3, Figure 2*). From our analysis, we were able to group all 18 cysteine mutants into one of three types. Type I mutants replicate and synthesize E2, but release low or undetectable levels of core in the supernatant. Most of the cysteine mutants fall into this category (15/18), and it is likely that their defect lies in improper E2 folding in the endoplasmic reticulum or placement on the viral particle prior to egress. Type II mutants produce low (C11A) or undetectable (C1A) levels of virus, and low levels of core protein. For C11A, we reasoned that the location of this cysteine in a hypervariable region of E2 (HVR3, amino acids 575-587) allows for greater plasticity upon alteration. However, it is more difficult to rationalize the phenotype of C1A. It is possible that disruption of the disulfide bond in this mutant allows for the C1 partner to transiently associate with another cysteine in E2 or E1, creating a bond that allows for placement on the virion surface and egress from the cell. Once exposed to the extracellular milieu, this non-native bond may orient the large extracellular loop of E2 in such a way as to mask residues in domain II and prevent CD81 or additional co-receptor binding, rendering C1A non-infectious.

Type III mutants are comprised of only one clone, C6A. This mutant was surprising, in that it produced large amounts of viral particles as assessed by core release (*Chapter 3, Figure 2C, 4D*) and RNA content in sucrose gradient fractions (*Chapter 3, Figure 3A*), but repeatedly failed to infect naïve cells (*Chapter 3, Figure 3B, 4C*). To ensure that this phenotype was due to C6 alone and not the surrounding region, which is thought to be a highly conserved putative fusion peptide, alanine substitution was performed on adjacent residues. These experiments proved that C6A was unique in its ability to release core in the supernatant but remain uninfectious (*Chapter 3, Figure 4*). The defect of C6A was not due to structural defects, as demonstrated by circular dichroism spectroscopy (*Chapter 3, Figure 5C*). Instead, we showed using purified eE2 proteins that C6A is unable to bind CD81, and the surrounding region also shows moderate CD81-binding defects (*Chapter 3, Figure 5A*). We confirmed this result using C6A protein in viral neutralization assays, but we did not study the surrounding region due to a lack of viral particle secretion by these mutants (*Chapter 3, Figure 5B*).

Our studies open up many questions about the orientation and function of disulfide bonds in HCV E2. This molecule is relatively intolerant of cysteine substitution, which is expected of a glycoprotein with complex structure and may reflect specific orientations required for hetero (E1)- or homo (E2) -dimerization. For comparison, it has been shown recently that HIV-1 Env protein is very tolerant of cysteine substitution despite strict conservation of sequence, with five out of ten disulfide bonds being completely dispensable for folding and two of these five dispensable for viral replication [52]. Perhaps the most striking observation made in our study is the lack of an identical C6A

phenotype in the 17 remaining mutants. This would seemingly indicate that C6 has no binding partner, but this has been disproven using N-ethylmaleimide (NEM) and iodoacetamide (IAM) protective labeling [53]. We currently have two hypotheses as to why C6A is unique. First, mutation of C6 may cause its partner (proposed to be C7 by Krey *et al*.) to form an intermolecular disulfide bond with E1. Noncovalent E1E2 heterodimers are normally found at the virion surface [54,56], and the proximity of these two proteins in the endoplasmic reticulum suggests that bonding interactions may be possible. However, preliminary mutagenesis studies suggest that the cysteines of E1 are equivalently paired through intramolecular bonding. When substituted for alanine, C5 and C6 of E1 are dispensable for both replication and infectious particle production, and we hypothesize that these two residues may be connected via disulfide linkage (Figure 1). NEM and IAM labeling have not been performed on E1, but if its eight cysteines are paired, the interaction of the E2 C6 partner with E1 would be transient. We have very recently shown using non-reducing western blots and sucrose concentration techniques that E2 on the surface of Cp7 virions exist as monomers with a small percentage of dimers. Interestingly, surface E2 on C6A exists in a mostly dimeric form, with an additional higher molecular weight band present in the stacking gel when blotting with anti-E2 2C1 (data not shown). Experiments using monoclonal antibodies to detect E1 are forthcoming, and we have also engineered HCVcc viruses with integrated E1-HA tags to determine whether increased intermolecular disulfide bonding occurs in the C6A clone. A second hypothesis for the lack of equivalent C6A phenotype in other E2 mutants is that the C6 partner forms an intermolecular disulfide bond with another E2 molecule upon C6 substitution. E2 is predicted to homodimerize [55], but this model was published before

domain III was proposed, and also did not take into account the strictly conserved disulfide bonds of E2. Presently, homodimerization has not been demonstrated in intact viral particles. We have constructed a preliminary model focusing on amino acids 500-511 of eE2 that incorporates the C6A phenotype, potential homodimerization, and the prediction that C6 and C7 form a disulfide-bonded pair [25,55] (G. Mateu, L. Uebelhoer, *et al*. in submission) (Figure 2). This model suggests that E2 may form parallel homodimers, not head-to-tail homodimers as has previously been suggested [55]. Destruction of the C6-C7 bond by C6 substitution could be overcome by a forced pairing of the two resultant free C7 residues, which would explain why C6A produces viral particles (Figure 2, bottom left). Conversely, C7 substitution would result in two free C6 residues whose bonding would be constrained by distance (Figure 2, bottom right). In this situation, C6-C6 pairing would be energetically unfavorable, requiring a twist in one or both E2 molecules to overcome this distance.

Our results indicate that the current proposed fusion peptide of E2 encompasses a CD81 binding domain that has not been previously reported and may have important implications for this glycoprotein's structure and function. Accordingly, we have immunized mice with both long and short peptides spanning this region in hopes of creating neutralizing monoclonal antibodies as a proof of concept. These initial experiments failed to yield productive B cell hybridomas, presumably due to low immunogenicity of antigen and failure of B cell germinal center formation. To circumvent this, we have linked these same peptides to the highly immunogenic hapten keyhole limpet hemocyanin (KLH) prior to immunization, and fusion with an

immortalized B cell partner is forthcoming. It is clear from our studies that much more work needs to be done before an accurate model of HCV E2 can be proposed. We have contributed a great deal of data to the field, which will hopefully be useful in future analysis of E1-E2 or E2-E2 interactions. The inability of mutant C6A to infect or revert *in vitro* in the absence of immune pressure makes this clone a useful tool to study the viral life cycle, and could potentially have future use as an attenuated vaccine.

A new system to study HCVcc binding and entry

The data presented in Chapter 4 are preliminary, but represent important first steps in the development of a complete imaging system to study the binding and entry of HCVcc. We modified a spin-inoculation protocol that is common in other infectious systems, such as HIV-1 [26], and applied a panel of monoclonal antibodies raised against a variety of HCV proteins in mice (H. Scarborough, unpublished results). Our results thus far are consistent with HCVpp studies, and more importantly with a newer study tracking directly labeled single HCVcc particles [27]. We provide evidence that HCVcc particles can be visualized immediately upon initial binding at the apex of human hepatoma cells, and associate in tightly clustered puncta measuring between 1.5-3 μm in diameter. Furthermore, binding is dependent on CD81 expression, glycan interactions, and a rearrangement of host cytoskeletal actin which can often be found just adjacent to or coinciding with incoming virions. Surprisingly, initial binding events in this system seem to be a faithful predictor of future productive infection, and suggest that every hepatocyte that comes in contact with HCV puncta will eventually become infected.

We are currently using this system to probe several aspects of the early HCV life cycle. HCV entry is known to be dependent on clathrin-mediated endocytosis, as demonstrated by dominant negative mutants, siRNA depletion of clathrin heavy chain components, and inhibition of clathrin formation at the plasma membrane using chlorpromazine [28,29]. However, visualization of HCV inside these pits has been impossible until now. Our ability to concentrate large amount of HCVcc and visualize early binding and entry events should allow us to visualize virus interacting with clathrin or clathrin-associated molecules. The adaptor proteins involved in HCVcc clathrin-mediated internalization are not currently known, but studies of clathrin endocytosis in neurons implicate several candidates. For future experiments, we plan to use antibodies against the heavy and light chains of clathrin, AP180 [30,31,32,33], enthoprotin [34], clathrin assembly lymphoid myeloid leukemia (CALM) protein [35,36], huntingtin-interacting protein (HIP-1) [37], and others to probe the HCV-clathrin interaction. Additionally, the structure of a complete clathrin lattice has been solved at subnanometer resolution, so it may be feasible to study this interaction using electron cryomicroscopy [38].

Initial fluorescent signal quantification of early and late timepoints has suggested that every Huh-7.5 cell that comes in contact with the 1.5-3 μm punctate structures visualized using anti-E2 2C1 monoclonal antibody results in a productively infected cell (*Chapter 4, Figure 4*). However, this approach is indirect, and the size of these visible structures indicates that a large degree of clumping occurs as a byproduct of our methods. Ultimately, a real-time method for visualizing single viral particles binding to a cell and the subsequent production of viral proteins in that specific cell is needed. We have

generated full-length constructs with integrated GFP protein (R. Chinnadurai, G. Mateu, unpublished results), but these constructs are only visible upon protein translation at the host cell endoplasmic reticulum. For future investigation, we propose to directly label concentrated preparations of these GFP viruses using lipophilic dye as previously reported [27]. Once labeled, we will perform real-time imaging to correlate fluorescent binding events with subsequent GFP expression in single cells. This analysis will allow us to determine if all virus binding leads to productive infection. Furthermore, the use of human hepatoma cells stably expressing fluorescent CD81, clathrin, or Rab molecules will be used to generate a complete real-time view of early binding, endocytosis, and fusion.

Naïve B cell antigen presentation to CD4+ T cell subsets

The antigen presentation capacity of naïve B cells has traditionally been overshadowed by a dominating interest in dendritic cells. However, the involvement of B cells in priming and maintaining an effective immune response through CD4+ interaction and neutralizing antibody production has been demonstrated in a number of chronic infections, necessitating further dissection of the antigen presentation capacity of this subset [39,40,41,42,43,44]. In an effort to augment antigen presentation to CD4+ T cells through these B cells, we built upon a previously described recombinant chimeric antibody system to develop a humanized antibody that delivers integrated virus-specific antigenic peptides to the class II processing machinery [45]. This rAb targets surface IgD, and as such was only expected to bind to antigen-inexperienced B cells. Additional variable region specificity allowed us to limit IgD molecules targeted to those with a

specific allotype (allotype "a"). Binding of these antibodies is exquisitely specific both *in vitro* and *in vivo*, and large fractions of mature naïve splenic B cells display surface binding using very low concentrations of the purified molecules (*Chapter 5, Figure 1*). The observation that surface IgD is withdrawn on these B cells when bound by rAb is not surprising, as efficient IgD cross-linking is known to be a trigger for B cell maturation, leading to a replacement of IgD with other surface or secreted immunoglobulins [46]. We followed fluctuations of surface IgD on B cells throughout treatment with rAb, and found that IgD gradually reappears over time, suggesting that either treatment is not significant enough to induce full activation, or a replenishment of IgD+ B cells occurs from a different compartment. The former hypothesis is difficult to rationalize, as rAbs have high affinity for surface IgD. Instead, rAbs may target numerous IgD molecules, but the nature of the rAb-IgD interaction may not be adequate to recruit intracellular signaling molecules. This is in line with B cell phenotyping data not included in this work that demonstrates weak upregulation of activation (CD69), costimulatory (CD80, CD86), and germinal center differentation (GL-7, PNA) markers. Future studies in this particular system should focus on proper activation of B cells upon surface IgD ligation. However, this approach needs to be tempered: if the majority of B cells are bound by rAb and constitutively activated, the risk of B cell lymphomas or hypergammaglobulinemia will surely increase until all circulating rAb has been cleared from the system. Even after these molecules expire, mature B cells may already be destined for uncontrolled growth, and could represent a significant danger to the host.

Inadequate recruitment of intracellular B cell signaling molecules is consistent with the subsequent T cell responses observed in our *in vivo* studies. Exogenous anti-CD28 is needed for CD4+ T cells to fully divide upon presentation of rAb-antigen by B cells, signifying a defect in signal 2-driven T cell activation. Indeed, provision of anti-CD28 in conjunction with rAb drives SMARTA CD4+ T cells to divide and phenotypically resemble a primary LCMV challenge (*Chapter 5, Figure 4*). Although contrived, this approach is encouraging, as it suggests that modification of our system to appropriately stimulate B cells to display this molecule may be enough to develop a robust CD4+ T cell memory response. It should be mentioned, however, that multiple rAbs or multi-epitope bearing rAbs may be needed to achieve partial or complete pathogen clearance in infectious systems. We originally chose the GP61-80 peptide of LCMV as our integrated rAb antigenic component as it represents an immunodominant epitope that influences the I-A^b-restricted cellular response [47]. Because of this, we hypothesized that we could create a novel vaccination strategy by modifying GP61-80-specific CD4+ T cell responses before or during infection. However, we were unable to reduce viral burden despite numerous prophylactic or therapeutic dosing regimens (L. Uebelhoer, unpublished data). In retrospect, even if rAb targeting were to adequately activate B cells for functional T cell activation, multiple epitopes would most likely have been needed to limit viral burden in animals. LCMV infection presents multiple antigens to the host over a prolonged period of time, and we rationalize that priming CD4+ T cells through rAbs to only one of these antigens is inadequate.

The most compelling evidence that rAb-antigen presentation by naïve B cells results in dysfunctional CD4+ T cells was a series of adoptive transfer survival experiments. We had originally hoped to control infection by priming adoptively transferred SMARTA T cells prior to infection, but for reasons described above this method failed. Interestingly, we found over the course of these experiments that LCMV challenge resulted in a lethal course of infection that was dependent on number of transferred cells (*Chapter 5, Figure 5*). We used this reliable predictor of survival to test the *in vivo* functionality and persistence of SMARTA cells post-rAb treatment, and found repeatedly that treatment of rAb GP61-80 with anti-CD28 or anti-CD28 alone were able to protect mice from this cell-mediated lethality. While protection was absolute in these groups, treatment with rAb GP61-80 alone resulted in a 50% survival rate. We hypothesize that presentation of rAb-antigen to a SMARTA T cell in the absence of CD28 costimulation results in either anergy or apoptosis. Since these cells are non-existent or unable to release cytokines upon challenge with LCMV, hypercytokinemia is reduced and animals are able to survive. To determine whether transferred cells are cleared from circulation or persist with defective function, experiments are currently underway examining the fate and *ex vivo* cytokine profile of transferred cells in multiple organs post-treatment and post-infection.

The work presented in Chapter 5 lends support to the idea that mature naïve B cells do not adequately prime CD4+ T cells upon antigen presentation [48,49,50], even when antigen is specifically targeted to a B cell surface molecule for internalization. The main question is: where do we go from here? Induction of T cell tolerance through deletion has been demonstrated with rAbs in the thymus, indicating that this technology can be

applied to the study of autoimmunity [51]. Experimental autoimmune encephalomyelitis (EAE, a model of multiple sclerosis) and murine rheumatoid arthritis are two autoimmune models where rAb treatment has direct application, and could have serious real-world clinical application. In addition to new model systems, class I-restricted priming has yet to be explored in the context of rAbs, and may shed light on rare B-CD8 or B-CD4-CD8 crosstalk events. Finally, comparison studies of different APC subsets in both CD4+ and CD8+ rAb systems may help determine whether inadequate priming is a global phenomenon, or limited to a particular type of cell.

Future directions

Two decades have passed since the discovery of HCV, and we still know very little about this devastating human pathogen. An exciting era of research is upon us, as our tools to study the virus have finally caught up with our ability to ask relevant questions. The goal of this disseration was to utilize these tools to study how HCV gains access to permissive cells and persists in the human population despite an onslaught of diverse host antiviral responses. My work has demonstrated how HCV masterfully subverts the immune system without hindering its viral life processes, and provides a glimpse into the consequences of structural manipulation of this flavivirus. Along the way, I have developed new systems for future investigation of binding, entry, and viral antigen presentation, all aimed at better understanding how humans and HCV coexist. A greater knowledge of this host-pathogen relationship will be invaluable in the development of novel therapies aimed at complete eradication of the virus.

Figures

Figure 1

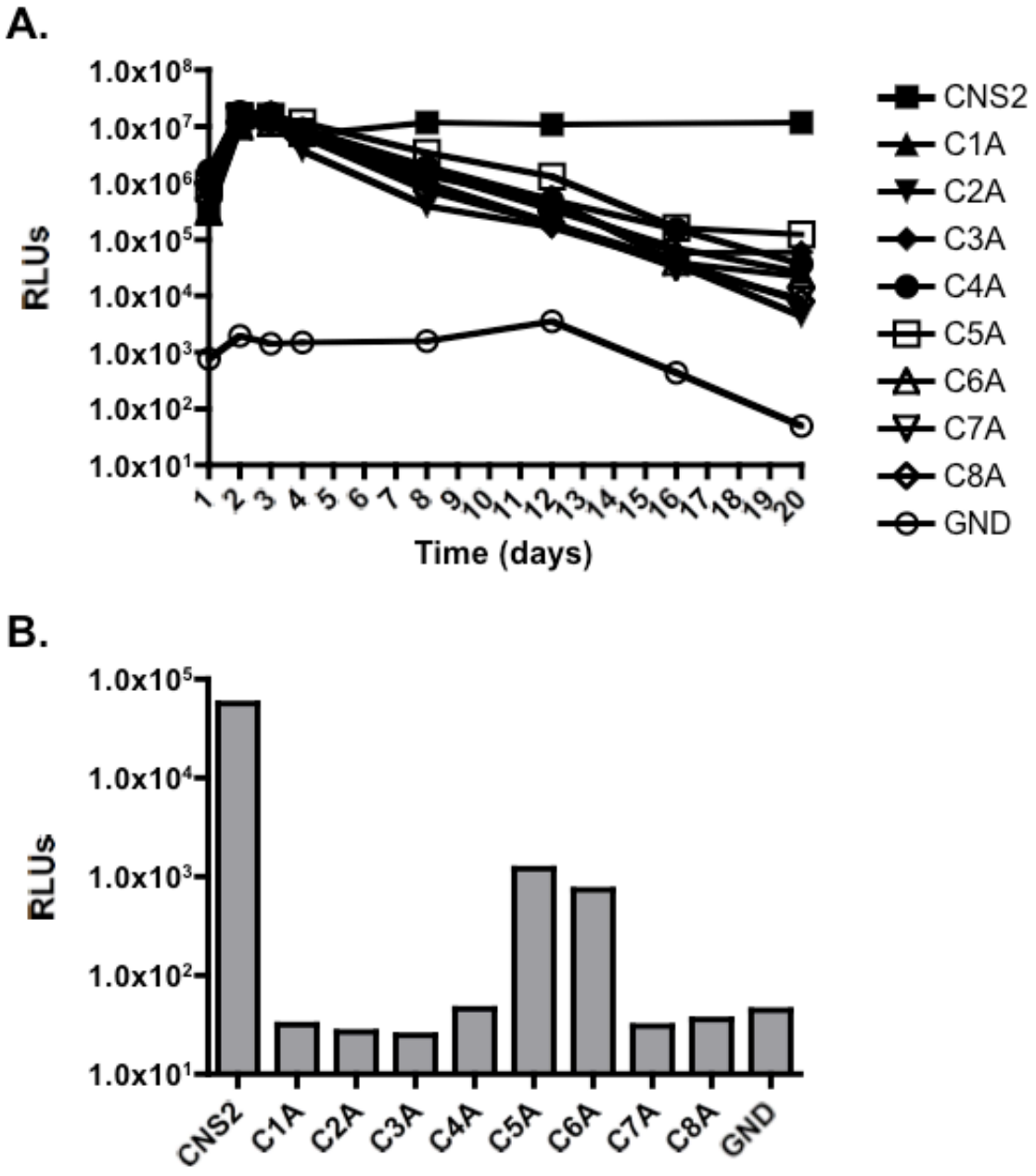

Figure 2

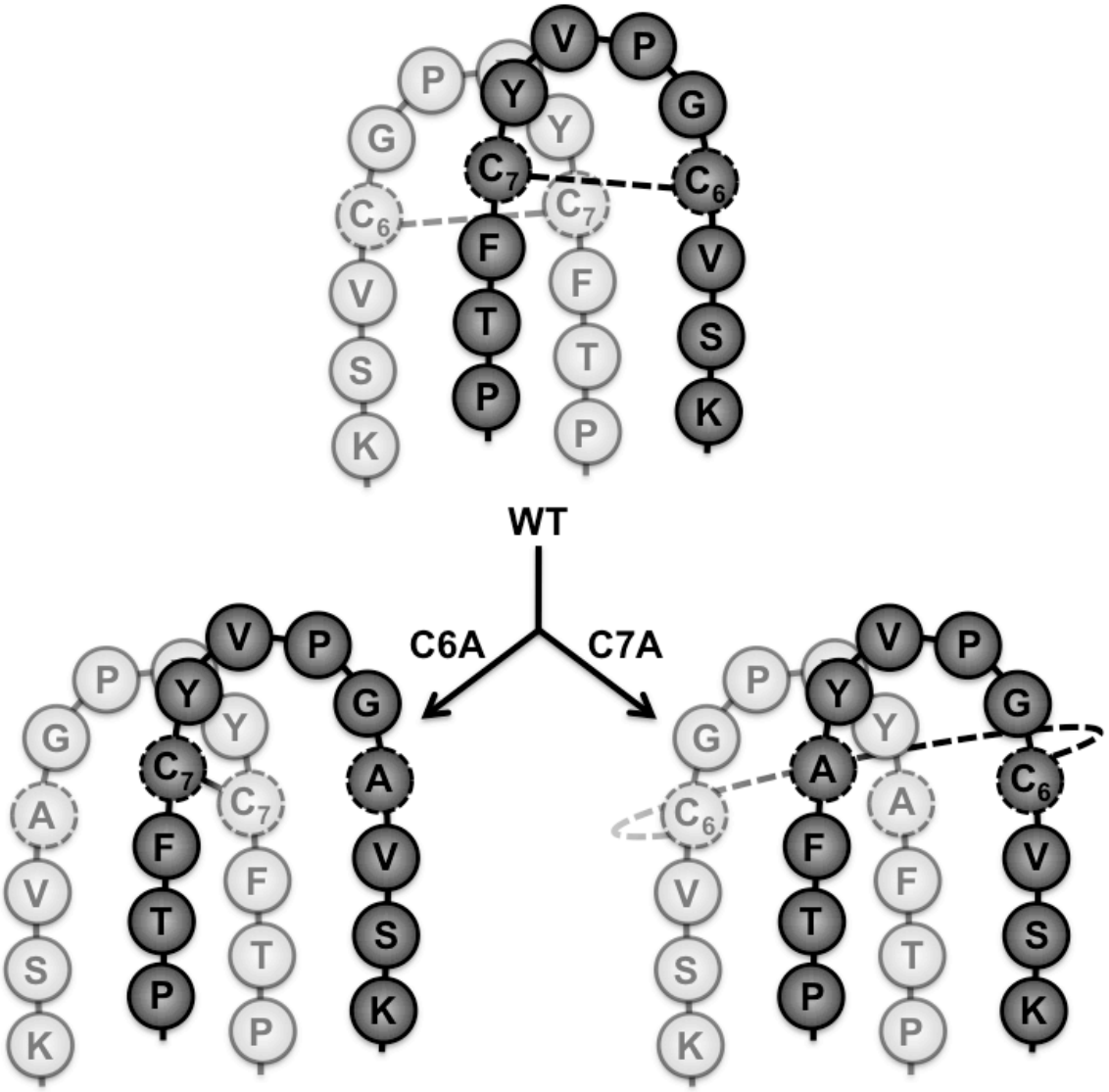

Figure Legends

Figure 1. Mutations in conserved cysteines of HCV E1 impair infectivity for all mutants except C_{82} (C5) and C_{91} (C6). E1 cysteine mutations were introduced in the CNS2Rluc clone to facilitate detection of replication. GND is a nonreplicative control genome. A) Replication of individual cysteine mutants as assayed by relative light units (RLUs) in cell lysates up to 20 days post-transfection. B) Infectivity of the E1 cysteine mutants four days post-tranfection. Supernatants from transfected cells were harvested at day four and used to infect naïve Huh-7.5 cells. Three days post-infection cells were lysed and tested for Renilla expression. For A) and B), data displayed is representative of two separate experiments.

Figure 2. Effect of alanine substitution on the proposed disulfide-bonding pattern between C_{505} (C6) and C_{510} (C7) of HCV E2. The amino acid sequence of HCV H77 E2 is depicted from residues 502-513 starting with lysine (K). This diagram was adapted from the Krey *et al*. model, and assumes parallel head-to-head homodimer formation with lightly shaded beads representing the background loop. Dashed lines indicate potential disulfide bond connectivity.

References

1. Tester I, Smyk-Pearson S, Wang P, Wertheimer A, Yao E, et al. (2005) Immune evasion versus recovery after acute hepatitis C virus infection from a shared source. J Exp Med 201: 1725-1731.

2. Timm J, Lauer GM, Kavanagh DG, Sheridan I, Kim AY, et al. (2004) CD8 epitope escape and reversion in acute HCV infection. J Exp Med 200: 1593-1604.

3. Chang KM, Rehermann B, McHutchison JG, Pasquinelli C, Southwood S, et al. (1997) Immunological significance of cytotoxic T lymphocyte epitope variants in patients chronically infected by the hepatitis C virus. J Clin Invest 100: 2376-2385.

4. Thimme R, Oldach D, Chang KM, Steiger C, Ray SC, et al. (2001) Determinants of viral clearance and persistence during acute hepatitis C virus infection. J Exp Med 194: 1395-1406.

5. Neumann AU, Lam NP, Dahari H, Gretch DR, Wiley TE, et al. (1998) Hepatitis C viral dynamics *in vivo* and the antiviral efficacy of interferon-alpha therapy. Science 282: 103-107.

6. Bukh J, Miller RH, Purcell RH (1995) Genetic heterogeneity of hepatitis C virus: quasispecies and genotypes. Semin Liver Dis 15: 41-63.

7. Thimme R, Bukh J, Spangenberg HC, Wieland S, Pemberton J, et al. (2002) Viral and immunological determinants of hepatitis C virus clearance, persistence, and disease. Proc Natl Acad Sci U S A 99: 15661-15668.

8. Erickson AL, Kimura Y, Igarashi S, Eichelberger J, Houghton M, et al. (2001) The outcome of hepatitis C virus infection is predicted by escape mutations in epitopes targeted by cytotoxic T lymphocytes. Immunity 15: 883-895.

9. Cooper S, Erickson AL, Adams EJ, Kansopon J, Weiner AJ, et al. (1999) Analysis of a successful immune response against hepatitis C virus. Immunity 10: 439-449.

10. Choo QL, Kuo G, Ralston R, Weiner A, Chien D, et al. (1994) Vaccination of chimpanzees against infection by the hepatitis C virus. Proc Natl Acad Sci U S A 91: 1294-1298.

11. Dazert E, Neumann-Haefelin C, Bressanelli S, Fitzmaurice K, Kort J, et al. (2009) Loss of viral fitness and cross-recognition by CD8+ T cells limit HCV escape from a protective HLA-B27-restricted human immune response. J Clin Invest 119: 376-386.

12. Wang JH, Layden TJ, Eckels DD (2003) Modulation of the peripheral T-Cell response by CD4 mutants of hepatitis C virus: transition from a Th1 to a Th2 response. Hum Immunol 64: 662-673.

13. von Hahn T, Yoon JC, Alter H, Rice CM, Rehermann B, et al. (2007) Hepatitis C virus continuously escapes from neutralizing antibody and T-cell responses during chronic infection *in vivo*. Gastroenterology 132: 667-678.

14. Frasca L, Del Porto P, Tuosto L, Marinari B, Scotta C, et al. (1999) Hypervariable region 1 variants act as TCR antagonists for hepatitis C virus-specific CD4+ T cells. J Immunol 163: 650-658.

15. Fuller MJ, Shoukry NH, Gushima T, Bowen DG, Callendret B, et al. (2010) Selection-driven immune escape is not a significant factor in the failure of CD4 T cell responses in persistent hepatitis C virus infection. Hepatology 51: 378-387.

16. Puig M, Mihalik K, Tilton JC, Williams O, Merchlinsky M, et al. (2006) CD4+ immune escape and subsequent T-cell failure following chimpanzee immunization against hepatitis C virus. Hepatology 44: 736-745.

17. Day CL, Lauer GM, Robbins GK, McGovern B, Wurcel AG, et al. (2002) Broad specificity of virus-specific CD4+ T-helper-cell responses in resolved hepatitis C virus infection. J Virol 76: 12584-12595.

18. Urbani S, Amadei B, Fisicaro P, Tola D, Orlandini A, et al. (2006) Outcome of acute hepatitis C is related to virus-specific CD4 function and maturation of antiviral memory CD8 responses. Hepatology 44: 126-139.

19. Smyk-Pearson S, Tester IA, Klarquist J, Palmer BE, Pawlotsky JM, et al. (2008) Spontaneous recovery in acute human hepatitis C virus infection: functional T-cell thresholds and relative importance of CD4 help. J Virol 82: 1827-1837.

20. Day CL, Seth NP, Lucas M, Appel H, Gauthier L, et al. (2003) *Ex vivo* analysis of human memory CD4 T cells specific for hepatitis C virus using MHC class II tetramers. J Clin Invest 112: 831-842.

21. Pileri P, Uematsu Y, Campagnoli S, Galli G, Falugi F, et al. (1998) Binding of hepatitis C virus to CD81. Science 282: 938-941.

22. Scarselli E, Ansuini H, Cerino R, Roccasecca RM, Acali S, et al. (2002) The human scavenger receptor class B type I is a novel candidate receptor for the hepatitis C virus. EMBO J 21: 5017-5025.

23. Drummer HE, Poumbourios P (2004) Hepatitis C virus glycoprotein E2 contains a membrane-proximal heptad repeat sequence that is essential for E1E2 glycoprotein heterodimerization and viral entry. J Biol Chem 279: 30066-30072.

24. Falkowska E, Kajumo F, Garcia E, Reinus J, Dragic T (2007) Hepatitis C virus envelope glycoprotein E2 glycans modulate entry, CD81 binding, and neutralization. J Virol 81: 8072-8079.

25. Krey T, d'Alayer J, Kikuti CM, Saulnier A, Damier-Piolle L, et al. (2010) The disulfide bonds in glycoprotein E2 of hepatitis C virus reveal the tertiary organization of the molecule. PLoS Pathog 6: e1000762.

26. Miyauchi K, Kim Y, Latinovic O, Morozov V, Melikyan GB (2009) HIV enters cells via endocytosis and dynamin-dependent fusion with endosomes. Cell 137: 433-444.

27. Coller KE, Berger KL, Heaton NS, Cooper JD, Yoon R, et al. (2009) RNA interference and single particle tracking analysis of hepatitis C virus endocytosis. PLoS Pathog 5: e1000702.

28. Blanchard E, Belouzard S, Goueslain L, Wakita T, Dubuisson J, et al. (2006) Hepatitis C virus entry depends on clathrin-mediated endocytosis. J Virol 80: 6964-6972.

29. Meertens L, Bertaux C, Dragic T (2006) Hepatitis C virus entry requires a critical postinternalization step and delivery to early endosomes via clathrin-coated vesicles. J Virol 80: 11571-11578.

30. Kohtz DS, Puszkin S (1988) A neuronal protein (NP185) associated with clathrin-coated vesicles. Characterization of NP185 with monoclonal antibodies. J Biol Chem 263: 7418-7425.

31. Murphy JE, Pleasure IT, Puszkin S, Prasad K, Keen JH (1991) Clathrin assembly protein AP-3. The identity of the 155K protein, AP 180, and NP185 and demonstration of a clathrin binding domain. J Biol Chem 266: 4401-4408.

32. Morris SA, Schroder S, Plessmann U, Weber K, Ungewickell E (1993) Clathrin assembly protein AP180: primary structure, domain organization and identification of a clathrin binding site. EMBO J 12: 667-675.

33. Zhou S, Tannery NH, Yang J, Puszkin S, Lafer EM (1993) The synapse-specific phosphoprotein F1-20 is identical to the clathrin assembly protein AP-3. J Biol Chem 268: 12655-12662.

34. Wasiak S, Legendre-Guillemin V, Puertollano R, Blondeau F, Girard M, et al. (2002) Enthoprotin: a novel clathrin-associated protein identified through subcellular proteomics. J Cell Biol 158: 855-862.

35. Dreyling MH, Martinez-Climent JA, Zheng M, Mao J, Rowley JD, et al. (1996) The t(10;11)(p13;q14) in the U937 cell line results in the fusion of the AF10 gene and CALM, encoding a new member of the AP-3 clathrin assembly protein family. Proc Natl Acad Sci U S A 93: 4804-4809.

36. Tebar F, Bohlander SK, Sorkin A (1999) Clathrin assembly lymphoid myeloid leukemia (CALM) protein: localization in endocytic-coated pits, interactions with clathrin, and the impact of overexpression on clathrin-mediated traffic. Mol Biol Cell 10: 2687-2702.

37. Legendre-Guillemin V, Metzler M, Lemaire JF, Philie J, Gan L, et al. (2005) Huntingtin interacting protein 1 (HIP1) regulates clathrin assembly through direct binding to the regulatory region of the clathrin light chain. J Biol Chem 280: 6101-6108.

38. Fotin A, Cheng Y, Sliz P, Grigorieff N, Harrison SC, et al. (2004) Molecular model for a complete clathrin lattice from electron cryomicroscopy. Nature 432: 573-579.

39. Farci P, Alter HJ, Wong DC, Miller RH, Govindarajan S, et al. (1994) Prevention of hepatitis C virus infection in chimpanzees after antibody-mediated *in vitro* neutralization. Proc Natl Acad Sci U S A 91: 7792-7796.

40. Farci P, Shimoda A, Wong D, Cabezon T, De Gioannis D, et al. (1996) Prevention of hepatitis C virus infection in chimpanzees by hyperimmune serum against the hypervariable region 1 of the envelope 2 protein. Proc Natl Acad Sci U S A 93: 15394-15399.

41. Yu MY, Bartosch B, Zhang P, Guo ZP, Renzi PM, et al. (2004) Neutralizing antibodies to hepatitis C virus (HCV) in immune globulins derived from anti-HCV-positive plasma. Proc Natl Acad Sci U S A 101: 7705-7710.

42. Hangartner L, Zellweger RM, Giobbi M, Weber J, Eschli B, et al. (2006) Nonneutralizing antibodies binding to the surface glycoprotein of lymphocytic choriomeningitis virus reduce early virus spread. J Exp Med 203: 2033-2042.

43. Zhou T, Georgiev I, Wu X, Yang ZY, Dai K, et al. (2010) Structural basis for broad and potent neutralization of HIV-1 by antibody VRC01. Science 329: 811-817.

44. Wu X, Yang ZY, Li Y, Hogerkorp CM, Schief WR, et al. (2010) Rational design of envelope identifies broadly neutralizing human monoclonal antibodies to HIV-1. Science 329: 856-861.

45. Lunde E, Munthe LA, Vabo A, Sandlie I, Bogen B (1999) Antibodies engineered with IgD specificity efficiently deliver integrated T-cell epitopes for antigen presentation by B cells. Nat Biotechnol 17: 670-675.

46. Abbas AK, Lichtman, A. H., Pober, J. S. (2005) Cellular and Molecular Immunology 5th Ed.: 192-194.

47. Kamperschroer C, Quinn DG (1999) Quantification of epitope-specific MHC class-II-restricted T cells following lymphocytic choriomeningitis virus infection. Cell Immunol 193: 134-146.

48. Lassila O, Vainio O, Matzinger P (1988) Can B cells turn on virgin T cells? Nature 334: 253-255.

49. Fuchs EJ, Matzinger P (1992) B cells turn off virgin but not memory T cells. Science 258: 1156-1159.

50. Ronchese F, Hausmann B (1993) B lymphocytes *in vivo* fail to prime naive T cells but can stimulate antigen-experienced T lymphocytes. J Exp Med 177: 679-690.

51. Schjetne KW, Thommesen JE, Fredriksen AB, Lunde E, Sandlie I, et al. (2005) Induction of central T cell tolerance: recombinant antibodies deliver peptides for deletion of antigen-specific (CD4+)8+ thymocytes. Eur J Immunol 35: 3142-3152.

52. van Anken E, Sanders RW, Liscaljet IM, Land A, Bontjer I, et al. (2008) Only five of 10 strictly conserved disulfide bonds are essential for folding and eight for function of the HIV-1 envelope glycoprotein. Mol Biol Cell 19: 4298-4309.

53. Whidby J, Mateu G, Scarborough H, Demeler B, Grakoui A, et al. (2009) Blocking hepatitis C virus infection with recombinant form of envelope protein 2 ectodomain. J Virol 83: 11078-11089.

54. Deleersnyder V, Pillez A, Wychowski C, Blight K, Xu J, et al. (1997) Formation of native hepatitis C virus glycoprotein complexes. J Virol 71: 697-704.

55. Yagnik AT, Lahm A, Meola A, Roccasecca RM, Ercole BB, et al. (2000) A model for the hepatitis C virus envelope glycoprotein E2. Proteins 40: 355-366.

56. Lavie M, Goffard A, Dubuisson J (2007) Assembly of a functional HCV glycoprotein heterodimer. Curr Issues Mol Biol 9: 71-86.